



UNIVERSITY OF UDINE

Department of Agricultural, Food, Environmental and Animal Sciences
(DI4A)

Doctor of Philosophy in:
FOOD AND HUMAN HEALTH

XXXI Cycle

Title of the thesis

Novel Ruthenium Carboxylate Complexes Bearing Electron
Rich Diphosphines for the Synthesis of Food Relevant and
Bioactive molecules

Ph.D. Student:
Rosario Figliolia

Supervisor:
Prof. Walter Baratta

Co-Supervisor:
Dr. Antonio Zanotti-Gerosa

In collaboration with





UNIVERSITÀ DEGLI STUDI DI UDINE

Dipartimento di Scienze AgroAlimentari, Ambientali e Animali (Di4A)

Dottorato di Ricerca in:
ALIMENTI E SALUTE UMANA

XXXI Ciclo

Titolo della tesi

**Nuovi Complessi Carbossilati di Rutenio Contendenti Difosfine
Elettron-Ricche per la sintesi di Molecole di Interesse
Alimentare e Biologico**

Dottorando:
Rosario Figliolia

Supervisore:
Prof. Walter Baratta

Co-Supervisore:
Dr. Antonio Zanotti-Gerosa

In collaborazione con



Table of contents

Table of contents	iv
Summary	vi
Acknowledgments	viii
Abbreviations Table	x
1.0 Introduction	1
1.1 Homogeneous transition metal-promoted catalysis: history and applications ..	1
1.2 Purpose of a catalyst: theoretical aspects and practical considerations.....	4
1.3 Phosphine based ruthenium complexes in reductive processes	8
1.4 Aim of this thesis work	10
2.0 Results and Discussion	11
2.1 Synthesis of novel acetate Ru complexes	11
2.1.1 Background of Ru carboxylate catalysts.....	11
2.1.2 Synthesis of carboxylate complexes Ru(OAc) ₂ (PP)	13
2.1.3 Reactivity of Ru(OAc) ₂ (PP) species	15
2.1.4 Carbonyl compounds deriving from Ru(OAc) ₂ (DiPPF)	19
2.1.5 Carbonyl compounds deriving from Ru(OAc) ₂ (CO)(PPh ₃) ₂	22
2.1.6 Reactivity of Ru(OAc) ₂ (CO)(DiPPF) (9).....	23
2.1.7 Conclusions	25
2.2 Transfer Hydrogenation of ketones	27
2.2.1 Background of Ru promoted reductions catalysis.....	27
2.2.2 TH of acetophenone promoted by acetate complexes.....	30
2.2.3 TH in presence of terdentate ligand Hamtp	34
2.2.4 Conclusions	37
2.3 Aldehyde Hydrogenation	38
2.3.1 Background of Ru promoted Hydrogenation	38
2.3.2 Hydrogenation of Benzaldehyde in presence of KOH.....	40
2.3.3 Hydrogenation of benzaldehyde in presence of KOH and ampy	43
2.3.4 Hydrogenation of Benzaldehyde in presence of acidic additives	45
2.3.5 Hydrogenation of benzaldehyde promoted by non-carbonyl compounds.....	50
2.3.6 KOH vs TFA in HY of benzaldehyde	52
2.3.7 Hydrogenation of α,β -unsaturated aldehydes.....	53
2.3.8 Hydrogenation of other substrates in neat conditions	61
2.3.9 Conclusions	62
2.4 Hydrogen Borrowing Reaction.....	64

2.4.1 Background of Ru promoted alkylation of amines	64
2.4.2 N-ethylation of N-methylcyclohexylamine with ethanol	66
2.4.3 N-alkylation of amines with primary alcohols	68
2.4.4 N-alkylation of cyclohexylamine with diols	74
2.4.5 Study of the reaction mechanism	74
2.4.6 Conclusions	78
3.0 Experimental Part	80
3.1 General	80
3.2 Synthesis of novel acetate complexes	80
3.3 Transfer Hydrogenation	126
3.4 Hydrogenation of aldehydes	127
3.5 N-alkylation	131
4.0 Conclusions and Future Perspectives	148
5.0 References	151

Summary

The aim of this thesis was the synthesis of novel catalytic systems based on acetate ruthenium complexes, bearing basic and relatively bulky diphosphines and their application in the reduction of carbonyl substrates to their corresponding alcohols, with molecular hydrogen and *via* transfer hydrogenation reaction using 2-propanol as hydrogen source. Moreover, the employment of these systems as catalysts in the alkylation of aliphatic and aromatic amines with primary alcohols and diols *via* borrowing hydrogen was studied. In addition. The work performed on this subject can be split out into four parts as follows:

1. The first part has concerned the synthesis and the characterization of the complexes $\text{Ru}(\text{OAc})_2(\text{PP})$ [PP=1,1'-bis(diisopropylphosphino)ferrocene; 1,1'-bis(dicyclohexylphosphino)ferrocene), $\text{Ru}(\text{OAc})_2(\text{PP})(\text{NN})$ (NN= 2-(aminomethyl)pyridine; ethylenediamine) and the monocarbonyl derivatives $\text{Ru}(\text{OAc})_2(\text{CO})(\text{PP})$.
2. The second part has been focused on the study on the catalytic performances of $\text{Ru}(\text{OAc})_2(\text{PP})$ and *in situ* generated $\text{Ru}(\text{OAc})_2(\text{PP})(\text{NN})$ in the transfer hydrogenation of carbonyl compounds in basic 2-propanol
3. During the third part the unprecedented hydrogenation of benzaldehyde in neat conditions (solvent-less) catalyzed by $\text{Ru}(\text{OAc})_2(\text{CO})(\text{PP})$ with hydrogen at low and high pressure, has been studied, affording benzyl alcohol with high purity. The scope of this reaction has been extended to different aromatic and α,β -unsaturated aldehydes, with high chemoselectivity for the C=O vs. C=C bond, and to ketone and imine substrates, under basic and also acidic conditions at very high S/C (10^5). In particular, *trans*-cinnamaldehyde, citral have been reduced to the corresponding food relevant alcohols.
4. The final part has regarded the application of the new developed $\text{Ru}(\text{OAc})_2(\text{CO})(\text{PP})$ systems in the ethylation of *N*-ethylcyclohexylamine with ethanol *via* borrowing hydrogen at relatively mild conditions (30 - 100 °C). To broaden the scope of this transformation, primary aliphatic and aromatic amines and different alkylating agents, including diols allowing formation of substituted pyrrolidines and piperazines, have been employed. Intramolecular reaction of 2-hydroxyethylaniline has also been investigated to obtain indoles, which as the pyrrolidine and piperazine derivatives are biologically relevant pharma frameworks.

The wide reactivity and productivity exhibited by these new class of ruthenium catalysts make them very attractive for industrial applications.

Acknowledgments

I would like to take some time to thank all the people without whom this project would never have been possible. Firstly, to my supervisor; Prof. Walter Baratta by choosing and granting me this opportunity, you have created an invaluable experience for myself to develop as a researcher in the best possible way. I greatly appreciate the freedom you given to me to try “new solutions” (cit.), in addition to the guidance and support you offered when I was in need. Thank you for all the feedback and encouragement throughout my time with you. Infinite thanks to the company Johnson Matthey for funding this project. In particular to my co-supervisor Dr. Antonio Zanotti-Gerosa and Dr. Hans Nedden for investing your time in to me, always providing great support with interesting and valuable feedback. Moreover, I need to thank you again Antonio for your kindness, availability and the long discussions. This made me feel part of the great JM family from the day-one in Cambridge. I send a final big hug to all the members of the Unit28 for all the practical support and kind acceptance that was given to me. You all have helped me to commit myself entirely to the spirit and ideals of your outstanding company. I'm also very grateful to Prof. Ruffo for the long-distance support in both scientific and personal needs.

Coming back to my close collaborators I would like to thank Salvo in particular, as I have come to regard you as one of my supervisors. You have always been there for me for everything I needed, kept me in check and over the years you have become a friend as well. Your mix of great experience, new ideas and heart-warming support have given me great confidence in the lab and, at the same time, made me realise that it's only the beginning in this challenging profession. I truly hope that we will be given the opportunity to work together in the future, and I wish you all the best for your starting academic career, you will be a great professor for sure!!!. I also want to take a moment to thank all “The CUBE”: Christian, Denise, Gerard, Gina, Hasseeb, Iacopo, Maria, Mattia, Maurizio, Matteo, Rossella, Rabail, Ruben and all the technicians Domelio, Luciano, Martino (Paolo), Pier, people of outstanding importance for my daily life in Udine for infinite reasons in both scientific and not. Three years ago, I met you all as colleagues but now, close to the end of the journey of the PhD, I leave you as friends; without your effort, help and support I would have been nowhere. I would like to offer special thank to Stefano Turco, who, although no longer with us, continues to inspire

his family and his friends with his great love and his invaluable sage advices on life. All of you will be forever special for me! Thank You ALL!

Of course, I also thank my parents and my brother for helping me during this years and being there for any practical support in all those things of life beyond doing a PhD, my friends from "CHrella", Marco, Massimiliano, Niko, Phoulvio, Roberto always present even from many Km away, and finally, Liliana, you are my solid pillar and my soft cloud, you have been always at my side reassuring and accompanying me, from any distance, through this hard and long period away. You will be a foundation of any of my projects and dreams, my first and last intent of all my choices for the future. There are not enough words to explain what you represent for me, now and forever, Thanks!!!!

Abbreviations Table

4Cy-Josiphos	1-{2-[dicyclohexylphosphine]ferrocenyl}ethyldicyclohexylphosphine
Acac	acetylacetonate
Ampy	2-(aminomethyl)pyridine
Ar	Aryl
BINAP	2,2'-Bis(diphenylphosphino)-1,1'-binaphthyl
Bipy	2,2'-Bipyridine
CAL	Cinnamaldehyde; (2 <i>E</i>)-3-Phenylprop-2-enal
COD	(1 <i>Z</i> ,5 <i>Z</i>)-cycloocta-1,5-diene
COL	Cinnamyl alcohol; (2 <i>E</i>)-3-phenylprop-2-en-1-ol
Cy	Cyclohexyl
CyNEt ₂	<i>N,N</i> -diethylcyclohexylamine
CyNEtMe	<i>N</i> -ethyl- <i>N</i> -methylcyclohexylamine
CyNHET	<i>N</i> -ethylcyclohexylamine
CyNHMe	<i>N</i> -methylcyclohexylamine
CyNMe(CH ₂ Ph)	<i>N</i> -benzyl- <i>N</i> -methylcyclohexylamine
DBU	1,8-Diazabicyclo[5.4.0]undec-7-ene
DcyPF	1,1'-bis(dicyclohexylphosphino)ferrocene
DCyPP	1,3-bis(cyclohexylphosphino)propane
DiPPF	1,1'-bis(diisopropylphosphino)ferrocene
DME	1,2-dimethylethanol
DMF	<i>N,N</i> -dimethylformamide
Dppb	1,4-bis(diphenylphosphino)butane
dppe	1,2-bis(diphenylphosphino)ethane
dppf	1,1'-bis(diphenylphosphino)ferrocene
dppm	1,1-bis(diphenylphosphino)methane
dppp	1,3-bis(diphenylphosphino)propane
en	ethylenediamine
Et	Ethyl
EtOH	Ethanol
FAL	Furfural
FOL	Furfuryl alcohol

GC	Gas Chromatography
GDP	Gross domestic product
Gly	Glycine; aminoethanoic acid
Hamtp	6-(4-methylphenyl)-2-(aminomethyl)pyridine
HCAL	Hydrocinnamaldehyde; 3-Phenylpropionaldehyde
HCOL	hydrocinnamyl alcohol; 3-Phenyl-1-propanol
HY	Hydrogenation
IPA or <i>i</i> PrOH	2-propanol
<i>i</i> Pr	Isopropyl
Me	Methyl
MeOH	Methanol
MTBE	methyl, <i>tert</i> -butyl ether
<i>n</i> BuOH	1-butanol
NMR	Nuclear Magnetic Resonance
NN	diamine
OAc	acetate
Ph	Phenyl
PP	diphosphine
<i>t</i> Bu	<i>tert</i> -butyl
<i>t</i> -BuOH	<i>tert</i> -butanol
<i>t</i> -BuONa	sodium <i>tert</i> -butoxide
TFA	Trifluoroacetic acid
TH	Transfer Hydrogenation
TOF	Turnover frequency
TON	Turnover number
Triphos	1,1,1-Tris(diphenylphosphinomethyl)ethane

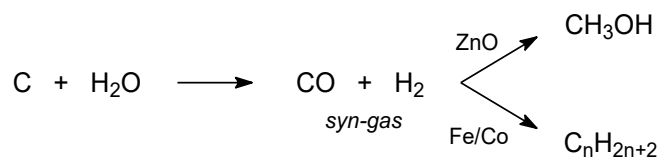
1.0 Introduction

1.1 Homogeneous transition metal-promoted catalysis: history and applications

Since a long time, a large number of processes have been accelerated by the addition of suitable substances that, as J.J. Berzelius stated ^[1], contribute to “produce decomposition in bodies, and form new compounds into the composition of which, they do not enter”. He called “catalytic force” the ability of these substances to accelerate the reaction rate without being affected at the end of the process. As a realistic example, the production of bread or beer stranding from wheat consists of procedures developed many centuries ago, but already at that time was well-known, although not well-understood, the key role played by yeast to obtain those products. In the early ‘800, S.K. Kirchoff reported the conversion of starch solution into sugars mixture promoted by mineral acid additives,^[2] the latter entirely recovered at the end of the reaction. J. W. Döbereiner (1816) studied the fermentation of starch into alcohols, assuming that sugars were plausible intermediates involved in the process. Fermentative processes were thus the first fundamental trials that highlighted the importance of certain compounds for the selective production of desired products. Afterwards, the experiments performed by L.J. Thenard ^[3] on ammonia decomposition into nitrogen and hydrogen promoted by metals and those made by J. W. Döbereiner (1823) on hydrogen combustion in open air with formation of water promoted by platinum, successively extended to palladium and iridium, had led to the foundation for all the research activity on transition metals in catalysis, boosting the development of novel and original heterogeneous systems between the 19th and 20th centuries. The studies of F. Haber and C. Bosch in the early 20th century led to the synthesis of ammonia directly from nitrogen and hydrogen, catalysed by iron oxides at high pressure and temperature. This research carried out in the laboratories of BASF led to the creation of a big industrial process for the synthesis of ammonia, opening the access for the production of fertilizers, explosives and a wide range of nitrogen containing products.

In the same period, BASF also developed the synthesis of methanol from syngas, a mixture of CO and H₂ obtained directly from carbon and water, using a ZnO catalyst (Scheme 1). Starting from syngas through an iron/cobalt-based catalyst, a broad range of organic products were prepared, e.g. alcohols, aldehydes, ketones, fatty acids, ethers and hydrocarbons, which were used as feedstocks for the chemical industry and as fuels for internal combustion engines (1925, Fischer-Tropsch synthesis). Therefore, it became common practice to perform the catalytic reaction by employing the metal compound in a different phase with respect to the reagents involved. Meanwhile, the development of the synthesis of transition metal complexes bearing organic ligands, such as phosphines and alk(en)yl fragments, was growing more and more flourishing. Only after a century since Döbereiner's pioneering experiments, the discovery and the setup of iron or cobalt complexes that could solubilize in the same media of the reactants, were applied by O. Roelen (1938; RUHRCHEMIE) for hydroformylation of alkenes to obtain saturated aldehydes ("oxo" process) and by W. Reppe (1953; BASF) for high pressure transformations of acetylene gas. In particular, Reppe's chemistry unlocked the access to suitable monomers for polymerization, leading to the production of materials still in use in our daily life, e.g. PVC, PMMA. Since during the 1950s the interest in metal catalysts was focused on the chemistry of polymers and plastics, it is worth mentioning G. Natta's group work on the development of a methodology for obtaining isotactic polypropylene catalysed by titanium salts. Homogeneous catalysis for reductive processes underwent the most significant advance during the 1960s, thanks to Wilkinson,^[4] who developed the well-defined rhodium complexes RhCl(PPh₃)₃ and RhH(CO)(PPh₃)₃ for efficient olefin hydrogenation and hydroformylation, respectively. From that point on, the rise of homogeneous catalysis started, opening the way for the wide and vibrant research of the last century on the application of transition metal complexes in a broad range of chemical transformations. On Wilkinson's findings, several processes were set up in the same decade for hydroformylation of olefins (Union Carbide Corporation). But it was only in the 1990s that the studies for the synthesis of fine chemicals, products with high added value which have applications also in food industry, took off, exploiting the research results of the bulk chemical area and the large academic effort that had been set up in the meantime. Some of these interesting molecules are vitamins (K₁, E), pharmaceutical ingredients (*l*-dopa, chloramphenicol, (*R*)-carnitine, taxol, (*S*-

propranolol, (S)-tetramisol, naproxen, ibuprofen, morphine), fragrances (nerol, citronellol, damascene, (-)-menthol) and herbicides (S-metolachlor) (Figure 1).



Scheme 1 Synthesis of methanol (a) and hydrocarbons (b) reacting syngas obtained from carbon and water.

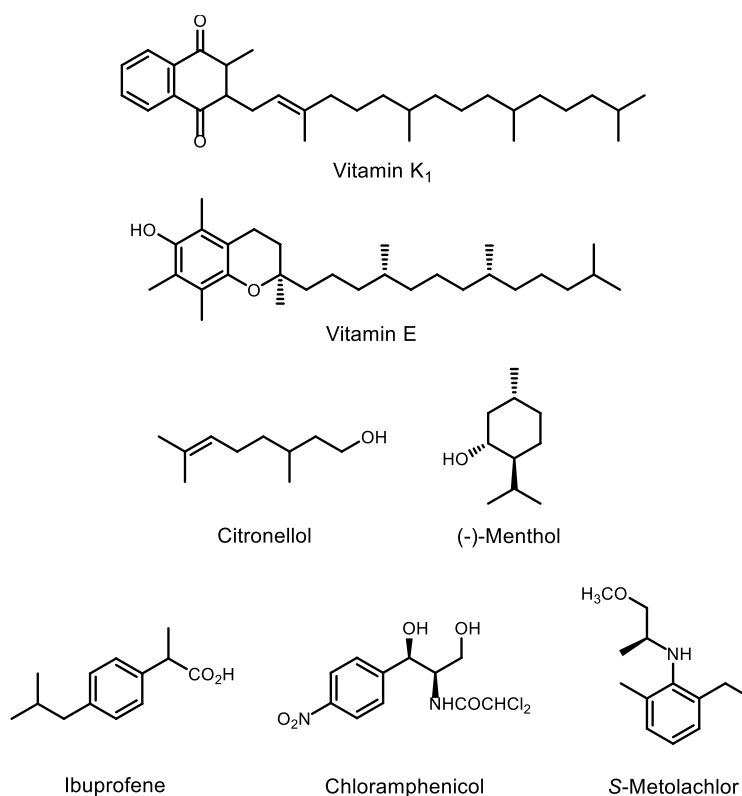


Figure 1 Some of the high added value products obtained via transition metal catalysed processes.

1.2 Purpose of a catalyst: theoretical aspects and practical considerations

As anticipated in the previous section, the term catalysis was coined by Berzelius over 150 years ago, when he had noticed that some substances undergo transformations when they were brought in contact with small amounts of certain species called "ferments". The definition used today reads as follows: *A catalyst is a substance which increases the rate at which a chemical reaction approaches equilibrium without becoming itself permanently involved.* The catalyst may be added to the reactants in a different form, the catalyst precursor, which has to be brought into an active form ("activated"). During the catalytic cycle the catalyst may be present in several intermediate forms when we look more closely at the molecular level. An active catalyst will pass a number of times through this cycle of states; in this sense the catalyst remains unaltered. Many chemical reactions, allowed by a thermodynamic point of view, are kinetically disadvantaged, thus increasing the speed of a reaction is crucial for obtaining the desired products. As a matter of fact, a temperature increase, which leads to an increase in the reaction rate is not always feasible (e.g. exothermic reactions). The general method to increase the speed of a reaction is to choose the pathway involving a lower activation energy by means of a catalyst.

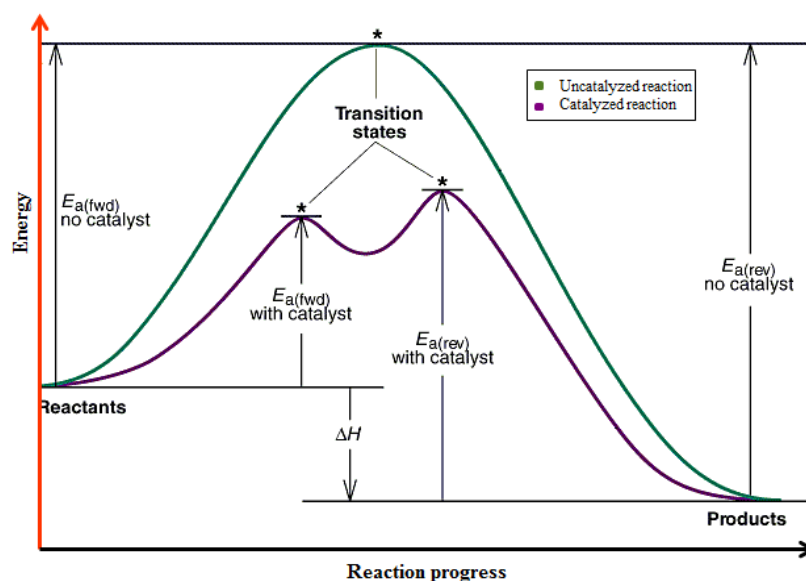


Figure 2 Different trends of the reaction with (purple) or without (green) a catalyst.

In the reaction the catalyst takes part in the formation of intermediate species that do not appear at the beginning and at the end of the reaction, lowering the activation energy (E_a) and resulting in increased speed and decreased reaction time (Figure 2). Two important parameters for studying a catalyst are its productivity and its activity. The first is defined as turnover number (TON), *i.e.* the number of moles of product produced with one mole of catalyst. This number determines the catalyst costs. If a catalyst can be re-used, its productivity is increased. The second factor, defined as turnover frequency (TOF), *i.e.* how many moles of product one mole of the catalyst produces per time unit, determines the production capacity of a given system. Substrates are present in larger amounts than the catalyst, when we report on catalytic reactions the ratio of substrate to catalyst is an important aspect. An inhibitor is a substance that retards a reaction, it is also present in catalytic or sub-stoichiometric amounts. In a metal catalysed reaction an inhibitor could be a substance that adsorbs onto the metal making it less active or blocking the site for substrate co-ordination. Organometallic catalysts consist of a central metal surrounded by organic (and inorganic) ligands. Both the metal and the large variety of ligands determine the properties of the catalyst. The set of ligands forming the coordination sphere of the complex and the number of ligands is called coordination number (CN) which usually ranges from 3 to 6. Parameters affecting the coordination number are the oxidation state of the metal centre, the electronic configuration of the central ion, the type of ligands (big and bulky ligands reduce the CN) and the interactions within the complex. Examples of transition metal complexes, their geometry and preferred reactions are reported in Table 1.

Table 1 Preferred geometry and reactivity of transition metals

Metal, oxidation state	Example	Geometry	Preferred reactions
Ni ⁰	Ni(CO) ₄	Tetrahedral	Ligand dissociation
Pd ⁰	Pd(PR ₃) ₂	Linear	Oxidative addition
Rh ^I , Ir ^I , Ru ^{II}	[Rh(PR ₃) ₂ (μ-Cl)] ₂	Square planar	Oxidative addition
Ru ^{II}	RuX ₂ (PR ₃) ₃	Trigonal pyramid	Ligand dissociation, oxidative addition
Ru ^{II} , Rh ^{III} , Ir ^{III}	Rh(PR ₃) ₃ XH ₂	Octahedral	Reductive elimination

The ligands can form one or more links with the central atom and, in the latter case are called chelating agents. Depending on the number of the atoms bonded with the

central atom (denticity), a ligand could be monodentate, bidentate, tridentate, or, in general, polydentate (Figure 3). Ligands of the same denticity but with different stereo-electronic properties can dramatically affect the catalytic activity of the complex employed in the process, resulting in enhancing or lowering it, depending on the modifications that have been carried out.

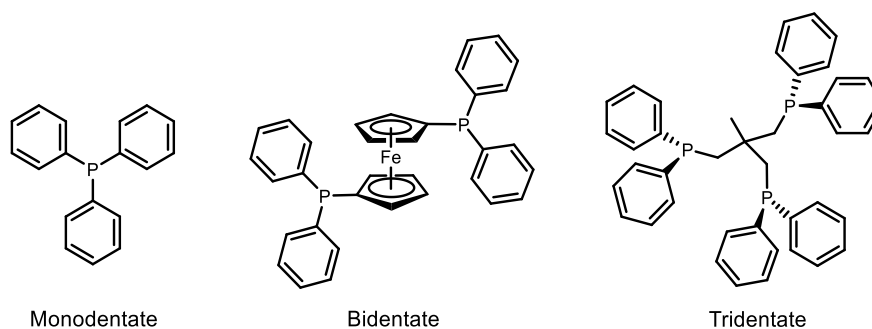


Figure 3 Example of phosphine ligands with different denticity.

The pursuit of highly efficient transition metal catalysts for the synthesis of valuable organic compounds is a matter of paramount importance for both academia and industry. Among the different transition metals, ruthenium is greatly considered because of its high performance in several organic reactions.^[5] In the last decades great efforts have been devoted within academia to the improvement of catalyst selectivity for achieving clean organic transformations. On the other hand, on account of the more and more stringent health and safety regulations for the metal content in food relevant synthetic substances,^[6] the desirable conditions are generally offset by relatively low turnover numbers with depletion of efficiency. Productivity and selectivity of the catalysts are the decisive factors in the development of sustainable chemical processes, especially in regard of large-scale industrial applications. Therefore, the attention of industrial research has been focused on the atom economy and high performance of the catalysts, which must possess very low (or absent) toxicity and should be employed at low loadings. In order to be competitive, the transition metal catalysts should also display moderate sensitivity toward air, moisture and substrate impurities. Therefore, robustness and (de)activation of the ruthenium species are important parameters that have to be carefully taken into account for the design of a practical catalyst.^[7]

Among hydrogenative processes, reduction of carbonyl compounds to alcohols is one of the main chemical transformation on industrial scale and continues to attract wide interest because of its fundamental importance for the synthesis of biologically active molecules as well as the transformations of both biomass feedstocks and petroleum chemicals.^[8] In principle, these compounds can be selectively hydrogenated by using homogeneous complexes, but the heterogeneous catalysts are environmentally more friendly and easier to separate and re-use than their homogeneous counterparts. The rational design of an active and selective heterogeneous metal supported catalyst is not however a very easy task. There are several factors, which can affect the activity and selectivity of a catalyst, namely the proper choice of the metal and its precursor, the support selection, the catalyst preparation and activation methods, the choice of reaction conditions and operation mode (e.g. gas or liquid phase system). Conversely, with homogeneous catalysts is possible to tailor and optimize their structure, by adapting the stereo-electronic properties of the ligands around the metal centre, to the particular requirements needed. This opportunity offered by homogeneous catalysts may have drastic consequences on their activity and selectivity. Within this context, the catalytic homogeneous reduction of carbonyl compounds using molecular hydrogen or a hydrogen donor^[9], such as 2-propanol, formic acid or formate salts, represents a green and economic procedure to access valuable alcohols for the production of fine and bulk chemicals.^[8]

1.3 Phosphine based ruthenium complexes in reductive processes

In 1966 Wilkinson reported the synthesis of the ruthenium complex $\text{RuCl}_2(\text{PPh}_3)_3$,^[10] Even though this catalyst was not as active as its rhodium analogue $\text{RhCl}(\text{PPh}_3)_3$, later it was broadly applied in several catalysed organic transformations and, more importantly, $\text{RuCl}_2(\text{PPh}_3)_3$ has also been used as suitable precursor for the synthesis of ruthenium complexes which are highly active in homogeneous hydrogenation and transfer hydrogenation of unsaturated $\text{C}=\text{X}$ bonds ($\text{X} = \text{C}, \text{N}, \text{O}$), i.e. olefin, imine and carbonyl substrates, respectively.^[11] Over the last decades, a wide range of highly productive homogeneous catalysts based on noble metals have been developed for this purpose. R. Noyori (Nobel prize in 2001) showed that the combination of Ru-phosphine complexes with diamines exponentially enhanced the chemoselectivity of the catalyst toward carbonyl hydrogenation vs. olefin reduction, reporting in the early 2000's the synthesis of ruthenium(II) complexes $\text{RuCl}_2(\text{P})_2(\text{diamine})$ e $\text{RuCl}_2(\text{PP})(\text{diamine})$ ($\text{P} = \text{phosphane}$, $\text{PP} = \text{diphosphane}$), which are excellent catalysts for selective homogeneous hydrogenation (HY) of simple ketone substrates.^[12] Moreover, by a suitable combination of chiral diphosphines and diamines on the ruthenium centre is possible to perform asymmetric HY of carbonyl compounds for the production of chiral alcohols with high optical purity. Nowadays, *trans*- $\text{RuCl}_2(\text{BINAP})(1,2\text{-diamine})$ systems under H_2 pressure are employed in the industry for the asymmetric reduction of $\text{C}=\text{O}$ bonds.^[13] Alternatively, in order to avoid the risks implied with the use of H_2 , $(\eta^6\text{-arene})\text{RuCl}(\text{Tsdpen})$ complexes ($\text{Tsdpen} = \text{TsNCHPhCHPhNH}_2$, $\text{Ts} = \text{SO}_2\text{C}_6\text{H}_4\text{CH}_3$) have been developed,^[14] which are active catalysts for TH, using 2-propanol, formic acid and its derivatives as hydrogen sources.

In the last fifteen years, Udine research group guided by Prof. W. Baratta has developed a protocol for the synthesis and the use of Ru- and Os-based catalysts^[15] in the enantioselective TH of $\text{C}=\text{O}$ bond to CH-OH functionality of ketones and aldehydes. These catalysts contain bidentate phosphines and bidentate nitrogen ligands, such as 2-(aminomethyl)pyridine (ampy)^[16] or tridentate ligands such as 6-phenyl-2-(aminomethyl)pyridine (HCNN)^[17] and showed high values of TOF (turnover frequency, herein defined as moles of substrate converted to alcohol per hour at 50%

conversion), up to 10^6 h^{-1} and TON up to 10^5 . In order to improve the catalytic activity, the design of the HCNN ligand was modified to possess a more rigid structure, synthesizing 2-(aminomethyl)benzo[*h*]quinoline ligands (HCNN') and conferring to their corresponding Ru- and Os-complexes a higher robustness and thermal stability under harsh reaction conditions.^[18] In addition, these complexes are also able to catalyze the enantioselective HY of carbonyl compounds to alcohols^[19] and, very recently, of aldimines to amines,^[20] when the proper alcohol solvent is used.^[21] A further extension of HCNN' ligands has been recently achieved, combining the proper Ru-phosphane complex with 4-substituted-2-(aminomethyl)benzo[*h*]quinoline compounds (HCNN^R, R=Me, Ph), developing a new preparation of the HCNN^R ligands, employing less toxic intermediate precursors and allowing a longer shelf-life of the final ligand, isolated as a hydrochloride salt (HCNN^R·HCl).^[21d] It is worthy to point out that RuCl(CNN^R)(PP) complexes are very active catalysts in the TH and HY of commercial-grade ketones and aldehydes (carbonyl substrates, especially aldehydes, are often pre-treated or distilled before use, in order to improve the catalytic activity, by removing impurities that may be deleterious for the catalyst). The TH being promoted by different hydrogen sources, such as 2-propanol, formic acid/triethylamine mixtures, sodium formate and ammonium formate. In the present case S/C ratios up to 10^5 are reached, employing substrates and solvents not previously pre-treated or distilled, thus showing high tolerability toward substrate impurities.^[21a-c] The complexes of general formulae MCl₂(PP)(ampy), MCl(CNN)(PP), MCl(CNN')(PP) and RuCl(CNN^R)(PP) (M = Ru, Os, R=Me, Ph), all types isolated for the first time in Udine, are among the most active and productive catalysts reported in the literature so far, and the results achieved on this subject have produced several papers and patents, some of them were licensed to Johnson Matthey company and extended worldwide. RuCl₂(PP)(ampy) (PP= dppb, dppf) catalysts are marketed and used in industrial reactions for the preparation of organic intermediates. Moreover, MCl₂(PP)(ampy) (M=Ru, Os) have demonstrated to be active catalysts in C-H activation reactions, such as dehydrogenation, racemization, deuteration, isomerization and alkylation processes involving ketones and alcohols.^[22]

1.4 Aim of this thesis work

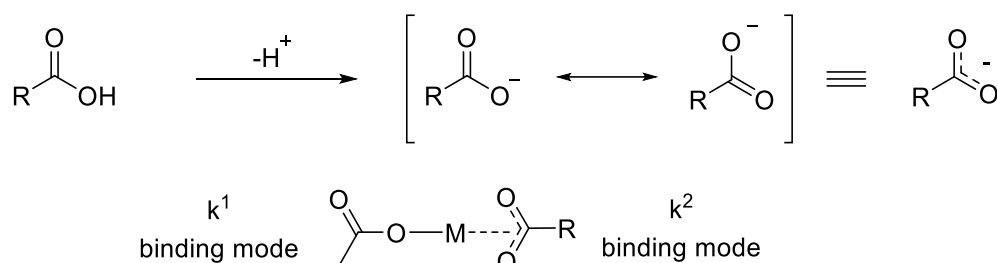
The group of organometallic chemistry of Udine, where this work was carried out, has recently shown that the acetate precursor $\text{Ru}(\text{OAc})_2(\text{PPh}_3)_2$, as well as its chloride congener $\text{RuCl}_2(\text{PPh}_3)_3$, can be a suitable starting material for the synthesis of a series of well-defined mononuclear complexes containing aryl diphosphines with the two P atoms connected through an alkyl chain as dppm, dppe, dppb or bridged by a ferrocenyl fragment as dppf, in combination with a chiral or achiral 2-aminomethylpyridine type ligands, or pincer CNN ligands bound to the metal center. Whilst the coordination chemistry and the effects in catalysis of P-aryl diphosphines have extensively been studied, the behaviour of more basic P-alkyl diphosphines has been poorly reported. As a matter of fact, only few examples of complexes bearing basic diphosphine ligands have been isolated, and studies have been mostly focused on their structural characterization, whereas little is reported on their catalytic applications. The work of this thesis has been focused on the synthesis, characterisation and applications of new bulky and basic diphosphine carboxylate ruthenium complexes, with or without diamine and carbon monoxide ligands. In addition to these studies of the reactivity of these complexes (i.e. protonation reactions and formation of hydride species), they were also investigated in catalytic organic reactions. As matter of fact, the acetate complexes efficiently catalyse the transfer hydrogenation and hydrogenation of carbonyl compounds and the alkylation of amines *via* borrowing hydrogen. The employment of these catalysts for the on g-scale hydrogenation of unsaturated aldehydes (*trans*-cinnamaldehyde, citral) and imines and the synthesis of nitrogen containing heterocycles holds promise for their applications for the synthesis of relevant frameworks in food and medicinal chemistry.

2.0 Results and Discussion

2.1 Synthesis of novel acetate Ru complexes

2.1.1 Background of Ru carboxylate catalysts

The first studies on the chelating effect of the carboxylate ligands were reported by Rai and Mehrotra in the '50s. They showed that the reaction of $\text{Al}(\text{OBut})_3$ with carboxylic acids yields to the carboxylate monomeric product $\text{Al}(\text{OBut})(\text{OOCR})_2$ or $\text{Al}(\text{OBut})(\text{OOCR})_3$, according to the moles of acids added. They demonstrated that reactions of metal alkoxides with carboxylic acids are facilitated thermodynamically since the carboxylate moiety after the deprotonation is able to bind the metal in a monodentate (k^1) or bidentate (k^2) mode.^[23] (Scheme 2) In view of Mehrotra's methodology, the reactions of alkoxides of a number of other metals and metalloids, Ti, Zr, Si, Ge, Ga, Ln, Fe, V, Nb, Ta, and Sb have been studied extensively in the following years and several acetate complexes have been described.^[24]

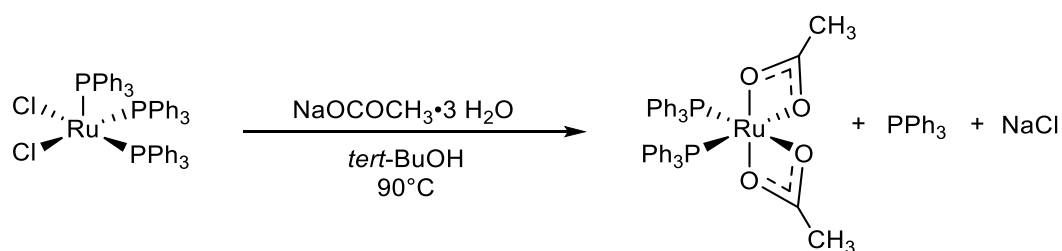


Scheme 2 Denticity of carboxylate ligands

As regards ruthenium, later in the '70s a big contribution was made by G. Wilkinson, S. D. Robinson, A. Dobson with their studies on the Ru carboxylate fragment in presence of other ligands such as triphenylphosphines (PPh_3), hydride (H), carbonyl (CO), acetylacetonate (acac), affording active complexes for the C-H activation, namely the hydrogenation and transfer hydrogenation of carbonyl compounds or the inverse dehydrogenation of alcohols.^[25] In the following decades great attention has been focused on the optimization of this class of compounds thanks to the unique success deriving from Noyori's studies during '80s and '90s on the hydrogenation of $\text{C}=\text{C}$ ^[26] and $\text{C}=\text{O}$ ^[27] double bond promoted by ruthenium acetate with chiral

diphosphines (R)- or (S)-binap, $[\text{Ru}(\text{BINAP})(\text{OCOCH}_3)_2]$. These carboxylates complexes in the presence of strong acids, such as HCl or HBr, undergo ligand substitution reactions affording the di-chloride or di-bromide derivatives that paved the way for the high productive asymmetric homogenous hydrogenation, promoted by the well known $[\text{RuH}_2\text{PPNN}]$ type complexes, *via* bifunctional catalysis. From then a large number of catalysts containing diamine ligands were developed, whereas the acetate derivatives were mainly investigated in the frame of their coordination chemistry and only marginally for catalytic applications.^[28]

Interestingly, the carboxylate complex $\text{Ru}(\text{OAc})_2(\text{PPh}_3)_2$ (**1**) was firstly reported by G. Wilkinson et al. in 1974 (Scheme 3),^[29] but its reactivity was barely explored for more than twenty years. It is worth noting that the structure of this compound was fully solved experimentally only 35 year after the first report, thanks to the study of Lynam et al.^[30] The two acetate ligands in this compound undergo a rapid exchange on the NMR time scale, showing for ^{31}P NMR a tight singlet at 64 ppm, and 2 equivalent CH_3 of the acetates as singlet at ^1H NMR. However, this exchange was detected by IR spectroscopy and the *cis* coordination of the triphenylphosphines was confirmed also in solution from the difference of resonance of the characteristic binding mode ($\Delta\nu$). The acetate ligand thus easily provides the generation of a vacant sites in the coordination sphere thanks to its lability and without the need to eliminate ligands. Moreover the orange color of **1** is in agreement with a coordinatively unsaturated Ru(II) complex, suggesting that, even **1** is octahedral, it is prone to undergo addition reactions^[31]



Scheme 3 Condition proposed by Wilkinson for the synthesis of $\text{Ru}(\text{OAc})_2(\text{PPh}_3)_2$

Carboxylate species similar to **1** were lately prepared also by reaction of suitable carboxylic acids or silver salts with dinuclear ruthenium species^[32] When encumbered aryl or alkyl-phosphines are coordinated in this way a *trans* configuration was usually obtained in monomeric complexes.^[33] To better profit the *trans* effect granted by the

phosphine ligands as enhance of the well know lability of the acetate ligands^[34], or increase the hydricity of metal hydride generated in trans during reduction processes, a simple switch to diphosphine ligands may open to a class of more reactive compounds. The chelate effect exerted by diphosphines allow to retain the desired cis configuration of phosphorus, thus the use of compounds as dppe could lead to the formation of $\text{Ru}(\text{k}^2\text{-OAc})_2(\text{dppe})$ by reaction with complex **1**. Wong et al. have already shown that the products obtained strongly depend on the bite angle of the chelating phosphine.^[28b] The diphosphines dppm, dppe and dppp, displaying a small bite angle, favoured the displacement of only one PPh_3 ligand forming complexes of type $\text{Ru}(\text{OAc})_2(\text{PP})(\text{PPh}_3)$. However, when the ligand dppb is used $\text{Ru}(\text{OAc})_2(\text{dppb})$ is formed, as for the dppf analogue $\text{Ru}(\text{OAc})_2(\text{dppf})$ that was also synthesised *via* this route by Lu et al.^[35] The exchange reaction of two phosphine with diphosphines on the precursors $\text{RuCl}_2(\text{PPh}_3)_3$ ended up in fluxional monomeric three phosphorus complexes or derivatives of the type *trans*- $\text{RuCl}_2(\text{PP})_2$.^[36] In presence of more basic alkyl-diphosphines, on the other hand, dimeric species $[\text{RuCl}_2(\text{PP})]_2$ are formed with bridged chlorine atoms. By using strongly coordinating solvent, such as the dimethylformamide (DMF) or nitriles, the formation of monomeric species $\text{RuCl}_2(\text{PP})(\text{solvent})_n$ are obtained.^[37]

Thus, no well-defined monomeric complexes of the type $\text{RuCl}_2(\text{PP})(\text{P})$ bearing basic diphosphines are reported in literature starting from $\text{RuCl}_2(\text{PPh}_3)_3$. Conversely, a series of derivatives with bulky and basic phosphines have been prepared starting from the precursors $\text{Ru}_2\text{Cl}_4(\eta^5\text{-p-cymene})_2$, $\text{RuCl}_2(\text{COD})_2$ and $\text{Ru}(\text{Me-allyl})_2(\text{COD})_2$.

Since the carboxylate ligands RCOO^- show different coordinating properties that strongly depend on the R substituent (i.e, Me, *t*Bu, CF_3), the resulting complexes have significantly different reactivity and catalytic behaviour with the same set of additional ligands. For instance, it is possible to switch from a carboxylate ligand to the corresponding fluorine derivative which displays a weaker coordination ability, and resulting in active dehydrogenation catalysts, as reported by Robison^[38] and Spek.^[28d]

2.1.2 Synthesis of carboxylate complexes $\text{Ru}(\text{OAc})_2(\text{PP})$

The complex $\text{Ru}(\text{OAc})_2(\text{PPh}_3)_2$ (**1**) was prepared from $\text{RuCl}_2(\text{PPh}_3)_3$ and sodium acetate in *tert*-butanol, following a slightly modified synthesis with respect to that

reported by Wilkinson, leading to an improved yield of (91%) at the laboratory scale of 10g per batch. In order to favour a complete precipitation of the insoluble carboxylate product the concentration of reagents was increased (spectrum 5, Figure 4). However, *tert*-butanol, which is a solvent with relatively high melting point, tends to be solid at room temperature, resulting not practical for industrial scale applications. To retain the liquid state it must be constantly warmed above 26°C, this problem can be usually solved by preparing *tert*-butanol/water solutions, but it didn't fitted the purpose of this complex synthesis since great amount of water in the system afforded a low yield of the desired product. Thus, several solvents and conditions were tested in the search of the more suitable solvent for a possible scale-up process. Among toluene, methanol, ethanol, 1,2-dimethyl ethanol (DME), the more volatile methyl-*tert*-butyl ether (MTBE) (bp. 55°C) was found to be a good alternative (Spectrum 4, Figure 4). It worked as non-solvent for the Ru(OAc)₂(PPh₃)₂ (**1**) and resulted easy to be removed under vacuum. However, to carry out the reaction at 90 °C (35 °C above its boiling point) an efficient condensation system was required. By carrying out the reaction at room temperature a lower yield was obtained with formation of a different product in which 3 phosphorus are coordinated to the metal centre, two in the square plane and one in axial position (AX₂ system), as established by ³¹P NMR (spectrum 3, Figure 4). Increasing the temperature to 40 °C allowed the reaction to proceed to the desired product but longer time were needed, while at 60 °C good productivity and purity were obtained in shorter reaction times (spectrum 1, Figure 4).

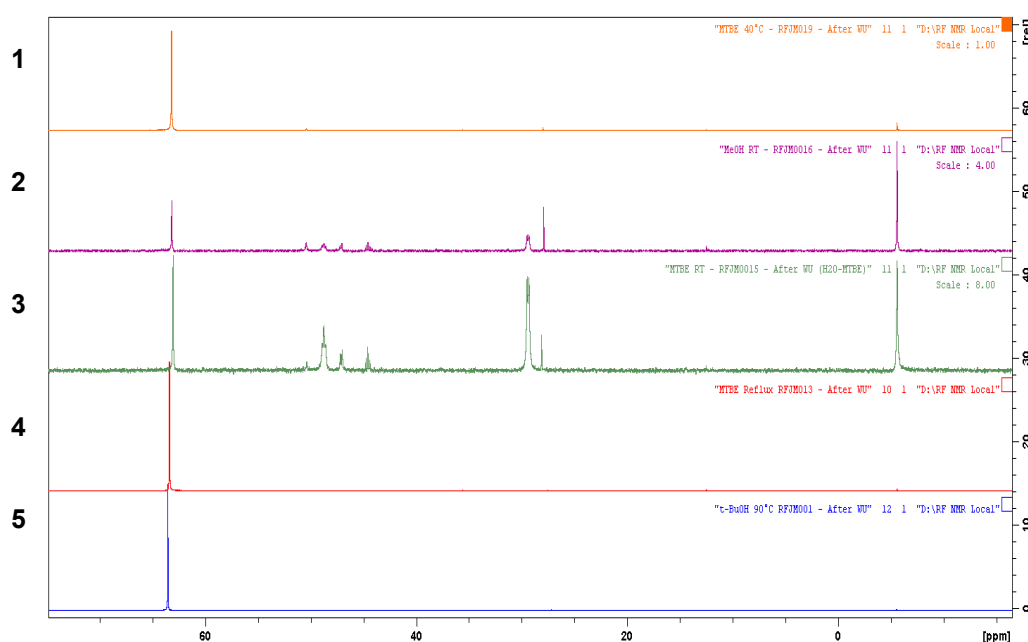
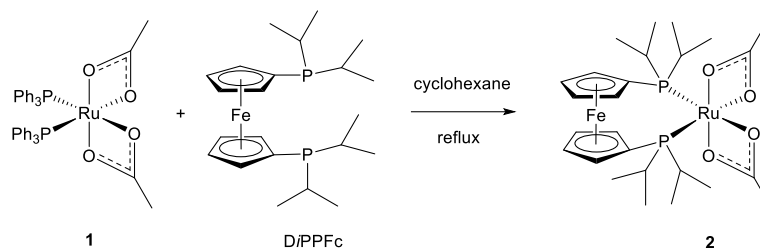


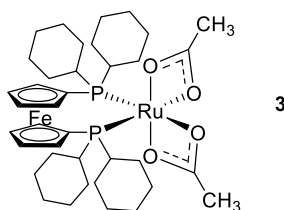
Figure 4 ³¹P{¹H} NMR spectra comparison 1-5 for the synthesis of complex **1** in different conditions.

The bisacetatotris(triphenylphosphine)ruthenium(II) precursor has proven to be a versatile precursor for the synthesis of diphosphine complexes by a simple exchange reaction. Thus reaction of **1** with the bulky alkyl diphosphine 1,1'-bis(diisopropylphosphino)ferrocene (DiPPF) afforded $\text{Ru}(\text{OAc})_2(\text{DiPPF})$ (**2**) in high yield (Scheme 4).



Scheme 4 Exemplar of exchange reaction with DiPPF diphosphine

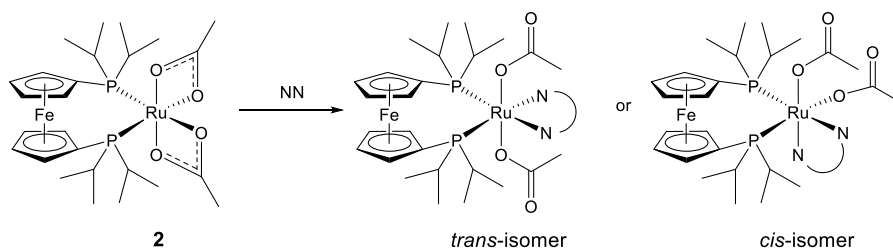
Similarly, by using 1,1'-bis(dicyclohexylphosphino)-ferrocene (DCyPF) the corresponding $\text{Ru}(\text{OAc})_2(\text{DCyPF})$ (**3**) was readily prepared.



For each diphosphines different solvents were tested cyclohexane being the solvent of choice for obtaining **2**. As a matter of fact, this media acted as non solvent for the precursor and the product, allowing the precipitation of **2** upon formation, driving the reaction to a clean product. To form complex **3** toluene resulted more suitable due to the presence of the bulkier cyclohexyl substituent on the phosphorus of DCyPF ligand, granting solubility in many solvents and requesting slightly higher reaction temperature for its synthesis. Compounds **2** and **3** showed ^{31}P NMR as sharp singlets hardly down shifted at 67.6 and 64.1 ppm, respectively (Figure 42, pag.83 and Figure 44, pag.84). Complex **2** displays a simple spectrum in ^1H NMR (Figure 40, pag.82), while **3** showed very broad signals due to cyclohexyl moieties (Figure 43, pag.84).

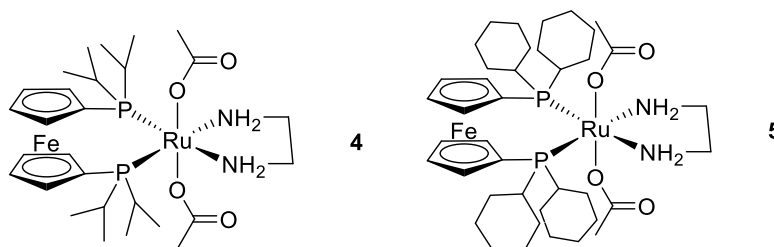
2.1.3 Reactivity of $\text{Ru}(\text{OAc})_2(\text{PP})$ species

The ability of carboxylate complexes to readily react with amines and diamines to form stable complex is well known (Scheme 5).



Scheme 5 Exemplar reaction of complex **2** with a generic diamine to form a *cis* or *trans* isomer.

Addition of the diamine en to compounds **2** and **3** promptly afforded two new derivatives *trans*-Ru(OAc)₂(DiPPF)(en) (**4**) and *trans*-Ru(OAc)₂(DCyPF)(en) (**5**), as thermally stable complexes, as expected from the strong coordinating property of the en ligand.



These two derivatives showed ³¹P NMR singlets at 44.9 and 38.2 ppm, respectively. The shelf life of these compounds in the solid state is very long in air at RT (several months), indicating that upon coordination these basic alkyl diphosphines become relatively unreactive towards oxygen. Conversely, upon reaction of **2** with the ampy ligand, which displays a coordination ability similar to en, a mixture of products is obtained. By addition of one equivalent of ampy to **2**, formation of the *cis* and *trans* isomers of Ru(OAc)₂(ampy)(DiPPF) in 4/1 ratio, respectively, is observed. In addition, these species equilibrate with **2** at room temperature, as inferred from ³¹P NMR measurements. This behaviour is not shown by complexes containing aryl diphosphines and is due to the strong *trans* effect exerted by the more basic alkyl PP ligand. The characterization of the *trans* isomer **6a**, showed in chapter 3, was carried out by low temperature NMR measurements upon addition of ampy at -60 °C (213 K), leading to two doublets at δ 45.3 and 43.5 ppm (Figure 53, pag.92), this species is stable at very low temperature, while warming up to 0 °C the coalescence of the two doublets into a singlet was induced (Figure 5). The ¹H NMR also showed diastereotopic protons of the NH₂ at δ 8.80 and 4.86 ppm at -60 °C (Figure 51, pag.91), while upon heating at 0°C they appeared as a broad singlet at δ 3.5 ppm (Figure 6). This suggests that at low temperature the acetate ligands interact with a H-N, stabilizing the *trans*

geometry. When the system was let to reach the room temperature the cis isomers started to form, giving only trace of cis product in 5 min, while full equilibration of the mixture between cis and trans isomers was reached in 1 h. Moreover, during this equilibration process a broad signal of the acetate precursor ($\delta \sim 67$ ppm) raised, indicating that the interconversion take place through the ampy de-coordination (Figure 7). A similar behaviour was observed with complex **3** in presence of ampy at RT. The kinetic ampy derivative *trans*-Ru(OAc)₂(DCyPF)(ampy) (**7**) was readily formed at room temperature, affording two doublets at δ 39.3 and 37.0 ppm with a $^2J(P,P) = 28.8$ Hz in the ³¹P NMR spectrum (Figures 57, 58, pag.97). However, within 24 h this complex slowly converts to a mixture of cis and trans isomers in equilibrium with the precursor **2**, displaying a broad singlet at δ 64.2 ppm (Figure 8).

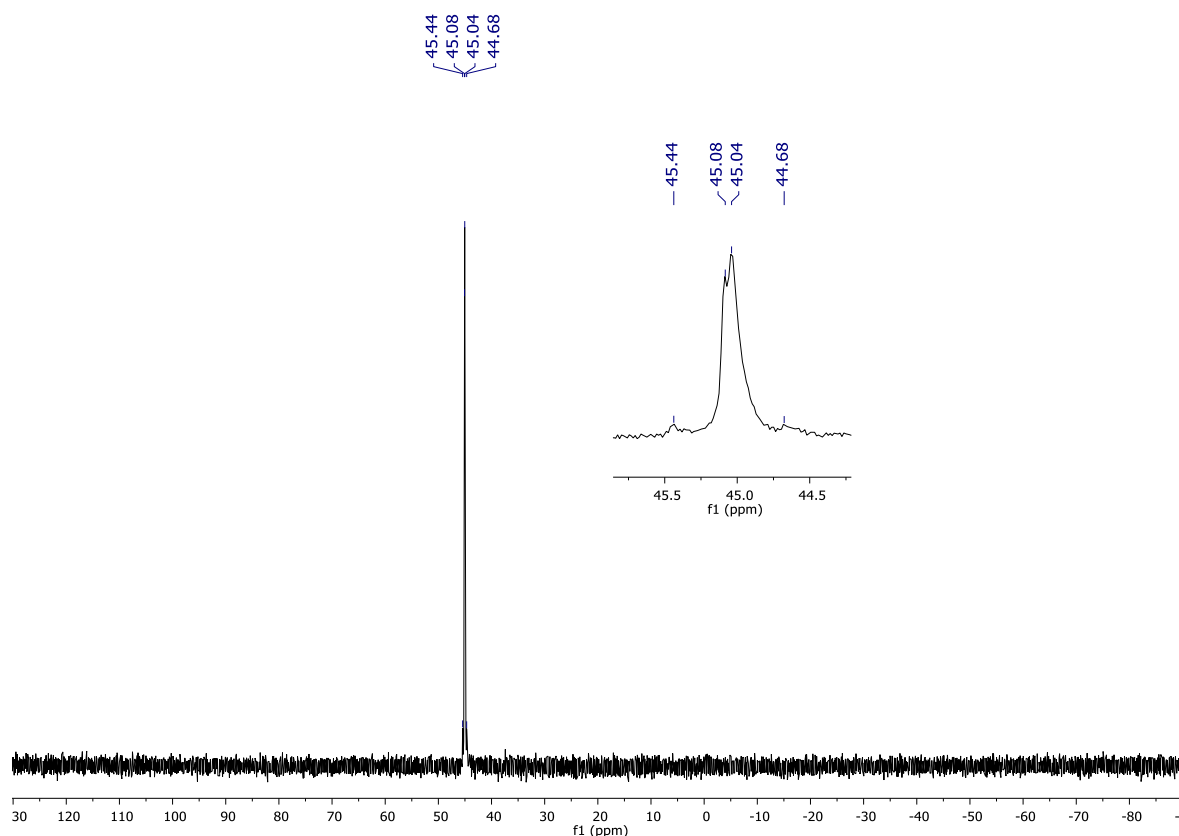


Figure 5 ³¹P{¹H} NMR spectrum of *trans*-Ru(OAc)₂(DiPPF)(ampy) (**6a**) in CD₂Cl₂ at 0°C

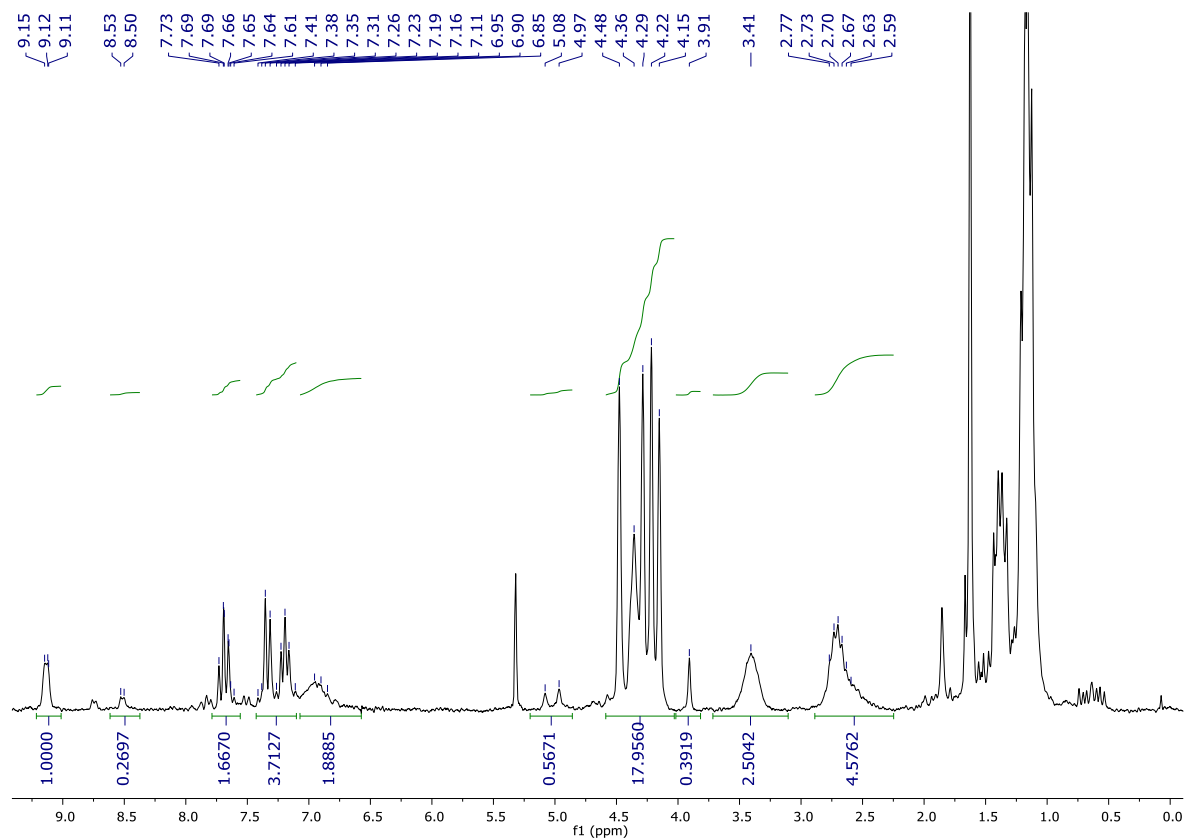


Figure 6 ^1H NMR spectrum of *trans*- $\text{Ru}(\text{OAc})_2(\text{DiPPF})(\text{ampy})$ (**6a**) in CD_2Cl_2 at 0°C

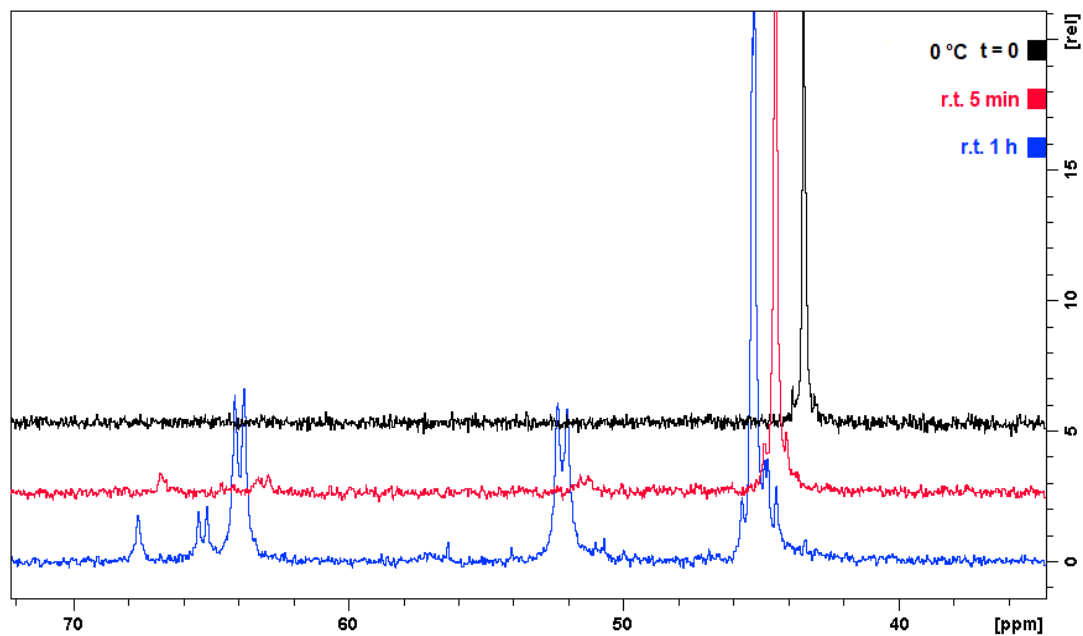


Figure 7 $^{31}\text{P}\{^1\text{H}\}$ NMR spectra of *trans*- $\text{Ru}(\text{OAc})_2(\text{DiPPF})(\text{ampy})$ (**6a**) in CD_2Cl_2 at 0°C , with the same tube after 5 min and 1 h at room temperature.

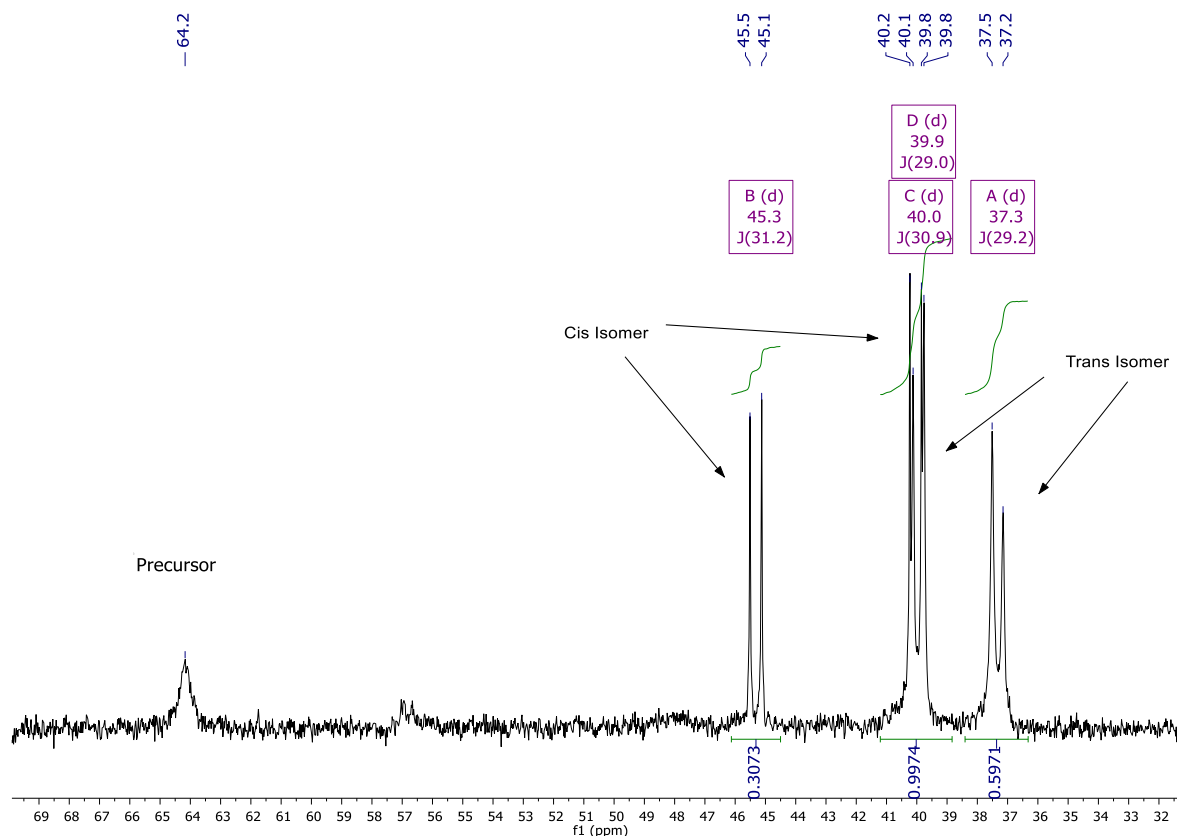
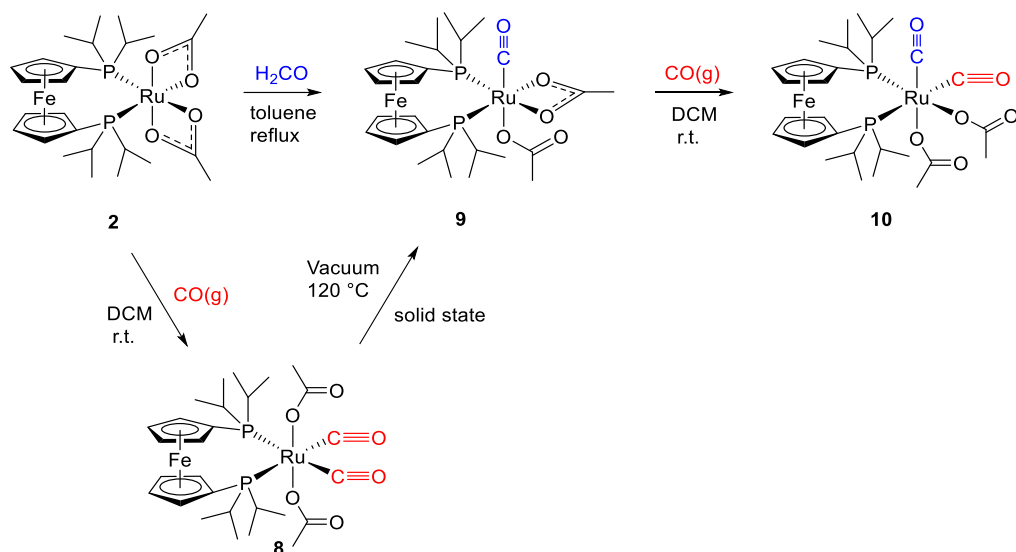


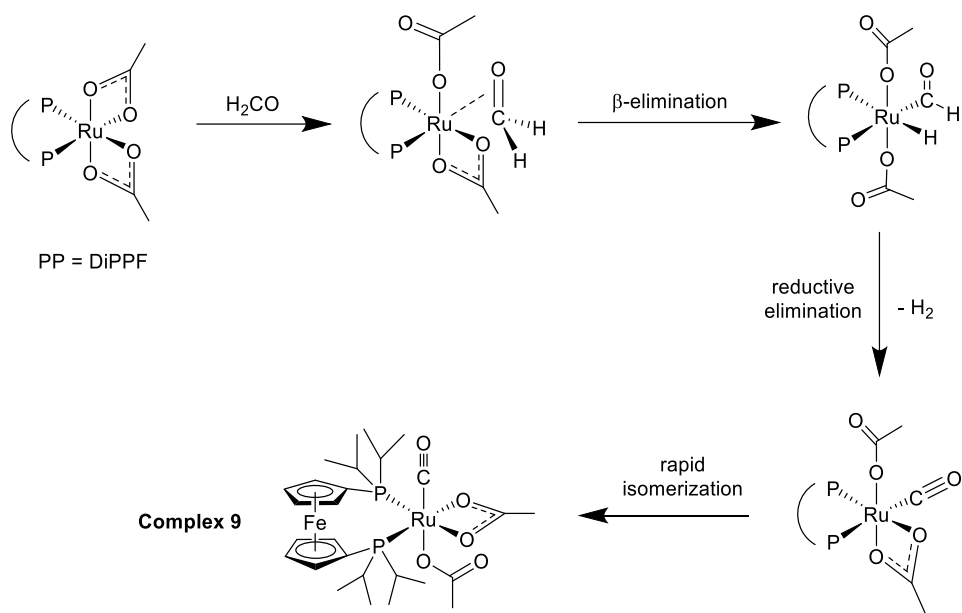
Figure 8 $^{31}\text{P}\{^1\text{H}\}$ NMR spectra of *trans*- $\text{Ru}(\text{OAc})_2(\text{DCyPPF})(\text{ampy})$ (**7**) in CD_2Cl_2 at after 24 h at RT.

2.1.4 Carbonyl compounds deriving from $\text{Ru}(\text{OAc})_2(\text{DiPPF})$

In the view of extending the reactivity of the $\text{Ru}(\text{OAc})_2(\text{DiPPF})$ (**2**) fragment we have investigated the preparation of the corresponding carbonyl derivatives. Treatment of **2** with $\text{CO}(\text{g})$ at 1 atm in DCM led to the formation of *trans,cis*- $\text{Ru}(\text{OAc})_2(\text{CO})_2(\text{DiPPF})$ (**8**) in high yield (Scheme 6). The complex gave in the ^{31}P NMR one sharp singlet at δ 26.5 ppm (Figure 61, pag.100) and showed in the $^{13}\text{C}\{^1\text{H}\}$ NMR a dd at δ 195.8 ppm with $^2J(\text{C},\text{P}) = 105.2$ Hz and 20.9 Hz, indicating that the two carbonyl ligands were coordinated *trans* to the phosphorus atoms, confirming the formation of the kinetic product (Figure 60, pag.99). By heating the isolated product in solid state at 120 °C under high vacuum overnight, one of the carbonyl was released, affording selectively $\text{Ru}(\text{OAc})_2(\text{CO})(\text{DiPPF})$ (**9**). Attempts to obtain mono carbonylation with $\text{CO}(\text{g})$ by using different solvents or reaction temperatures failed, due to the high lability of the acetate ligands *trans* to phosphorus atoms. A selective method to produce compound **9** involves the use of aqueous formaldehyde or paraformaldehyde *via* a decarbonylation reaction (Scheme 7).



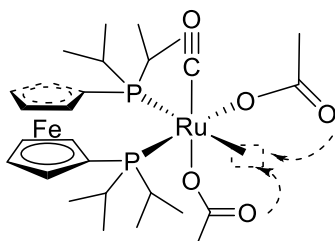
Scheme 6 Reactivity of acetate complex with CO(g) or formaldehyde to produce **9** or **10** starting from **2** or **9**.



Scheme 7 Mechanism for the decarbonylation reaction of formaldehyde.

Complex **2** in fact reacted cleanly with formaldehyde (aq.) (5 equiv.) in toluene at reflux within 2 h, affording the monocarbonyl acetate complex **9** in 78% yield. Alternatively, complex **9** was also prepared by reaction of **2** with paraformaldehyde in toluene with a slower conversion rate. At RT the $^{31}\text{P}\{^1\text{H}\}$ NMR spectrum of **9** in CD_2Cl_2 shows a very broad singlet at $\delta = 61.7$ ppm ($\Delta\nu_{1/2} = 110$ Hz), while the ^1H NMR spectrum exhibited four C-H signals for the ferrocene C_5H_4 moiety and a singlet at $\delta = 1.92$ ppm for the two acetate ligands, furthermore, the signals of all the quaternary carbons were

not detectable in the $^{13}\text{C}\{^1\text{H}\}$ NMR spectrum regardless of the deuterated solvent, concentration, duration and relaxation time (4 – 10 s) selected for the analysis, even on different NMR instruments. This indicates a rapid exchange of the OAc groups on the NMR time scale at RT (Figures 62, 63, 64, pag.102) Scheme 8.



Scheme 8 Fluxionality of the acetate ligands on the position in trans to one phosphorus.

Upon cooling at -75°C both the ^{31}P and ^1H NMR spectra become more complex, in particular the phosphorus NMR exhibits two major signals, namely two doublets and one singlet. Moreover the ^{13}C showed two different carbonyl signals, a doublet of doublets at δ 206.0 ppm with $^2J(\text{C},\text{P}) = 21.8$ and 15.9 Hz, and a triplet at δ 204.4 ppm with $^2J(\text{C},\text{P}) = 17.9$ Hz (Figures 65, 66, 67, pag.103). This is possibly due to the formation of conformers due to the steric hindrance exerted by the bulky isopropyl ferrocene ligand. The CO stretching of **9** was at relatively low wavelength (1939 cm^{-1}), in agreement with the presence of the electron-rich diphosphines. Addition of different amounts of benzylamine showed the coordination of only one amine ligand, indicating compound **9** is a monomer.

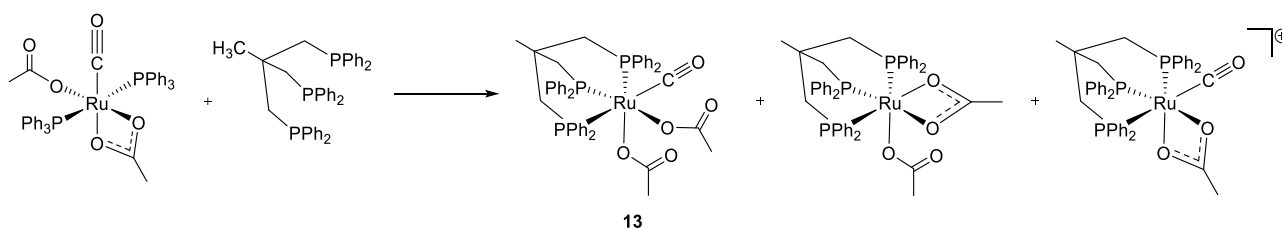
Under 1 atm of $\text{CO}(\text{g})$ in DCM, complex **9** converted to the derivative *cis,cis*- $\text{Ru}(\text{OAc})_2(\text{CO})_2(\text{DiPPF})$ (**10**) in 24 h (Scheme 6). This complex shows two sharp doublets in the ^{31}P NMR spectrum at δ 50.8 and 39.2 ppm, with a doublet of doublets and a triplet in the ^{13}C spectrum for the two CO ligands, confirming the *cis,cis*-geometry (Figures 68, 69, 70, pag.106). Keeping complex **10** for 40 h in DCM at RT under inert atmosphere, the precursor **9** spontaneously formed (26% conversion) as inferred from the characteristic broad singlet at δ 60.6 ppm in the ^{31}P NMR spectrum. This confirmed that the second carbonyl in trans to the phosphorus resulted barely coordinated due to a strong trans effect compared to the other strongly coordinated in axial position (Figure 71).

Finally, a different synthetic pathway has been investigated to produce complex **9**, using a precursor with higher ruthenium content per mole with respect to **1**. Starting

from the polymer precursor $[\text{Ru}(\text{CO})_2(\text{Cl})_2]_n$ by addition of DiPPF and 10 equivalents of sodium acetate. This route displays a higher atom economy and is relevant for possible industrial applications. Among the different solvents, toluene at reflux led to a straightforward production of **9** with good yield, while with tert-butanol and other alcohols (ethanol, 2-propanol) the reaction was very slow or it failed. The rate of formation of the desired product plays a crucial role, too long reaction times could drive the formation of undesired products due to the oxygen sensitive diphosphine. Furthermore, in the presence of 10 equivalents of CHCl_3 the $\text{RuCl}(\text{k}^2\text{-OAc})(\text{CO})(\text{DiPPF})$ (**16**) was obtained in low yields (Figures 87, 88, page 126).

2.1.5 Carbonyl compounds deriving from $\text{Ru}(\text{OAc})_2(\text{CO})(\text{PPh}_3)_2$

The complex $\text{Ru}(\text{OAc})_2(\text{CO})(\text{PPh}_3)_2$ was firstly reported by Wilkinson. In his procedure bubbling CO through a solution of **1** in MeOH results in a pale green precipitate. This complex was applied successfully as precursor for the production of $\text{Ru}(\text{OAc})_2(\text{CO})(\text{PP})$ type complexes with a number of diphosphines in Baratta's research group, whereas the substitution of the monodentate triphenylphosphine with bulky chelating diphosphines, such as 1,3-dicyclohexylphosphinopropane (DCyPP), 4Cy-josiphos or triphos was still unreported. Unfortunately, the ^1H NMR characterization of the Cy phosphine derivatives $\text{Ru}(\text{OAc})_2(\text{CO})(\text{DCyPP})$ (**11**) and $\text{Ru}(\text{OAc})_2(\text{CO})(4\text{Cy-Josiphos})$ (**12**) was difficult because of the presence of very broad signals in the region below 2 ppm (Figures 72, 74, 109). On the other hand, the ^{31}P NMR showed broad signals, similar to that of related fluxional complexes, such as **9** or $\text{Ru}(\text{OAc})_2(\text{CO})(\text{dppf})$ (Figures 73, 75, 109) explained above in Scheme 8. The reaction with triphos led to a mixture of three species showed in Scheme 9 (Figures 76, 77, pag.113).



Scheme 9 Reaction of the triphos ligand with the $\text{Ru}(\text{OAc})_2(\text{CO})(\text{PPh}_3)_2$ precursor

The major one 75 mol% is consistent with the formation of the desired product $\text{Ru}(\text{OAc})_2(\text{CO})(\text{Triphos})$ (**13**) in which the tridentate ligand exhibits an A_2X signal pattern at the phosphorus NMR. The second more important species (~ 20 mol% of the mixture) showed a broad singlet at 40.3 ppm, this belongs to the already reported $\text{Ru}(\text{OAc})_2(\text{Triphos})^{[39]}$ and derives from the de-coordination of the carbonyl ligand favoured by the k^2 chelating ability of two acetate ligand in cis position to the CO. The less abundant species in the mixture (less than 10%) was attributed to the cationic complex in which one acetate is k^2 -coordinated and the second act as counter anion. If optimized, this should be a viable new synthetic route for the synthesis of this compound without the need of using the expensive precursor $\text{Ru}(\text{Me-allyl})_2(\text{COD})$ that requires inert atmosphere and very dry solvents, however these studies being outside the scope of this thesis. All these reactions were carried out in toluene that allows solubilization of the precursor and higher operational temperatures, leading to an increase of the reaction rates.

2.1.6 Reactivity of $\text{Ru}(\text{OAc})_2(\text{CO})(\text{DiPPF})$ (9**)**

Preparation of trifluoroacetate complexes by protonation of acetate ligands on the metal with TFA and subsequent substitution, is an easy way to achieve more reactive compounds. During this thesis work a great effort has been addressed to isolate and characterize new trifluoro acetate derivatives from Ru acetate complexes, starting from precursor **1**. Addition of TFA (1 and 2 equiv) to **9** in CD_2Cl_2 leads to new species, as inferred from the ^{31}P NMR measurements. With 1 equivalent of TFA two broad singlets were detected at δ 67.8 and 59.8 ppm, consistent with the formation of two new species which equilibrate with the precursor **9** (Figure 83, pag.118). Upon addition of a second equivalent of TFA the two peaks disappear leading to a new broad signal at δ 63.4, indicating the successful exchange of all acetate ligands with the stronger acid (Figure 9). Among the several procedures developed for the isolation of the trifluoro acetate derivate $\text{Ru}(k^1\text{-OCOCF}_3)(k^2\text{-OCOCF}_3)(\text{CO})(\text{DiPPF})$ (**14**), the most efficient is the treatment of **9** with an excess of TFA, followed by addition of calcium carbonate to eliminate the excess of TFA and the generated acetic acid as calcium salts. The isolated product shows a sharp singlet at ^{31}P NMR in $[\text{D}_3]\text{toluene}$ (Figure 80, pag.116) which broaden with the time in solution to match the signal observed in situ formation (Figure 10). The ^{13}C NMR spectra of **14** at room temperature are poor due to the high

fluxionality of this compound, whereas the more sensitive ^{19}F NMR showed two distinct CF_3 groups (Figure 81).

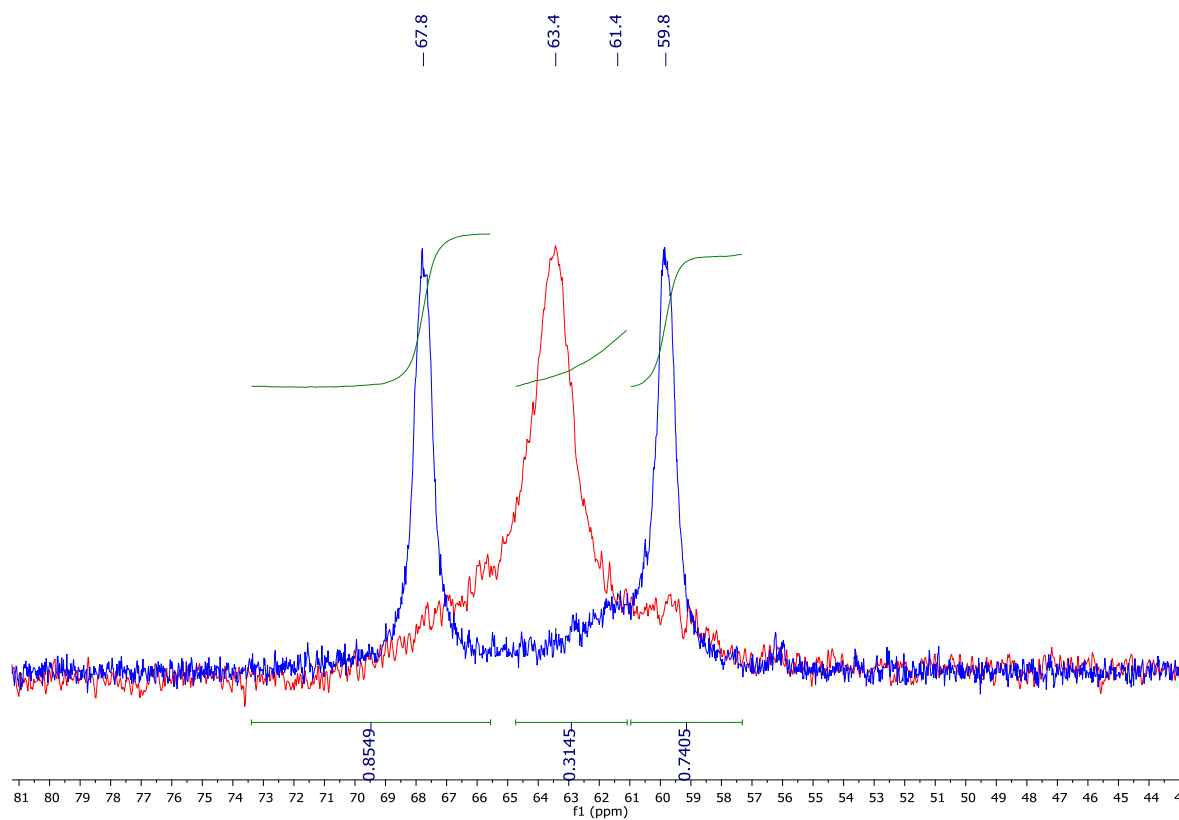


Figure 9 Superimposition of ^{31}P NMR spectra of **9** after one and two equiv. of TFA in CD_2Cl_2

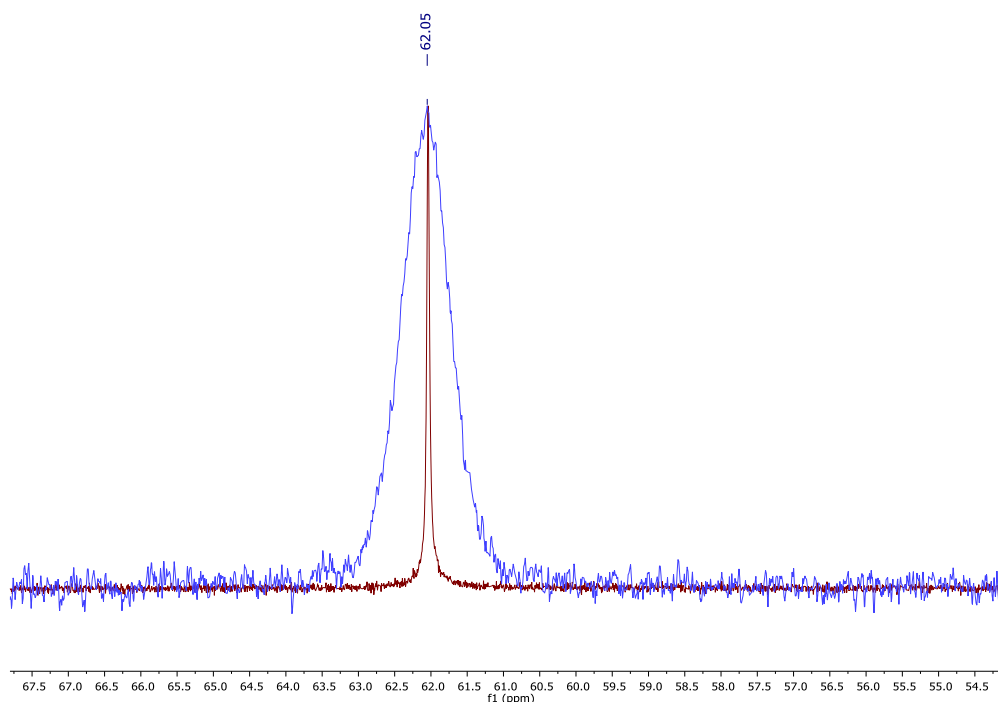


Figure 10 Superimposition of ^{31}P NMR spectra of **14** freshly dissolved in $[\text{D}_8]\text{Toluene}$ at 25°C (red) and after 24h (blue).

The reactivity of Ru carboxylate in the activation of terminal alkynes is well known.^[40] Compound **9** that possesses a high electron density on the metal, with respect to the complexes bearing aryl diphosphines, in the presence of phenylacetylene (1 equiv.) and a base in toluene affords the corresponding acetylide $\text{Ru}(\text{k}^2\text{-OAc})(\text{CO})(\text{DiPPF})(\text{C}\equiv\text{CPh})$ (**15**), with no formation of the corresponding vinylidene complex. The crystal structure of this compound (Figure 11) showed a Ru – C₁ bond of 2.040 Å, significantly longer than vinylidene complexes, with a C₁ – C₂ length of 1.200 Å, that was in the range of a normal C≡C triple bond. The angle Ru – C₁- C₂ of 172.3 was close to the linear as expected for this kind of complexes whereas the O₁ – Ru – O₂ was narrowed by the k^2 binding mode of the acetate.

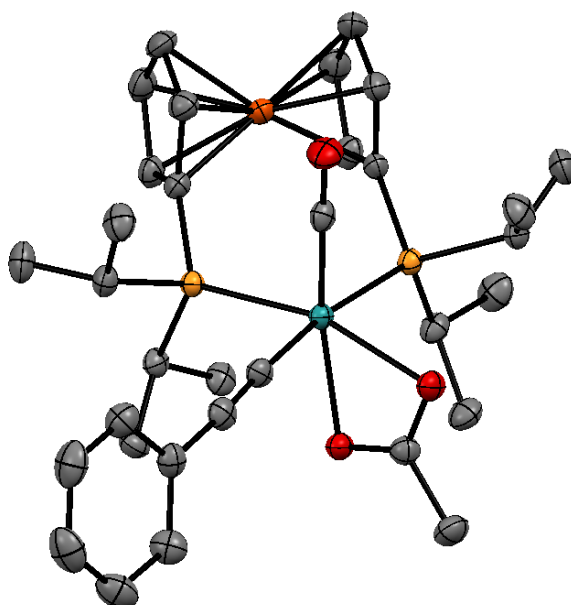


Figure 11 ORTEP style plot of compound **15** in the solid state. Ellipsoids are drawn at the 50% probability level. H-atoms are omitted for clarity. Selected bond lengths [Å] and angles [°]: Ru1 - P2 2.3018(6), Ru1 - P1 2.4658(7), Ru1 - O3 2.1936(17), Ru1 - O2 2.2013(17), Ru1 - C1 2.040(2), Ru1 - C9 1.816(3), C1 - C2 1.199(3), P2 - Ru1 - P1 100.28(2), O3-Ru1-O2 59.51(6), C1 - Ru1 - P1 172.56(7).

2.1.7 Conclusions

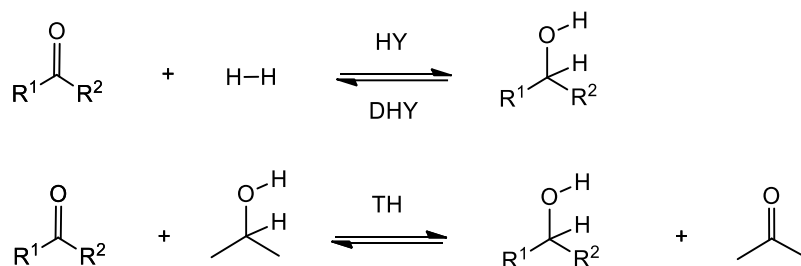
In conclusion, the straightforward exchange reaction of triphenylphosphine with metallocene based bulky alkyl-diphosphines DiPPF and DCyPFc on the acetate complexes $\text{Ru}(\text{OAc})_2(\text{PPh}_3)_3$ and $\text{Ru}(\text{OAc})_2(\text{CO})(\text{PPh}_3)_3$ afforded novel versatile precursors $\text{Ru}(\text{OAc})_2(\text{PP})$ and $\text{Ru}(\text{OAc})_2(\text{CO})(\text{PP})$. Since the Ru chemistry of bidentate alkyl phosphines is practically unexplored and a significant difference in the chemical

reactivity and catalytic activity is expected compared to the commonly employed aryl diphosphines, these precursors open the way to new Ru based catalytic systems. Preliminary studies show that compound $\text{Ru}(\text{OAc})_2(\text{CO})(\text{DiPPF})$ **9** in the presence of TFA undergoes easy protonation of the acetate ligands, affording the corresponding more reactive trifluoroacetate species, whereas interaction of phenylacetylene with **9** in a basic environment leads to the mono acetylide derivative.

2.2 Transfer Hydrogenation of ketones

2.2.1 Background of Ru promoted reductions catalysis

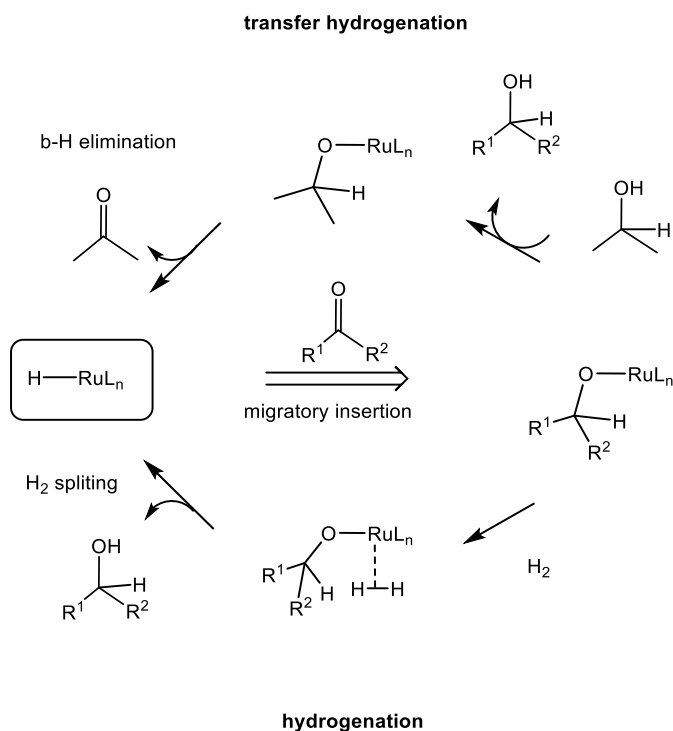
Starting from the observation performed during the first half of the past century,^[41] significant improvements have been made in the synthesis and development of late transition metal catalysts for hydrogenative processes. A great variety of transition metal centers, ligands, conditions, solvents and hydrogen sources, have been studied for the reduction of unsaturated compounds, reaching nowadays an advanced technological level, enough to be applied on industrial scale. Ir, Ru, Rh, Os^[19b] and, very recently Mn,^[42] have exhibited a very good potential. Complexes bearing P-, O-, S-, C- and N-ligands in various forms, ranging from monodentate to tetradentate ligands (such as N-heterocyclic carbenes, half sandwich, multidentate phosphines, amines and their proper combinations) are typically the most popular catalysts for metal-promoted reductions. As shown in Scheme 10, hydrogenation (HY) process occurs with the reduction of the C=O group by molecular hydrogen (top), while transfer hydrogenation (TH) formally involves two H atoms provided by a hydrogen donor molecule (bottom), such as 2-propanol.



Scheme 10 Hydrogenation and transfer hydrogenation reactions.

Alternative feasible hydrogen donors are formic acid, formic acid/triethylamine mixtures and formate salts. Primary alcohols, such as ethanol or methanol, are generally less suitable hydrogen donors than secondary alcohols such as 2-propanol, due to their unfavourable redox potential.^[43] On these bases, HY is thermodynamically easier and should afford complete conversion at lower temperatures. However, TH with 2-propanol is an equilibrium reaction which can be shifted to the alcohol product by mass effect using it as solvent. Because of its operational simplicity and the absence of the risks associated with the use of H₂, TH has increasingly been used in industrial

plants, representing a valid alternative to HY. In both catalytic TH and HY reactions, a metal-hydride species is usually involved as key intermediate,^[44] then reaction with the carbonyl substrate leads to a metal alkoxide complex *via* migratory insertion reaction^[45] (Scheme 11). The upper part of the scheme presents the “inner sphere mechanism” in which the metal alkoxide reacts with 2-propanol, then the produced metal-isopropoxide undergoes a β -hydrogen elimination to release acetone and regenerating the active M-H species. Conversely, in the HY, the metal alkoxide reacts with H₂, possibly involving a η^2 -coordination to the complex,^[46] with consecutive H-H splitting and regeneration of the M-H bond (lower part of Scheme 11). It is worth noting that C-H activation generally requires a *cis* vacant site,^[47] although a facile β -hydrogen elimination reaction promoted by 18-electrons Ir(III) complexes has been claimed by Milstein.^[48]



Scheme 11 Reduction of carbonyl compounds via inner sphere TH and HY pathway.

On the turn of 2000s a breakthrough in asymmetric TH (ATH) and HY (AHY), was the development by Noyori of the catalysts $\text{RuCl}(\eta^6\text{-arene})(\text{N-arylsulfonyl-dpen})$ and the following work on $\text{trans-RuCl}_2(\text{BINAP})(1,2\text{-diamine})$,^[13] which are highly active in the ATH and the AHY of various aromatic ketones^[49] and imines^[50]; respectively (Figure 12).

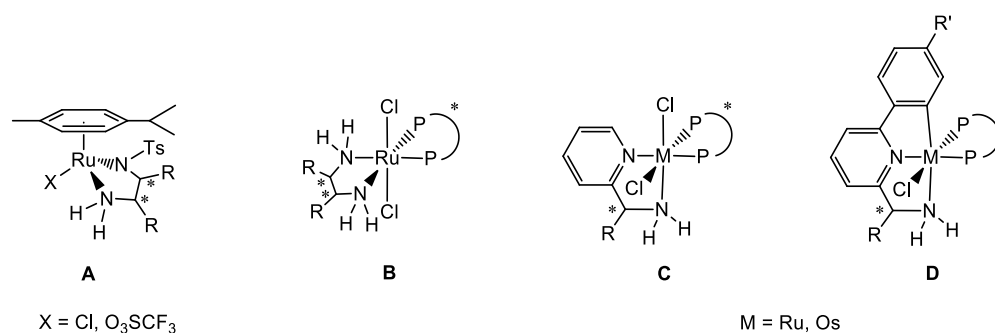
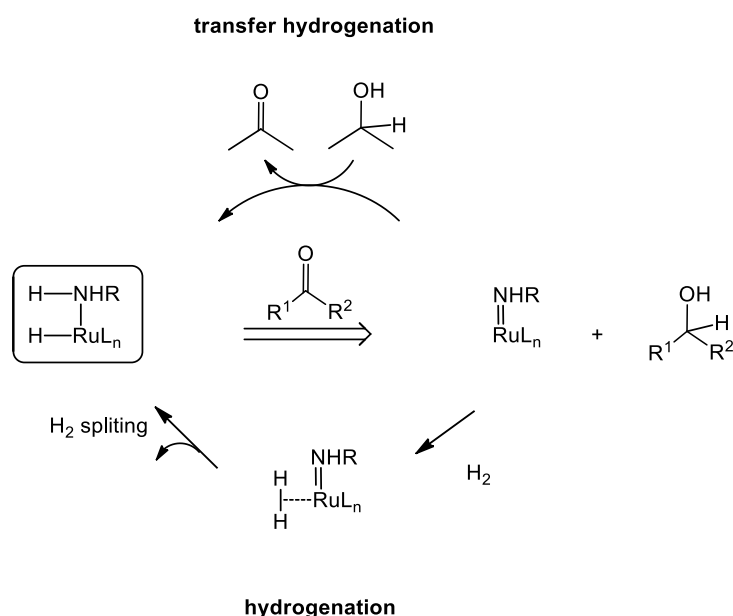


Figure 12 Highly efficient Ru and Os catalysts for asymmetric transfer hydrogenation and hydrogenation of ketones.

The high activity of these systems is attributed to the presence of the NH₂ group, that leads to the formation of 16-electron Ru-amide species. For example during the TH promoted by the Ru(η^6 -arene) complex (system **A** Figure 12), after the formation of a metal-hydride intermediate, both the Ru-H and Ru-NH₂ linkages react with the substrate leading to the alcohol product and a Ru-amide species (also characterized in the solid state^[49]) which is rapidly converted back to the active metal hydride species by the reductive media (IPA or hydrogen) (Scheme 12)



Scheme 12 Reduction of carbonyl compounds via outer sphere TH and HY pathway.

The Ru-ammide species was also confirmed starting from the RuCl₂(PP)(1,2-diamine)^[51] (**B**, Figure 12), which is better suited for HY affording the alcohol product and the Ru-amide. Conversely, Bergens reported that reacting Ru(H)₂(BINAP)(dppe) with acetophenone the corresponding alkoxide RuH(OR)(BINAP)(dppe) (OR=1-

phenyl-1-ethoxide) is formed and that the generation of the Ru-amide and 1-phenylethanol occurs involving a transition state with a partial Ru-O linkage.^[52]

The compounds $\text{RuCl}_2(\text{PP})(\text{ampy})$ ^[53] (**C**, Figure 12) are highly active catalysts for both TH and HY reactions. Moreover, these type of complexes have been proven to promote a series of organic transformations involving the C-H bond activation of alcohols, such as dehydrogenation, allylic alcohol isomerization, ketone α -alkylation,^[22c] amine alkylation, and amide formation.^[54] Expanding the work on the catalysts of the type **C**, the pincer complexes $\text{MCl}(\text{CNN})(\text{PP})$ (**D**, Figure 12) ($\text{M} = \text{Ru}$,^[17a, 17b, 53b, 55] Os ;^[19a, 56] $\text{HCNN} = 1$ -(6-arylpyridin-2-yl)methanamine) were designed. They are one of the most efficient catalysts for the TH of carbonyl compounds in 2-propanol, affording TOF up to 10^6 h^{-1} and extremely high productivity ($\text{TON} \approx 10^5$) showing enantioselectivity (up to 99 % *ee*). In this view, the carboxylate precursors described in the previous chapter, perfectly fit the will to design new complexes with an increased and wide reactivity for a growing number of reactions, accomplished by changing and optimizing coordination motif on the metal. Thanks to their modularity was possible to put together the robustness of a strong facial configuration of diphosphine and CO ligands borrowed from the arene and Cp^* complexes, with the trans induction of the basic phosphines. Moreover, the acetate fragment was an attractive ligand due to its lability. In fact, switching from k^2 to k^1 coordination it's able to generate a free position on the metal, without changing its oxidation state. This is an interesting feature still poorly exploited.

2.2.2 TH of acetophenone promoted by acetate complexes

The catalytic activity of some of the acetate complexes obtained in chapter 2.1 was investigated in the reduction of the model substrate acetophenone *via* TH in the presence of sodium 2-propoxide as the base. Figures 13 - 16 show time-conversion profiles, built trough GC data.

Precursor **2**, was tested in the presence of diamine ligands ampy and en and also without NN ligands, showing an increased activity in presence of the NH_2 group (entries 1, 5, 6 Table 2) affording TOF between 1500 and 2500 h^{-1} (Figure 13) Unexpectedly, in the absence of amine ligands, complex $\text{Ru}(\text{OAc})_2(\text{dppf})$ (TOF 4500 h^{-1}) resulted in a better catalytic performance (entry 2, Table 2, Figure 14). Also, the preformed ampy derivative as a cis/trans mixture of compounds **6b/6b'** (entry 3, Table 2), showed a

reduced activity compared with the *in situ* generated complex according with the relatively easy release of the diamine ligands (see chapter 2.1.3). Moreover, complex **7**, for which the dissociation of ampy was much slower, exhibited a higher catalytic activity with a TOF of 3000 h⁻¹ (entry 4, Table 2, Figure 15) indicating that, in this catalytic condition the deactivation processes occurred as soon as the NN ligand was released. When higher substrate/catalyst ratio (S/C 20000) was used (entries 7,8 Table 2) the conversion of acetophenone was very low (<10%) for both ampy and en complexes.

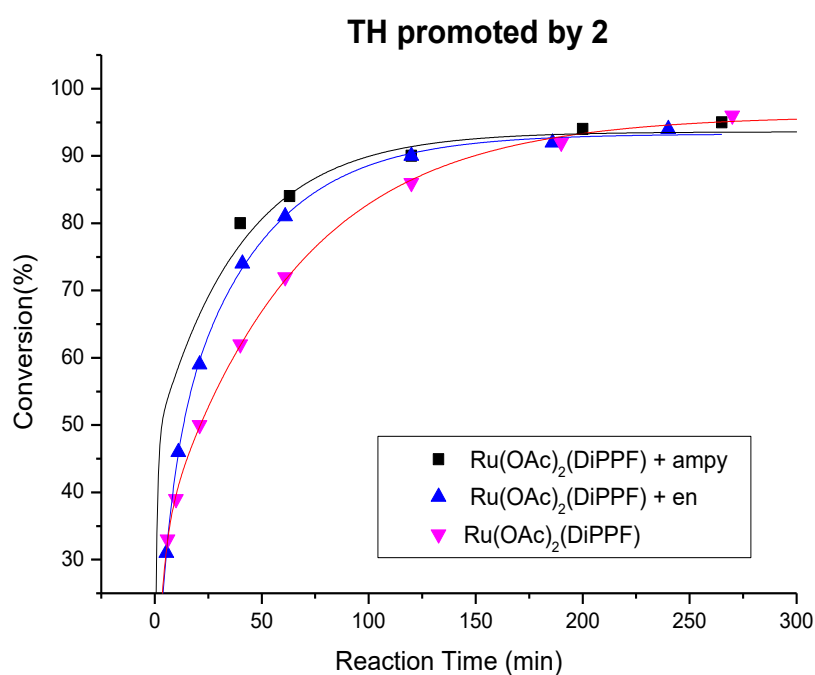


Figure 13 TH of acetophenone promoted by **2** in presence of diamine ligands.

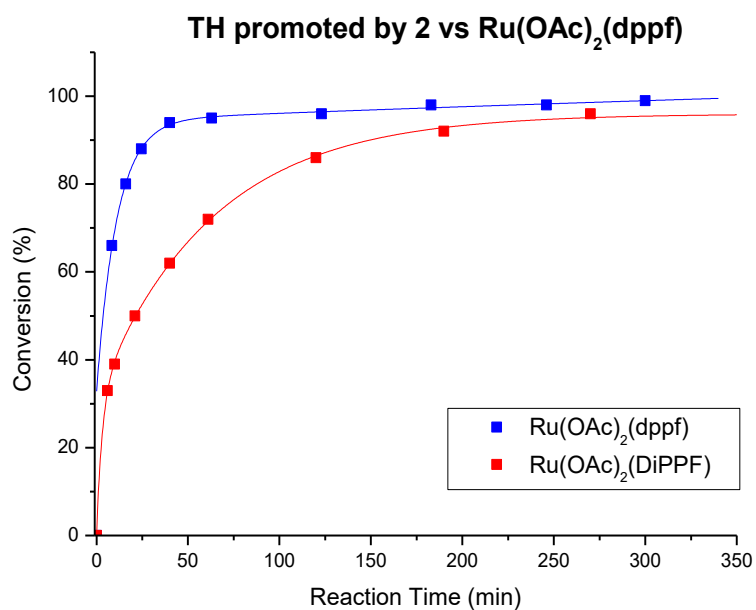


Figure 14 TH of acetophenone promoted by 2 vs Ru(OAc)₂(dppf)

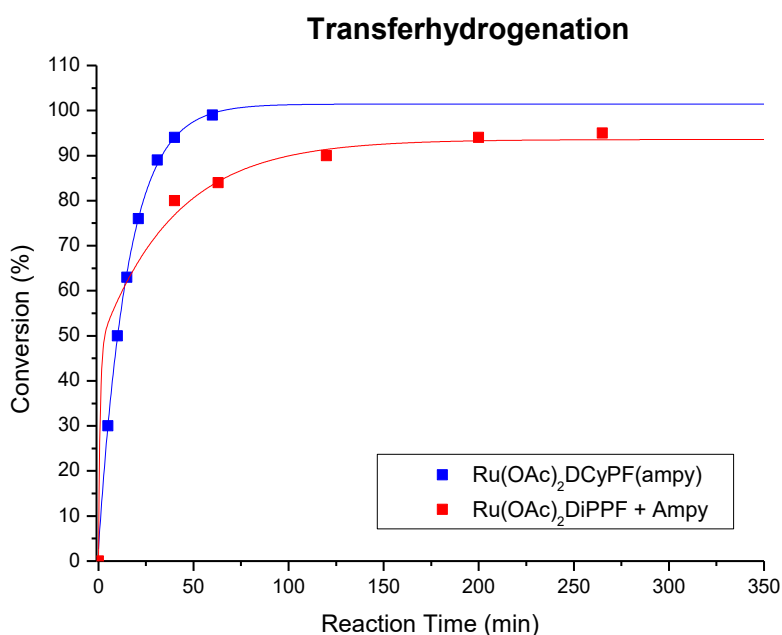


Figure 15 Comparison complex 7 with 6 generated in situ

Moving to the carbonyl complex **9**, higher activity was observed with TOF 8000 h⁻¹, indicating a higher robustness of the catalyst conferred by the CO ligand. The presence of diamine boosted the activity to TOF 30000 h⁻¹ (entries 7, 8 Table 2), and upon addition of ampy to **9** a great acceleration effect was detected but, unfortunately, deactivation occurred in less than 2 min. Conversely, productivity of dicarbonyl species

8 was very low, in accordance with the fact that this complex entered the catalytic cycle only after the release of one CO ligand from the coordination sphere. The reaction carried out in the presence of benzylamine as the only base, showed low reaction rate (entry 13, Table 2) suggesting that no carbometallation process occurred during the reduction. The time-conversion profiles of compound **9** with different amine ligands, indicate that addition of ampy dramatically increases the reaction rate (Figure 16). However, all the systems reported in figure 16 were not able to match the catalytic activity of Ru(OAc)₂(dppf), which in the presence of ampy is able to reach TOF up to 10⁵.^[22c]

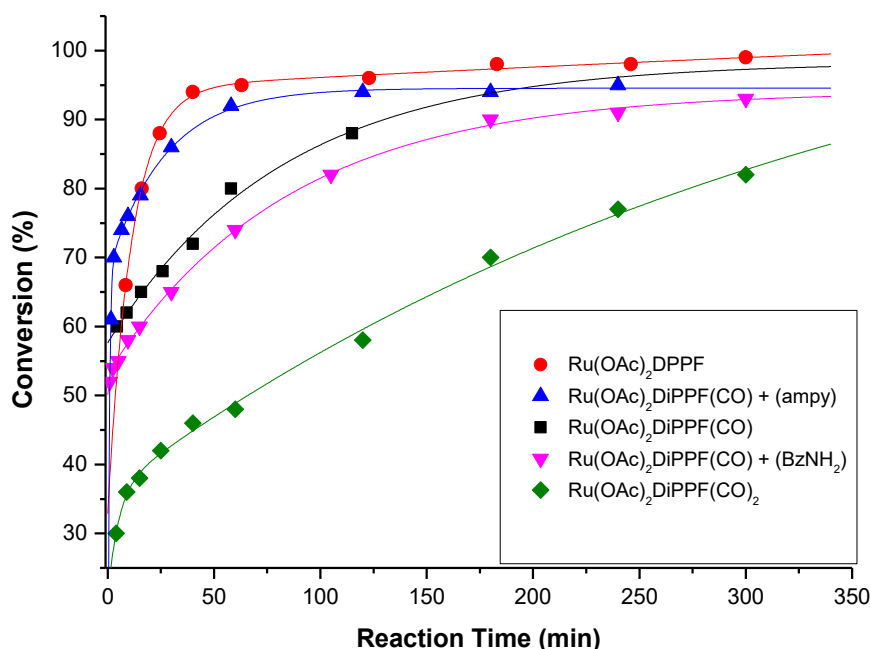


Figure 16 TH of acetophenone promoted by **9** with NN ligands

Surprisingly, complex Ru(OAc)₂(CO)(4Cy-Josiphos) (**12**) was found to be very active in the reduction of acetophenone with an S/C = 1000, in mild temperature conditions down to 30 °C, the reactions completed in 5 min showed TOF = 80000 h⁻¹ (entries 14 – 17, Table 2). It has to be noticed that **9** showed poor catalytic activity at 30 °C, hinting that the catalyst activation requires higher temperature.

Table 2 TH of acetophenone promoted by complexes 2 – 12 in presence of NaOiPr

Entry	Catalyst	Additive (equiv.)	S/C	Time (h)	Conv.[a] [%]	TOF [h ⁻¹]
1	Ru(OAc) ₂ (DiPPF)		1000	4.5	96	1500
2	Ru(OAc) ₂ (DPPF)		1000	1	95	4600

Entry	Catalyst	Additive (equiv.)	S/C	Time (h)	Conv.[a] [%]	TOF [h ⁻¹]
3	Ru(OAc) ₂ (DiPPF)(ampy)		1000	1	56	250
4	Ru(OAc) ₂ (DCyPF)(ampy)		1000	1	99	3000
5	Ru(OAc) ₂ (DiPPF)	ampy (10)	1000	3.5	94	1200
6	Ru(OAc) ₂ (DiPPF)	en (10)	1000	4	94	2500
7	Ru(OAc) ₂ (DiPPF)(ampy))		20000	1	13	-
8	Ru(OAc) ₂ (DiPPF)(en)		20000	1	4	-
9	Ru(OAc) ₂ (CO)(DiPPF)		1000	2	80	8000
10	Ru(OAc) ₂ (CO)(DiPPF)	ampy (10)	1000	1	92	24500
11	Ru(OAc) ₂ (CO)(DiPPF)	BzNH ₂ (10)	1000	3	90	30000
12	Ru(OAc) ₂ (CO) ₂ (DiPPF)		1000	5	82	250
13	Ru(OAc) ₂ (CO)(DiPPF)	BzNH ₂ (10)	1000	3	80 ^[b]	500
14	Ru(OAc) ₂ (CO)(4Cy-Josiphos)		1000	1.5 min	98	38000
15	Ru(OAc) ₂ (CO)(4Cy-Josiphos)	ampy (10)	1000	10 min	98	30000
16	Ru(OAc) ₂ (CO)(4Cy-Josiphos)		1000	1 min	96 ^[c]	58100
17	Ru(OAc) ₂ (CO)(4Cy-Josiphos)		2000	5 min	99 ^[d]	80000

[a] The conversion was determined by GC analysis. [b] no addition of NaOiPr in the system
[c] Temperature = 60°C. [d] Temperature = 30°C

2.2.3 TH in presence of terdentate ligand Hamtp

Unfortunately, attempts of TH with complex 9 on other substrate as (L)-menthone or citral (a 2/1 mixture of the geometrical isomers geranial/neral) did not result in the desired outcomes. In particular, the product of the reduction of (L)-menthone in the best conditions found for acetophenone, was a mixture of 4 of all the possible isomers namely (+)-neomenthol, (+)-isomenthol, (-)-menthol, (+)-neoisomenthol, (Figure 17) with no appreciable degree of stereoselectivity, whereas citral attained only partial conversion into the corresponding alcohols.

Table 3 TH of (L)-menthone promoted by 9.

Complex	Additive	Time (h)	Conv. (%)	Selectivity (%)			
				A ^[a]	B ^[b]	C ^[c]	D ^[d]
9	-	6	40	16	7	34	43
9	ampy	6.5	92	20	9	29	42

[a] (+)-neomenthol; [b] (+)-isomenhol; [c] (-)-menthol; [d] (+)-neoisomenthol

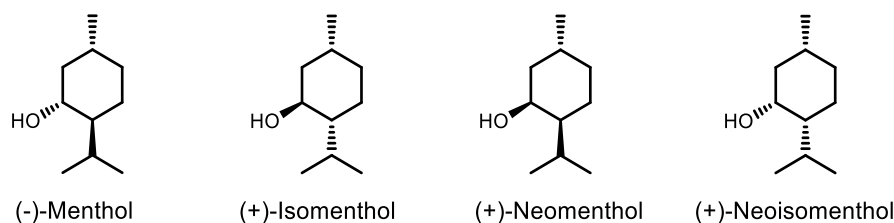
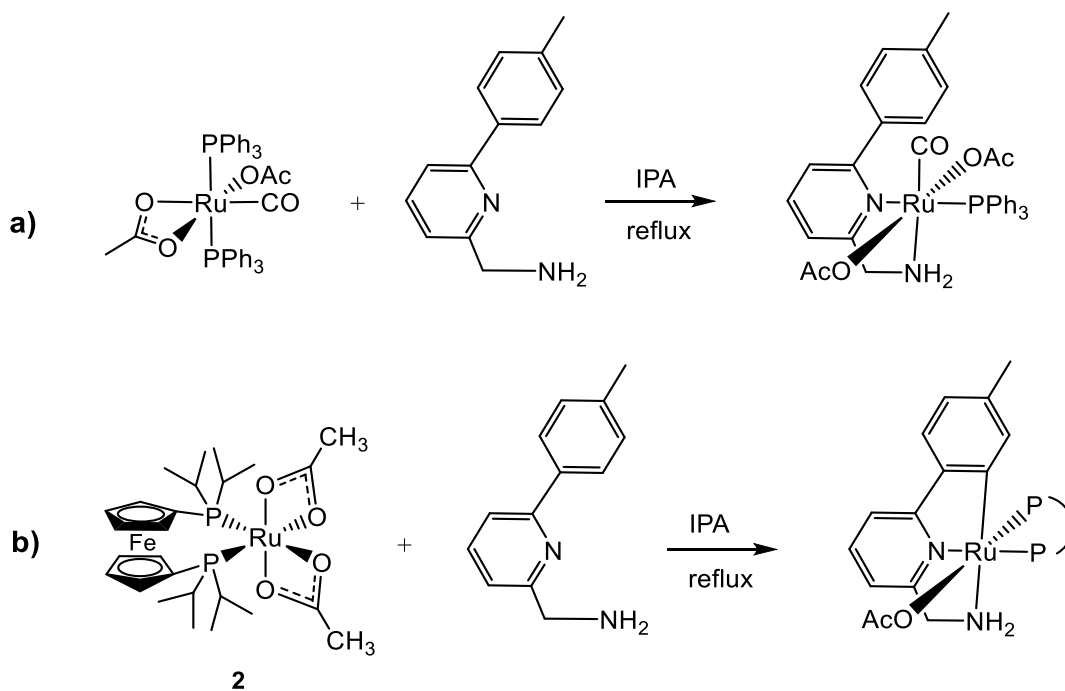


Figure 17 All possible menthol isomers deriving from the reduction of (*L*)-mentone

Our attempts of enhancing the catalytic activity of the novel acetate systems pointed the attention on the combination between $\text{Ru}(\text{OAc})_2(\text{CO})(\text{PPh}_3)_2$ or precursor **2** with the tridentate ligand Hamtp (Scheme 13), for the in situ formation of acetate homologs of type D in Figure 12 of the previous section, using the weaker base K_2CO_3 . As a matter of fact, it has been observed that k^1 -acetate complex $\text{Ru}(\text{OAc})(\text{CNN})(\text{dppb})$ displays a higher rate of reaction with respect to the chloride congener $\text{RuCl}(\text{CNN})(\text{dppb})$ in the TH of acetophenone.^[17c, 57]



Scheme 13 Proposed catalytic species from the in situ reaction of Hamtp with complexes $\text{Ru}(\text{OAc})_2(\text{CO})(\text{PPh}_3)_2$ (**a**) and **2** (**b**)

Indeed very good results were achieved with complex bearing triphenylphosphine as precursor with TOF of 8000 and 900 h^{-1} (Table 4; Figure 18) with a good selectivity in favour of desired (-)-menthol (77%). No enhancement of the catalytic activity was observed in the presence of the bulky diphosphine DiPPF, suggesting that the

increased electro donation properties of this ligand do not significantly affect the catalytic performances of this system.

Table 4 TH of (*L*)-menthone (0.1 M) with $\text{Ru}(\text{OAc})_2(\text{CO})(\text{PPh}_3)_2$ or **2** in 2-propanol at 82 °C in the presence of 5 mol% K_2CO_3 .

Complex	Additive	S/C	Time	Conv. (%)	Selectivity (%)			
					A ^[a]	B ^[b]	C ^[c]	D ^[d]
$\text{Ru}(\text{OAc})_2(\text{CO})(\text{PPh}_3)_2$	Hamtp	1000	30 min	99	18	3	77	1
$\text{Ru}(\text{OAc})_2(\text{CO})(\text{PPh}_3)_2$	Hamtp	10k	56 h	81	15	3	53	10
2	Hamtp	1000	6 h	20	4	3	5	7

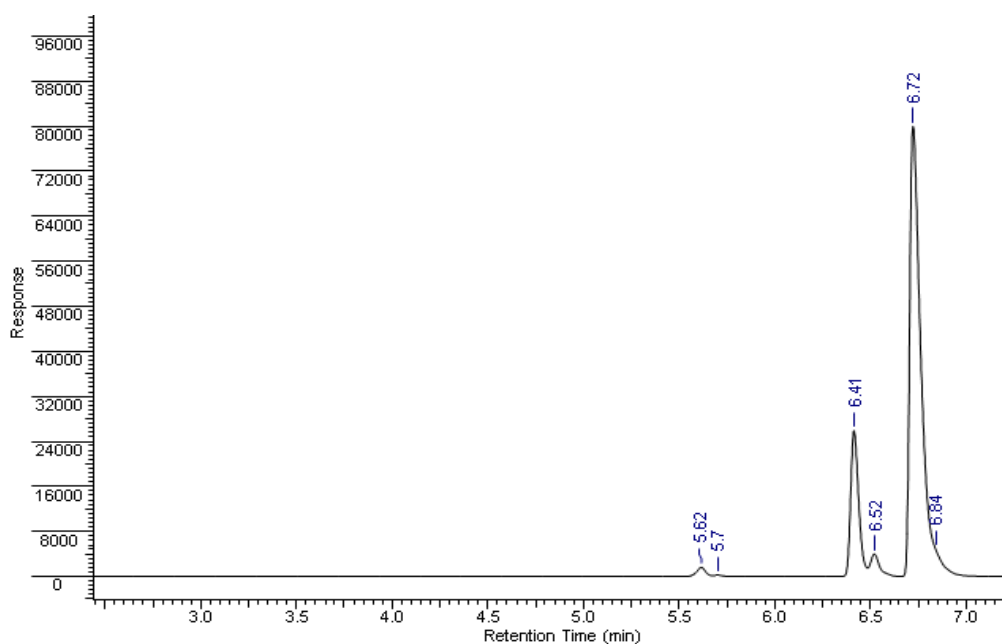


Figure 18 GC chromatogram of the reduction of menthone in presence of Hamtp (S/C 1000).

A confirmation of the high robustness and productivity of the active species obtained from the system $\text{Ru}(\text{OAc})_2(\text{CO})(\text{PPh}_3)_2$ / Hamtp, was found in the TH of citral in the same condition applied with (*L*)-menthone (Table 5). Full conversion was attained with S/C in the range 1000 and 10000 in 10 and 90 min, respectively.

Table 5 TH of citral (0.1 M) with $\text{Ru}(\text{OAc})_2(\text{CO})(\text{PPh}_3)_2$ in 2-propanol at 82 °C in the presence of 5 mol% K_2CO_3 .

Complex	Additive	S/C	Time	Conv. (%)
$\text{Ru}(\text{OAc})_2(\text{CO})(\text{PPh}_3)_2$	Hamtp	1000	10	99
$\text{Ru}(\text{OAc})_2(\text{CO})(\text{PPh}_3)_2$	Hamtp	10k	90	98

2.2.4 Conclusions

The TH of acetophenone catalysed by the novel acetate complexes $\text{Ru}(\text{OAc})_2(\text{PP})$ (PP= DiPPF, DCyPPF) and $\text{Ru}(\text{OAc})_2(\text{PP})(\text{NN})$ (NN= ampy, en), has been investigated. They showed good activity with TOFs up to 30000 but low TONs up to 2000; no important differences were observed between the systems $\text{Ru}(\text{OAc})_2(\text{PP})$ and $\text{Ru}(\text{OAc})_2(\text{PP})(\text{ampy})$. As a matter of fact, the joint steric hindrance with the strong trans-effect of the basic diphosphines weakens the coordination of the ampy ligand, hinting that the $\text{Ru}(\text{OAc})_2(\text{PP})(\text{ampy})$ systems eventually end up in the same catalytic active species of the $\text{Ru}(\text{OAc})_2(\text{PP})$ congeners. This fact likely determines the reduced acceleration effect granted by the bifunctional NH_2 moiety when in the metal coordination sphere. On the other hand, the complex $\text{Ru}(\text{OAc})_2(\text{DiPPF})(\text{en})$ with a more coordinating diamine, that appears to release very slowly the nitrogen ligand, but with no significant improvement in the catalytic outcomes.

The carbonyl complexes $\text{Ru}(\text{OAc})_2(\text{CO})_n(\text{PP})$ ($n= 1, 2$; PP= DiPPF, Cy-Josiphos) showed good performances with $n=1$, whereas with $n=2$ moderate catalytic performances were observed, hinting that the de-coordination of CO is a key step to obtain catalytically active species. The addition of nitrogen ligands to monocarbonyl complexes dramatically increased the reaction rate, suggesting that carbonyl complexes produce more robust and stable species than their $\text{Ru}(\text{OAc})_2(\text{PP})$ congeners.

The carbonyl precursor $\text{Ru}(\text{OAc})_2(\text{CO})(\text{PPh}_3)_2$ in combination with the tridentate ligand Hampt proved to be successful in the reduction of citral to its corresponding alcohol mixture and of bulky (L)-menthone to (-)-menthol with good stereoselectivity and productivity (S/C 1000).

Further studies are in progress to better understand the catalytic activity of these complexes and for broadening the scope of the TH reaction to other unsaturated substrates.

2.3 Aldehyde Hydrogenation

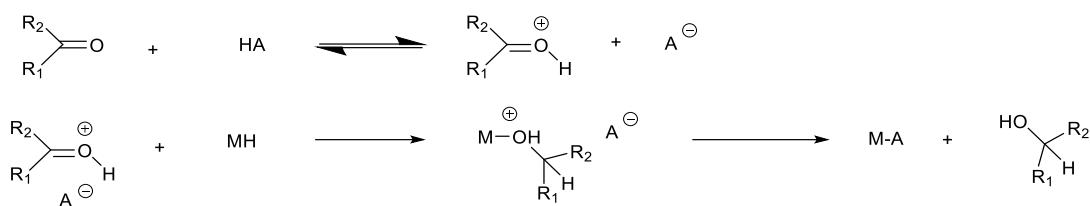
2.3.1 Background of Ru promoted Hydrogenation

Reports on reductions in a monophasic system date back to 1938 when Calvin described the hydrogenation of quinone using copper acetate system with hydrogen. Since then catalysis started to acquire an increasing attention and relevance in view of the manifold applications. A breakthrough in the development of homogeneous hydrogenation came as direct result of the discovery of the $\text{RhCl}(\text{PPh}_3)_3$ system, reported by Wilkinson, which was found to catalyse the olefin hydrogenation. Because of the growing interest in the catalytic hydrogenation, from the middle of the 60' the literature has become vast and a lot of reviews and books appeared, focusing mainly on the C=C bond reduction. Nowadays, hydrogenation is applied in many synthesis of pharmaceuticals, flavors, and fragrances.^[58] It has been estimated that approximately 25% of all chemical processes include at least a catalytic hydrogenation step,^[59] contributing also to ca. 8% of the world's GDP. As a matter of fact, hydrogenation is one of the most applied reaction for the manufacture of chemicals and it is not surprising that HY remains one of the widest areas of research in catalysis.

As regards the hydrogenation of carbonyl compounds several ruthenium compounds were reported in 70' to display moderate to good activity. In these studies, the systems were generally based on the phosphine-coordinated ruthenium carbonyl compounds, previously employed in catalytic C-C forming reaction involving CO. Thus, the hydroformylation catalyst $\text{Ru}(\text{CO})_3(\text{PPh}_3)_2$ was shown to be effective in the hydrogenation of propionaldehyde under 20 bar H_2 and at 120 °C^[60] Tsuji and Suzuki used the complex $\text{RuCl}_2(\text{PPh}_3)_3$ to hydrogenate a series of aliphatic and aromatic aldehydes^[61] The derivatives $\text{RuHCl}(\text{PPh}_3)_3$, $\text{RuHCl}(\text{CO})(\text{PPh}_3)_3$, and $\text{RuCl}_2(\text{PPh}_3)_3$ were used to reduce both aliphatic and aromatic aldehydes, although benzaldehyde reduction was less efficient than with the previously mentioned $\text{RuCl}_2(\text{CO})_2(\text{PPh}_3)_2$ catalyst. Although $\text{RuHCl}(\text{PPh}_3)_3$ displayed good activity, the catalysis occurs with concomitant decarbonylation of the aldehyde, as proven by the formation of metal carbonyl species at the end of reaction. Carbonyl complexes appeared more robust toward this side deactivation reaction of the catalyst, $\text{RuHCl}(\text{CO})(\text{PPh}_3)_3$ was found to be one of the most efficient catalyst. Using propionaldehyde with a S/C of 50000, turnover numbers of up to 32000 were achieved after 50 h at 140° C under 30 bar of

H₂ [62] Highly selective reduction of citral was described by Hotta using RuHCl(PPh₃)₃ [63], achieving poor selectivity (66%) in toluene under 50 bar H₂ at 30° C. Interestingly, addition of 12.5% HCl, and performing the reaction in toluene : ethanol mixture (27 : 3), afforded 99% conversion with increased selectivity (98%).

Although significant progress has been made concerning the selective reduction of carbonyl groups in presence of C=C double bonds, [12, 64] only few examples of catalysts are known which exhibit high selectivity for the hydrogenation of carbonyl group vs. olefin moieties. The chemistry becomes even more challenging when a formyl and a ketone group are present in the same molecule. In particular, such reaction is important for the production of flavours, fragrances [65] and pharmaceuticals. [66] Very recently, Dupau and coworkers reported a general and highly efficient method for the chemoselective catalysed aldehyde hydrogenation, under base-free conditions, of a variety of different ketoaldehydes reaching turnover numbers (TON) up to 40000, by replacing the halide ion in RuCl₂(diphosphine)(diamine) with a carboxylate ion, which led to a great improvement of catalytic efficiency and a high selective hydrogenation of aldehydes fragment. However, this Ru(OCO*t*Bu)₂(dppe)(en) catalyst needs 1 mol% of carboxylic acid (e.g., benzoic acid) as additive to obtain higher turnover numbers. [67] Several systems have been reported involving stoichiometric hydrogenation of ketones or aldehydes by metal hydrides in the presence of acids. The ionic hydrogenation mechanism accounts for most of these hydrogenations. An early example came from the report in 1985 by Darensbourg et al. with a Cr complex [CrH(CO)₄P(OMe)₃]₃⁻ [68] which catalysed propionaldehyde reduction to propanol in presence only of AcOH. Hydride transfer from [RuH(CO)(bpy)₂]⁺ occurs in the hydrogenation of acetone even in aqueous solutions. [69] Mechanistic studies on the dependence of the reaction rate upon the acid concentration occurring with hydride transfer mechanism, showed a first order dependence for the acid and the metal hydride species, thus the general proposed mechanism for this kind of catalysis reports a pre-equilibrium protonation of the aldehyde followed by hydride transfer from the metal to the substrate. [70]



Scheme 14 Proposed ionic mechanism for hydrogenation.

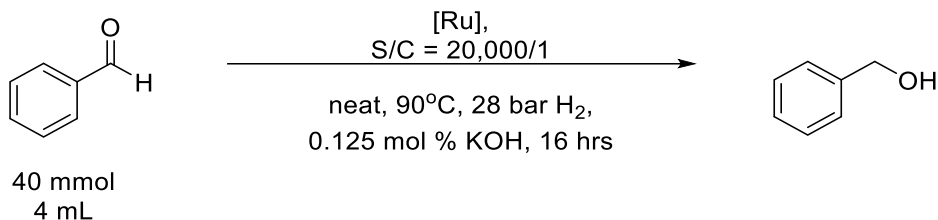
The growing number of fields in which HY is employed is also increasing the amount of solvents needed to run the reactions, especially on a huge scale productions, with more than 15 billion kilograms of organic solvents produced each year.^[71] This environmental problem force to place an intense emphasis on the development of chemical reactions that reduce wastes, as stated in one of the Principles of the Green Chemistry.^[72] It indicates that the use of a solvent should be avoided whenever possible. Moreover, in carbonyl compounds hydrogenation the presence of various type of solvents (organic, aqueous, or acidic solvents) may cause serious problems in product separation.^[71, 73] Therefore, it is desirable to develop solvent-free hydrogenation processes for efficient and clean productions, aimed to the sustainability of the chemical industry.

Herein, we report our results on solvent-free hydrogenation of aldehydes. Furthermore, all the catalytic hydrogenations were carried out using as substrates neat undistilled (aged or freshly opened) and not degassed aldehydes. In this way it was possible to simulate the exploitation of raw starting materials, reducing as much as possible the treatments needed for a large or mid-scale applications. As a matter of fact, it is of paramount importance to establish the activity of catalysts for substrates of commercial grade purity for example not under strict inert atmosphere, since the experimental conditions of industrial plants may significantly differ from the model reactions carried out in academic labs.

2.3.2 Hydrogenation of Benzaldehyde in presence of KOH

The activity of the novel ruthenium acetate complexes was investigated starting on a 40 mmol scale of benzaldehyde, with 28 bar H₂ pressure, using a high substrate/catalyst ratios, aiming to reduce the metal content in the final product (50 ppm or lower of Ru). Since the catalytically active ruthenium-hydride species are usually generated in basic media,^[44, 74] where aldehydes undergo undesirable side

reactions, very low amount of $\text{KOH}_{(\text{aq})}$ (less than 0.125%) was added to neat aldehyde, to minimize the formation of high weight by-products (i.e. aldol condensation,^[75] Tishchenko^[76] or Cannizzaro reactions^[77] (Scheme 15).



Scheme 15 General condition for HY of benzaldehyde in presence of the basic additive 1M $\text{KOH}_{(\text{aq})}$.

Good performances were exhibited by the complexes $\text{Ru}(\text{OAc})_2(\text{CO})(\text{DiPPF})$, $\text{Ru}(\text{OAc})_2(\text{CO})(\text{dppf})$, $\text{RuCl}(\text{OAc})(\text{CO})(\text{DiPPF})$ and the $\text{RuCl}_2(\text{dppb})(\text{ampy})$ with TOF of 1356, 1827, 2262, 1795 h^{-1} respectively (Figure 19, entries 1, 2, 11, 15, Table 6), while in the same conditions the precursors **1** and $\text{Ru}(\text{OAc})_2(\text{CO})(\text{PPh}_3)_2$, with the corresponding complexes bearing the diphosphines 4Cy-Josiphos, DCyPP and dppb, resulted in poor conversions (entries 9, 10, Table 6). Complexes $\text{Ru}(\text{OAc})_2(\text{CO})(\text{DiPPF})$ (**9**) and $\text{Ru}(\text{OAc})_2(\text{CO})(4\text{Cy-Josiphos})$ (**12**) were also tested at 35 and 50 °C, but no or poor conversion was achieved indicating that higher temperatures are required for their activation (entries 6, 7, 8, Table 6). Notably, in the presence of base these complexes showed very high activity in the transfer hydrogenation of acetophenone at 30 °C with TOF= 80000 h^{-1} (see chapter 2.2.2). Conversely, the well-known triphos complexes $\text{Ru}(\text{OAc})_2(\text{CO})(\text{Triphos})$ (**13**) and $\text{RuH}_2(\text{CO})(\text{Triphos})$ (entries 12, 13, Table 6) catalyze the carbonyl compounds reduction only under harsher conditions ($\sim 140^\circ\text{C}$), thus the activation occurs at higher temperature.^[78]

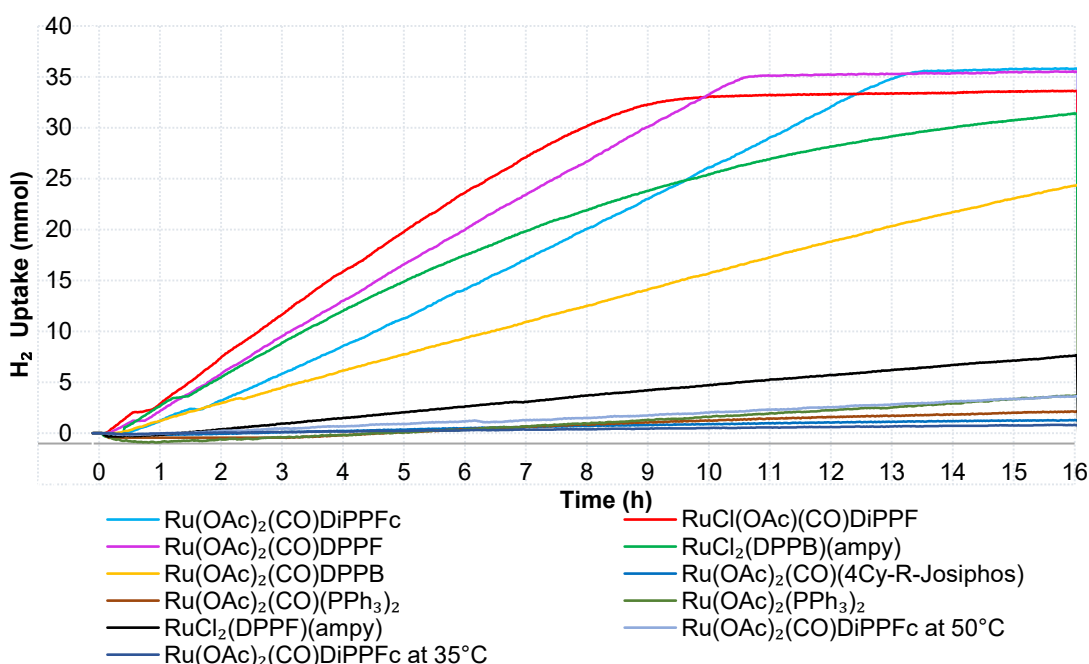


Figure 19 H_2 Uptake in HY promoted by carboxylate catalysts in presence of basic additive 1M $KOH_{(aq)}$.

The replacement of one acetate ligand with a chloride on the ruthenium monocarbonyl moiety in the $RuCl(OAc)(CO)(DiPPF)$, resulted in slightly higher activity and shorter time to reach the maximum uptake of H_2 (entry 11 Table 6) with respect to the corresponding diacetate complex. It is worth noting that the analogous dichloride carbonyl complexes have been described by Gimeno as dinuclear species $[RuCl_2(CO)(PP)]_2$ and were found active in TH reactions.^[28e] To investigate the effect of the acetate vs. chloride in catalysis, the complexes *cis*- $RuX_2(dppb)(ampy)$ ($X = Cl, OAc$) were tested in the hydrogenation of aldehydes. The carboxylate complex shows poor activity (entry 17 Table 6). By contrast, for the monocarbonyl derivatives the presence of acetate ligands which allows rapid activation, through dihydrogen splitting, appears to be crucial for the catalysis in neat condition (see section 2.4.5).

Table 6 HY promoted by acetate complexes in presence of basic additive KOH.

Entry	Catalyst	T [°C]	H_2 Uptake [h] ^[a]	Conversion [%] ^[b]	by-product [%] ^[b]
1	$Ru(OAc)_2(CO)DiPPF$	90	13.5	100	-
2	$Ru(OAc)_2(CO)dppf$	90	10.5	100	0.6
3	$Ru(OAc)_2(CO)(dppb)$	90	16	74.3	3.6
4	$Ru(OAc)_2(CO)(DCyPP)$	90	-	23.9	0.7
5	$Ru(OAc)_2(CO)(4Cy-Josiphos)$	90	-	55.7	4.3
6	$Ru(OAc)_2(CO)(4Cy-Josiphos)$	50	-	2.5	-
7	$Ru(OAc)_2(CO)DiPPF$	50	-	11.7	3.9
8	$Ru(OAc)_2(CO)DiPPF$	35	-	1.4	0.7

Entry	Catalyst	T [°C]	H ₂ Uptake [h] ^[a]	Conversion [%] ^[b]	by-product [%] ^[b]
9	Ru(OAc) ₂ (CO)(PPh ₃) ₂	90	-	12.0	2.2
10	Ru(OAc) ₂ (PPh ₃) ₂	90	-	11.8	-
11	RuCl(OAc)(CO)DiPPF	90	10	99.5	-
12	Ru(OAc) ₂ (CO)(Triphos)	90	-	75 ^[c]	-
13	RuH ₂ (CO)(Triphos)	90	-	67.4	0.8
14	NO [Ru]/None	90	-	1.9	1.9
15	RuCl ₂ (dppb)(ampy)	90	16	97.2	0.2
16	RuCl ₂ (dppf)(ampy)	90	-	31.1	0.4
17	<i>cis</i> -Ru(OAc) ₂ (dppb)(ampy)	90	-	7.5	2.6

[a] Approximate time for completion according to the hydrogen consumption data. [b] calculated by GC. [c] calculated by NMR. Substrate/Catalyst/1M KOH = 20,000/1/25, 90°C, 28 bar H₂

2.3.3 Hydrogenation of benzaldehyde in presence of KOH and ampy

Diamine ligands are well-known additive able to boost the rate of hydrogenation reactions of aldehydes and ketones, since the pioneering work of Noyori et al. ^[13] The effect of addition of ampy (10 equiv.) to the catalysts Ru(OAc)₂(CO)(DiPPF) and Ru(OAc)₂(CO)(dppf) was investigated in the HY under the same catalytic conditions described in section 3.1 (Figures 20, 21). For the complex **9** a slight acceleration effect, in comparison with the catalysis without ampy, was observed (Figure 20). The addition of ampy ligand neat or diluted in methanol led to much of the same results (TOF 2340 and 2350 h⁻¹ respectively) (entries 1, 3, Table 7). Lowering the amount of ampy to 5 equiv. resulted in a strong decreasing of activity (entry 2, Table 7), while in absence of base (KOH) partial conversion (73.9%) was achieved; suggesting that the activation of the catalyst occurs under relatively strong basic conditions (entry 5, Table 7).

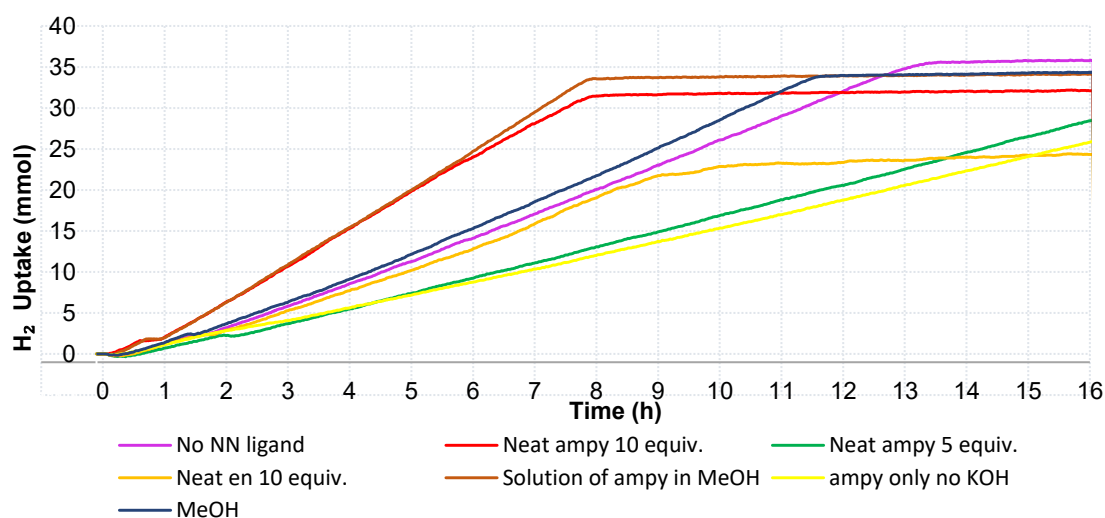


Figure 20 H_2 uptake in HY promoted by $Ru(OAc)_2(CO)(DiPPF)$ in presence of diamine additives.

The presence of MeOH in small quantity (50 μ L, 1.25 mmol) was also proven to enhance the activity of the ruthenium catalyst (entry 4, Table 7). Conversely, addition of ethylenediamine ligand had a detrimental effect resulting in a decreasing of the activity (entry 6, Table 7). By using the complex $Ru(OAc)_2(CO)(dppf)$ in presence of ampy modest conversion (53.9%) was achieved, as well as with ampy solution or with addition of methanol (Figure 21) (entries 7 - 9, Table 7).

Table 7 HY promoted by catalysts **9** and $Ru(OAc)_2(CO)(dppf)$ in the presence of nitrogen ligands and MeOH.

Entry	Catalyst	Additive/Solvent	H_2 Uptake [h] ^[a]	Conversion [%] ^[b]	by-product [%] ^[b]
1	$Ru(OAc)_2(CO)(DiPPF)$	neat ampy 10 equiv.	8.5	100	-
2	$Ru(OAc)_2(CO)(DiPPF)$	neat ampy 5 equiv.	-	82.8	-
3	$Ru(OAc)_2(CO)(DiPPF)$	ampy solution ^[d]	8	99.8	2.0
4	$Ru(OAc)_2(CO)(DiPPF)$	MeOH 50 μ L	11.5	99.9	0.1
5	$Ru(OAc)_2(CO)(DiPPF)$	neat ampy 10 equiv.	-	73.9 ^[e]	0.9
6	$Ru(OAc)_2(CO)(DiPPF)$	neat en 10 equiv.	14	95.4	-
7	$Ru(OAc)_2(CO)(dppf)$	neat ampy 10 equiv.	16	53.9	0.1
8	$Ru(OAc)_2(CO)(dppf)$	ampy solution ^[d]	-	38.1	2.4
9	$Ru(OAc)_2(CO)(dppf)$	MeOH 50 μ L	-	44.8	1.6
10	NO [Ru]	ampy solution ^[d]	-	2.0	2.0

[a] Approximate time for completion according to the hydrogen consumption data. [b] calculated by GC on. [c] calculated by NMR. [d] ampy 0.4 M in MeOH [e] no KOH was added. Substrate/Catalyst/1M KOH = 20,000/1/25, 90°C, 28 bar H_2

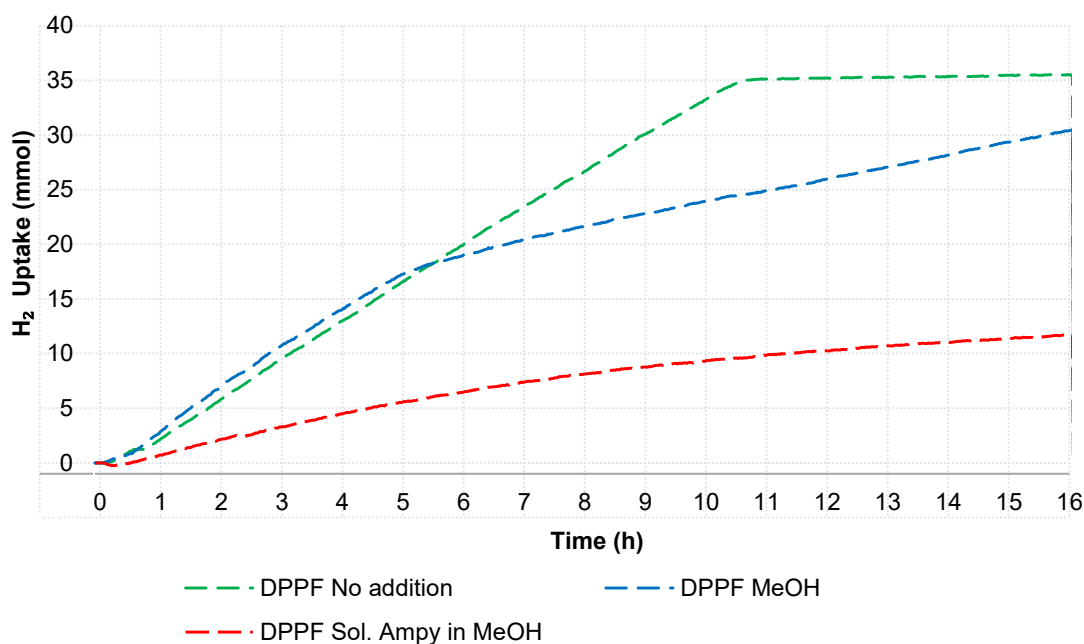
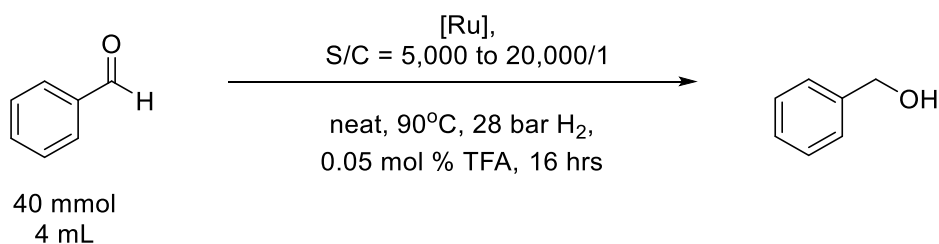


Figure 21 H_2 uptake in HY promoted by $Ru(OAc)_2(CO)(dppf)$ in presence of diamine additives.

2.3.4 Hydrogenation of Benzaldehyde in presence of acidic additives

Only few examples of Noyori's type catalysts, able to promote the HY under base free conditions, have been reported. Furthermore, Dupau et al. have shown the importance of the anionic ligand (i.e. carboxylate) that paves the way to the hydrogenation in acidic conditions.^[79] According to these studies, the H-H activation may occur through coordination of H_2 to the metal, followed by heterolytic dihydrogen splitting by a carboxylate oxygen of the ligand, affording the catalytically active Ru(II) hydride intermediate.

Herein, a modified version of the reduction in neat condition presented above was applied with three representative carboxylic acids as additive, namely acetic, trifluoroacetic and benzoic acid. Among them, the best enhancing effect on catalytic efficiency was found for the complexes bearing the basic DiPPF diphosphine in presence of trifluoroacetic acid (Scheme 16, Table 8).



Scheme 16 General condition for HY of benzaldehyde in presence of TFA additive.

The most active complexes found with KOH (1 M), were tested in absence of any additive, usually defined as *base free* catalysis or more generally under *neutral condition*, resulting in poor results (entries 1, 2, Table 8).

The activity of complexes, bearing aryl- or alkyl-diphosphines, were also tested in presence of carboxylic acids. In particular the activity of complex Ru(OAc)₂(CO)(DiPPF) (**9**) (0.01 - 0.25 mol%) was also investigated with different amounts of TFA (2 - 50 equiv.) (Figure 22) (entries 3 - 7, Table 8). By increasing the quantity of acid, the selectivity to the desired product is not affected, as well as the amounts of benzyl trifluoro acetal. Moreover, no observation of self-induced hydrogenation of the TFA to trifluoro ethanol was observed by NMR measurements, unlike previously reported for carboxylate complexes^[80] The best accordance between the H₂ consumption and final conversion data was obtained with 10 equiv. of acid (TOF 1900 h⁻¹). In all other cases, the plateau of the uptake curve, used to track the end of the reaction, was reached in shorter times, indicating higher activity (TOFs up to 4000 h⁻¹), but it lay at relatively low values of H₂ mmol consumed in comparison with the higher conversion observed by NMR. The slightly lower conversion calculated from the H₂ uptake with respect to the conversion calculated by NMR analysis was likely due to the low accuracy of the value for the hydrogen pressure. The conversion and activity calculated by NMR at the end of 16 h were in accordance with the ones obtained by GC (entries 8, 9, Table 8). Lower pressure of hydrogen and different substrate/catalyst ratios were also tested, founding that complex **9** was able to reach almost full conversion at 5 bar of H₂ with a S/C of 10000:1 in 16 h (entries 10 - 13, Table 8). Regarding complexes **11**, **12**, dppb and dppf analogs under the same conditions, none of them was able to reach high conversions (entries 14 - 18, Table 8). Only the RuCl(OAc)(CO)(DiPPF) showed an activity comparable to the Ru(OAc)₂(CO)(DiPPF) (entry 19, Table 8) with TOF 1350 h⁻¹ and a conversion to the desired product of 98.5%. Interestingly, in slightly acidic condition the hydrogenation of benzaldehyde was not promoted by dichloride or diacetate complexes without the CO ligand, namely RuCl₂(dppb)(ampy) RuCl₂(dppf)(ampy) and cis-Ru(OAc)₂(dppb)(ampy) (entries 20 - 22, Table 8). Furthermore, addition of acetic and benzoic acid gave no appreciable improving of the reaction rate with respect to the test without additives, for both chloride and carboxylate complexes (entries 25 - 30, Table 8).

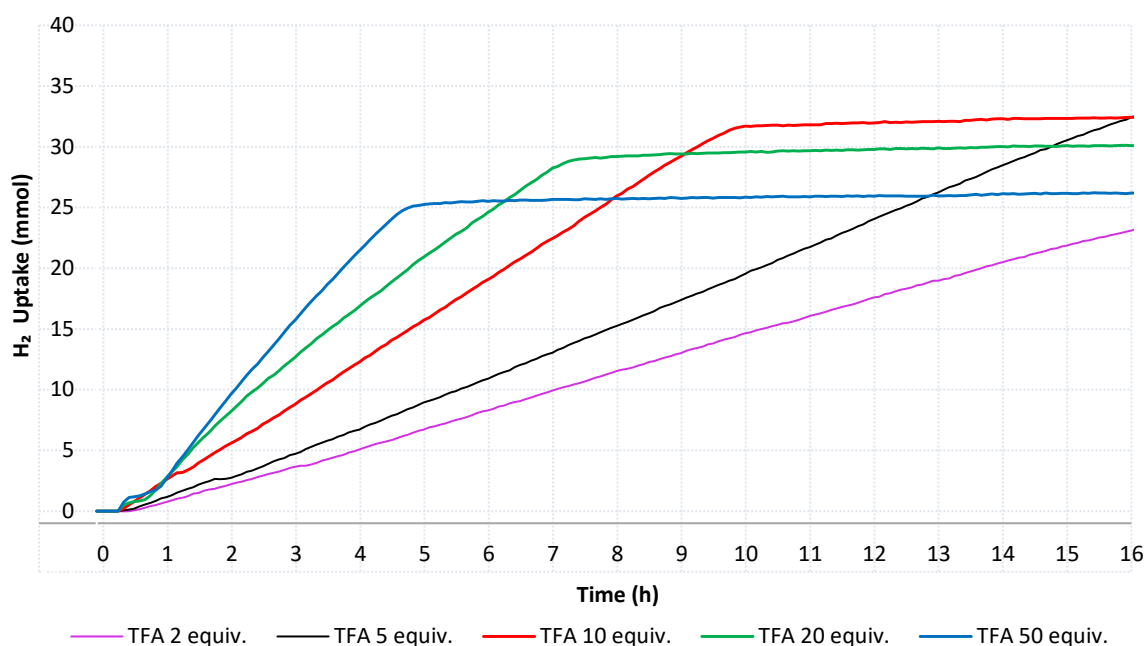


Figure 22 H₂ Uptake in HY promoted by Ru(OAc)₂(CO)(DiPPF) with different equiv. of TFA

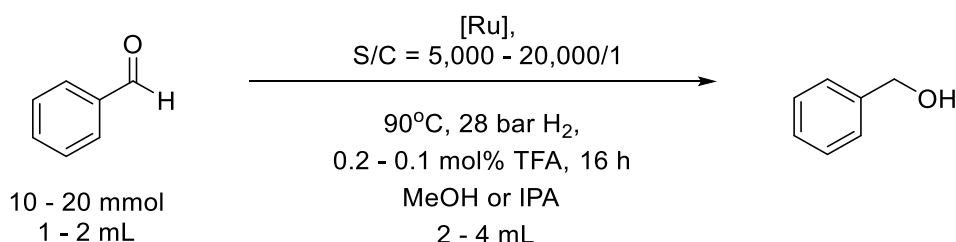
Table 8 HY neat promoted by acetate catalysts **9**, **12** and other ruthenium congeners in slightly acid condition

Entry	Catalyst	S/C	T [°C]	P [bar]	Additive % ^[d] (equiv. to [Ru])	H ₂ uptake [h] ^[a]	Conv. [%] ^[b]	by-product [%] ^[b]
1	Ru(OAc) ₂ (CO)(DiPPF)	20k:1	90	28	NO ADDITIVE	-	45.5	0.5
2	Ru(OAc) ₂ (CO)(dppf)	20k:1	90	28	NO ADDITIVE	-	37.1	2.5
3	Ru(OAc) ₂ (CO)(DiPPF)	20k:1	90	28	TFA 0.01 (2)	-	72.7 ^[c]	7.2 ^[c]
4	Ru(OAc) ₂ (CO)(DiPPF)	20k:1	90	28	TFA 0.025 (5)	16	93.8 ^[c]	0.9 ^[c]
5	Ru(OAc) ₂ (CO)(DiPPF)	20k:1	90	28	TFA 0.1 (10)	11	98.0 ^[c]	0.6 ^[c]
6	Ru(OAc) ₂ (CO)(DiPPF)	20k:1	90	28	TFA 0.2 (20)	8	99.5 ^[c]	0.3 ^[c]
7	Ru(OAc) ₂ (CO)(DiPPF)	20k:1	90	28	TFA 0.5 (50)	6	99.9 ^[c]	0.8 ^[c]
8	Ru(OAc) ₂ (CO)(DiPPF)	20k:1	90	28	TFA (10)	13	100.0	4.0
9	Ru(OAc) ₂ (CO)(DiPPF)	20k:1	90	28	TFA (15)	11	100.0	-
10	Ru(OAc) ₂ (CO)(DiPPF)	20k:1	90	10	TFA (10)	-	36.0	-
11	Ru(OAc) ₂ (CO)(DiPPF)	20k:1	90	5	TFA (10)	-	29.8	4.7
12	Ru(OAc) ₂ (CO)(DiPPF)	20k:1	90	5	TFA (10)	-	21.3	-
13	Ru(OAc) ₂ (CO)(DiPPF)	10k:1	90	5	TFA (10)	16	94.8	2.0
14	Ru(OAc) ₂ (CO)(DCyPP)	20k:1	90	28	TFA (10)	-	17.7	3.2
15	Ru(OAc) ₂ (CO)(4Cy-Josiphos)	20k:1	90	28	TFA (10)	-	69.5	4.9
16	Ru(OAc) ₂ (CO)(4Cy-Josiphos)	20k:1	50	28	TFA (10)	-	3.4	2.8
17	Ru(OAc) ₂ (CO)(dppb)	20k:1	90	28	TFA (10)	-	21.5	2.7
18	Ru(OAc) ₂ (CO)(dppf)	20k:1	90	28	TFA (10)	-	62.6	2.2
19	RuCl(OAc)(CO)(DiPPF)	20k:1	90	28	TFA (10)	15	99.3	0.8
20	RuCl ₂ (dppb)(ampy)	20k:1	90	28	TFA (10)	-	5.6	-
21	RuCl ₂ (dppf)(ampy)	20k:1	90	28	TFA (10)	-	2.0	-
22	<i>cis</i> -Ru(OAc) ₂ (dppb)(ampy)	20k:1	90	28	TFA (10)	-	12.1	4.8
23	Ru(OAc) ₂ (CO)(Triphos)	20k:1	90	28	TFA (10)	-	22	9.6
24	RuH ₂ (CO)(Triphos)	20k:1	90	28	TFA (10)	-	13.3	2.8

Entry	Catalyst	S/C	T [°C]	P [bar]	Additive % ^[d] (equiv. to [Ru])	H ₂ uptake [h] ^[a]	Conv. [%] ^[b]	by-product [%] ^[b]
25	Ru(OAc) ₂ (CO)(DiPPF)	20k:1	90	28	HOAc (10)	-	63.8	1.7
26	Ru(OAc) ₂ (CO)(DiPPF)	20k:1	90	28	Benzoic Acid (10)	-	58.9	4.9
27	Ru(OAc) ₂ (CO)(dppf)	20k:1	90	28	Benzoic Acid (10)	-	47.7	9.3
28	RuCl ₂ (dppb)(ampy)	20k:1	90	28	Benzoic Acid (10)	-	9.2	-
29	RuCl ₂ (dppf)(ampy)	20k:1	90	28	Benzoic Acid (10)	-	3.4	-
30	<i>cis</i> -Ru(OAc) ₂ (dppb)(ampy)	20k:1	90	28	Benzoic Acid (10)	-	7.7	2.7
31	NO [RU] / NONE	-	90	28	TFA 0.1	-	2.0	2.0

[a] Approximate time for completion according to the hydrogen consumption data. [b] calculated by GC. [c] calculated by NMR. [d] 0.1% respect to the substrate.

Tests were also carried out at 10 and 20 mmol scale with S/C 5000 – 20000, using methanol and 2-propanol as solvents at 90 °C and 28 bar of H₂ (Scheme 17, Table 9).



Scheme 17 General condition for the HY of benzaldehyde in MeOH or IPA in presence of TFA

Employment of MeOH afforded up to 50% of undesired condensations products. The formation of by-products, such as hemiacetal or acetal of benzaldehyde with the methanol, is favoured in acidic conditions. This rapid equilibrium reduces the amount of available substrate, leading to a lower selectivity and reaction rate (entries 1, 2, Table 9). This behaviour was not observed in 2-propanol (IPA), in which full conversion was obtained in 2 - 4 h, depending on the concentration of the substrate (10 or 5 M). Reducing the amount of catalyst to S/C = 20k:1 resulted in a drop of activity (entries 3, 4, 5, Table 9). Control experiments show that in absence of H₂ pressure, no conversion was observed, indicating that the contribution of TH to the reduction process appears negligible (entry 6, Table 9). The non-carbonyl precursor Ru(OAc)₂(DiPPF) **2** in the same conditions showed a modest 38.8% conversion (entry 7, Table 9).

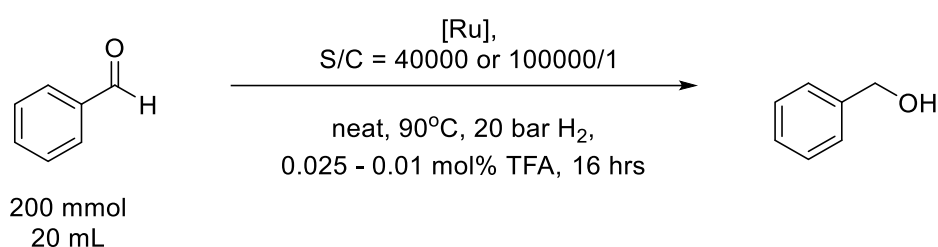
Table 9 HY in solution promoted by catalysts **9** and **2** in slightly acid conditions.

Entry	Catalyst	Sub. Conc. [M]	S/C	T	P	Solvent/ Additive (equiv. to [Ru])	H ₂ Uptake ^[a] [h]	Conversion ^[b] [%]	by-product [%] ^[b]
1	Ru(OAc) ₂ (CO)(DiPPF)	2.5	5k:1	90	28	MeOH, TFA (10)	9	100	25.0
2	Ru(OAc) ₂ (CO)(DiPPF)	2.5	5k:1	60	20	MeOH, TFA (10)	16	93.4	47.6
3	Ru(OAc) ₂ (CO)(DiPPF)	10	10k:1	90	28	IPA, TFA (10)	2	99.5 ^[c]	0.1 ^[c]
4	Ru(OAc) ₂ (CO)(DiPPF)	5	10k:1	90	28	IPA, TFA (10)	3.5	99.9 ^[c]	0.3 ^[c]

Entry	Catalyst	Sub. Conc. [M]	S/C	T	P	Solvent/ Additive (equiv. to [Ru])	H ₂ Uptake ^[a] [h]	Conversion ^[b] [%]	by-product [%] ^[b]
5	Ru(OAc) ₂ (CO)(DiPPF)	10	20k:1	90	28	IPA, TFA (10)	14	97.1 ^[c]	0.6 ^[c]
6	Ru(OAc) ₂ (CO)(DiPPF)	10	20k:1	90	0	IPA, TFA (10)	-	1.0 ^[c]	-
7	Ru(OAc) ₂ (DiPPF)	10	20k:1	90	28	IPA, TFA (10)	-	38.8 ^[c]	4.0 ^[c]

[a] Approximate time for completion according to the hydrogen consumption data. [b] calculated by GC. [c] calculated by NMR.

In order to verify the scalability of this solvent free catalysis, the hydrogenation benzaldehyde was performed on 200 mmol scale at S/C of 40000 and 100000 in a 50 ml Parr Autoclave at 20 bar of H₂ and 90 °C with the optimized acidic conditions.



Scheme 18 General condition for HY of benzaldehyde in slightly acidic conditions in Parr Autoclave.

Full conversion of the benzaldehyde to benzyl alcohol has been observed with the Ru(OAc)₂(CO)(DiPPF) at both loadings in 23 and 50 h (entries 1, 2, Table 10, Figure 23), reaching TON of 965000. The relative increase of impurities in the system from the undistilled aldehyde could induce deactivation processes,^[7] interestingly, the catalyst activity, was not altered by the decreased loading (S/C 25000 and 100000) with TOF of 1380 and 2280 h⁻¹ respectively), while the analogous dpf complex achieved only 30% conversion at S/C 100000 (Table 10).

Table 10 HY of neat benzaldehyde in slightly acidic conditions on 200 mmol scale in Parr Autoclave.

Entry	Catalyst	S/C	Additive (equiv. to [Ru])	H ₂ Uptake [h] ^[a]	Conversion [%] ^[b]	by-product [%] ^[b]
1	Ru(OAc) ₂ (CO)(DiPPF)	40k:1	TFA (10)	18	100.0	3
2	Ru(OAc) ₂ (CO)(DiPPF)	100k:1	TFA (10)	50	100.0	3.5
3	Ru(OAc) ₂ (CO)(dpf)	100k:1	TFA (10)	-	30.0	-

[a] Approximate time for completion according to the hydrogen consumption data. [b] calculated by GC

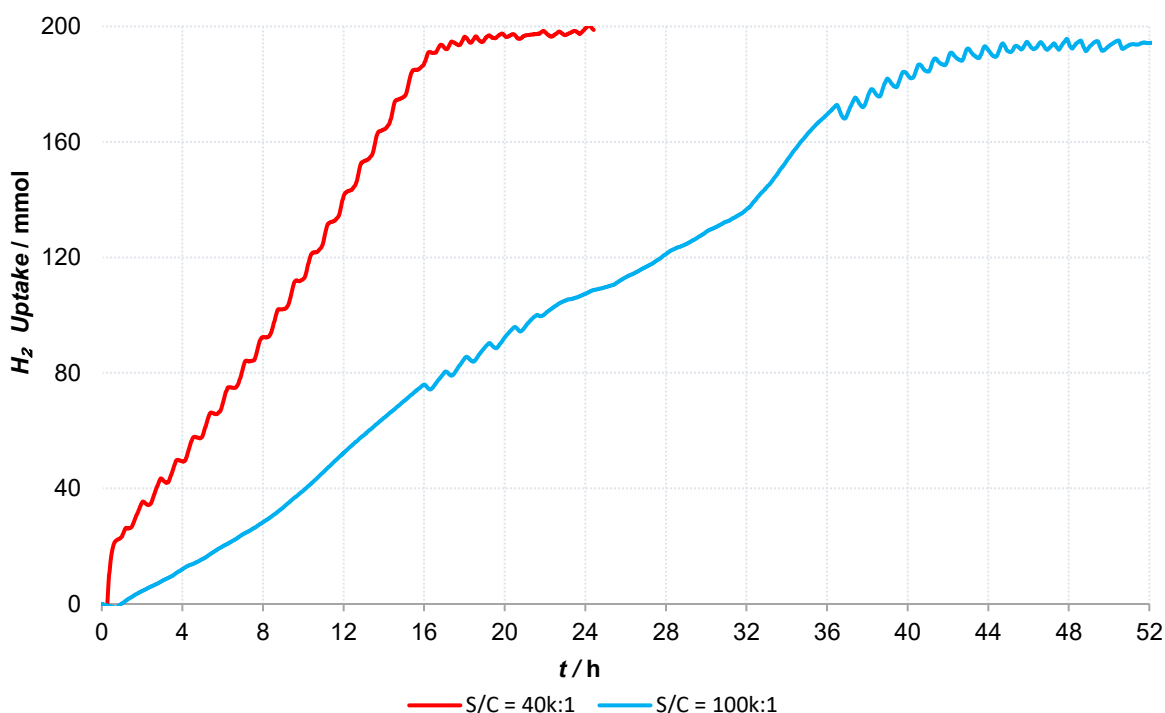


Figure 23 H₂ uptake in HY in slightly acidic conditions promoted by Ru(OAc)₂(CO)(DiPPF) at S/C 40k:1 and 100k:1.

2.3.5 Hydrogenation of benzaldehyde promoted by non-carbonyl compounds

The activity of the diacetate non-carbonyl ruthenium complexes **1**, **2** and Ru(OAc)₂(rac-BINAP) was compared to that of the carbonyl derivatives in neat conditions and by adding both basic (KOH) and acidic (TFA) additives (Table 11). In all the tests non-carbonyl acetate complexes gave generally poor or no conversion, regardless of the nature of the phosphines, indicating the crucial role of the CO ligand, in retarding catalyst deactivation *via* poisoning processes.

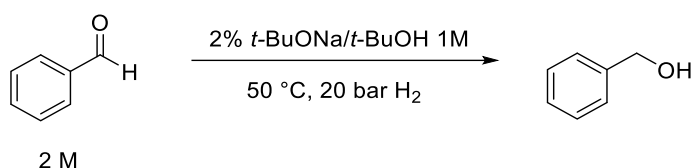
Table 11 HY of neat benzaldehyde of Ru(OAc)₂(PP) complexes with KOH or TFA additives (S/C= 20k:1, 90°C, 28 bar H₂).

Entry	Catalyst	S/C	T	P	Base ^[a]	Additive (equiv. to [Ru])	Conversion [%] ^[a]	by-product [%] ^[a]
1	Ru(OAc) ₂ (PPh ₃) ₂	20k:1	90	28	KOH	-	11.8	-
2	Ru(OAc) ₂ (PPh ₃) ₂	20k:1	90	28	KOH	Ampy sol.(10)	4.6	4.6
3	Ru(OAc) ₂ (rac-BINAP)	20k:1	90	28	KOH	-	2.3	-
4	Ru(OAc) ₂ (rac-BINAP)	20k:1	90	28	-	TFA (10)	6.0	-
5	Ru(OAc) ₂ (DiPPF)	20k:1	90	28	KOH	-	8.2	0.4
6	Ru(OAc) ₂ (DiPPF)	20k:1	90	28	KOH	Ampy neat (10)	4.2	-
7	Ru(OAc) ₂ (DiPPF)	20k:1	90	28	-	TFA (15)	3.3	0.9

Entry	Catalyst	S/C	T	P	Base [a]	Additive (equiv. to [Ru])	Conversion [%] [a]	by-product [%] [a]
8	Ru(OAc) ₂ (dppb)	20k:1	90	28	KOH	Ampy neat (10)	15.3	-
9	Ru(OAc) ₂ (dppb)	20k:1	90	28	-	Ampy neat (10)	7.9	4.5
10	Ru(OAc) ₂ (dppb)	20k:1	90	28	-	TFA (15)	4.9	1.2

[a] Solution of 1M KOH 0.125 mol%; [b] calculated by GC

Furthermore, the influence of methanol as solvent was investigated, under the same conditions previously described by Baldino et al. (benzaldehyde 10 mmol, 1mL, 2M in MeOH 4mL, S/C 1000:1).^[81]



Scheme 19 General condition for the HY of benzaldehyde in MeOH

By contrast to the acidic conditions, in the presence of a base no formation of the acetal was observed as main product, affording high conversions in all reactions (Table 12). Finally, the activity of the diacetate dppb complex was found to enhance in presence of the ampy ligand, in accordance with the *in situ* formation of the Noyori's type complex RuL₂(PP)(NN), resulting higher with respect to the preformed complex Ru(OAc)₂(dppb)(ampy) (entry 6, Table 12). This indicates that non-carbonyl complexes give better performance in presence of MeOH, while in solvent free systems the monocarbonyl complexes are superior.

Table 12 HY of benzaldehyde in MeOH promoted by non-carbonyl complexes containing dppb.

Entry	Catalyst	T	P	Base	Solvent/Additive	H ₂ Uptake [h] [a]	Conversion [%] [b]	by-product [%] [b]
1	cis-Ru(OAc) ₂ (dppb)(ampy)	90	28	<i>t</i> -BuONa 1M 2%	MeOH 4 mL	2	100	3.9
2	cis-Ru(OAc) ₂ (dppb)(ampy)	50	28	<i>t</i> -BuONa 1M 2%	MeOH 4 mL	3	99.9	5.0
3	cis-Ru(OAc) ₂ (dppb)(ampy)	50	20	<i>t</i> -BuONa 1M 2%	MeOH 4 mL	1	100	6.7
4	cis-Ru(OAc) ₂ (dppb)(ampy)	90	20	1M KOH 0.5%	MeOH 4 mL	5	100	0.8
5	cis-Ru(OAc) ₂ (dppb)(ampy)	90	28	1M KOH 0.5%	MeOH 4 mL	12	100	1.3
6	Ru(OAc) ₂ (dppb)	50	20	<i>t</i> -BuONa 1M 2%	MeOH 4 mL, ampy ^[c]	0.5	100	0.7
7	Ru(OAc) ₂ (dppb)	50	20	<i>t</i> -BuONa 1M 2%	MeOH 4 mL	15	89.8	1.3
8	Ru(OAc) ₂ (PPh ₃) ₂	50	20	<i>t</i> -BuONa 1M 2%	MeOH 4 mL	16	92.2	3.0

[a] Approximate time for completion according to the hydrogen consumption data. [b] calculated by GC

[c] Neat ampy 2.5 equiv. (benzaldehyde 10mmol, 1mL, 2M, S/C 1000:1)

2.3.6 KOH vs TFA in HY of benzaldehyde

To clarify the dependence of the performance of different classes of complexes upon the additive used, a graphical comparison of the activity in the HY of benzaldehyde with KOH (0.125 mol%) or TFA (0.05 mol%) is presented in Figure 24. Based on the data collected in Table 13, each bar represents the conversion, while the top flags indicate the corresponding time for the maximum uptake of H₂.

Table 13 Comparison of catalytic activity with KOH and TFA additives in the same reaction conditions (S/C= 20k:1, 90°C, 28 bar H₂).

Catalyst	Product with KOH [%]	H ₂ Uptake with KOH [h]	Product with TFA [%]	H ₂ Uptake with TFA [h]
Ru(OAc) ₂ (CO)(DiPPF)	100.0	13.5	98.2	9.5
Ru(OAc) ₂ (CO)(dppf)	99.4	10.5	60.4	-
Ru(OAc) ₂ (CO)(dppb)	70.7	16.0	18.8	-
Ru(OAc) ₂ (CO)(DCyPP)	23.2	-	14.5	-
Ru(OAc) ₂ (CO)(4Cy-Josiphos)	51.4	-	64.6	-
RuCl(OAc)(CO)(DiPPF)	99.5	10.0	98.5	15.0
RuH ₂ (CO)(Triphos)	66.6	-	15.0	-
RuCl ₂ (dppb)(ampy)	97.0	16.0	5.6	-
RuCl ₂ (dppf)(ampy)	30.7	-	2.0	-
cis-Ru(OAc) ₂ (dppb)(ampy)	4.9	-	7.3	-

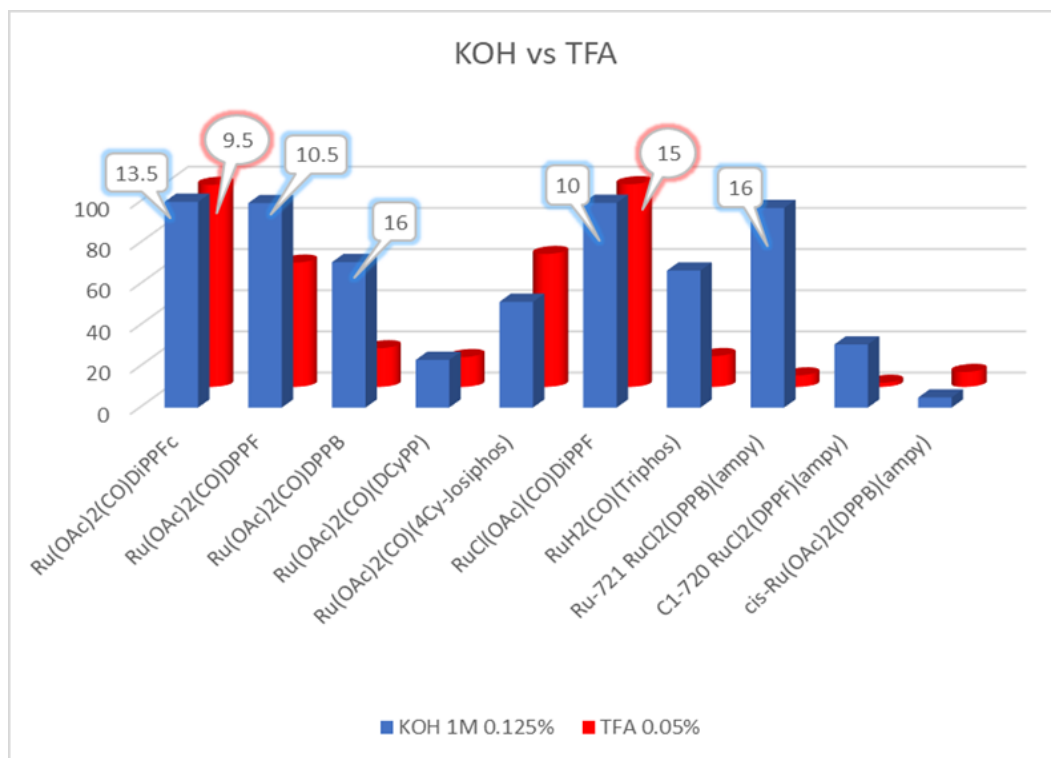


Figure 24 Graphical comparison of the obtained conversions with KOH and TFA in the same reaction conditions (S/C= 20k:1, 90°C, 28 bar H₂)

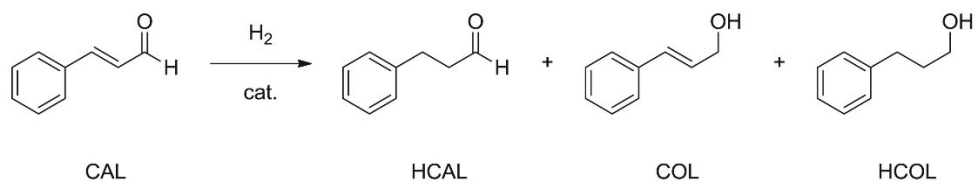
The presence of base proven to be a more general condition in which both acetate and chloride complexes were able to be activated. On the other hand, with TFA, only the acetate complexes showed activity. Among them, only the alkyl DiPPF diphosphine ligand promoted high conversions. Its strong trans effect favours the exchange between the hemilabile carboxylate acetate ligands and the TFA, through a protonation reaction.

The activity of the Ru monocarbonyl complexes without base additives opens the way for the reduction of aldehydes at new pH conditions in which the classical halide complexes tested are not active at all. Moreover, only the complexes that bears the CO ligand proved to be active in solvent free conditions, this is a confirmation that the fragment Ru(PP)(CO) is very robust even in presence of bulky and basic diphosphines that in principle would be easier to be oxidised or protonated.

2.3.7 Hydrogenation of α,β -unsaturated aldehydes

Since one of the aim of this PhD work was the synthesis of food relevant and bioactive compounds, the best catalytic system found during the precedent screening was applied to the reduction of α,β -unsaturated aldehydes; a class of naturally occurring molecules appealing to the industry for the production of unsaturated primary alcohols used as aromas, flavours or drugs.^[82] However, catalytic hydrogenation of organic compounds possessing multiple unsaturated bonds is particularly challenging and requires complexes able to promote the preferential activation of the C=O function with respect to the thermodynamically more favoured reduction of the C=C by ca. 35 kJ/mol.^[83]

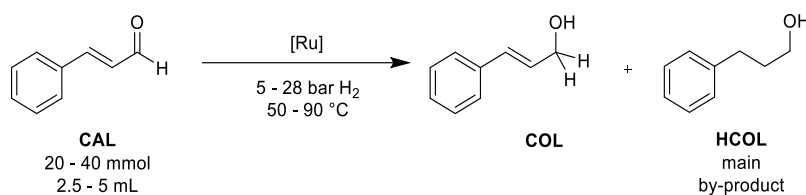
The selective hydrogenation of cinnamaldehyde (CAL) to cinnamyl alcohol (COL) is an exemplar substrate of industrial interest. The hydrogenation of CAL can produce COL, hydrocinnamaldehyde (HCAL), hydrocinnamyl alcohol (HCOL), since the hydrogenation of the C=C bond is thermodynamically favoured (Scheme 20). COL is commercially manufactured from CAL *via* the well-known Meerwein–Ponndorf–Verley reduction, where the strong oxophilic aluminum triisopropoxide is used as a reagent. Although COL is obtained in high yields by this process, disposal of aluminum salts is a major drawback of this method.^[84]



Scheme 20 All possible products deriving from the HY of trans-cinnamaldehyde.

High selectivity up to 90% toward COL has been reported for supported ruthenium catalysts,^[85] with turn-over frequencies ranging between 6 and 450 h⁻¹. In homogeneous HY the catalysts exploited are usually based on Ru, Os, Rh and Ir, bearing diphosphine/diamine ligand pairs or pincer ligands.^[49, 86] In industrial applications, ruthenium is strongly preferred thanks to the lower price with respect to Rh or Ir. High selectivity towards the allylic alcohols were obtained with ruthenium complexes based on water-soluble ligands, but slow deactivation reactions between the product and the phosphine ligand could poison the catalyst.^[87]

Therefore, the neat conditions found in this work for benzaldehyde represent the best compromise between the advantages granted by heterogeneous applications, like solvent free systems and no treatments of substrates, and the well-defined metal center of the homogeneous catalysis. Those conditions were tuned to achieve the best performance with regard to conversion, productivity and chemo-selectivity in presence of different Ru(OAc)₂(CO)(PP) complexes, bearing various diphosphines, starting at S/C 20000. The best results have been achieved by the complex Ru(OAc)₂(CO)(dppb) and the DiPPF analogous **9** (entries 1, 12, Table 14) with TOF 810 and 1795 h⁻¹. Higher loadings of catalyst were exploited (10k:1 and 5k:1) and lower pressure of H₂ was operated, to avoid the C=C double bond reduction (entries 13 – 21, Table 14). Interestingly, lowering the amount of catalyst and the pressure did not alter significantly the activity; the 5k:1 loading under 10 bar of hydrogen showed TOF 1412 h⁻¹ and a selectivity of 88% for the carbonyl group, whereas with 5 bar pressure TOF 1062 h⁻¹ was found. The lower pressure also gave the best chemo-selectivity of 92% toward the C=O over the C=C, but unfortunately require longer reaction time to fully convert the substrate. On the other hand, at temperature lower than 90°C poor activity is observed (entries 15 - 17, 20 - 21, Table 14). Surprisingly, the reactions in presence of basic additive 1M KOH resulted in very low conversions regardless of the complex used (entries 3, 5, 7, 9-11, Table 14).



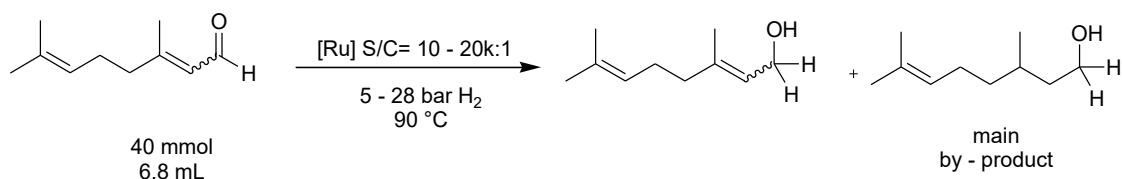
Scheme 21 Reaction conditions for the HY of neat cinnamaldehyde (CAL).

Table 14 Hydrogenation of trans-cinnamaldehyde in solvent free conditions

Entry	Catalyst	S/C	T [°C]	P [bar]	Base [a]	Acid (equiv. to Ru)	H ₂ Uptake [h] ^[b]	Conv. [%] ^[c]	by-products [%] ^[c]
1	Ru(OAc) ₂ (CO)(dppb)	20k:1	90	28	-	TFA (10)	16	64.8	7.2
2	Ru(OAc) ₂ (CO)(dppb)	20k:1	90	10	-	TFA (10)	-	18.0	-
3	Ru(OAc) ₂ (CO)(dppf)	20k:1	90	28	KOH	-	-	35.7	3.5
4	Ru(OAc) ₂ (CO)(dppf)	20k:1	90	28	-	TFA (10)	-	8.8	2.0
5	Ru(OAc) ₂ (CO)(PPh ₃) ₂	20k:1	90	28	KOH	-	-	12.0	2.2
6	Ru(OAc) ₂ (CO)(PPh ₃) ₂	20k:1	90	28	-	TFA (10)	-	6.9	0.1
7	RuCl(OAc)(CO)(DiPPF)	20k:1	90	28	KOH	-	-	37.4	6.4
8	RuCl(OAc)(CO)(DiPPF)	20k:1	90	28	-	TFA (10)	-	42.6	15.5
9	RuCl ₂ (dppb)(ampy)	20k:1	90	28	KOH	-	-	8.0	6.1
10	cis-Ru(OAc) ₂ (dppb)(ampy)	20k:1	90	28	KOH	-	-	7.5	2.6
11	Ru(OAc) ₂ (CO)(DiPPF)	20k:1	90	28	KOH	-	-	53.5	8.0
12	Ru(OAc) ₂ (CO)(DiPPF)	20k:1	90	28	-	TFA (10)	10h	89.8	19.5
13	Ru(OAc) ₂ (CO)(DiPPF)	20k:1	90	10	-	TFA (10)	-	37.7	7.9
14	Ru(OAc) ₂ (CO)(DiPPF)	10k:1	90	10	-	TFA (10)	-	74.8	11.6
15	Ru(OAc) ₂ (CO)(DiPPF)	10k:1	60	10	-	TFA (5)	-	14.0	5.0
16	Ru(OAc) ₂ (CO)(DiPPF)	10k:1	50	10	-	TFA (10)	-	12.0	7.0
17	Ru(OAc) ₂ (CO)(DiPPF)	10k:1	50	5	-	TFA (10)	-	10.5	7.5
18	Ru(OAc) ₂ (CO)(DiPPF)	5k:1	90	10	-	TFA (10)	14	98.5	13.5 ^{[d][e]}
19	Ru(OAc) ₂ (CO)(DiPPF)	5k:1	90	5	-	TFA (10)	16	85.2	10.9 ^{[d][f]}
20	Ru(OAc) ₂ (CO)(DiPPF)	5k:1	50	10	-	TFA (10)	-	22.9	9.3
21	Ru(OAc) ₂ (CO)(DiPPF)	5k:1	50	5	-	TFA (10)	-	27.3	21.8
22	NO RU / NONE	-	RT	28	-	TFA 0.2% ^[h]	-	85.0	85.0 ^[g]

[a] Solution of KOH 1M 0.125 mol%; [b] Approximate time for completion according to the hydrogen consumption data; [c] Calculated by GC; [d] Calculated by NMR; [e] 11.3% HCOL; [f] 6.4% HCOL; [g] 0% HCOL; [h] 0.2% in respect of the aldehyde; S/C= 5 – 20k:1, T=50 - 90°C, P= 5 – 28 bar

The same procedure was applied to the citral, a 2:1 mixture of the aldehydes geranial and neral with remarkable industrial interest for the synthesis of geraniol and nerol. For the HY in neat conditions, this substrate was used without any treatment, affording a mixture of alcohol products which were analyzed by GC and NMR techniques. The literature about the separation of the resulting terpenic alcohols is extensive and can be performed on silica,^[88] with enzymes or on β-cyclodextrins with high yield and low loss of nerol isomer, as recently established.^[89]



Scheme 22 Reaction conditions for the HY of neat citral mixture.

After some testing at 20k:1 loading of $\text{Ru}(\text{OAc})_2(\text{CO})(\text{DiPPF})$, the best performance in terms of conversion and chemo-selectivity was achieved at S/C = 10k:1 with 28 and 10 bar H_2 with TOF 1600 and 910 h^{-1} (entries 4, 5, Table 15). Increasing the temperature led to lower selectivity and conversion (entry 3 Table 15). It worth noting that the complexes $\text{Ru}(\text{OAc})_2(\text{CO})(\text{dppf})$ and $\text{RuCl}(\text{OAc})(\text{CO})(\text{DiPPF})$ showed a better turn over frequencies (2000 and 1428 h^{-1}) and high productivity, but the chemo-selectivity was lower with respect to the $\text{Ru}(\text{OAc})_2(\text{CO})(\text{DiPPF})$ (**9**) complex, as established by GC and NMR techniques. It is worth pointing out that the NMR analysis was crucial for the determination of the nerol and \pm -citronellol content, since the GC separation of these compounds resulted a difficult task. Figure 25 and Figure 26 display the overlapping of the GC peaks of nerol and \pm -citronellol (t_R 5.41-5.43), and how the shape of the peak changed according to the ratio nerol\citronellol. The citronellal chromatogram in Figure 26 showed that no production of saturated aldehyde occurs during HY in neat acidic conditions.

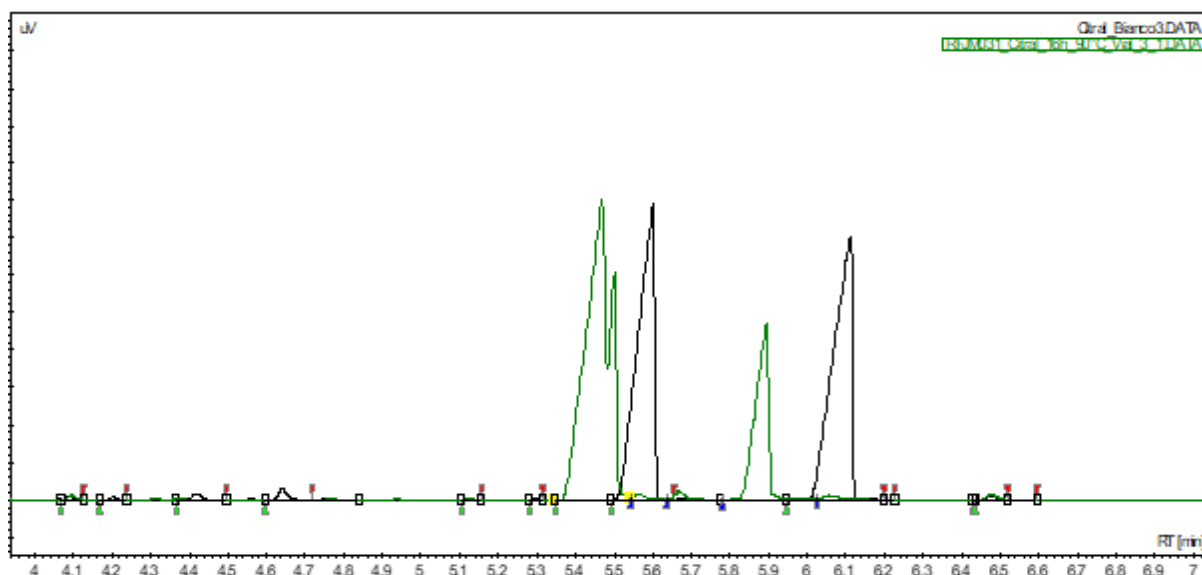


Figure 25 exemplar GC of high conversion HY of citral (entry 5, Table 15): alcohols (t_R 5.41-5.43, 5.86 min) superimposed with citral (t_R 5.54, 6.1 min) chromatogram.

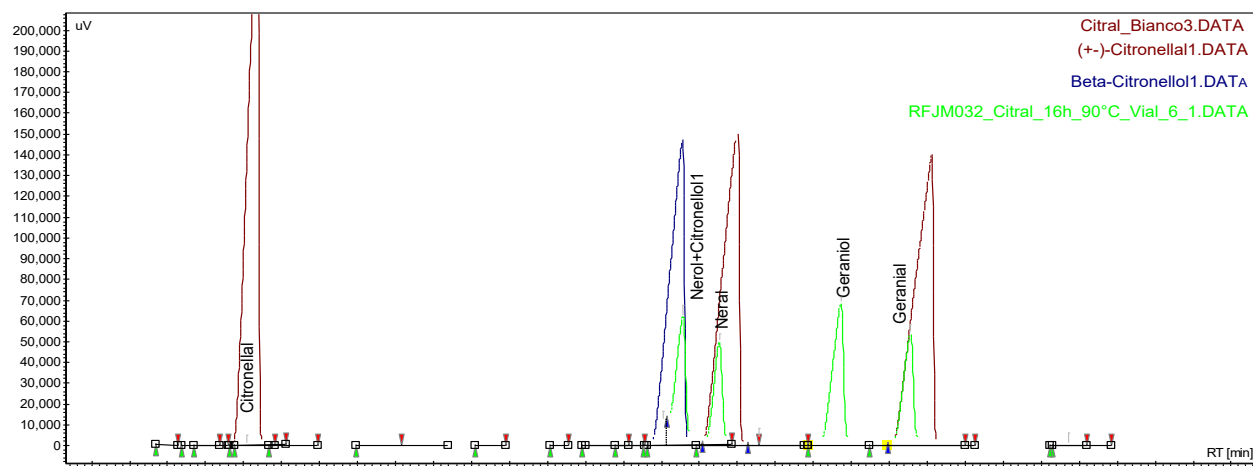


Figure 26 exemplars GC of low conversion HY of citral (entry 3, Table 15): alcohols (t_R 5.41-5.43, 5.86) superimposed with starting material (t_R 5.54, 6.1), citronellal (t_R 4.31) and \pm -citronellol (t_R 5.41) chromatograms.

Table 15 Hydrogenation of citral with $Ru(OAc)_2(CO)PP$ complexes.

Entry	Catalyst	S/C	T [°C]	P [bar]	Base ^[a]	Acid (equiv. to Ru)	H ₂ Uptake [h] ^[b]	Conv. [%] ^[c]	by-products [%] ^[d]	Selectivity C=O/C=C [%] ^[d]
1	$Ru(OAc)_2(CO)(DiPPF)$	20k:1	90	28	KOH	-	-	15.4	-	-
2	$Ru(OAc)_2(CO)(DiPPF)$	20k:1	90	28	-	TFA (10)	-	80.5	12.4	87%
3	$Ru(OAc)_2(CO)(DiPPF)$	20k:1	120	10	-	TFA (10)	-	61.4	23.9	74%
4	$Ru(OAc)_2(CO)(DiPPF)$	10k:1	90	28	-	TFA (10)	8	97.2	8.5	93%
5	$Ru(OAc)_2(CO)(DiPPF)$	10k:1	90	10	-	TFA (10)	11	90.3	11.7	90%
6	$Ru(OAc)_2(CO)(DiPPF)$	10k:1	90	5	-	TFA (10)	16	86.3	11.1	88%
7	$Ru(OAc)_2(CO)(dppf)$	20k:1	90	28	KOH	-	-	27.6	-	-
8	$Ru(OAc)_2(CO)(dppf)$	20k:1	90	28	-	TFA (10)	16	78.7	27.2	70%
9	$Ru(OAc)_2(CO)(dppf)$	10k:1	90	28	-	TFA (10)	10	98.3	22.4	78%
10	$Ru(OAc)_2(CO)(dppb)$	20k:1	90	28	-	TFA (10)	-	10.4	-	-
11	$Ru(OAc)_2(CO)(dppb)$	20k:1	90	10	-	TFA (10)	-	19.3	-	-
12	$RuCl(OAc)(CO)(DiPPF)$	20k:1	90	28	KOH	-	-	22.2	5.4	-
13	$RuCl(OAc)(CO)(DiPPF)$	20k:1	90	28	-	TFA (10)	14	98.7	55.3	45%
14	$Ru(OAc)_2(CO)(DiPPF)$	20k:1	90	28	-	Benzoic Acid (10)	-	19.3	-	-
15	$Ru(OAc)_2(CO)(DiPPF)$	10k:1	90	28	-	Benzoic Acid (10)	-	49.3	-	-
16	$Ru(OAc)_2(CO)(dppf)$	20k:1	90	28	-	Benzoic Acid (10)	-	26.4	-	-
17	NO RU	-	90	28	-	-	-	0	-	-
18	NO RU	-	90	28	-	TFA 0.7%	-	0	-	-

[a] Solution of KOH 1M 0.125 mol%; [b] Approximate time for completion according to the hydrogen consumption data; [c] Calculated by GC; [d] Calculated by NMR.

Furfural (FAL) is also an important chemical, readily accessible from carbohydrate cellulosic biomass that has attracted significant attention worldwide, as a cheap feedstock for renewable liquid fuels and chemical productions as furan and furfuryl alcohol (FOL).^[90] FOL finds application in the manufacture of resins, rubbers and fibres^[91] Due to the broad variety of hydrogenation products of furfural, the design of

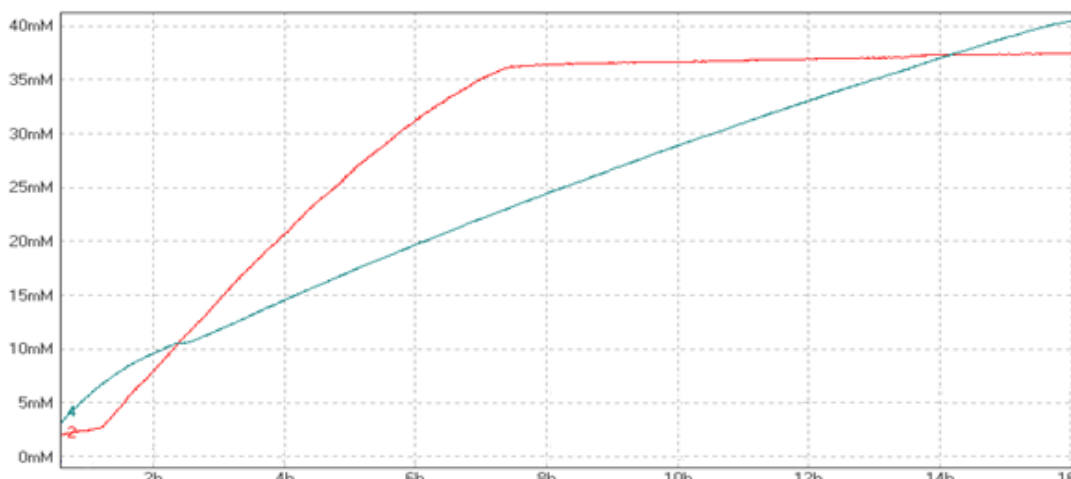


Figure 27 Comparison of the hydrogen consumption during HY of furfural promoted by $Ru(OAc)_2(CO)(DiPPF)$ at 28 (red) and 10 bar (blue) of H_2 with TFA (entries 4, 6, Table 16).

Surprisingly, the monochloride catalyst showed higher productivities together with high selectivity for the C=O in presence of 1M KOH with TOF 3300 h^{-1} at 20k:1 loading, whereas in acidic conditions displayed TOF 1660 h^{-1} (Figure 29). As expected for an aromatic compound with stabilization energy of 16 kcal mol^{-1} (67 kJ mol^{-1}),^[75] the furan ring was hence particularly resilient to reduction in this conditions (entries 7, 8, Table 16).

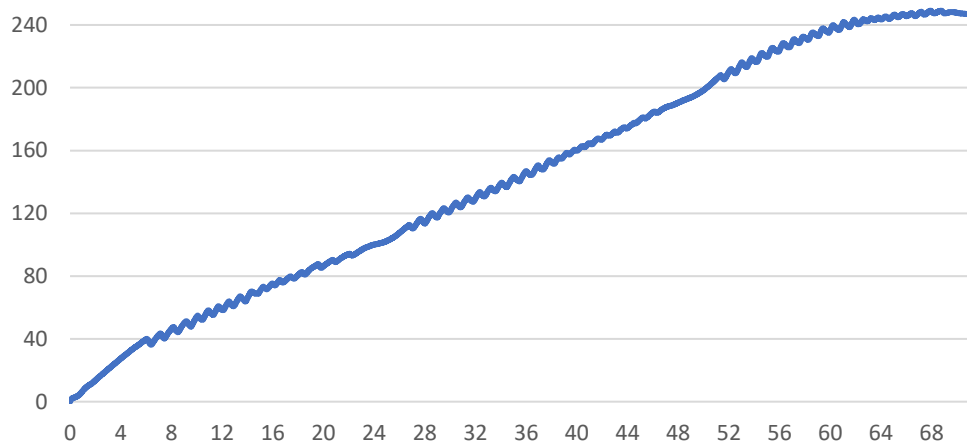


Figure 28 Hydrogen consumption during HY of furfural on 240 mmol (20 mL) scale promoted by $Ru(OAc)_2(CO)(DiPPF)$ at 20 bar, 90°C , $S/C = 100000$, (entries 11, Table 16).

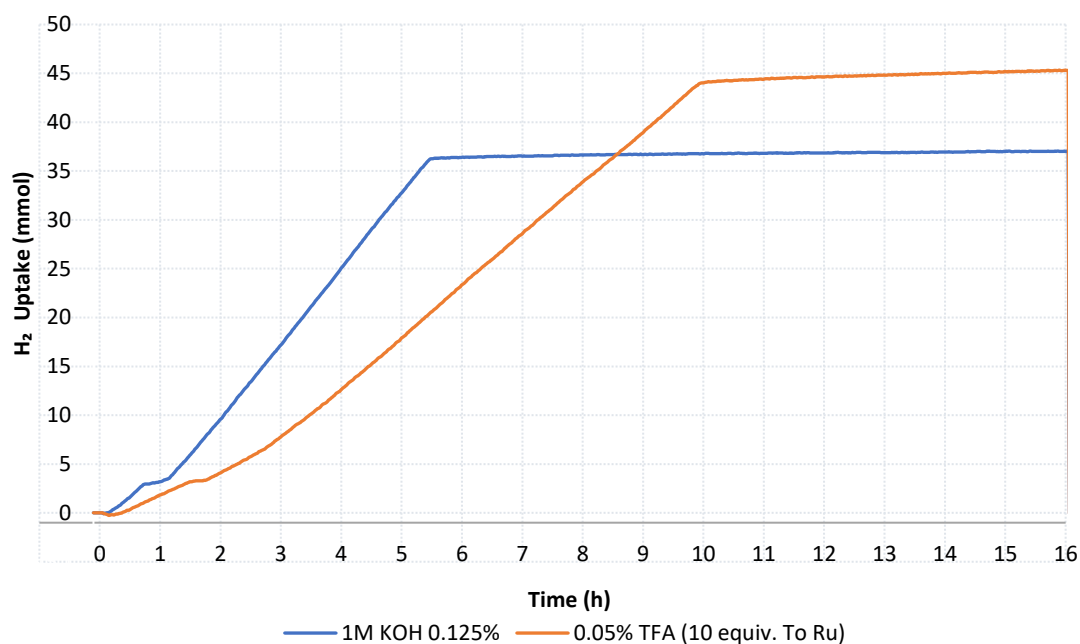


Figure 29 Hydrogen consumption comparison during HY of furfural promoted by $Ru(OAc)_2(CO)(DiPPF)$ with basic or acidic additive.

Sulfur heterocycles are incorporated in the structures of many biological active compounds like drugs, pesticides and agrochemical.^[94] The HY of 2-thiophencarboxyaldehyde promoted by the DiPPF complex **9** showed an inversed trend in respect of all the catalytic tests carried out before. In presence of KOH, the highest reactivity was observed in solvent free conditions with TOF 6650 h⁻¹, while in acidic conditions a modest conversion of 64% to the corresponding thioalcohol and TOF 910 h⁻¹ were observed (entries 12, 13, Table 16, Figure 30). The reason of this enhanced activity in basic conditions is unclear and may be ascribed to the higher coordinating ability of the formed alcohol containing sulfur, with respect to that with oxygen, requiring a strong base to displace the product from the metal center.

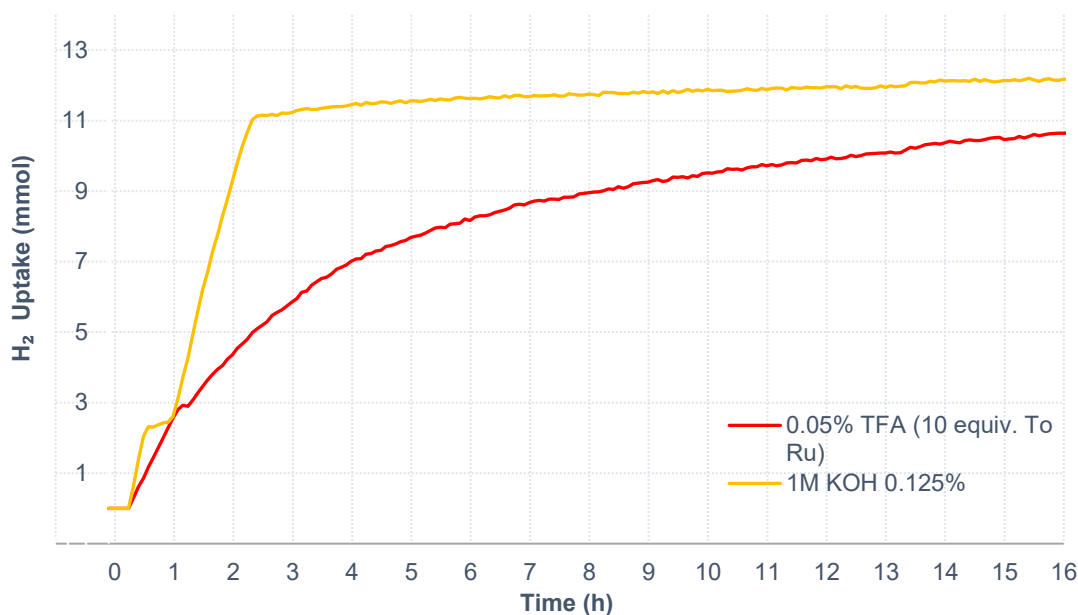


Figure 30 Hydrogen consumption comparison during HY of 2-thiophenecarboxyaldehyde promoted by $\text{Ru}(\text{OAc})_2(\text{CO})(\text{DiPPF})$ with basic or acidic additive.

Table 16 HY of neat furfural or 2-thiophenecarboxyaldehyde with $\text{Ru}(\text{OAc})_2(\text{CO})(\text{DiPPF})$ and $\text{RuCl}(\text{OAc})(\text{CO})(\text{DiPPF})$.

Entry	Catalyst	S/C	T [°C]	P [bar]	Base ^[a]	Acid [equiv. to Ru]	H ₂ Uptake ^[b] [h]	Conv. ^[c] [%]	by-products ^[c] [%]
1	$\text{Ru}(\text{OAc})_2(\text{CO})(\text{DiPPF})$	10k:1	90	20	KOH		4	100	-
2	$\text{Ru}(\text{OAc})_2(\text{CO})(\text{DiPPF})$	10k:1	90	28	-	TFA 10 equiv.	3.5	100	-
3	$\text{Ru}(\text{OAc})_2(\text{CO})(\text{DiPPF})$	20k:1	90	28	KOH			48.8	-
4	$\text{Ru}(\text{OAc})_2(\text{CO})(\text{DiPPF})$	20k:1	90	28	-	TFA 10 equiv.	8	100	-
5	$\text{Ru}(\text{OAc})_2(\text{CO})(\text{DiPPF})$	20k:1	90	10	KOH			31.0	-
6	$\text{Ru}(\text{OAc})_2(\text{CO})(\text{DiPPF})$	20k:1	90	10	-	TFA 10 equiv.	16	99.3	3.8
7	$\text{RuCl}(\text{OAc})(\text{CO})(\text{DiPPF})$	20k:1	90	28	KOH		6	99.8	-
8	$\text{RuCl}(\text{OAc})(\text{CO})(\text{DiPPF})$	20k:1	90	28	-	TFA 10 equiv.	10	99.3	-
9	$\text{Ru}(\text{OAc})_2(\text{CO})(\text{DiPPF})$	20k:1	50	28	-	TFA 10 equiv.		11.0	0.5
10	$\text{Ru}(\text{OAc})_2(\text{CO})(\text{DiPPF})$	20k:1	50	10	-	TFA 10 equiv.		6.5	0.5
11	$\text{Ru}(\text{OAc})_2(\text{CO})(\text{DiPPF})$	100k:1	90	20	-	TFA 10 equiv.	68	100	-
12	$\text{Ru}(\text{OAc})_2(\text{CO})(\text{DiPPF})$	20k:1	90	28	-	TFA 10 equiv.	16 ^[d]	68.7 ^[e]	4.5 ^[e]
13	$\text{Ru}(\text{OAc})_2(\text{CO})(\text{DiPPF})$	20k:1	90	28	KOH		3 ^[d]	99.5 ^[e]	0.5 ^[e]

[a] Solution of 1M KOH 0.125 mol%; [b] Approximate time for completion according to the hydrogen consumption data; [c] Calculated by GC; [d] substrate = 2-thiophenecarboxyaldehyde; [e] Calculated by NMR.

2.3.8 Hydrogenation of other substrates in neat conditions

Different substrates were probed to test the possible expansion of the scope of the $\text{Ru}(\text{OAc})_2(\text{CO})(\text{DiPPF})$ catalyst in the solvent free (neat) conditions. The reduction of

acetophenone to 1-phenyl ethanol at 20k:1 loading, only in presence of TFA. Despite the good activity (TOF 2150 h⁻¹) there was no complete conversion over 16 h, highlighting that bulky substrates are more difficult to be reduced. In basic conditions the ketone was not reduced in acceptable amount (entries 1, 2, Table 17). Moving to bulkier substrate as (-)-menthone, any attempt of reduction in neat conditions, led to very low hydrogen uptake and poor menthol production, at S/C = 1k to 20k, with both KOH or TFA additives.

The carbonyl complex **9** was also found active in the *N*-alkylation of amines as described in the following chapters 2.4. The last step of the borrowing hydrogen mechanism for *N*-alkylation reaction is postulated to be the reduction of the imine derivative by the metal hydride to the final amine product. The HY of *N*-benzylideneaniline was then tested, to probe if the same complex was able to reduce a similar substrate with good results. Since the melting point of this imine is 54 °C, quite below the optimized reaction temperature, this substrate was used as solid, allowing a simple preparation of the reaction at 20 mmol scale, S/C = 10k and 5k:1 under 28 bar of H₂. The TFA additive showed a better reactivity also in imine hydrogenation, proving to be more selective toward the desired product with a TOF of 2500 h⁻¹ while in basic conditions there was almost 30% of benzyl alcohol as main impurity detected by NMR (entry 3, 4 Table 17).

Table 17 Reduction of Acetophenone and *N*-benzylideneaniline with Ru(OAc)₂(CO)(DiPPF).

Entry	Catalyst	S/C	T	P	Base ^[a]	Additive	H ₂ Uptake [h] ^[b]	Conv. [%] ^[c]	by-products [%] ^[c]
1	Ru(OAc) ₂ (CO)(DiPPF)	20k:1	90	28	-	TFA 10 equiv.	16	93.9 ^[d]	-
2	Ru(OAc) ₂ (CO)(DiPPF)	20k:1	90	28	KOH	-	-	16.8 ^[d]	-
3	Ru(OAc) ₂ (CO)(DiPPF)	10k:1	90	28	-	TFA 10 equiv.	8	96.3 ^[e]	4,7
4	Ru(OAc) ₂ (CO)(DiPPF)	5k:1	90	28	KOH	--	3	70.4 ^[e]	29.5

[a] Solution of 1M KOH 0.125 mol%;, [b] Approximate time for completion according to the hydrogen consumption data; [c] by NMR; [d] Substrate = acetophenone; [e] Substrate = *N*-benzylideneaniline

2.3.9 Conclusions

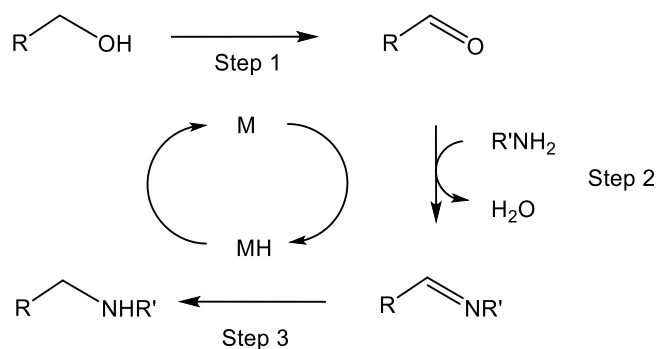
The Ru(OAc)₂(CO)(PP) type catalyst are proved to be active in the reduction under neat conditions, in particular the Ru(OAc)₂(CO)(DiPPF) complex and the corresponding monochloride RuCl(OAc)(CO)(DiPPF) are active in the presence of TFA toward the reduction of all the substrates tested. As matter of fact, Ru(OAc)₂(CO)(DiPPF) gave the better performances in terms of activity, productivity

and chemoselectivity with respect to the complexes bearing different aliphatic or aryl diphosphines, with both basic or acidic additive. The majority of the HY tests was focused on diacetate catalyst given its large availability, while for the mixed chloride-acetate complex a more efficient synthetic pathway should be developed in order to better explore its reactivity. Further studies should be dedicated to deeply understand the dependence of the reaction rate from the TFA concentrations, that can give more mechanistic insight. Moreover, to take advantage from the solvent free condition promoted by the TFA, avoiding undesired side reactions with the solvent, or to explore the hydrogenation in acidic IPA to run reductions without transfer hydrogenation contribution.

2.4 Hydrogen Borrowing Reaction

2.4.1 Background of Ru promoted alkylation of amines

Catalytic reactions involving nitrogen-containing compounds is an area of current research on account of the manifold applications. A large number of natural, agrochemical and pharmaceutical compounds are amines, amides or heterocycles, containing a single or double carbon-nitrogen bond. Selective transformations for the formation of C-N bonds are of high industrial relevance and several methods have been developed. As a matter of fact amines are commonly prepared in the pharma plants, *via* amination with aryl halide or tosylates^[95] or *via* reductive amination of carbonyl group or *N*-alkylation of amides followed by reduction.^[96] This kind of reactions entail the use of hazardous reactants and side products which have a strong environmental impact. The widely used nucleophilic substitutions (SN₂) require alkylating reagents which are toxic and whose thresholds as impurities in drugs are generally very low, this route being resulting less appealing to industry.^[96] The reduction of imines and amides is often carried out using flammable and hazardous reducing reagents, as LiAlH₄ and NaBH₃CN, which also afford a large amount of waste.^[97] In this context, the catalytic *N*-alkylation of amines using activated alcohols and affording water as only byproduct, is a more attractive atom-economic way for the C-N bond formation widely studied in academia and of great interest for industrial applications.^[98] Alcohols are in general low toxic and stable compounds, which are easy to handle and available from renewable sources, being a valid, environmentally friendly alternative to many alkylating agents. It is generally accepted that this reaction may occur through a catalytic hydrogen borrowing approach, also named autotransfer process,^[99] in which a primary alcohol undergoes a dehydrogenation reaction to a carbonyl compound promoted by the catalyst (step 1, Scheme 24). The more reactive aldehyde species generated *in situ* reacts with an amine, affording an imine (step 2, Scheme 24). Finally, the metal hydride species generated in the first step transfers the hydrogen to the imine leading to the final *N*-alkylated amine product (step 3, Scheme 24).

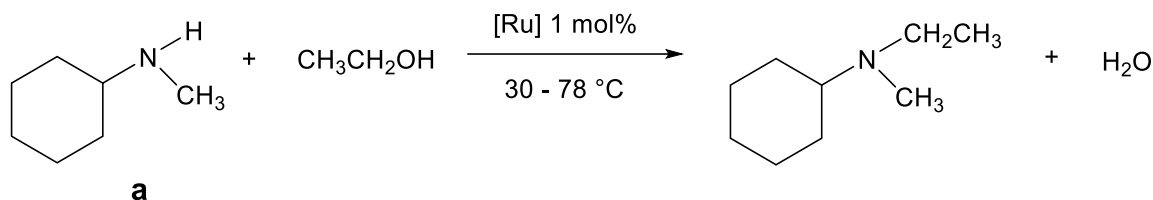


Scheme 24 *N*-alkylation of amines with alcohols via borrowing hydrogen

Main group metal hydroxides and alkoxides were found to catalyze the *N*-alkylation of amines with alcohols under harsh reaction conditions, resulting in low yield and selectivity.^[100] In the last decades, Ir, Ru,^[98] and more recently Mn and Fe^[101] have attracted a great deal of attention for *N*-alkylation *via* borrowing hydrogen. Examples of ruthenium catalysts, generated *in situ*, entails the use of the precursors $\text{RuCl}_3 \cdot n\text{H}_2\text{O}$,^[102] $\text{Ru}_3(\text{CO})_{12}$,^[103] $[\text{RuCl}_2(p\text{-cymene})]_2$,^[104] $[\text{Ru}(\text{COD})\text{Cl}_2]_n$,^[105] $\text{RuHCl}(\text{CO})(\text{PPh}_3)_3$,^[106] and $\text{RuH}_2(\text{CO})(\text{PPh}_3)_3$ ^[107] in combination with phosphanes, phosphates and nitrogen ligands. Conversely, well-defined catalysts are $\text{RuCl}_2(\text{PPh}_3)_3$,^[108] $\text{RuH}_2(\text{PPh}_3)_4$,^[109] $\text{RuCl}(\eta^5\text{-C}_5\text{H}_5)(\text{PPh}_3)_2$,^[110] $[\text{RuCl}(p\text{-cymene})(\text{PN})]\text{X}$,^[111] $\text{RuHCl}(\text{CO})(\text{PNY})$ ($\text{Y} = \text{N}, \text{P}$),^[112] $\text{RuCl}(\text{CNN})(\text{dppb})$ ^[113] and Ru pincer NNN complexes.^[114] *N*-alkylation is generally performed at high temperature (typically 120 or 180°C), and primary alcohols usually react faster than secondary. Therefore, the development of selective catalysts which can work at low temperature is of crucial importance for the application of this relevant sustainable transformation. It is worth pointing out that the coordination properties of carboxylate ligands, which display moderate stability with relatively high lability, are particularly attracting for catalytic reactions. Even if the mono-carbonyl Ru complexes, namely the Dobson catalyst $\text{Ru}(\text{OCOCF}_3)_2(\text{CO})(\text{PPh}_3)_2$ ^[38, 115] and $[\text{Ru}(\mu\text{-OCOC}_2\text{F}_4\text{OCO})(\text{CO})(\text{PP})]_2$ ($\text{PP} = \text{diphosphane}$),^[28d] are active for the alcohol dehydrogenation (the first step of the mechanism proposed for *N*-alkylation), whereas $\text{Ru}(\text{OCOCF}_3)_2(\text{CO})(\text{PPh}_3)_2$ / (*R*)-BINAP has been found active in the asymmetric C-C coupling between olefins and primary alcohols,^[116] no example of carboxylate Ru complex have been reported in the *N*-alkylation reaction.

2.4.2 N-ethylation of N-methylcyclohexylamine with ethanol

The carboxylates complexes Ru(OAc)₂(PPh₃)₂ (**1**), Ru(OAc)₂(DiPPF) (**2**) and Ru(OAc)₂(CO)(DiPPF) (**9**) (0.4 - 2 mol%) were found active in the N-ethylation of N-methylcyclohexylamine (**a**) using commercial grade untreated ethanol, under mild reaction conditions (Scheme 25). The ethanol has a double role, acting as solvent and reagent, avoiding the use of any additional solvent that may require further treatments. In presence of the diacetate precursor **1** or the derivative generate *in situ* in presence of the basic diphosphines DCyPP, the tertiary amine NMeEtCy is formed in 25% in 30 h at 78 °C, with a EtOH/NHMeCy ratio of 100 (entries 1, 2, Table 18).



Scheme 25 General conditions for N-ethylation of N-methylcyclohexylamine with ethanol catalyzed by ruthenium diacetate complexes.

Table 18 N-ethylation of methylcyclohexylamine (**a**) with EtOH catalyzed by ruthenium acetate complexes (1 mol%).

Entry	Complex	Ligand or additive (equiv.)	EtOH/NHMeCy	T [°C]	Time [h]	Conv. ^[a] [%]	By-products ^[a] [%]
1	Ru(OAc) ₂ (PPh ₃) ₂ 1	-	100	78	30	25	3
2	Ru(OAc) ₂ (PPh ₃) ₂	DCyPP (1.5)	100	78	12	5	2
3	Ru(OAc) ₂ (dppf)	-	100	78	16	6	< 1
4	Ru(OAc) ₂ (DiPPF) 2	-	10	65	15	80	
5	Ru(OAc) ₂ (DiPPF) 2	TFA (15)	10	65	14	100	1
6	Ru(OAc) ₂ (CO)(PPh ₃) ₂	-	10	78	29	0	0
7	Ru(OAc) ₂ (CO)(PPh ₃) ₂	DiPPF (1.5)	10	78	25	51	5
8	Ru(OAc) ₂ (CO)(PPh ₃) ₂	dppf (1.5)	10	78	25	1	5
9	Ru(OAc) ₂ (CO)(PPh ₃) ₂	DCyPP (1.5)	100	78	12	18	< 1
10	Ru(OAc) ₂ (CO)(DiPPF) 9	-	100	78	6	97	< 1
11	Ru(OAc) ₂ (CO)(DiPPF) 9	-	10	65	24	92	1
12	Ru(OAc) ₂ (CO)(DiPPF) 9	TFA (10)	10	65	6	98	< 1
13	Ru(OAc) ₂ (CO)(dppf)	-	10	78	25	6	5
14	Ru(OAc) ₂ (CO)(dppf)	TFA (10)	10	65	24	93	4
15	<i>trans,cis</i> -Ru(OAc) ₂ (CO) ₂ (DiPPF)	-	100	78	24	61	2
16	Ru(OAc) ₂ (CO)(DiPPF) 9 ^[b]	-	10	30	40	68	1
17	Ru(OAc) ₂ (CO)(DiPPF) 9 ^[b]	TFA (10)	10	30	40	97	< 1
18	RuCl(OAc)(CO)(DiPPF)	TFA (10)	10	65	19	1	-
19	NO Ru / NONE	-	10	78	22	0	-

[a] The conversion was determined by GC analysis. [b] Catalyst loading 2 mol%.

By employment of complex **2** bearing DiPPF, 80% conversion was achieved in 15 h at 65°C with also a lower EtOH/NHMeCy = 10 (entry 4, Table 18). Interestingly, an increased rate was observed by addition of CF₃COOH (TFA) 15 equiv., with respect to **2**, affording 100% of the ethylated derivate (entries 5, Table 18). The use of the corresponding dppf complex Ru(OAc)₂(dppf) led to poor conversion (6%) (entry 3, Table 18). The monocarbonyl derivative Ru(OAc)₂(CO)(PPh₃)₂ gives no conversion under these catalytic conditions (entry 6, Table 18). Addition of DiPPF (1.5 equiv.) to the latter derivative afforded 51% of NMeEtCy at 78°C in 25 h, whereas with dppf and DCyPP poor conversions were achieved (1% and 18%), indicating that DiPPF led to a more active catalytic species, with respect to the less basic dppf or more bulky dicyclohexyl homologous (entries 7 – 9, Table 18). Employment of the preformed monocarbonyl diacetate complex with DiPPF **9** results in 97% conversion in 6 h at 78°C, whereas 92% of product was achieved at 65°C in 24 h, with EtOH/NHMeCy = 100 and 10 respectively (entries 10, 11, Table 18). The higher catalytic activity of **9** in respect to the *in situ* system Ru(OAc)₂(CO)(PPh₃)₂ / DiPPF, can be ascribed to the incomplete diphosphine substitution on the metal center. In parallel to **2**, addition of TFA to **9** (10 equiv.) at 65°C results in a visible acceleration effect, affording 98% of desired product in 6 h (entry 12, Table 18). The analog isolated monocarbonyl diacetate complex with dppf did not show better catalytic activity with respect to the *in situ* system, and in presence of TFA almost full conversion was achieved but over 24 h (entries 13, 14, Table 18), indicating an activity six times lower than the isopropyl homologous derivative. Also the di-carbonyl **8** was tested, showing at 78°C 61% conversion in 24 h (entry 15, Table 18), the expected slower activity being in accordance with the process in which one of the carbonyl ligand is released from the complex allowing the monocarbonyl species involved in the catalytic cycle of **9**. The de coordination favored at high temperatures or vacuum, led to the more stable complex bearing the CO in *cis* position with respect to the phosphorus, as seen in section 2.1.4. Interestingly, by performing the reaction at 30 °C with **9** (at 2 mol% loading), 67% of NMeEtCy was attained in 40 h (entry 16, Table 18), whereas addition of TFA, resulted in 97% of product (entry 17, Table 18), indicating that quantitative N-alkylation can be achieved at very low temperature in presence of a well-designed carboxylate complex. By carrying out the reaction without Ru catalysts no N-ethylation was observed (entry

19, Table 18). An increase of rate by addition of acids has previously been reported for the $\text{RuH}_2(\text{CO})(\text{PPh}_3)_3$ / xantophos system,^[107] and for $\text{Ru}(\text{OCOCF}_3)_2(\text{CO})(\text{PPh}_3)_2$ ^[38, 115] in the alcohol dehydrogenation. Experiments carried out in presence of additive TFA from 1.5 to 50 equiv. with respect to **9** (Figure 31), showed a faster conversion of **a** into NMeEtCy within the range 3 - 10 equiv. of acid (TOF up to 200 h^{-1} at 50% conv. at 65°C), pointing out that the N-alkylation occurs in a suitable pH window. In addition, no formation of ethyl acetate was observed during the N-ethylation of **a** with **9**, suggesting that the in situ generated acetaldehyde undergoes a fast reaction with amine with respect to ethanol.

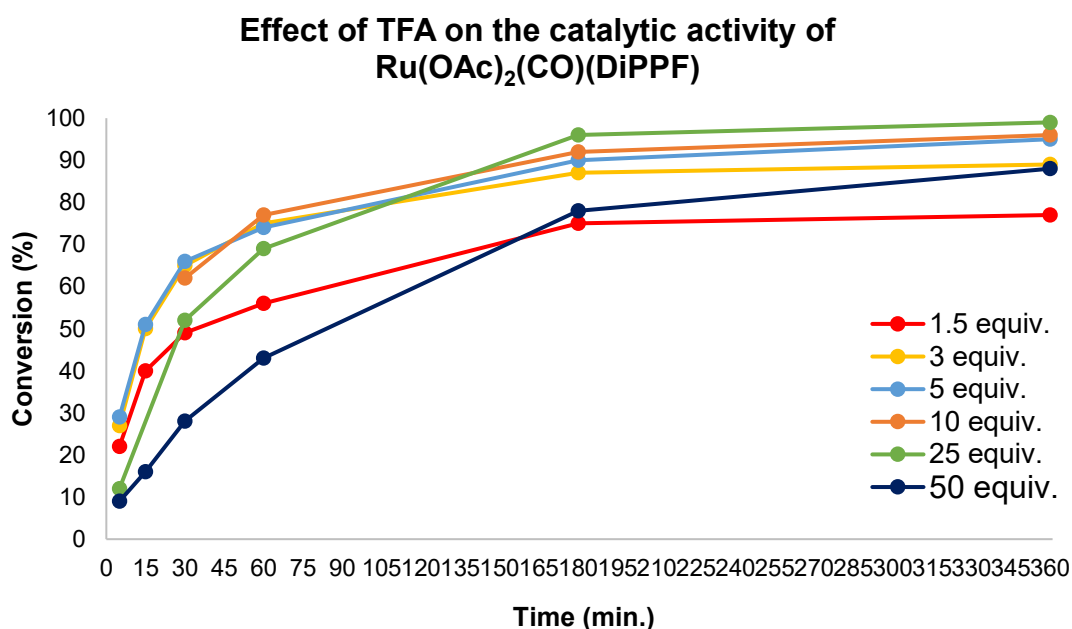
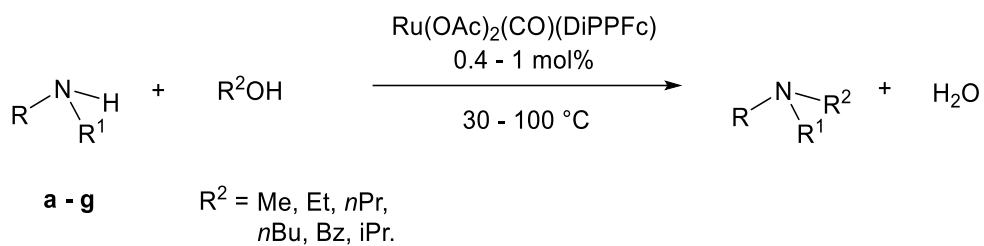


Figure 31 N-ethylation of **a** catalyzed by **9** (1 mol%) in the presence of TFA 1.5 – 50 equiv. at 65° .

2.4.3 N-alkylation of amines with primary alcohols

The $\text{Ru}(\text{OAc})_2(\text{CO})(\text{DiPPF})$ complex **9** (0.4 - 1 mol%) showed catalytic activity for the N-alkylation of primary and secondary amines with primary alcohols (Scheme 26, Figure 32). Cyclohexylamine **b** reacted with EtOH giving quantitatively the tertiary amine NEt₂Cy in 21 h at 78°C (entry 1, Table 19), while the monoalkylated NHEtCy intermediate was detected by GC analysis (Figure 106). The bulky amine NH₂/Pr₂ **c** led to NEt/Pr₂ in low conversion (15%) (entry 2, Table 19), whereas aniline **d** gave NEt₂Ph 70% at 65°C after 24 h (entry 3, Table 19). Conversely, secondary amine typically used as drug precursors N-benzylpiperazine **e**, N-phenylpiperazine **f** and morpholine **g** were quantitatively converted at 65°C to the corresponding amines in 5 h (entries 4, 5, Table 19) (Figure 107) and 6.5 h

(entry 6, Table 19), indicating that less sterically hindered and more basic amines undergo faster alkylation processes promoted by **9**. The 2-amino-1-phenylethanol **h** was slowly converted into the mono-ethylated product in 24 h (46%) (entry 7, Table 19, Figures 33, 34), whereas the dialkylated was not detected. This was probably due to the strong η^2 -coordination of the mono-alkylated amino alcohol intermediate to the metal center. This highly decreases the reaction rate, thus inhibiting the catalytic process from proceeding further. Interestingly, the 2-aminophenethyl alcohol neat slowly undergo intramolecular N-alkylation forming 65% of 1H-Benzo[b]pyrrole (indole) in 24 h, indicating that an additional step of dehydrogenation of the amine was possible in presence of the large stabilization energy granted by aromatization. Moreover, only 2% of saturated intermediate indoline was observed indicating a fast reactivity toward the final product (entry 8, Table 19, Figures 35, 36). Reacting cyclohexyl-methyl-amine **a** with different primary alcohols (C₁–C₄) afforded the alkylated products in lower yield. With MeOH at both temperature of 65 or 100°C (10 and 16%, entries 9, 10, Table 19), whereas *n*PrOH and *n*BuOH afforded the corresponding desired amines RNMeCy (R = Pr, Bu) in 68 and 60% yield in 27 and 30 h (entries 11, 12, Table 19). In view of the very feeble acidic character of nonfluorinated alcohols there was an expected lower rate of reaction with higher aliphatic alcohols (pK_a > 16) in respect of ethanol (pK_a 15.9). NMe(CH₂Ph)Cy was formed with benzyl alcohol in 87% yield at 100°C after 48 h (entry 13, Table 19). The use of the secondary alcohol *i*PrOH gave no conversion at 65°C (entry 14, Table 19). Although the dehydrogenation step is thermodynamically favored for secondary alcohols in comparison to primary ones,^[43] it is likely that the higher reactivity of primary carbinols is due to easier formation of the corresponding aldimines with respect to ketimines (step 2, Scheme 24). In chapter 3 is reported the characterization of products in table 19, Figure 108 Figure 115, pag.140) The practical potential of catalyst **9** for the on gram scale synthesis was tested on substrate **e** (1.98 g) and ethanol (5.7 mL) using 30 mg of **9** (0.4 mol%) obtaining 1-benzyl-4-ethylpiperazine (1.87 g, 81%) at 78°C in 15 h (entry 15, Table 19, Figures 120, 121, pag.146).



Scheme 26 General conditions for N-alkylation of amines with primary alcohols promoted by Ru(OAc)₂(CO)(DiPPF).

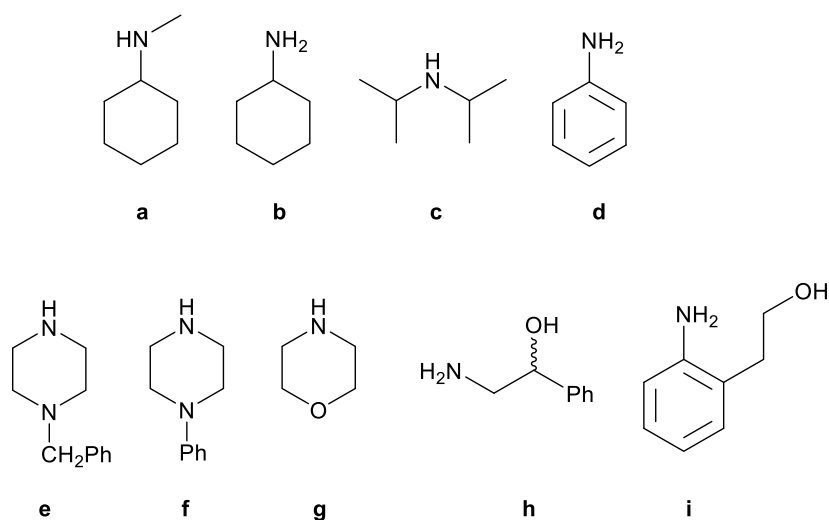
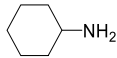

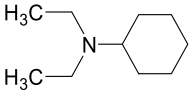
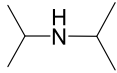

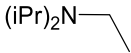
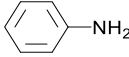

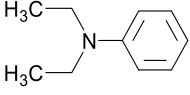
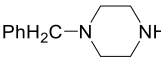

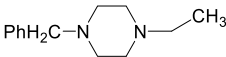
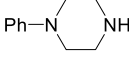

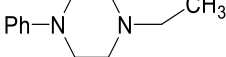
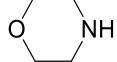

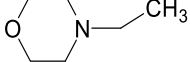
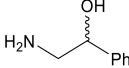

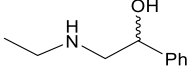
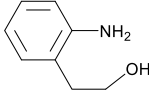
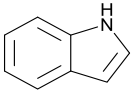
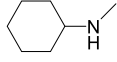
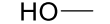
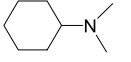
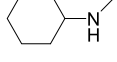
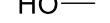
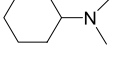
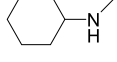
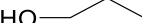
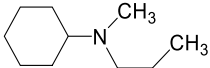
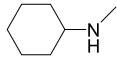

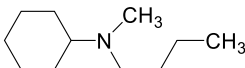
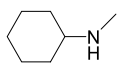
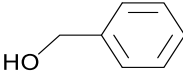
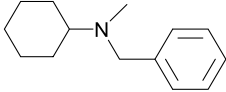
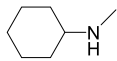
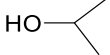
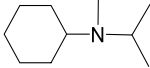
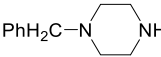
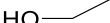


Figure 32 Primary and secondary amines **a** to **i** used in N-alkylation promoted by **9**.

Table 19 *N*-alkylation of amines with primary alcohols catalyzed by **9** (1 mol%).

Entry	Amine	Alcohol	Alcohol /Amine	T [°C]	Time [h]	Conv. ^[a] [%]	By-prod. ^[a] [%]	Products
1			100	78	21	96	3	
2			100	78	24	15	1	
3			10	65	24	70	2	
4			10	65	5	100	-	
5			10	65	5	99	1	
6			10	65	6.5	100	-	
7			10	65	24	46	-	
8		-	1	100	24	67	2	
9			10	65	24	10	1	
10			10	100	24	16	1	
11			10	65	27	68	1	
12			10	65	30	60	7	
13			5	100	48	87	1	
14			10	65	36	0	1	
15			10	78	15	100 ^[c]	-	

[a]The conversion was determined by GC analysis and assessed by ¹H NMR spectroscopy;
 [b] Dialkylated product; [c] Catalyst loading 0.4 mol%.

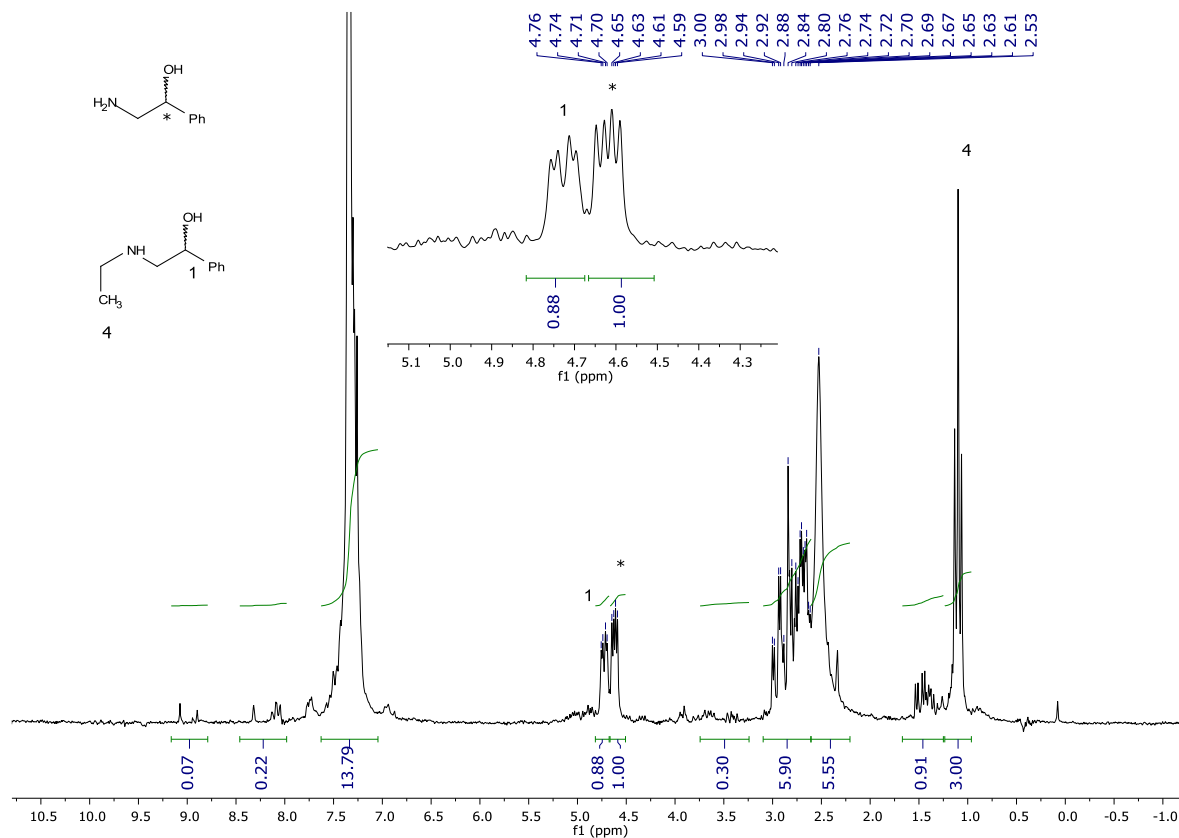


Figure 33 ^1H NMR spectrum of 2-amino-1-phenylethanol and its N-ethylated product mixture, ratio ~4:3 in CDCl_3 (entry 7, Table 19).

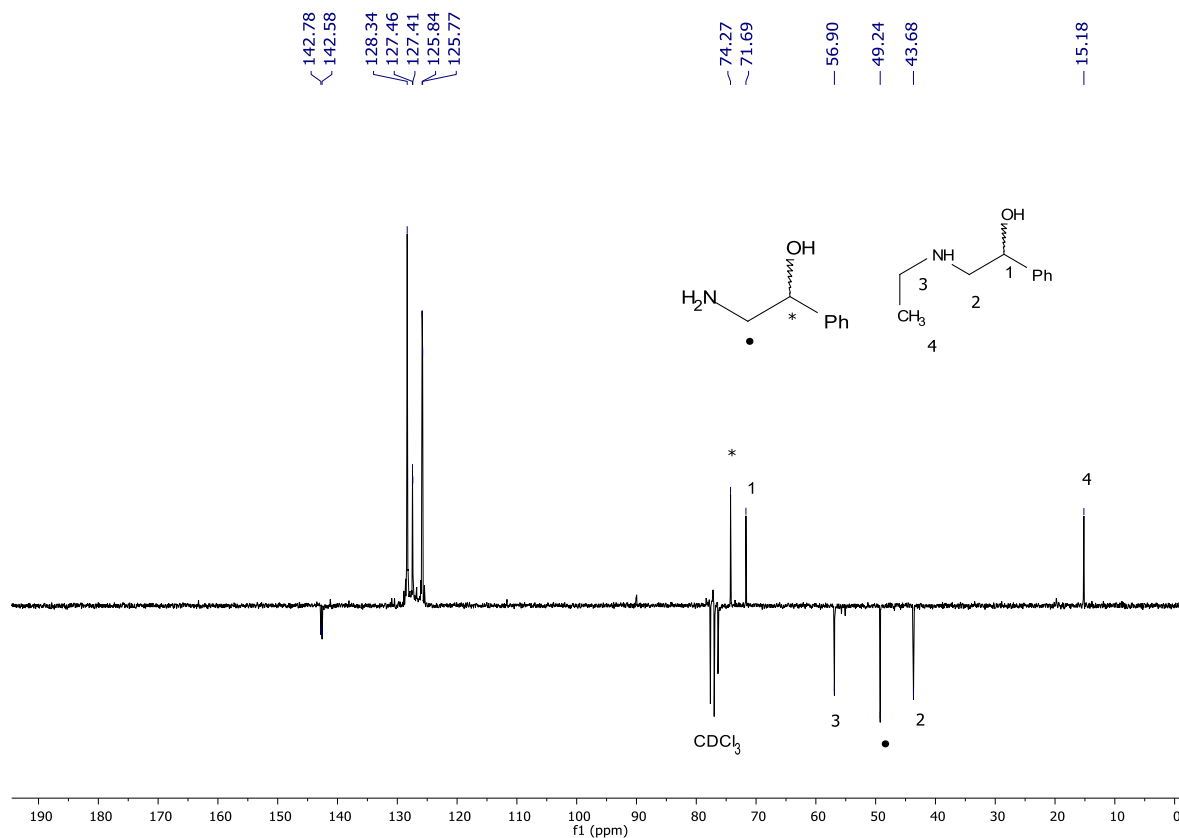


Figure 34 $^{13}\text{C}\{^1\text{H}\}$ NMR spectrum of 2-amino-1-phenylethanol and its N-ethylated product mixture, ratio ~4:3 in CDCl_3 (entry 7, Table 19).

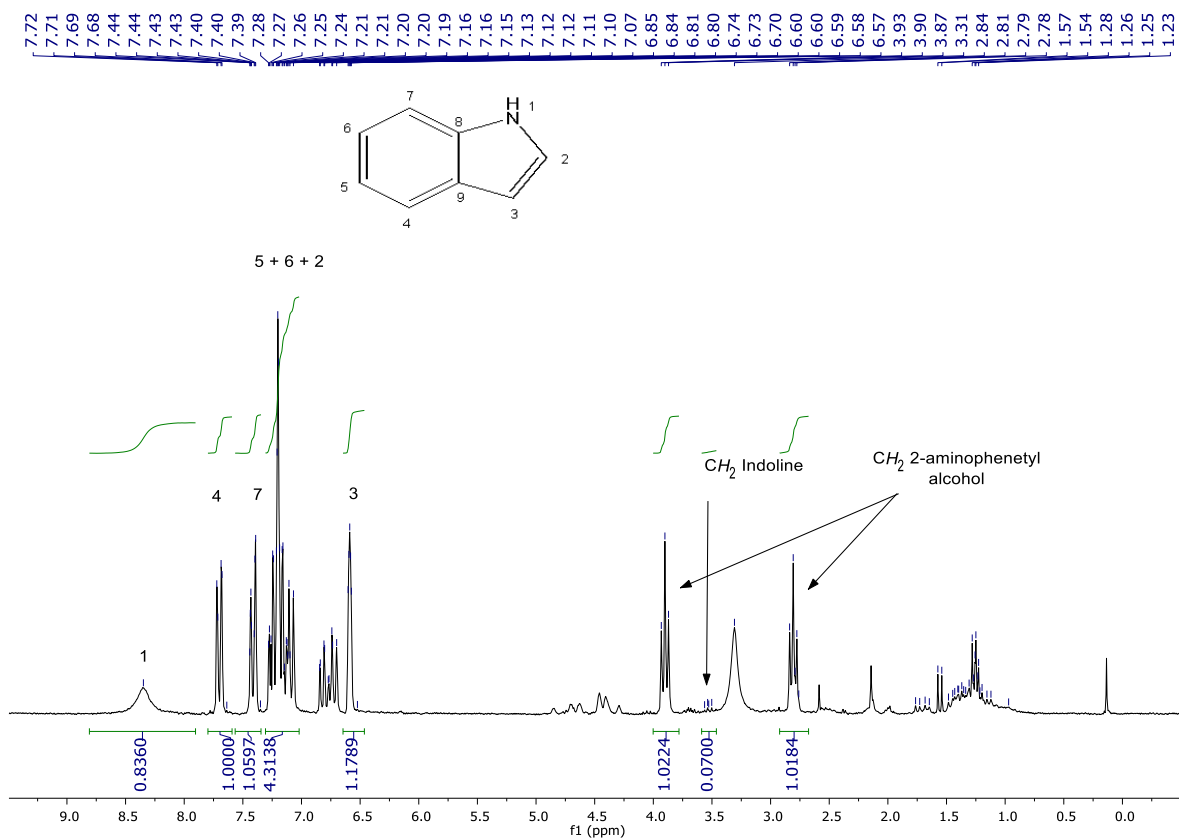


Figure 35 ¹H NMR spectrum of crude indole mixed with 2-aminophenethyl alcohol (entry 8, Table 19).

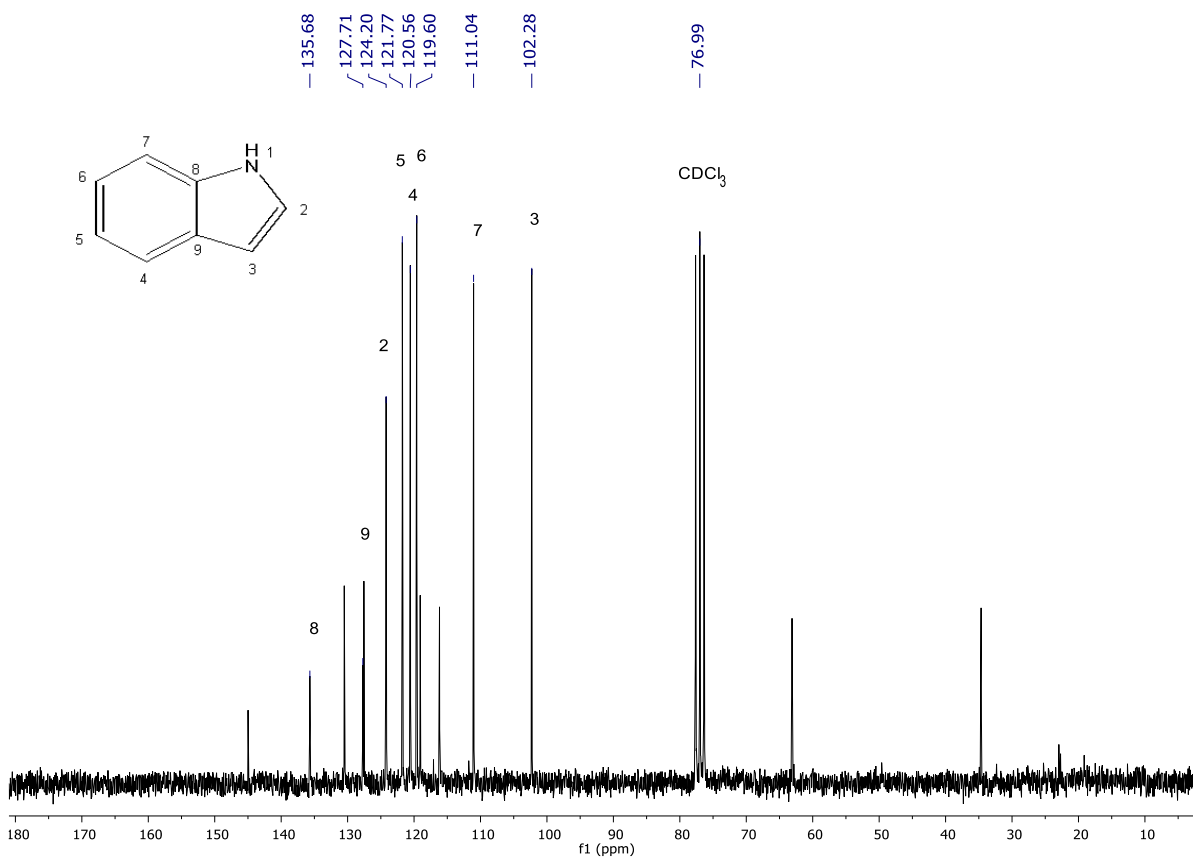
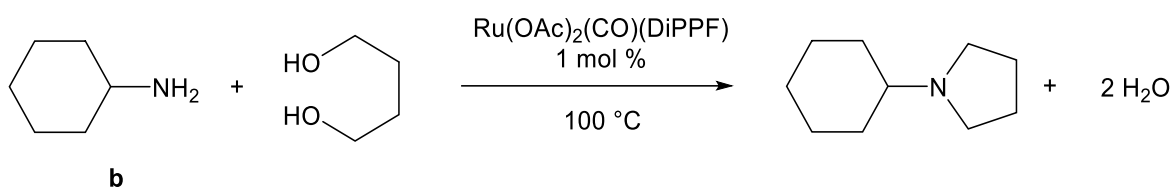


Figure 36 ¹³C{¹H} NMR spectrum of crude indole mixed with 2-aminophenethyl alcohol (entry 8, Table 19).

2.4.4 N-alkylation of cyclohexylamine with diols

The use of the 1,4-butanediol in a molar ratio 2/1 with respect to the primary amine **b** afforded the cyclic tertiary amine *N*-cyclohexylpyrrolidine in 87% yield at 100 °C after 30 h (entry 1, Table 20, Scheme 27, Figures 116, 117, pag.144). This reaction proceeded efficiently also with other diols, namely 1,5-pentanediol and 3-methyl-1,5-pentanediol with *N*-cyclohexylpyrrolidine affording the corresponding cyclic amines at relatively low alcohol / amine ratio (1.5) (entries 2, 3, Table 20, Figures 118, 119, pag.145). Preliminary studies on the reactivity of diamine substrates, such as ethylenediamine, propylenediamine, with ethanol failed, suggesting that the stronger coordination properties of these bidentate ligands may hindered the catalytic *N*-alkylation reaction.



Scheme 27 Exemplar reaction for the synthesis of heterocycles with terminal diols promoted by Ru(OAc)₂(CO)(DiPPF) (**9**).

Table 20 *N*-alkylation of cyclohexylamine with diols for heterocycles formation catalyzed by **9** (1 mol%).

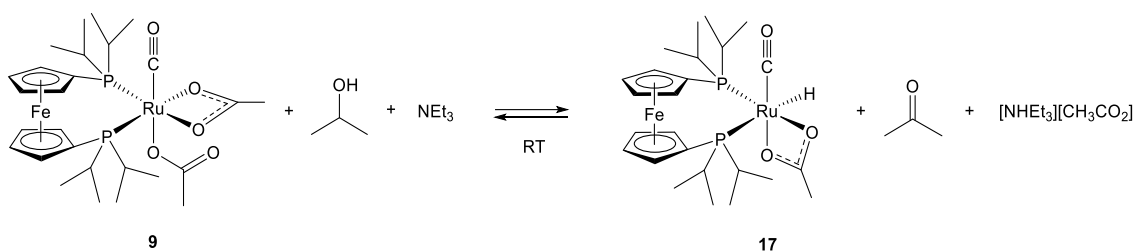
Entry	Amine	Alcohol	Alcohol /Amine	T [°C]	Time [h]	Conv. ^[a] [%]	By-prod. ^[a] [%]	
1			2	100	30	87	10 ^[d]	
2			1.5	100	48	99	<1	
3			1.5	100	48	99	<1	

[a]The conversion was determined by GC analysis and assessed by ¹H NMR spectroscopy; [d] Monoalkylated product.

2.4.5 Study of the reaction mechanism

In the catalytic *N*-alkylation reaction the formation of a Ru hydride species is expected during the alcohol dehydrogenation (Scheme 24).^[44, 117] Complex

$\text{Ru}(\text{OAc})_2(\text{CO})(\text{DiPPF})$ is soluble in alcohols (EtOH , $i\text{PrOH}$) affording a broad ^{31}P NMR singlet similar to that observed in CD_2Cl_2 (Figure 64). Interestingly, addition to **9** of the weakly coordinating NEt_3 amine (20 equiv.) at RT in 2-propanol led to the monohydride species $\text{RuH}(\text{OAc})(\text{CO})(\text{DiPPF})$ (**17**), which equilibrates with the dicarboxylate **9** (**17** / **9** = 1 / 9 molar ratio) (Scheme 28).



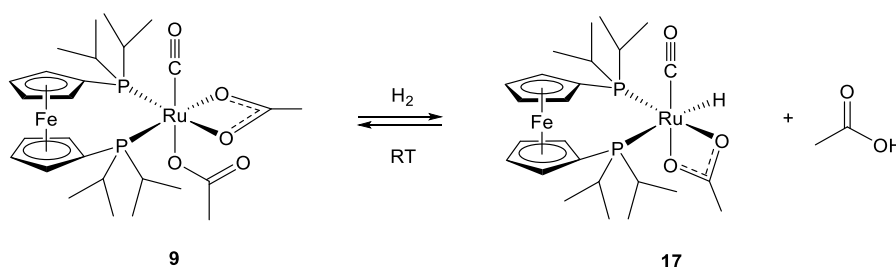
Scheme 28 Formation of the $\text{RuH}(\text{OAc})(\text{CO})(\text{DiPPF})$ in equilibrium with **9** in $i\text{PrOH}$ with 20 equiv NEt_3 .

The $^{31}\text{P}\{^1\text{H}\}$ NMR spectrum of metal-hydride showed two doublets at $\delta = 80.0$ and 24.6 ppm (external CDCl_3 lock) with a small $^2J(\text{P},\text{P})$ of about 7.7 Hz (Figure 97, pag.133), the P *trans* to the H was attributed to the higher field signal with a $^2J(\text{H},\text{P})$ of 135 Hz as established by a not decoupled ^{31}P NMR experiment (Figure 98, pag.133). Complex **17** also formed by reaction of **9** with dihydrogen (4 atm) in $[\text{D}_8]\text{toluene}$ (**17** / **9** = 1 / 9), with no need of base, according to the Scheme 29. In the ^1H NMR spectrum the doublet of doublets at $\delta = -5.98$ ppm is for the Ru-H with a $^2J(\text{H},\text{P})$ of 31.3 and 133 Hz for the *cis* and *trans* P atoms, respectively (Figure 100, pag.134), according to the data for the related hydride derivative $\text{RuH}(\text{CNN})(\text{dppb})$.^[55a, 118] Complex **17** showed a good stability under hydrogen over 24 h at RT and once heated to 50 °C the downfield $^{31}\text{P}\{^1\text{H}\}$ NMR signal loosed its fine structure, indicating fluxional behavior of the P atoms. On the other hand, in the same experiment the broad singlet of complex **9** became significantly sharper upon heating. This may highlight the protecting role of the acetate ligand that can accommodate weakly coordinating agents at low temperature, such as water, alcohols, and releases these molecules upon heating, switching between k^1 and k^2 -coordination, in agreement with the studies on the related adduct $\text{Ru}(\text{OCOCF}_3)_2(\text{CO})(\text{PPh}_3)_2(\text{ROH})$ ^[28d] (Figure 101, pag.135). It is worth pointing out that, the dinuclear hydride complex $[\text{Ru}(\mu\text{-H})(\text{CO})(\text{BINAP})]_2(\text{O}_2\text{CC}_2\text{F}_4\text{CO}_2)$ has been described as resting state in the alcohol dehydrogenation,^[28d] while the mononuclear species $\text{RuHX}(\text{CO})(\text{PP})$ ($\text{X} = \text{Cl}$, carboxylate) have been postulated to be

important in the catalytic dehydrogenation of alcohol,^[28d] and C-C coupling reactions.^[119]

Attempts to isolate RuH(OAc)(CO)(DiPPF) under harsher conditions, using strong reducing agents like NaBH₄, CaH₂ or NaOiPr, led to incomplete conversion with formation of several uncharacterized species. Reaction of **9** with NaOiPr in [D]₈-toluene under H₂ (2 atm), afforded a mixture of products containing the starting complex (Figure 37). Interestingly, by addition of benzylamine a new metal hydride was detected as main species in the ³¹P{¹H} NMR spectrum, with two doublets at 72.1 and 27.4 ppm with ²J(P,P) of 11.5 Hz, consistent with the formation of the amine hydride adduct RuH(OAc)(CO)(DiPPF)(PhCH₂NH₂) (Figure 38). The formation of new hydride species was also observed with several nitrogen containing compounds, depending on their coordination ability. As a matter of fact, in the presence of 2 equivalents of the weakly coordinating and sterically encumbered base DBU both complex **17** and a different hydride were observed (Figure 39). Amine hydride ruthenium adducts were also detected at the end of the alkylation reaction, as inferred from ³¹P{¹H} NMR spectroscopy, highlighting the protective role of the amine at high concentration (~1.7 M) on the ruthenium hydride toward deactivation processes.

As regards mechanism of the *N*-alkylation by **9**, it is thus likely that the monohydride **17** is formed by substitution of one acetate ligand with an alkoxide, formed in the basic media granted by the amine, followed by a β-H-elimination. Reaction between the formed aldehyde and the amine affords the imine (and water), which after insertion into the Ru-H bond and protonation by alcohol, leads to the alkylated amine with regeneration of the Ru-alkoxide and closing the catalytic cycle.



Scheme 29 Formation of the RuH(OAc)(CO)(DiPPF) **17** in equilibrium with **9** in [D₈]toluene under 4 atm of H₂.

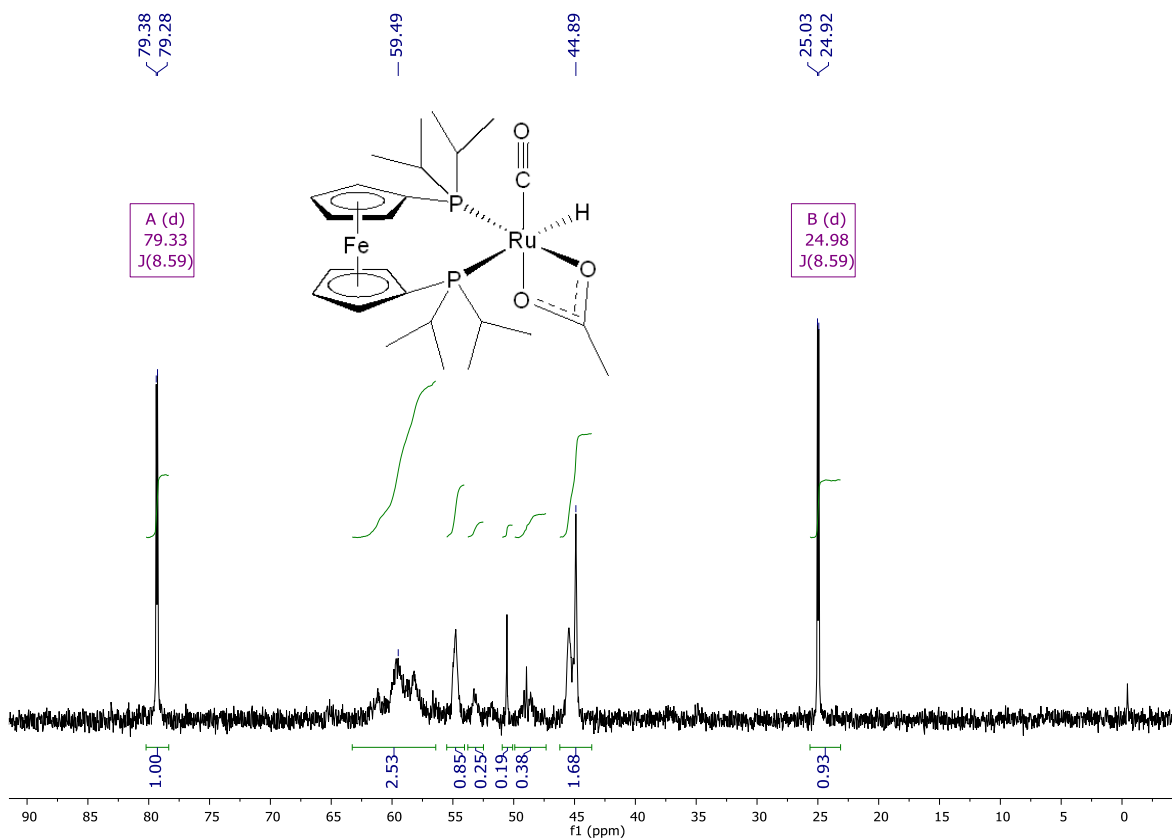


Figure 37 $^{31}\text{P}\{^1\text{H}\}$ NMR spectrum of the mixture of product obtained from $\text{Ru}(\text{OAc})_2(\text{CO})(\text{DiPPF})$ in presence of NaOiPr , H_2 2 atm in $[\text{D}]\text{8Toluene}$ at 25°C .

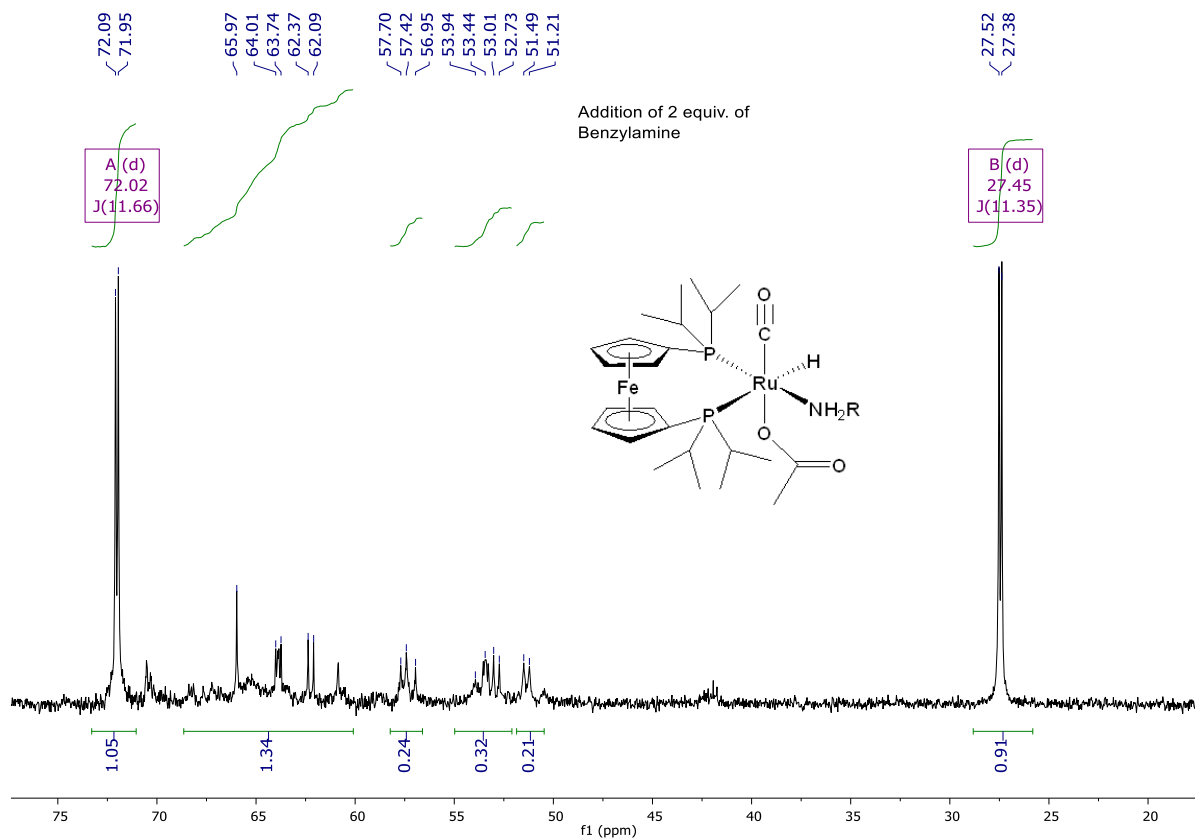


Figure 38 $^{31}\text{P}\{^1\text{H}\}$ NMR spectrum of mixture in Figure 37 in presence of benzylamine BzNH_2

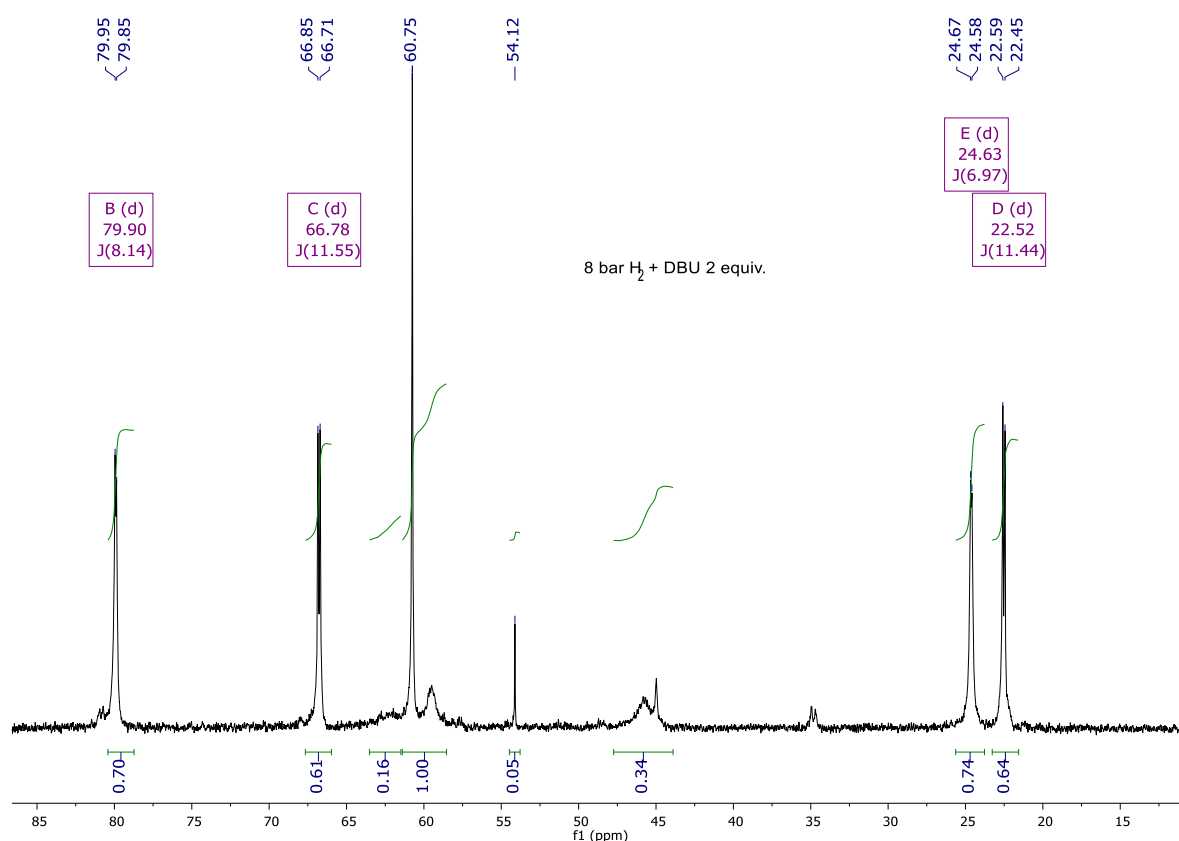


Figure 39 $^{31}\text{P}\{^1\text{H}\}$ NMR spectrum of $\text{Ru}(\text{OAc})_2(\text{CO})(\text{DiPPF}) + \text{NaOiPr} + \text{H}_2$ 8 bar after addition of DBU

2.4.6 Conclusions

In summary, the easily accessible carboxylate $\text{Ru}(\text{OAc})_2(\text{CO})(\text{DiPPF})$ (**9**), containing the bulky DiPPF diphosphine displayed high activity in the *N*-alkylation of amines with untreated primary alcohols *via* a borrowing hydrogen reaction. This ruthenium system allowed unprecedented mild *N*-alkylation of primary and secondary amine at temperature as low as 30°C and without the use of any additional base, resulting one of the most active catalysts reported to date. The carboxylate ligand in combination with basic diphosphines and the carbonyl ligand showed a preference for very concentrated solution of substrate allowing to perform the reaction in up to semi-neat condition in which commercial grade alcohols acted as substrates and solvents. The addition of TFA, up to 10 equivalents with respect to the catalyst, has a strong accelerating effect resulting in a rate 4 times higher. Further studies are required to fully rationalize the catalytic cycle in presence of TFA that is involved in the protonation of the amine substrate and in the formation of labile and active trifluoro carboxylate complexes.

3.0 Experimental Part

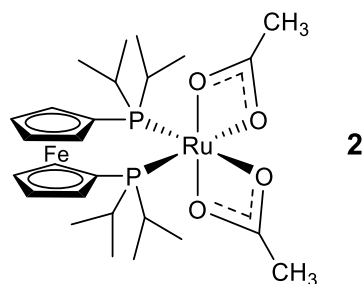
3.1 General

All reactions were carried out under argon atmosphere using standard Schlenk techniques. Commercial grade alcohols and toluene were purchased from Alfa Aesar, degassed and used without purification. Compounds **1**,^[29] Ru(OAc)₂(dppf),^[35] Ru(OAc)₂(CO)(PPh₃)₂,^[120] Ru(OAc)₂(CO)(dppf), RuCl₂(dppb)(ampy), RuH₂(CO)(Triphos), Ru(OAc)₂(CO)(dppb) RuCl₂(dppb)(ampy) RuCl₂(dppf)(ampy) cis-Ru(OAc)₂(dppb)(ampy), were prepared according to the literature procedures. Amines (Aldrich) were distilled, whereas all other chemicals (Aldrich and Johnson Matthey) were used without further purification. NMR measurements were recorded on a Bruker AC 200 spectrometer. Chemical shifts, in ppm, are relative to TMS for ¹H and ¹³C{¹H}, whereas 85% H₃PO₄ was used for ³¹P{¹H} and PhCF₃ for ¹⁹F NMR. Elemental analyses (C, H, N) were carried out with a Carlo Erba Flash EA1112 elemental analyzer, whereas the GC analyses were performed with a Varian GP-3380 gas chromatograph with a MEGADEX-ETTBDMS-β column of 25 m of length, internal diameter 0.25 mm, column pressure 5 psi, H₂ as carrier gas and flame ionization detector (FID). The injector and detector temperature were 250°C. All reactions were carried out under an argon atmosphere using standard Schlenk techniques. Solvents were purchased from Aldrich, Alfa Aesar and Carlo Erba; degassed and/or dried over sieves 3A.

3.2 Synthesis of novel acetate complexes

Synthesis of Ru(OAc)₂(PPh₃)₂ (1): RuCl₂(PPh₃)₃ (16.00 g, 0.0167 mol) and NaOCOCH₃ (23.00 g, 0.280 mol) were placed in a Schlenk tube and suspended in 250 mL of MTBE. The air was removed from the system with 5 vacuum/nitrogen cycles and then refluxed for 48 h, affording an orange precipitate. The system was cooled to RT. and 100 mL of water was added, the biphasic system was vigorously stirred for 1 h and filtered. The solid was washed with MTBE (2 x 35 mL), MeOH (2 x 20 mL) and again with MTBE (2 x 35 mL), and finally dried under reduced pressure. Yield: 11.19 g (90%). All the analytical and spectroscopic data were consistent with previous literature^[30]

Synthesis of Ru(OAc)₂(DiPPF) (2):



Ru(OAc)₂(PPh₃)₂ (**1**) (2.00 g, 2.69 mmol) and DiPPF (1.19 g, 2.84 mmol, 1.05 equiv) were placed in a Schlenk and suspended in 5 mL of degassed cyclohexane. The mixture was refluxed for 4 h, affording an orange crystalline precipitate, which was filtered, washed with cold *n*-pentane (3x1 mL) and dried under reduced pressure. Yield: 1.47 g (87%). ¹H NMR (200.1 MHz, CDCl₃, 20 °C): δ = 4.37 (s, 4H; C₅H₄), 4.28 (s, 4H; C₅H₄), 2.57 (*hept*, ³J(H,H) = 7.0 Hz, 4H; CH(CH₃)₂), 1.91 (s, 6H; CH₃CO₂), 1.17 ppm (*dd*, ³J(P,H) = 12.6 Hz, ³J(H,H) = 7.0 Hz, 24H; CH(CH₃)₂); ¹³C{¹H} NMR (50.3 MHz, CDCl₃, 20 °C): δ = 188.1 (t, ³J(C,P) = 0.8 Hz; OCOCH₃), 79.4 (*pseudo t*, J(C,P) = 20.0 Hz, *ipso*-C₅H₄), 73.7 (t, ²J(C,P) = 2.9 Hz; C₅H₄), 70.1 (t, ³J(C,P) = 2.5 Hz; C₅H₄), 27.9 (m; CH(CH₃)₂), 24.0 (s; OCOCH₃), 19.1 (s; CH(CH₃)₂), 19.0 ppm (s; CH(CH₃)₂); ³¹P{¹H} NMR (81.0 MHz, CDCl₃, 20 °C): δ = 67.6 ppm (s); elemental analysis (%) calcd for C₂₆H₄₂FeO₄P₂Ru: C 48.99, H 6.64; found: C 49.53, H 6.92.

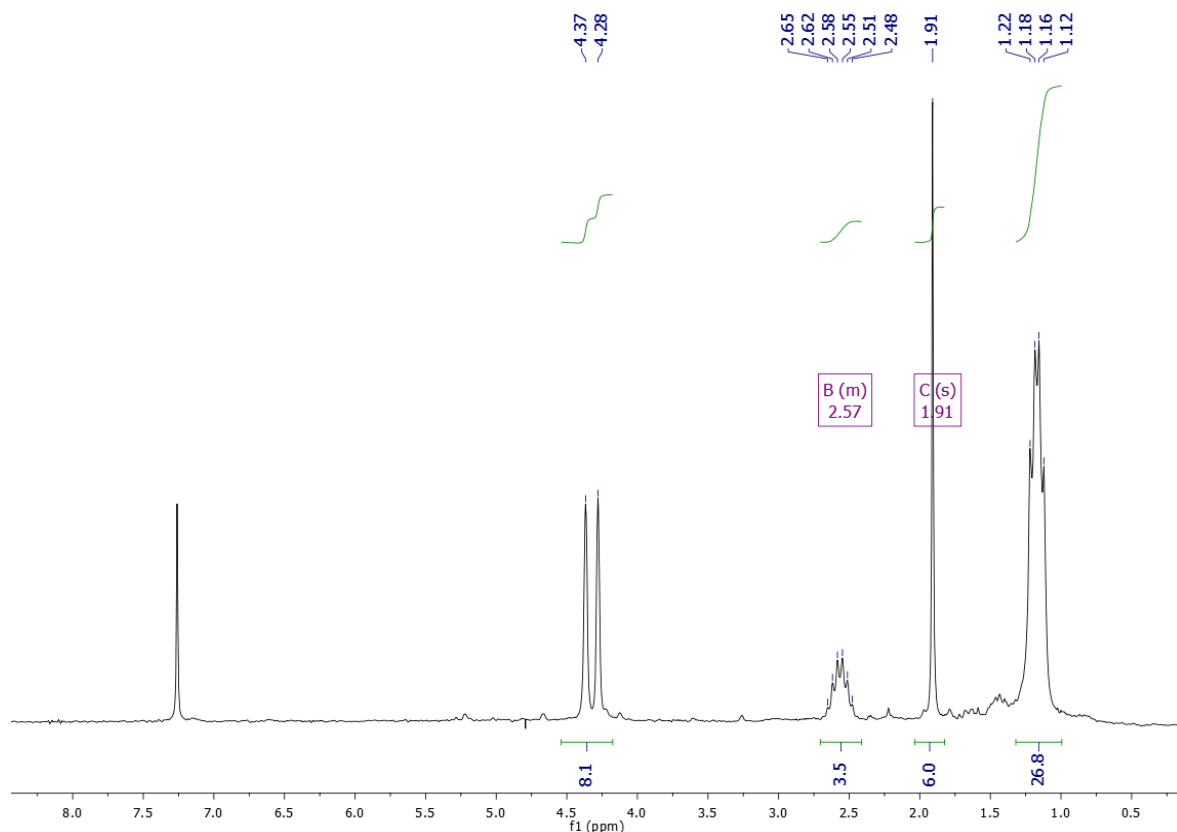


Figure 40 ^1H NMR spectrum of $\text{Ru}(\text{OAc})_2(\text{DiPPF})$ (**2**) in CDCl_3 at $20\text{ }^\circ\text{C}$.

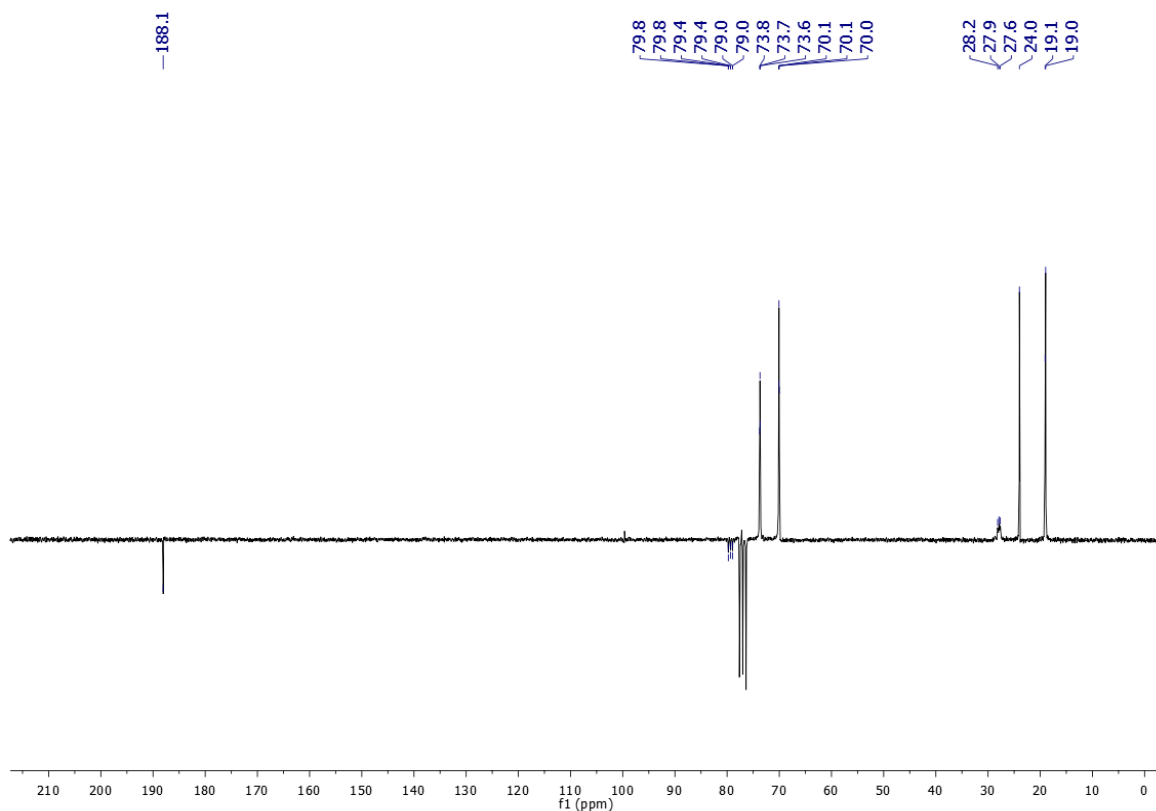


Figure 41 $^{13}\text{C}\{^1\text{H}\}$ NMR spectrum of $\text{Ru}(\text{OAc})_2(\text{DiPPF})$ (**2**) in CDCl_3 at $20\text{ }^\circ\text{C}$.

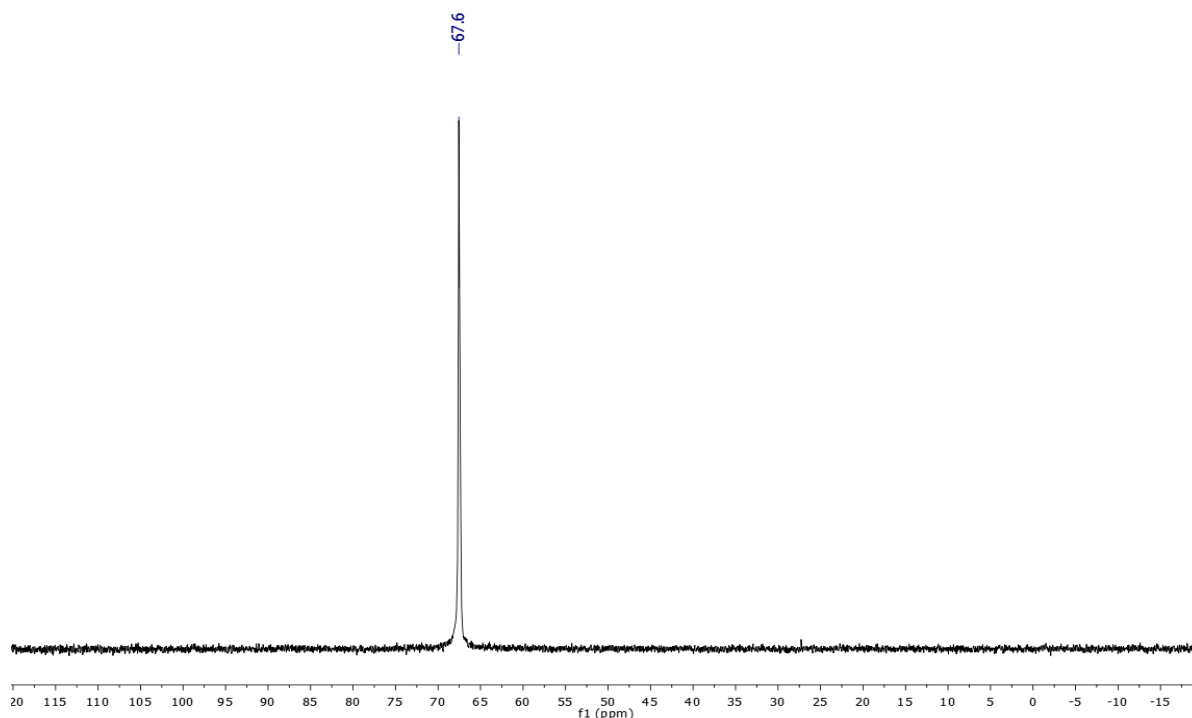
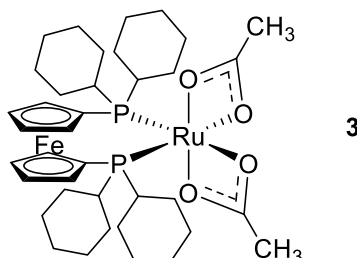


Figure 42 $^{31}\text{P}\{^1\text{H}\}$ NMR spectrum of $\text{Ru}(\text{OAc})_2(\text{DiPPF})$ (**2**) in CDCl_3 at $20\text{ }^\circ\text{C}$

Synthesis of $\text{Ru}(\text{OAc})_2(\text{DCyPF})$ (**3**):



$\text{Ru}(\text{OAc})_2(\text{PPh}_3)_3$ (100 mg, 0.134 mmol) and DCyPF (81.6 mg, 0.141 mmol, 1.05 equiv) were suspended in 0.75 mL of degassed toluene and the mixture was refluxed for 60 min. The obtained red solution was concentrated to almost 1 mL, evaporating the solvent under reduced pressure, and $\text{Ru}(\text{OAc})_2(\text{DCyPF})$ was precipitated by addition of *n*-pentane (10 mL). The solid was filtered, washed with *n*-pentane (2x3 mL) and dried under reduced pressure. Yield: 49.2 mg (46%). ^1H NMR (200.1 MHz, CD_2Cl_2 , $20\text{ }^\circ\text{C}$): δ = 4.28 (t, $^3J(\text{H,H})$ = 1.4 Hz, 4H; C_5H_4), 4.19 (t, $^3J(\text{H,H})$ = 1.7 Hz, 4H; C_5H_4), 2.23 (br s, 4H; PCH of Cy), 2.04-1.56 (br m, 20H; CH_2 of Cy) 1.85 (s, 6H; CH_3CO_2), 1.52-1.01 ppm (br m, 20H; CH_2 of Cy); $^{31}\text{P}\{^1\text{H}\}$ NMR (81.0 MHz, CD_2Cl_2 , $20\text{ }^\circ\text{C}$): δ = 64.1 ppm (s); elemental analysis (%) calcd for $\text{C}_{38}\text{H}_{58}\text{FeO}_4\text{P}_2\text{Ru}$: C 57.21, H 7.33; found: C 58.60, H 7.50.

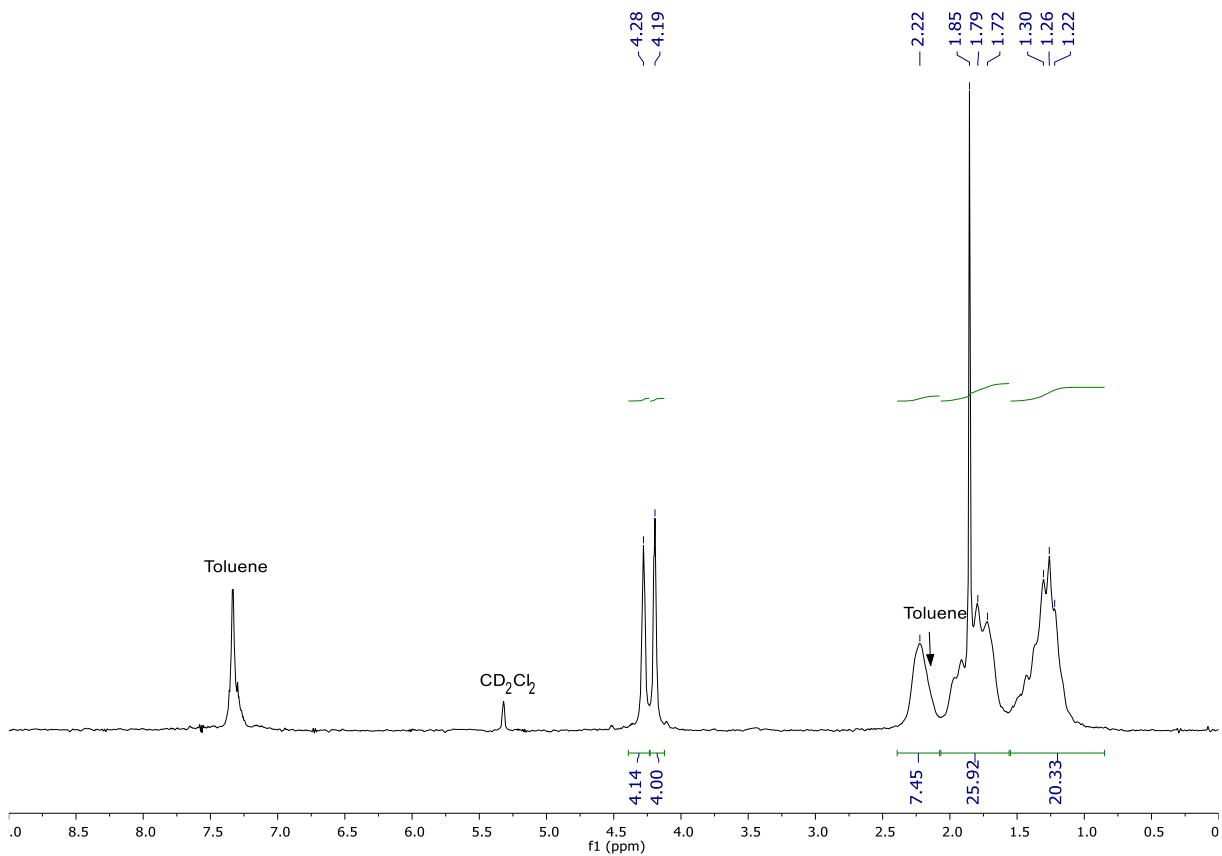


Figure 43 ^1H NMR of $\text{Ru}(\text{OAc})_2(\text{DCyPF})$ (**3**) in CD_2Cl_2 at $20\text{ }^\circ\text{C}$

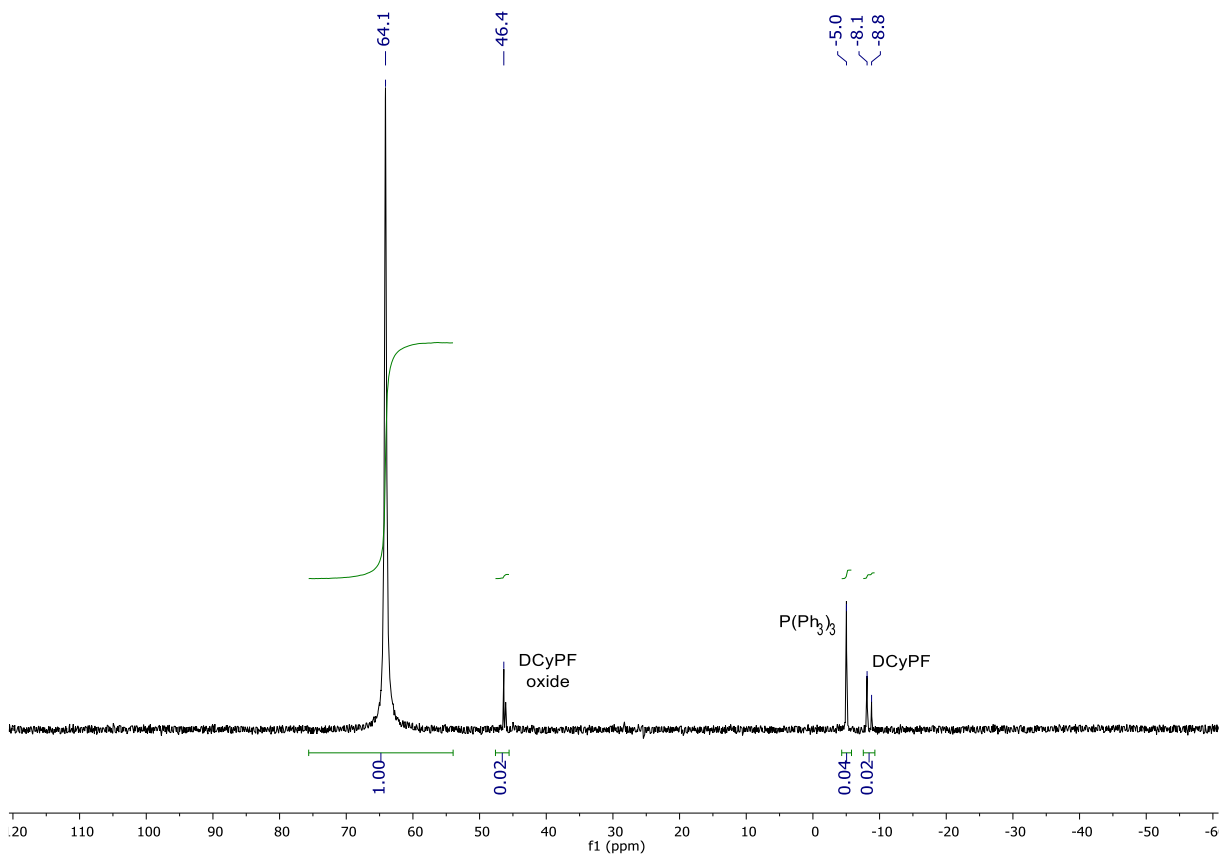
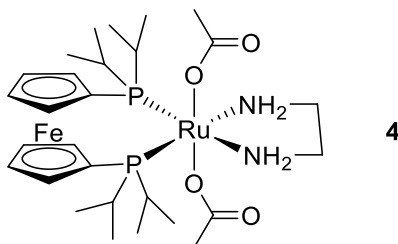


Figure 44 $^{31}\text{P}\{^1\text{H}\}$ NMR spectrum of $\text{Ru}(\text{OAc})_2(\text{DCyPF})$ (**3**) in CD_2Cl_2 at $20\text{ }^\circ\text{C}$

Synthesis of *trans*-Ru(OAc)₂(DiPPF)(en) (4):



Ru(OAc)₂(PPh₃)₃ (100 mg, 0.134 mmol) and DiPPF (82 mg, 0.141 mmol, 1.05 equiv) were suspended in 2 mL of degassed *n*-heptane and refluxed for 2 h leading to an orange suspension of Ru(OAc)₂DiPPF (checked by NMR). Ethylenediamine (9 μ L, 0.134 mmol, 1.0 equiv) was added and the mixture was stirred for 2 h, affording a yellow precipitate of Ru(OAc)₂(DiPPF)(en). The complex was filtered, washed with refrigerated *n*-pentane (2x1 mL) and dried under reduced pressure. Yield 48.6 mg (52%). ¹H NMR (200.1 MHz, CDCl₃, 20 °C): δ = 5.99 (br s, 4H; NH₂), 4.42 (br s, 4H; C₅H₄), 4.27 (pseudo t, *J*(H,H) = 1.7 Hz, 4H; C₅H₄), 2.97 (br s, 4H; CH₂N), 2.54 (hept, ³*J*(H,H) = 7.0 Hz, 4H; CH(CH₃)₂), 1.72 (s, 6H; CH₃CO₂), 1.26 (dd, ³*J*(P,H) = 12.1 Hz, ³*J*(H,H) = 7.0 Hz, 12H; CH(CH₃)₂), 1.15 ppm (dd, ³*J*(P,H) = 12.2 Hz, ³*J*(H,H) = 7.1 Hz, 12H; CH(CH₃)₂); ¹³C{¹H} NMR (50.3 MHz, CDCl₃, 20 °C): δ = 183.6 (dd, ³*J*(C,P) = 1.9 Hz, ³*J*(C,P) = 0.8 Hz; OCOCH₃), 79.4 (pseudo t, *J*(C,P) = 17.4 Hz, *ipso*-C₅H₄), 74.3 (pseudo t, *J*(C,P) = 3.1 Hz; C₅H₄), 69.9 (pseudo t, *J*(C,P) = 2.2 Hz; C₅H₄), 43.5 (s; CH₂), 27.8 (pseudo t, *J*(C,P) = 9.5 Hz; CH(CH₃)₂), 26.1 (s; OCOCH₃), 19.8 (s; CH(CH₃)₂), 19.7 ppm (s; CHCH₃); ³¹P{¹H} NMR (81.0 MHz, CDCl₃, 20 °C): δ = 44.9 ppm (s); elemental analysis (%) calcd for C₂₈H₅₀FeN₂O₄P₂Ru: C 48.21, H 7.22, N 4.02; found: C 48.20, H 7.20, N 3.60.

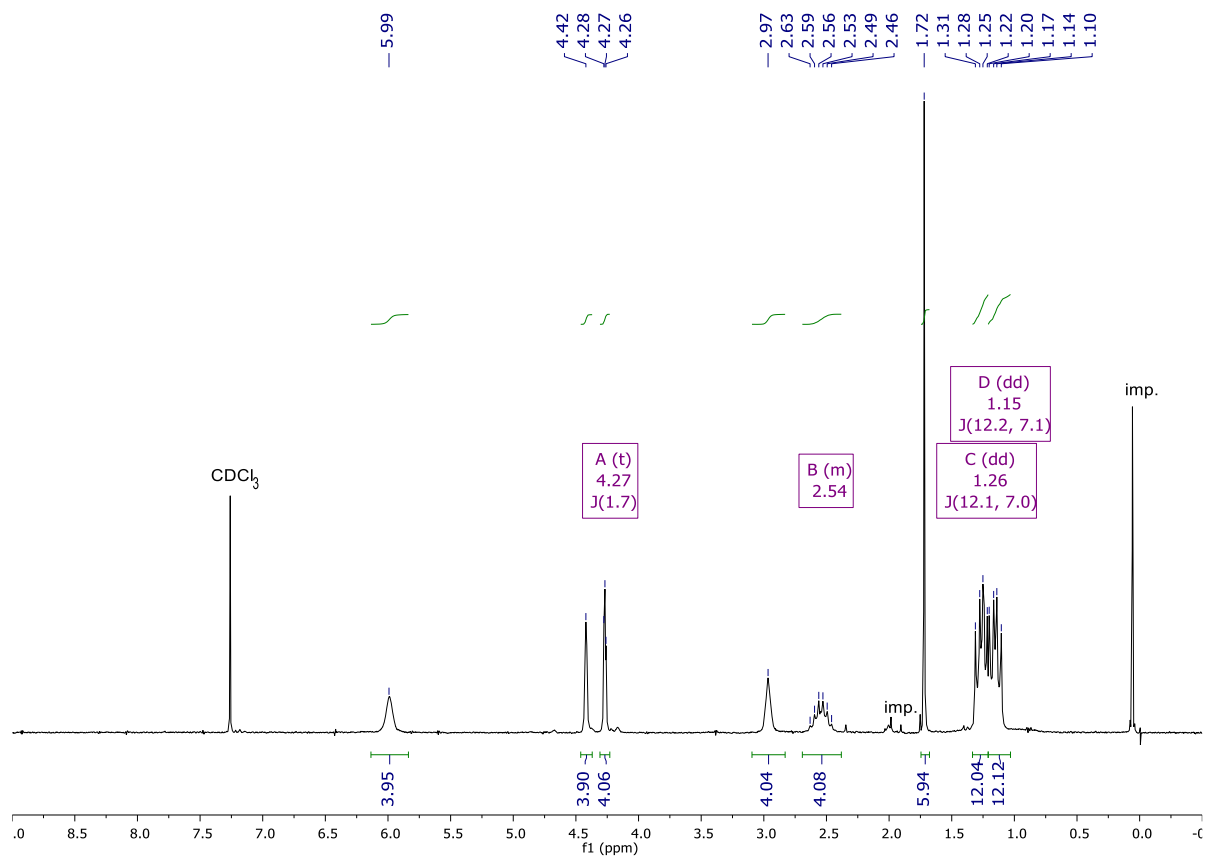


Figure 45 ^1H NMR of *trans*-Ru(OAc)₂(DiPPF)(en) (**4**) in CDCl₃ at 20 °C

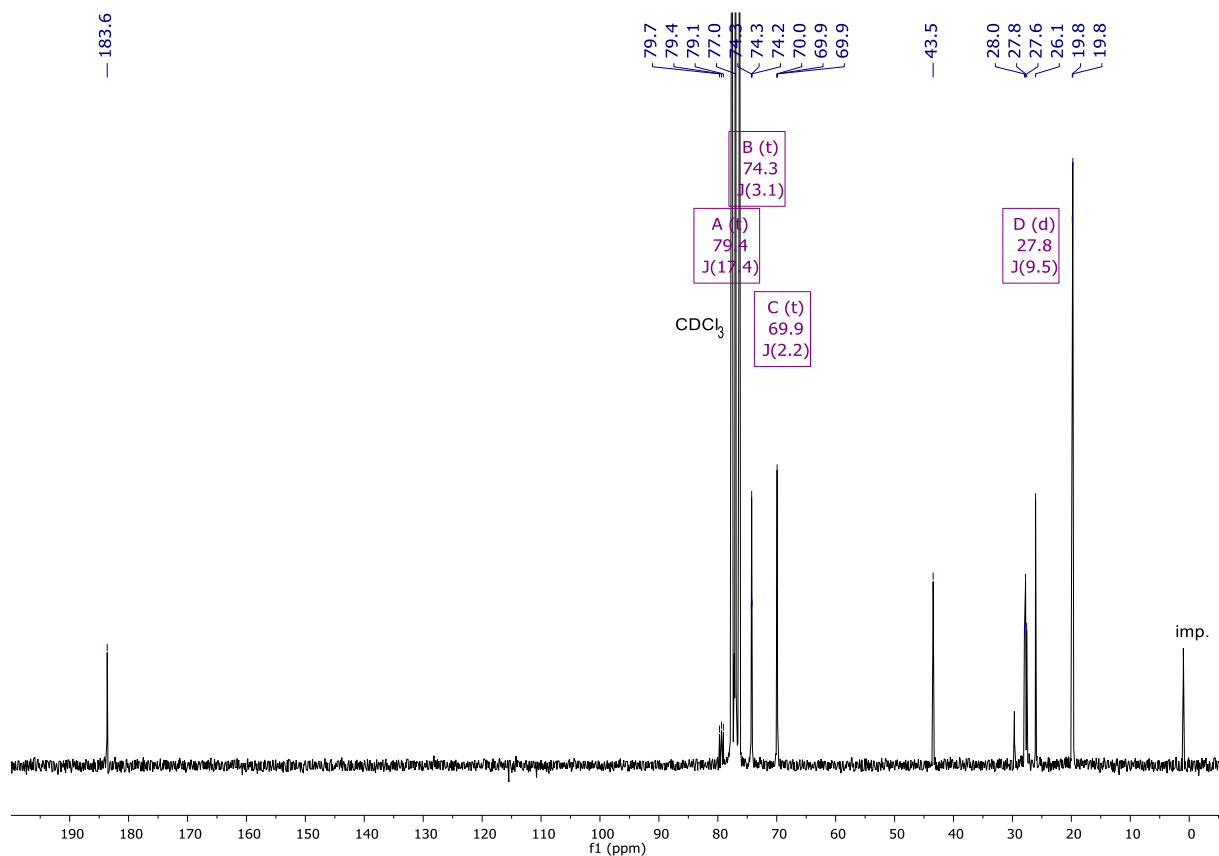


Figure 46 $^{13}\text{C}\{^1\text{H}\}$ NMR of *trans*-Ru(OAc)₂(DiPPF)(en) (**4**) in CDCl₃ at 20 °C

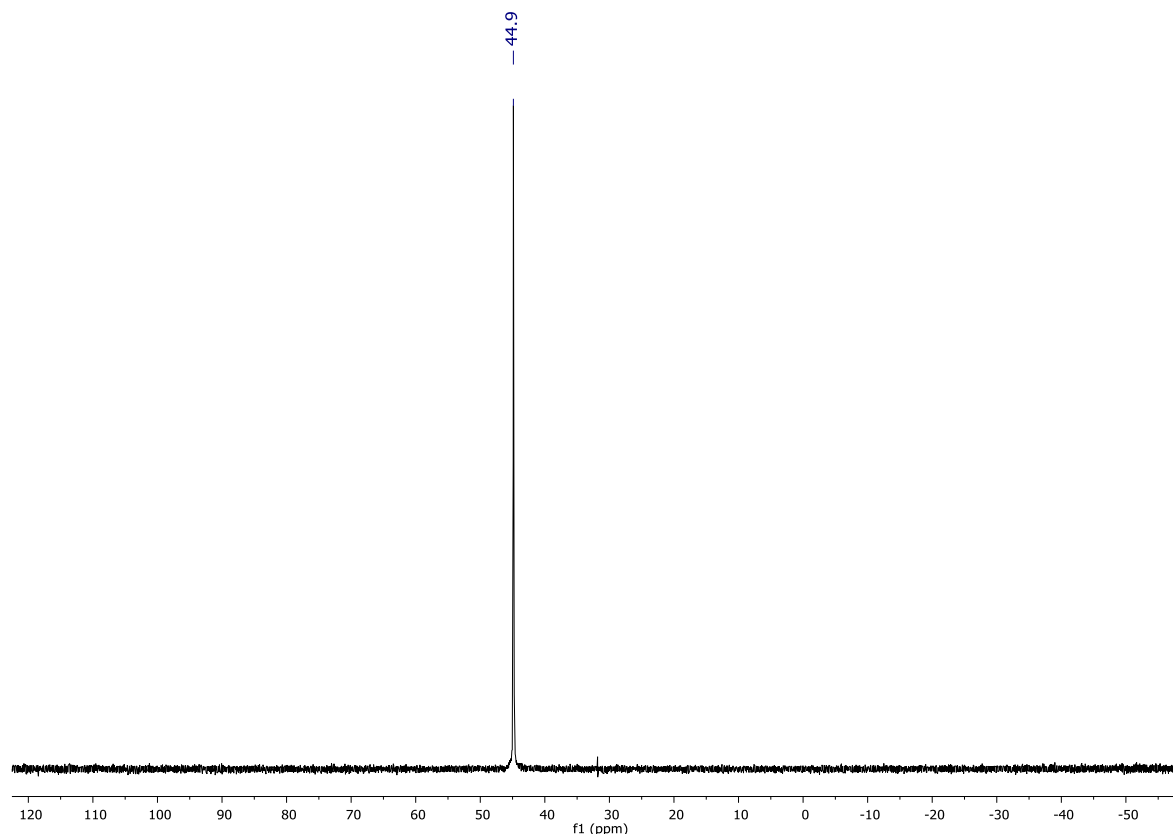
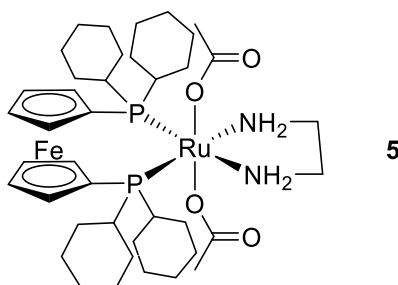


Figure 47 $^{31}\text{P}\{^1\text{H}\}$ NMR spectrum of *trans*- $\text{Ru}(\text{OAc})_2(\text{DiPPF})(\text{en})$ (**4**) in CDCl_3 at $20\text{ }^\circ\text{C}$

Synthesis of *trans*- $\text{Ru}(\text{OAc})_2(\text{DCyPF})(\text{en})$ (5**):**



$\text{Ru}(\text{OAc})_2(\text{PPh}_3)_3$ (98 mg, 0.132 mmol) and DCyPF (80 mg, 0.138 mmol, 1.05 equiv) were suspended in 1.5 mL of degassed *n*-heptane, and refluxed for 2 h, until a suspension containing $\text{Ru}(\text{OAc})_2\text{DCyPF}$ is formed (as verified by NMR analysis). Ethylenediamine (9 μL , 0.132 mmol, 1.0 equiv) was added to the mixture that was stirred at room temperature for 2 h affording a yellow solution. Cooling the solution in an ice-bath, a precipitate is formed. The solid was filtered, washed with cold *n*-heptane and then dried under reduced pressure. Yield 72 mg (63%). ^1H NMR (200.1 MHz, CD_2Cl_2 , $20\text{ }^\circ\text{C}$): δ = 6.09 (s, 4H NH_2), 4.32 (m, 4H; C_5H_4), 4.25 (pseudo t, $J(\text{H},\text{H}) = 1.7$

Hz, 4H; C₅H₄), 2.92 (s, 4H; CH₂N), 2.34-2.12 (br m, 8H; Cy), 2.01-1.84 (br m, 3H; Cy), 1.83-1.56 (br m, 9H; Cy), 1.69 (s, 6H; CH₃CO₂) 1.55-1.10 (br m, 22H; Cy); ¹³C{¹H} NMR (50.3 MHz, CDCl₃, 20 °C): δ = 183.4 (t; ³J(C,P) = 1.0 Hz; OCOCH₃), 79.6 (pseudo t, J(C,P) = 16.3 Hz, ipso-C₅H₄), 75.0 (pseudo t, J(C,P) = 3.0 Hz; C₅H₄) 70.3 (pseudo t, J(C,P) = 2.4 Hz; C₅H₄), 43.8 (s; CH₂N), 39.8 (t, ¹J(C,P) = 8.7 Hz; PCH), 29.8 (d, ²J(C,P) = 7.9 Hz; CH₂ of Cy), 28.4 (t, ³J(C,P) = 4.6 Hz; CH₂ of Cy), 26.9 (s; CH₂ of Cy), 26.1 ppm (s; OCOCH₃); ³¹P{¹H} NMR (81.0 MHz, CD₂Cl₂, 20 °C): δ = 38 ppm (s); elemental analysis (%) calcd for C₄₀H₆₆FeN₂O₄P₂Ru: C 56.01, H 7.76, N 3.27; found: C 58.10, H 7.20, N 2.90.

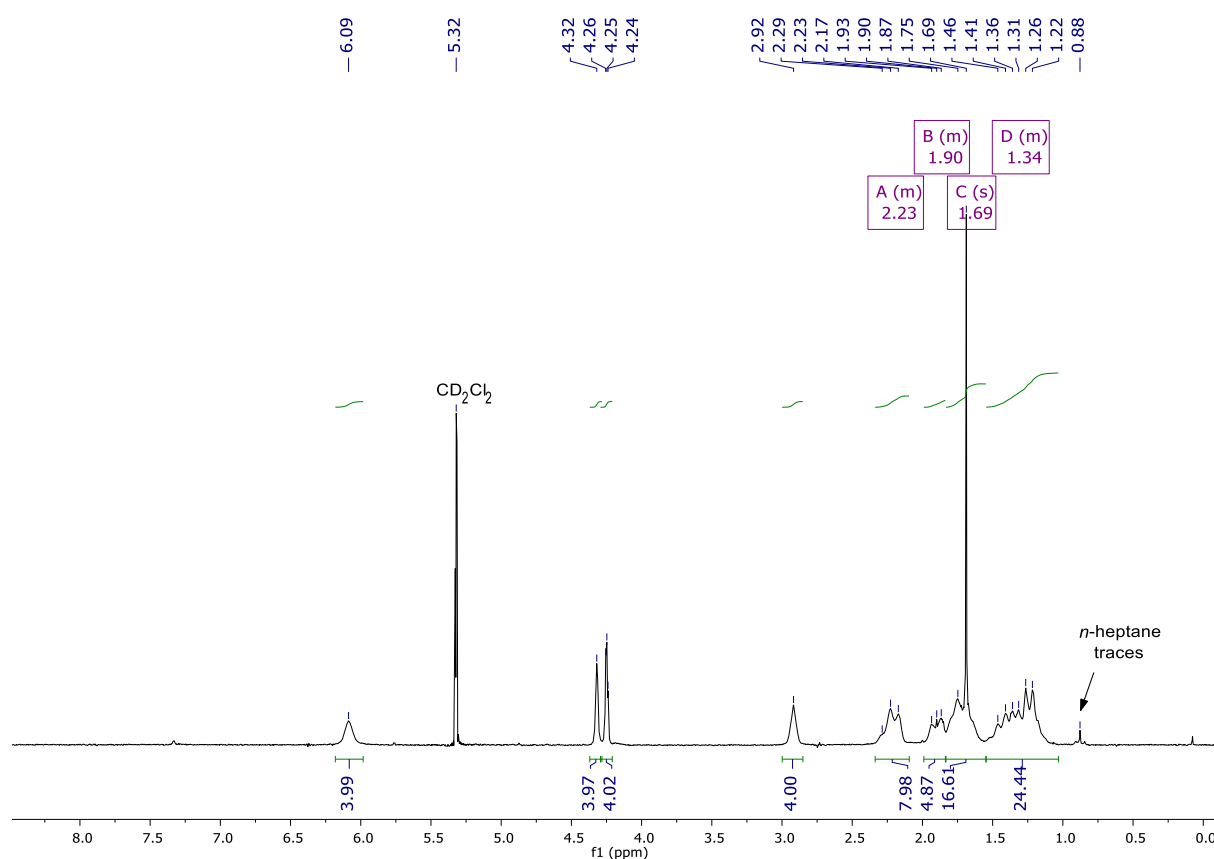


Figure 48 ¹H NMR of *trans*-Ru(OAc)₂(DCyPF)(en) (**5**) in CD₂Cl₂ at 20 °C

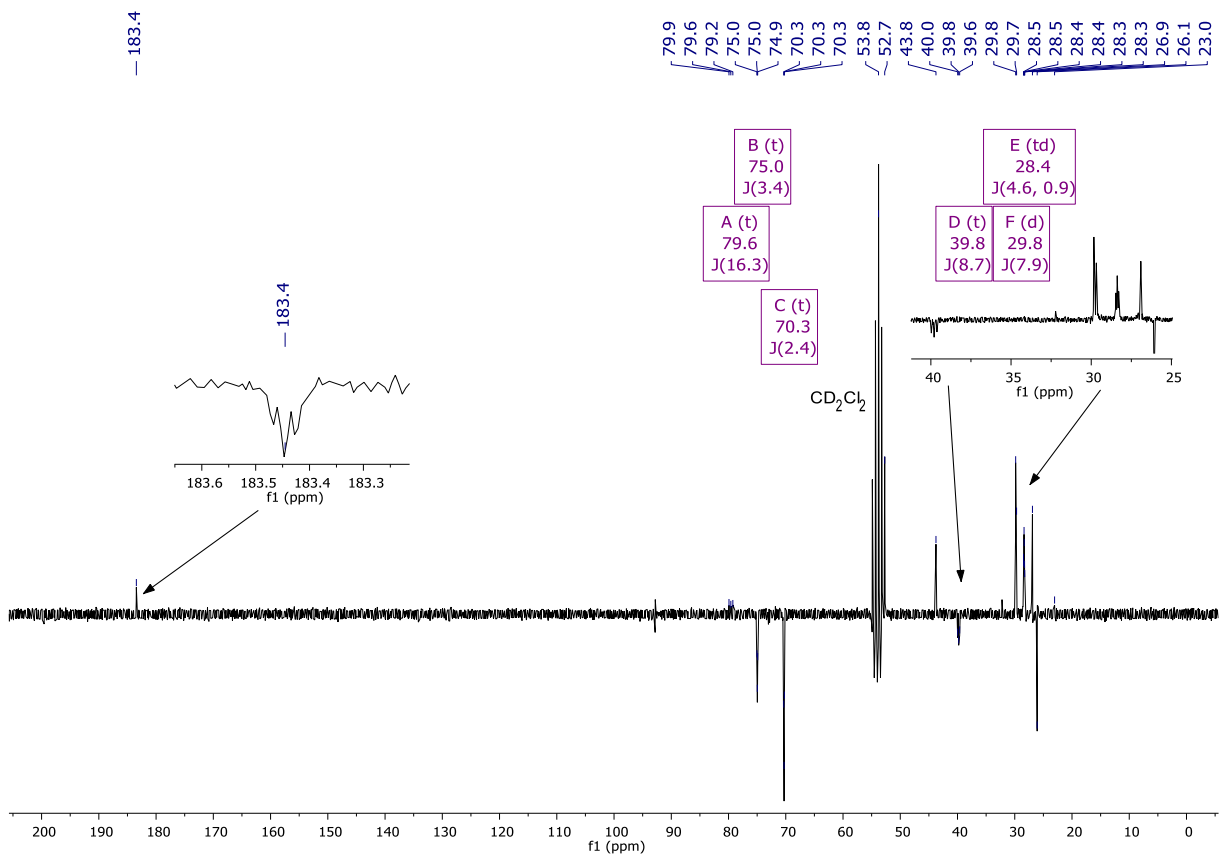


Figure 49 $^{13}\text{C}\{^1\text{H}\}$ NMR of *trans*-Ru(OAc)₂(DCyPF)(en) (**5**) in CD₂Cl₂ at 20 °C

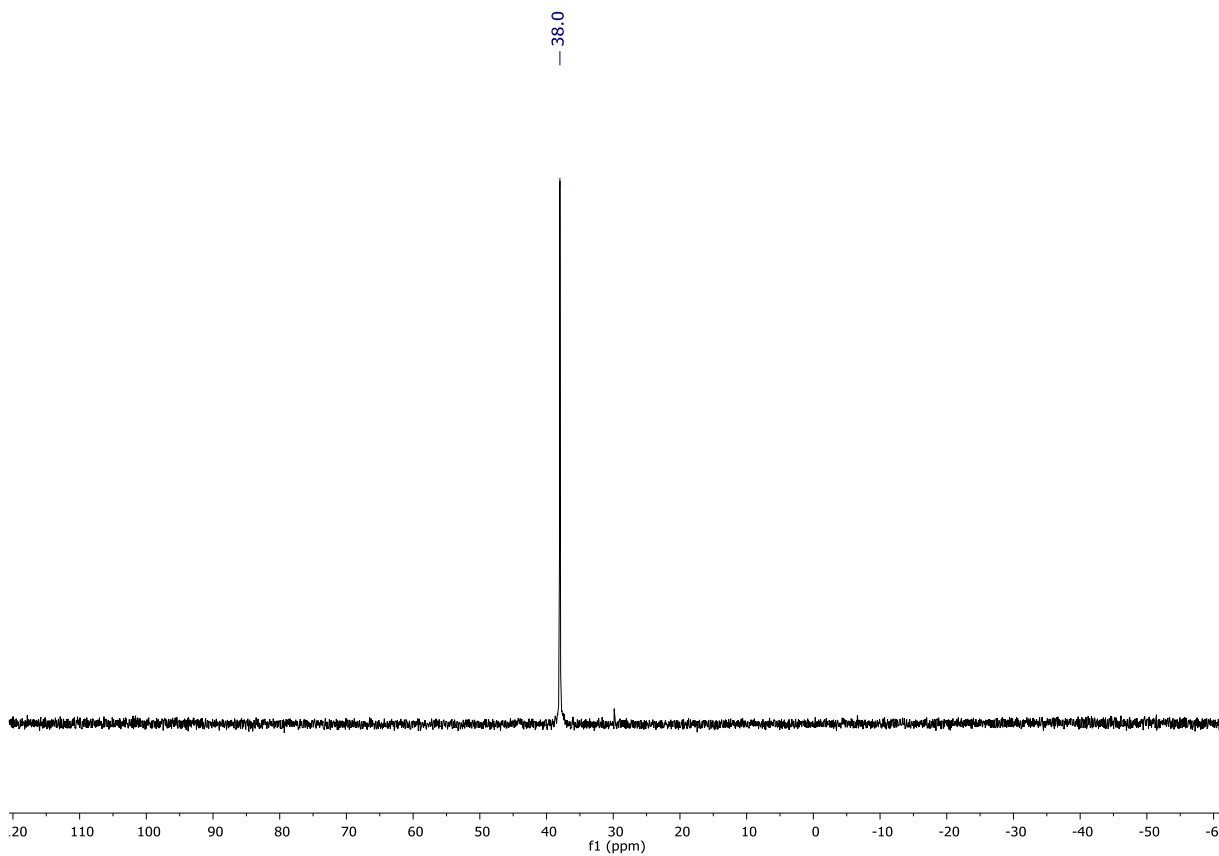
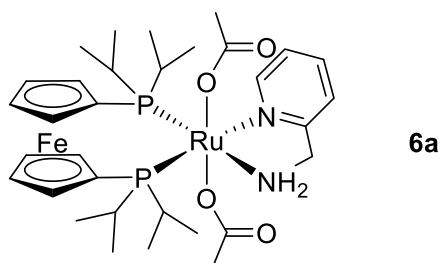


Figure 50 $^{31}\text{P}\{^1\text{H}\}$ NMR spectrum of *trans*-Ru(OAc)₂(DCyPF)(en) (**5**) in CD₂Cl₂ at 20 °C

Synthesis of the mixture of *cis*- and *trans*-Ru(OAc)₂(DiPPF)(ampy):

Ru(OAc)₂(PPh₃)₃ (2.0 g, 2.690 mmol) and DiPPF (1.181 g, 2.820 mmol, 1.05 equiv) were suspended in degassed cyclohexane (14 mL) and the mixture was refluxed for 2 h. The resulting orange suspension consists of Ru(OAc)₂DiPPF as verified by NMR analysis. A solution of ampy (277 μL, 2.690 mmol, 1.0 equiv) in 2 mL of degassed MEK was added to the mixture, that was stirred at room temperature for 4 h. A yellow precipitate containing *trans* and *cis*-Ru(OAc)₂(DiPPF)(ampy) (**6a**, **6b**, **6b'**) was formed. The solid was filtered, washed with a small amount of cold *n*-pentane and then dried under reduced pressure. Yield: 1.7 g (85%).

NMR evidences of *trans*-Ru(OAc)₂(DiPPF)(ampy):



The *trans* isomer (**6a**) (kinetic product) was characterized by the spectroscopic analysis of the reaction *in situ* between Ru(OAc)₂(DiPPF) (25 mg 0.039 mmol) and ampy (4.1 μL, 0.040 mmol, 1.02 equiv), conducted in an NMR tube at low temperature (-60 °C) in CD₂Cl₂. ¹H NMR (200.1 MHz, CD₂Cl₂, -60 °C): δ = 9.01 (d, ³J(H,H) = 5.5 Hz, 1H; *o*-C₅H₄N), 8.80 (br s, 1H; NH₂), 7.69 (t, ³J(H,H) = 7.7 Hz, 1H; *p*-C₅H₄N), 7.33 (d, ³J(H,H) = 7.7 Hz, 1H; *m*-C₅H₄N), 7.20 (t, ³J(H,H) = 6.7 Hz, 1H; *m*-C₅H₄N), 4.86 (br s, 1H; NH₂) 4.55-3.80 (br m, 8H; C₅H₄), 4.16 (s, 2H; CH₂N), 2.95-2.30 (br m, 4H; CH(CH₃)₂), 1.78 (s, 3H; CH₃CO₂), 1.67-1.10 (br m, 15H; CH(CH₃)₂), 1.42 (br s, 3H; CH₃CO₂), 0.88 (m, 3H; CH(CH₃)₂), 0.77 (m, 3H; CH(CH₃)₂), 0.57 ppm (m, 3H; CH(CH₃)₂); ¹³C{¹H} NMR (50.3 MHz, CD₂Cl₂, -60 °C): δ = 182.5 (s; OCOCH₃), 180.9 (s; OCOCH₃), 164.7 (s; NCCH₂), 154.4 (s; C(6) of Py), 135.8 (s; C(4) of Py), 122.0 (s; C(3) of Py), 119.6 (s; C(5) of Py), 84.8 (d, ¹J(C,P) = 35.0 Hz; *ipso*-C₅H₄) 83.7 (d; ¹J(C,P) = 31.0 Hz; *ipso*-C₅H₄), 73.1 (s; C₅H₄), 71.0 (s; C₅H₄), 70.0 (s; C₅H₄), 67.3 (s; C₅H₄), 50.8 (s; CH₂N), 31.3 (d, ¹J(C,P) = 17.9 Hz; CH(CH₃)₂), 29.8 (d, ¹J(C,P) = 14.3 Hz; CH(CH₃)₂), 27.5 (d, ¹J(C,P) = 18.7 Hz; CH(CH₃)₂), 25.2 (s; OCOCH₃), 24.8 (d, ¹J(C,P) = 17.2 Hz; CH(CH₃)₂), 23.5 (s; CH(CH₃)₂), 20.2 (br s; CH(CH₃)₂), 20.0 (s; CH(CH₃)₂),

19.1 (s; CH(CH₃)₂), 18.3 (s; CH(CH₃)₂), 17.8 (br s; CH(CH₃)₂), 17.6 (s; CH(CH₃)₂), 16.6 ppm (s; CH(CH₃)₂); ³¹P{¹H} NMR (81.0 MHz, CD₂Cl₂, -60 °C): δ = 45.2 (d, ²J(P,P) = 29.0 Hz), 43.5 ppm (d, ²J(P,P) = 29.0 Hz).

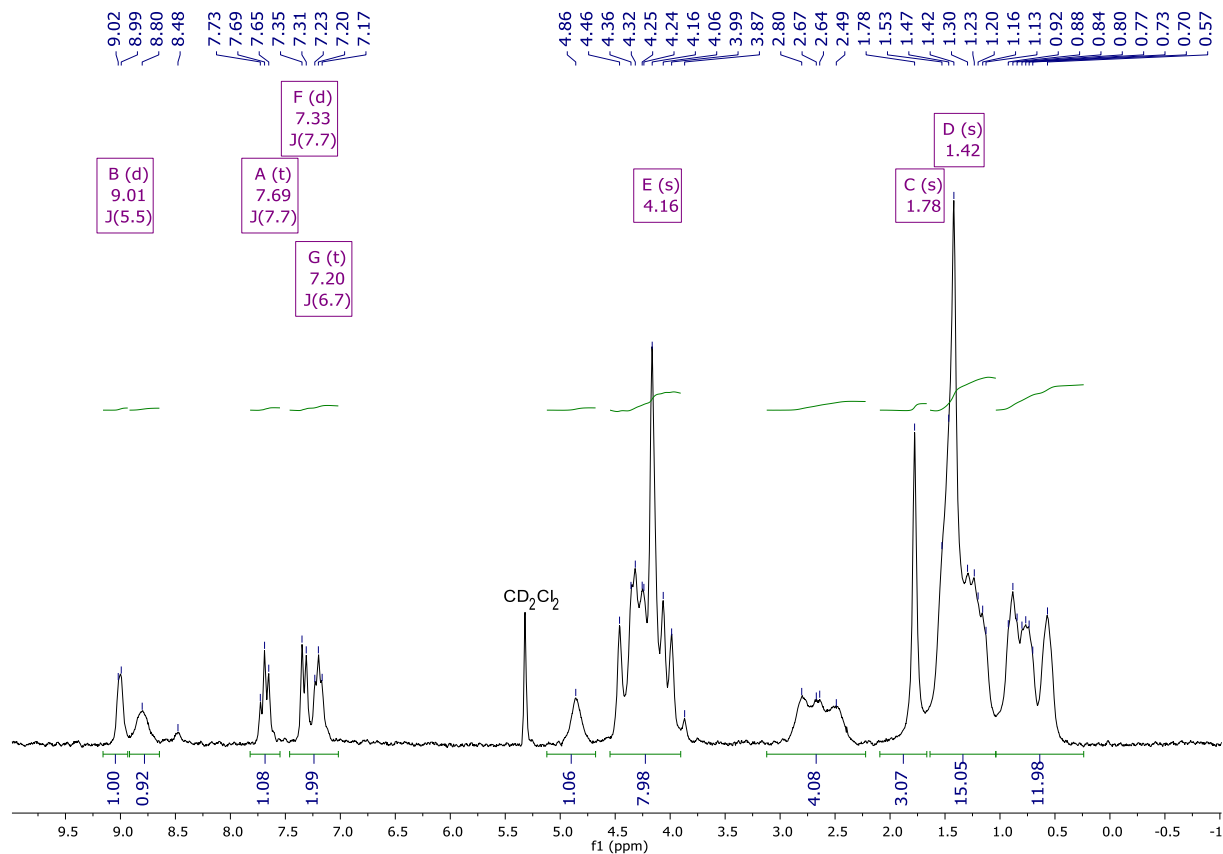


Figure 51 ¹H NMR spectrum of *trans*-Ru(OAc)₂(DiPPF)(ampy) (**6a**) in CD₂Cl₂ at -60 °C

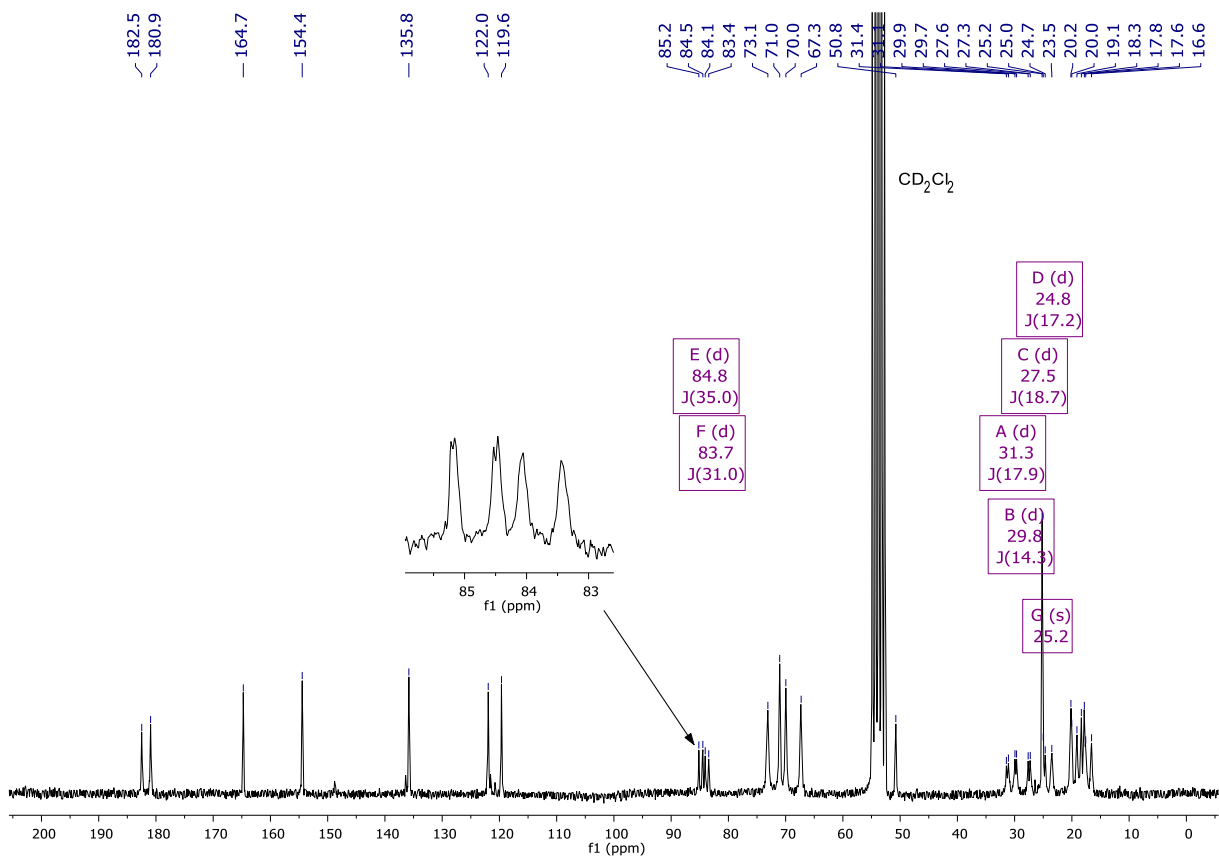


Figure 52 $^{13}\text{C}\{^1\text{H}\}$ NMR spectrum of *trans*-Ru(OAc)₂(DiPPF)(ampy) (**6a**) in CD₂Cl₂ at -60 °C

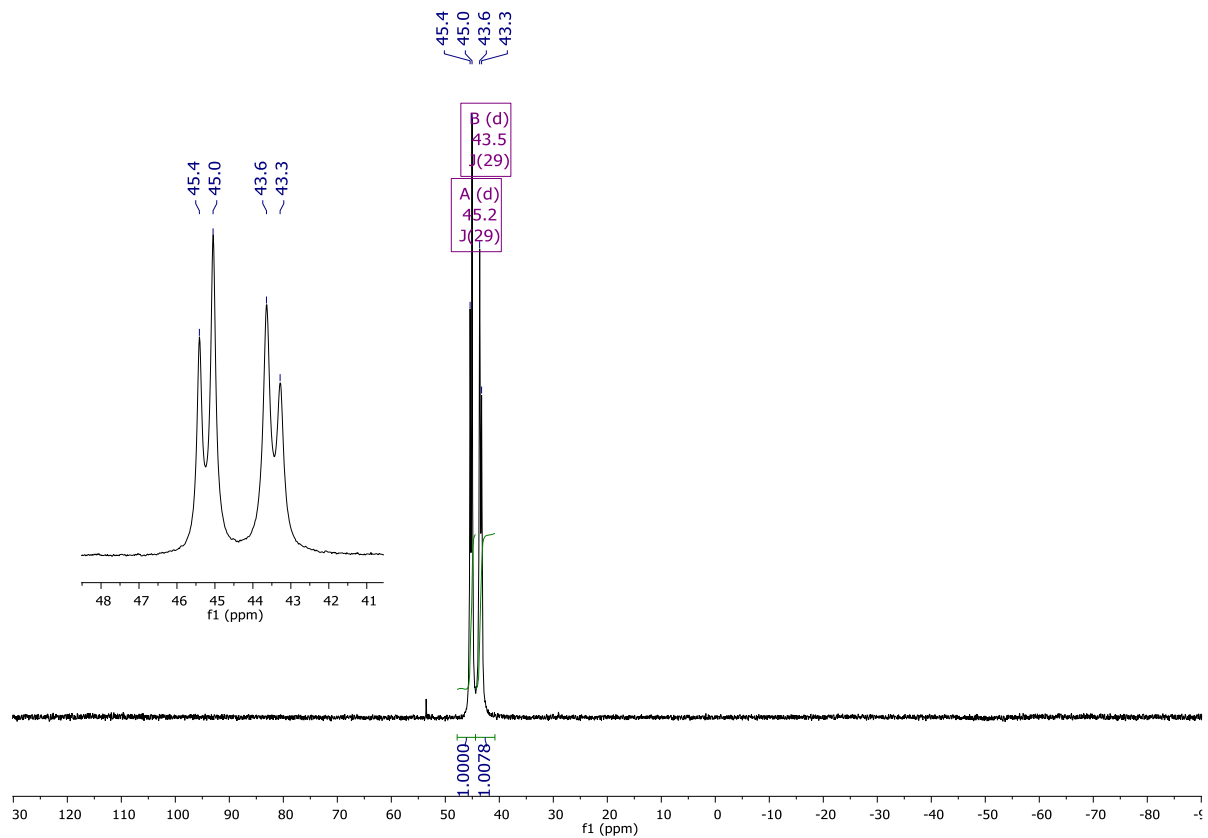
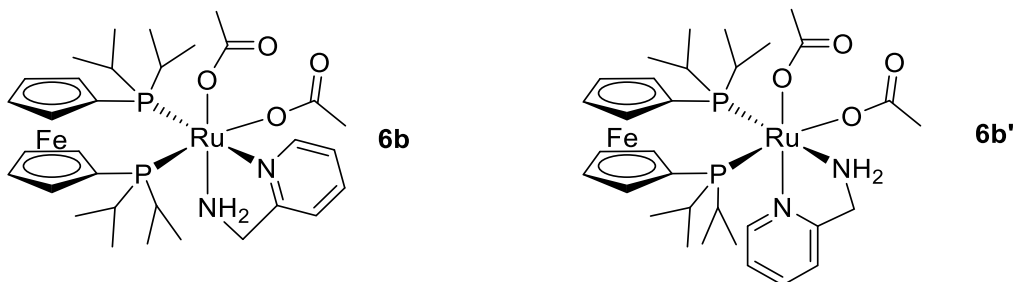


Figure 53 $^{31}\text{P}\{^1\text{H}\}$ NMR spectrum of *trans*-Ru(OAc)₂(DiPPF)(ampy) (**6a**) in CD₂Cl₂ at -60 °C

NMR evidences of the mixture of *cis*-Ru(OAc)₂(DiPPF)(ampy) isomers:

Addition to the NMR tube containing *trans*-Ru(OAc)₂(DiPPF)(ampy) of 50 μ L of CD₃OD at room temperature leading instantly to the two *cis* isomers **6b** and **6b'** in 4:1 mixture, as determined by the integration of the ³¹P and ¹H NMR signals.



¹H NMR (200.1 MHz, CD₂Cl₂, 20 °C): δ = 9.07 (d, ³J(H,H) = 5.6 Hz, 0.2H; *o*-C₅H₄N minor isomer), 8.73 (d, ³J(H,H) = 4.7 Hz, 0.8H *o*-C₅H₄N major isomer), 8.29 (m, 0.8H NH₂ major), 7.92 (t, ³J(H,H) = 7.7 Hz, 0.8H; *p*-C₅H₄N major), 7.71 (t, ³J(H,H) = 9.0 Hz, 0.2H, *p*-C₅H₄N minor), 7.59 (d, ³J(H,H) = 7.8 Hz, 0.8H; *m*-C₅H₄N major), 7.48 (t, ³J(H,H) = 6.2 Hz, 0.8H; *m*-C₅H₄N major), 7.22 (m, 0.4H; *m*-C₅H₄N minor), 4.55 (br s, 0.8H; CH₂N major), 4.41 (br s, 2H; C₅H₄), 4.33 (s, 2H; C₅H₄), 4.28 (br s, 1H; CH₂N and C₅H₄ minor), 4.19 (br s, 0.2H; CH₂N minor), 4.13 (br s, 3.2H; C₅H₄ major), 3.88 (s, 0.2H; CH₂N minor), 3.29 (s, 0.8H, NH₂ major), 2.76-2.32 (br m, 4H; CH(CH₃)₂ major + minor), 1.97 (s, 0.6H; CH₃CO₂ minor), 1.88 (s, 3H; CH₃CO₂ major + minor), 1.71 (s, 2.4H; CH₃CO₂ major), 1.48 (dq, ³J(P,H) = 15.0 Hz, ³J(H,H) = 7.0 Hz, 6H; CH(CH₃)₂ major + minor), 1.39-0.99 (br m, 12H; CH(CH₃)₂ major + minor), 0.67 ppm (dq, ³J(P,H) = 15.8 Hz, ³J(H,H) = 7.1 Hz, 6H; CH(CH₃)₂ major + minor); ¹³C{¹H} NMR (50.3 MHz, CD₂Cl₂, 20 °C): δ = 188.7 (s; OCOCH₃ minor isomer), 188.1 (d, ³J(C,P) = 2.0 Hz; OCOCH₃ major isomer), 179.1 (d, ³J(C,P) = 1.1 Hz; OCOCH₃ major), 177.4 (s; OCOCH₃ minor), 162.1 (d, ³J(C,P) = 1.1 Hz; NCCH₂ major), 150.5 (br s; C(6) of Py major), 149.1 (s; C(6) of Py minor), 138.4 (s; C(4) of Py major), 137.1 (s; C(4) of Py minor), 124.7 (d, ³J(C,P) = 2.3 Hz; C(3) of Py major), 123.2 (s; C(3) of Py minor), 122.5 (s; C(5) of Py minor), 121.5 (d, ³J(C,P) = 1.4 Hz; C(5) of Py major), 84.3 (d, ¹J(C,P) = 35 Hz; *ipso*-C₅H₄ major), 82.6 (d, ¹J(C,P) = 39 Hz; *ipso*-C₅H₄ major), 75.0 (br s; C₅H₄ minor), 74.1 (m; C₅H₄ minor), 73.9 (m; C₅H₄ minor), 73.5 (d, ²J(C,P) = 3.8 Hz; C₅H₄ major), 73.4 (d, ²J(C,P) = 3.4 Hz; C₅H₄ major), 73.2 (d, ²J(C,P) = 3.6 Hz; C₅H₄ minor), 72.6 (d, ²J(C,P) = 1.3 Hz; C₅H₄ minor), 72.2 (d, J(C,P) = 5.8 Hz; C₅H₄ major), 72.0 (d, J(C,P) = 2.0 Hz;

C₅H₄ major), 71.7 (d, $J(\text{C,P}) = 2.5$ Hz; C₅H₄ major), 71.6 (br s; C₅H₄ major), 70.0 (d; $J(\text{C,P}) = 3.6$ Hz; C₅H₄ major), 69.8 (d; $J(\text{C,P}) = 3.9$ Hz; C₅H₄ major), 52.6 (d; $^3J(\text{C,P}) = 2.8$ Hz CH₂N major), 30.6 (d, $^1J(\text{C,P}) = 28.6$ Hz; CH(CH₃)₂ major), 30.3 (d, $^1J(\text{C,P}) = 24.7$ Hz; CH(CH₃)₂ major), 29.8 (d, $J(\text{C,P}) = 22.0$ Hz; CH(CH₃)₂ major), 29.1 (d, $^1J(\text{C,P}) = 21.6$ Hz; CH(CH₃)₂ major), 24.5 (s; OCOCH₃ major), 24.5 (d, $^1J(\text{C,P}) = 1.5$ Hz; CH(CH₃)₂ minor), 24.2 (s; OCOCH₃ major), 21.8 (m; CH(CH₃)₂ minor), 20.9 (d, $^2J(\text{C,P}) = 4.6$ Hz; CH(CH₃)₂ major), 20.3 (d, $^2J(\text{C,P}) = 2.9$ Hz; CH(CH₃)₂ major), 20.2 (s; OCOCH₃ major), 20.1 (d, $^2J(\text{C,P}) = 2.0$ Hz; CH(CH₃)₂ major), 19.8 (d, $^2J(\text{C,P}) = 3.7$ Hz; CH(CH₃)₂ major), 19.6 (d, $^2J(\text{C,P}) = 3.7$ Hz; CH(CH₃)₂ major), 19.4 (br s; CH(CH₃)₂ major), 18.6 ppm (d, $^2J(\text{C,P}) = 1.2$ Hz; CH(CH₃)₂ major); $^{31}\text{P}\{^1\text{H}\}$ NMR (81.0 MHz, CD₂Cl₂, 20 °C): $\delta = 65.5$ (d, $^2J(\text{P,P}) = 25.5$ Hz; minor isomer), 62.9 (d, $^2J(\text{P,P}) = 27.5$ Hz; major isomer), 51.2 (d, $^2J(\text{P,P}) = 27.5$ Hz; major), 45.4 ppm (d, $^2J(\text{P,P}) = 24.7$ Hz; minor).

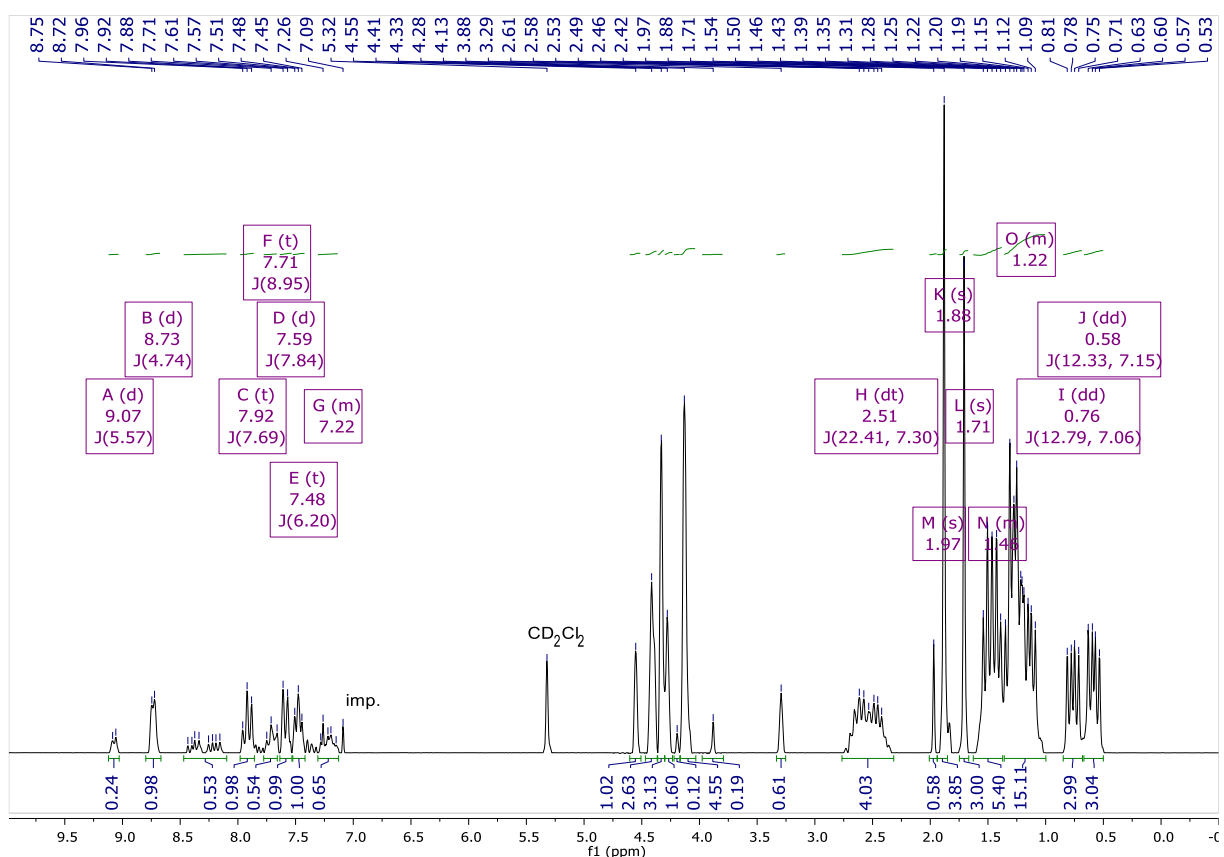


Figure 54 ^1H NMR spectrum of isomer mixture $\text{cis-Ru}(\text{OAc})_2(\text{DiPPF})(\text{ampy})$ (**6b**, **6b'**) in CD_2Cl_2 at 20°C

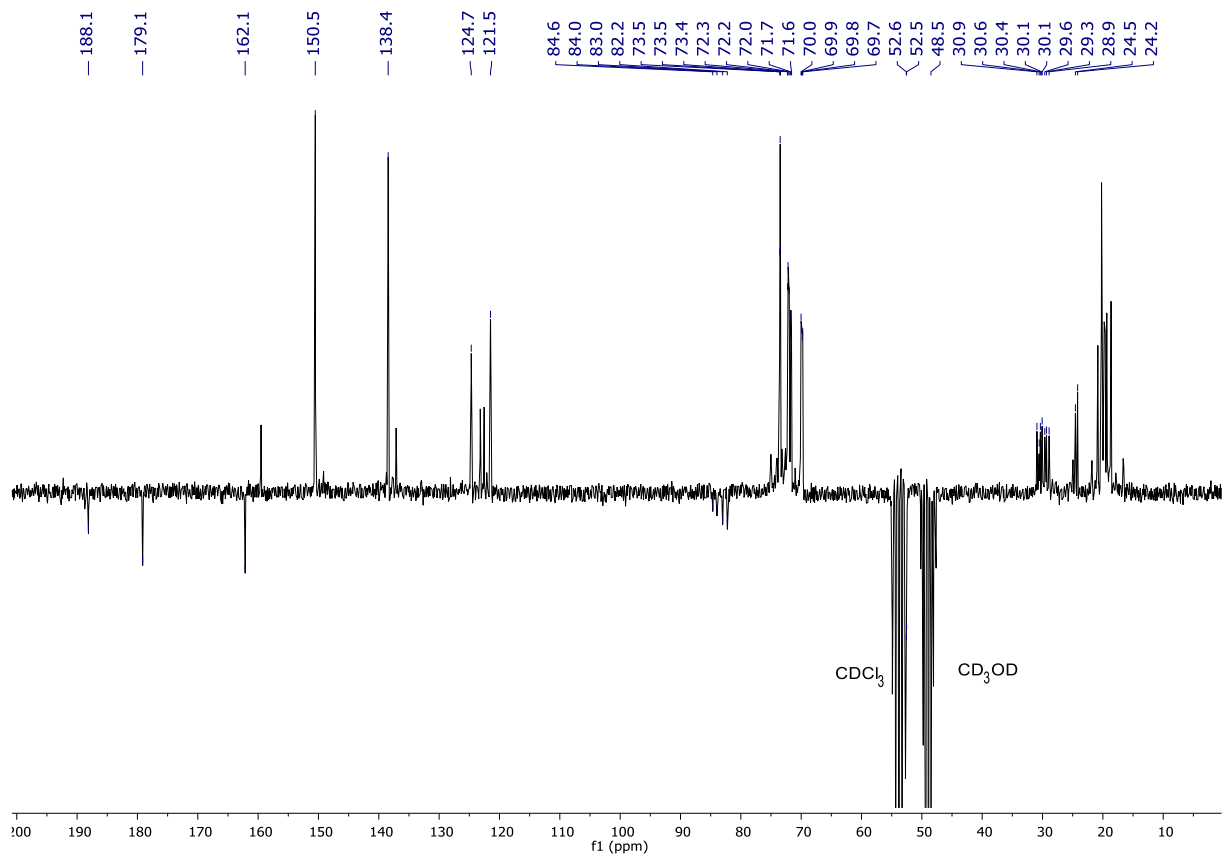


Figure 55 $^{13}\text{C}\{^1\text{H}\}$ NMR spectrum of isomer mixture *cis*-Ru(OAc)₂(DiPPF)(ampy) (**6b**, **6b'**) in CD₂Cl₂ at 20 °C

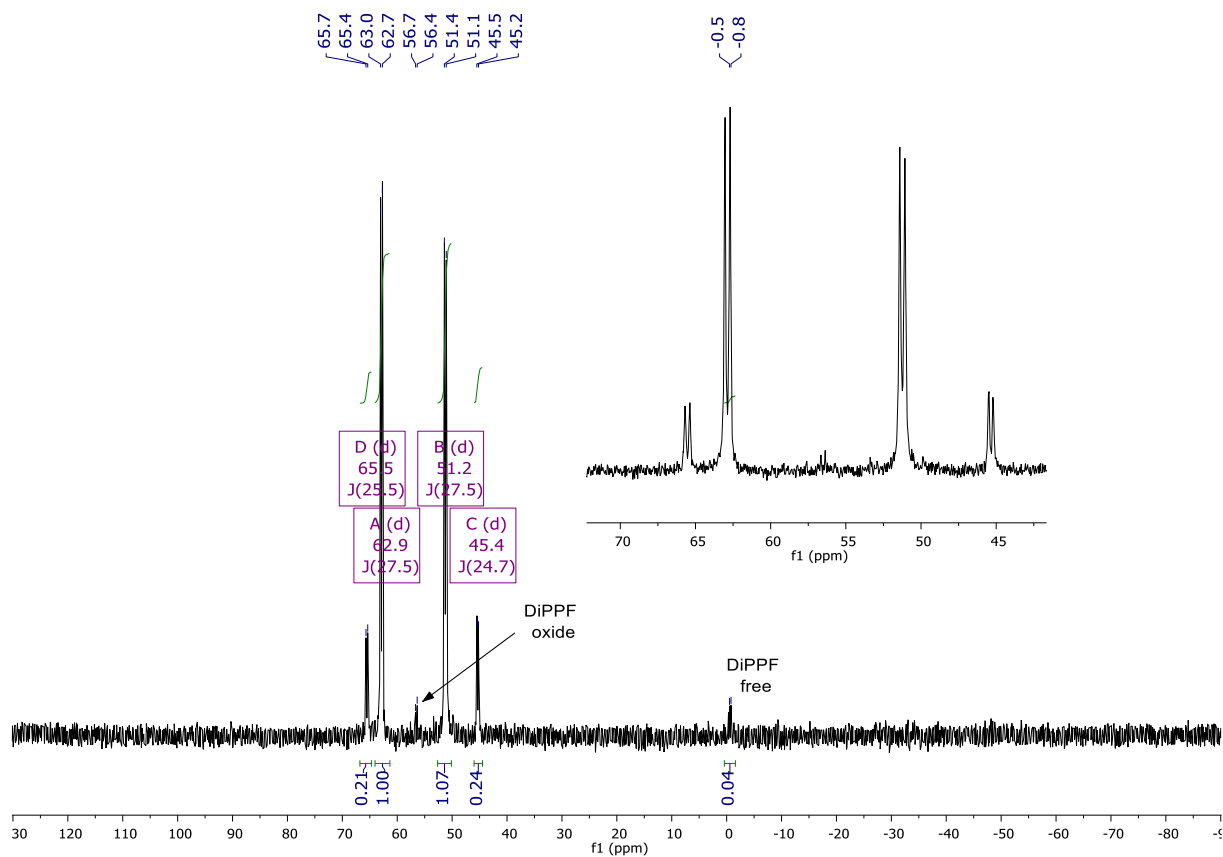
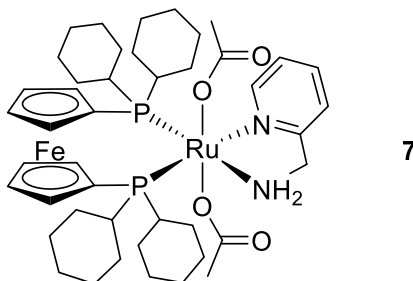


Figure 56 $^{31}\text{P}\{^1\text{H}\}$ NMR spectrum of isomer mixture *cis*- $\text{Ru}(\text{OAc})_2(\text{DiPPF})(\text{ampy})$ (**6b**, **6b'**) in CD_2Cl_2 at 20 °C

Synthesis *trans*- $\text{Ru}(\text{OAc})_2(\text{DCyPF})(\text{ampy})$ (7**):**



$\text{Ru}(\text{OAc})_2(\text{PPh}_3)_3$ (98 mg, 0.132 mmol) and DCyPF (80 mg, 0.138 mmol, 1.05 equiv) were suspended in 1.5 mL of degassed *n*-heptane. The mixture was refluxed for 1 h until a solution containing $\text{Ru}(\text{OAc})_2\text{DCyPF}$ is formed, as verified by NMR analysis. Ampy (14 μL , 0.132 mmol 1.0 equiv) was added to the solution leading rapidly to a yellow precipitate. The solid was filtered, washed with cold *n*-heptane (3x2 mL) and then dried under reduced pressure. Yield: 77 mg (65%). ^1H NMR (200.1 MHz, CDCl_3 , 20 °C): δ = 9.02 (d, $^3J(\text{H,H})$ = 2.0 Hz, 1H; *o*- $\text{C}_5\text{H}_4\text{N}$), 7.62 (t, $^3J(\text{H,H})$ = 7.1 Hz, 1H; *p*- $\text{C}_5\text{H}_4\text{N}$), 7.16 (pseudo t, $J(\text{H,H})$ = 6.7 Hz, 2H; *m*- $\text{C}_5\text{H}_4\text{N}$), 4.43 (br s, 2H; C_5H_4), 4.36 (br s, 2H; C_5H_4), 4.16 (br s, 4H; C_5H_4), 4.11 (m, 2H; CH_2N), 2.39 (s, 4H; PCH of Cy), 2.27-0.91 ppm (m, 46H; CH_3CO_2 and CH_2 of Cy). ^{31}P NMR (81.0 MHz, CDCl_3 , 20 °C): δ = 39.3 (d, $^2J(\text{P,P})$ = 28.9 Hz), 37.0 ppm (d, $^2J(\text{P,P})$ = 28.9 Hz); elemental analysis (%) calcd for $\text{C}_{44}\text{H}_{66}\text{FeN}_2\text{O}_4\text{P}_2\text{Ru}$: C 58.34, H 7.34, N 3.09; found: C 57.50, H 7.10, N 2.90.

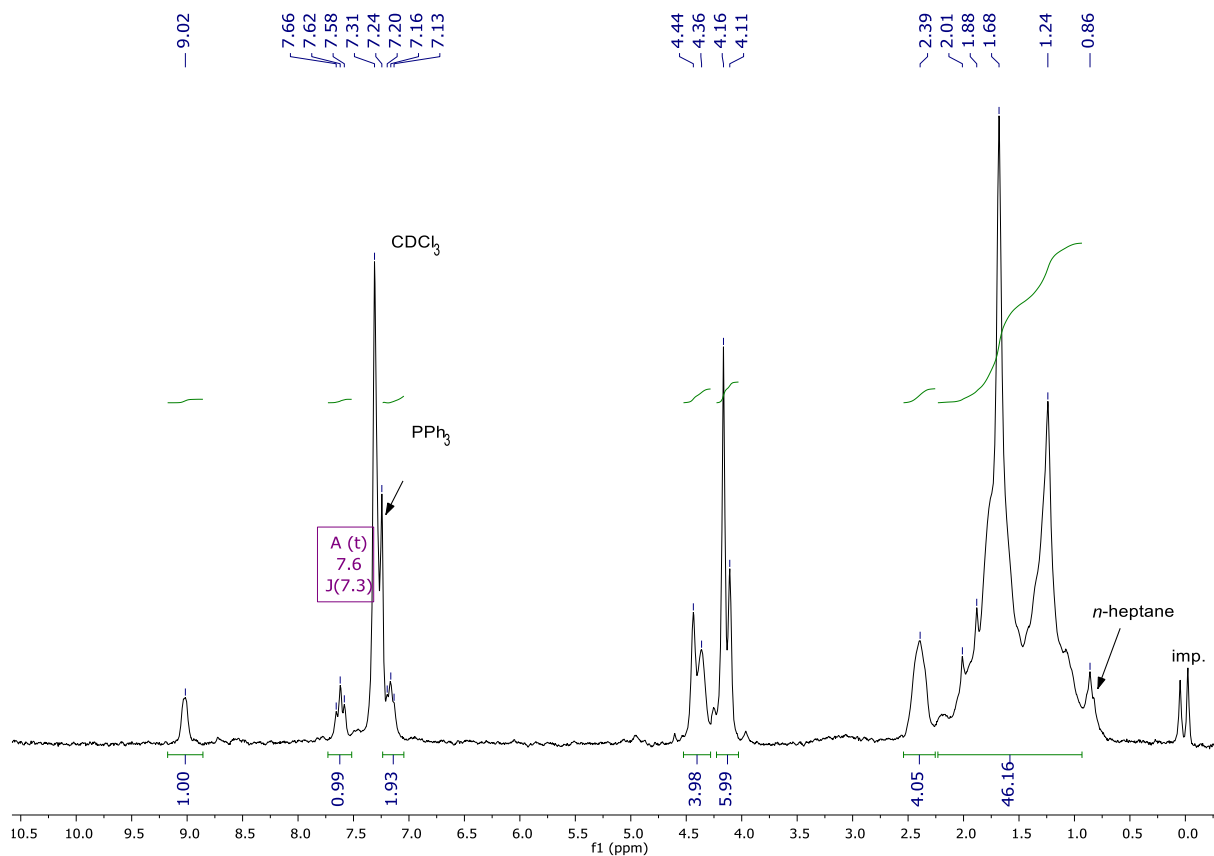


Figure 57 ¹H NMR spectrum of Ru(OAc)₂(DCyPF)(ampy) (**7**) in CDCl₃ at 20 °C.

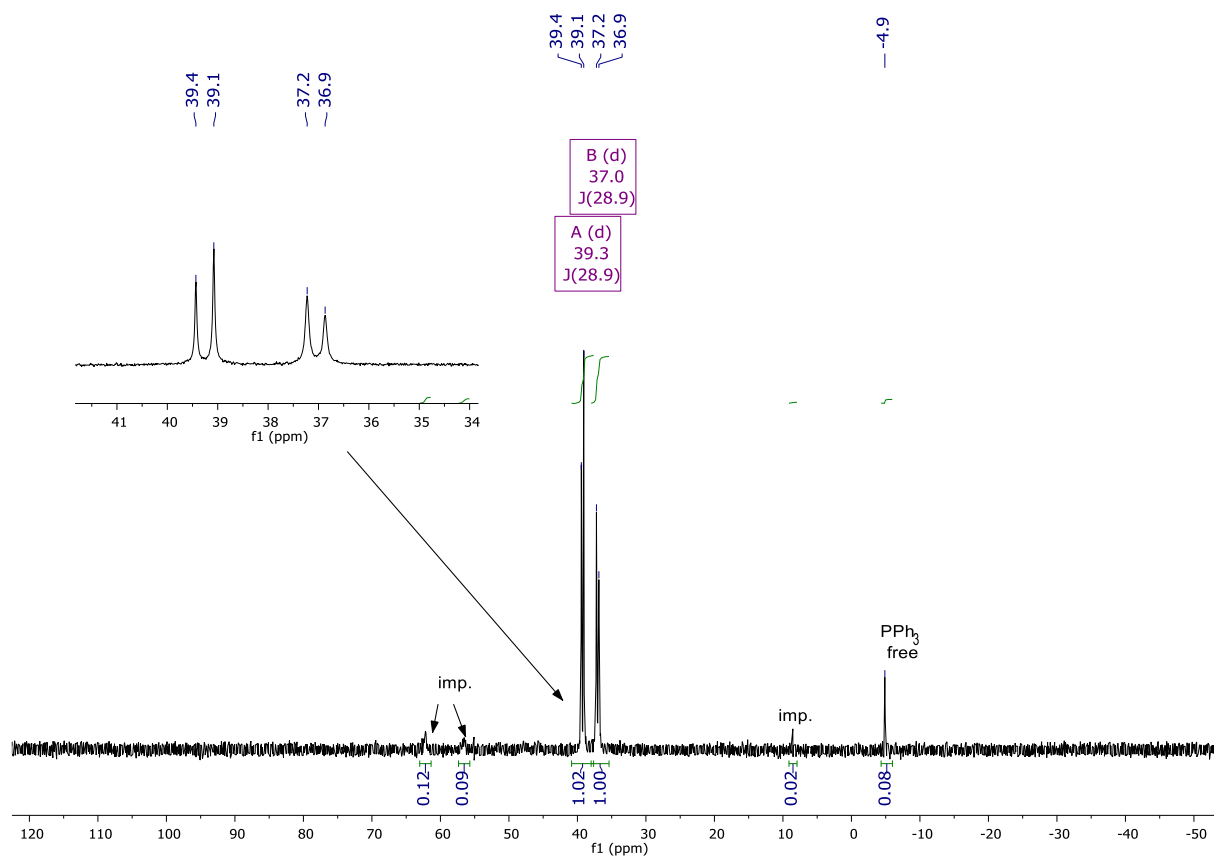
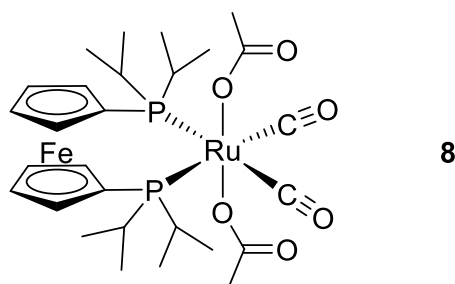


Figure 58 ³¹P{¹H} NMR spectrum of Ru(OAc)₂(DCyPF)(ampy) (**7**) in CDCl₃ at 20 °C.

Synthesis of *trans,cis*-Ru(OAc)₂(CO)₂(DiPPF) (8):



Ru(OAc)₂DiPPF (60 mg, 0.08 mmol) was dissolved in degassed CH₂Cl₂ (3 mL), and vigorously stirred under CO atmosphere (1 atm) for 30 minutes at room temperature. The solvent was evaporated under reduced pressure leading the product as a yellow powder. Yield: 54.4 mg (98%). ¹H NMR (200.1 MHz, CDCl₃, 20 °C): δ = 4.69 (s, 4H; C₅H₄), 4.48 (s, 4H; C₅H₄), 2.57 (hept, ³J(H,H) = 5.9 Hz, 4H; CH(CH₃)₂), 1.93 (s, 6H; CH₃CO₂), 1.29 (dd, ³J(P,H) = 13.2 Hz, ³J(H,H) = 7.1 Hz, 12H; CH(CH₃)₂), 1.14 ppm (dd, ³J(P,H) = 13.3 Hz, ³J(H,H) = 7.1 Hz, 12H; CH(CH₃)₂); ¹³C{¹H} NMR (50.3 MHz, CDCl₃, 20 °C): δ = 195.8 (dd, ²J(C,P) = 105.2 Hz, ²J(C,P) = 20.9 Hz; CO), 177.0 (t, ³J(C,P) = 1.9 Hz; OCOCH₃), 74.9 (t, ²J(C,P) = 3.6 Hz; C₅H₄), 74.4-73.2 (m; *ipso*-C₅H₄), 71.4 (t, ²J(C,P) = 2.8 Hz; C₅H₄), 27.3-26.1 (m; CH(CH₃)₂), 23.2 (s; OCOCH₃), 19.7 (s; CH(CH₃)₂), 18.8 ppm (s; CH(CH₃)₂); ³¹P{¹H} NMR (81.0 MHz, CDCl₃, 20 °C): δ = 26.5 ppm (s); elemental analysis (%) calcd for C₂₈H₄₂FeO₆P₂Ru: C 48.49, H 6.10; found: C 48.40, H 6.30.

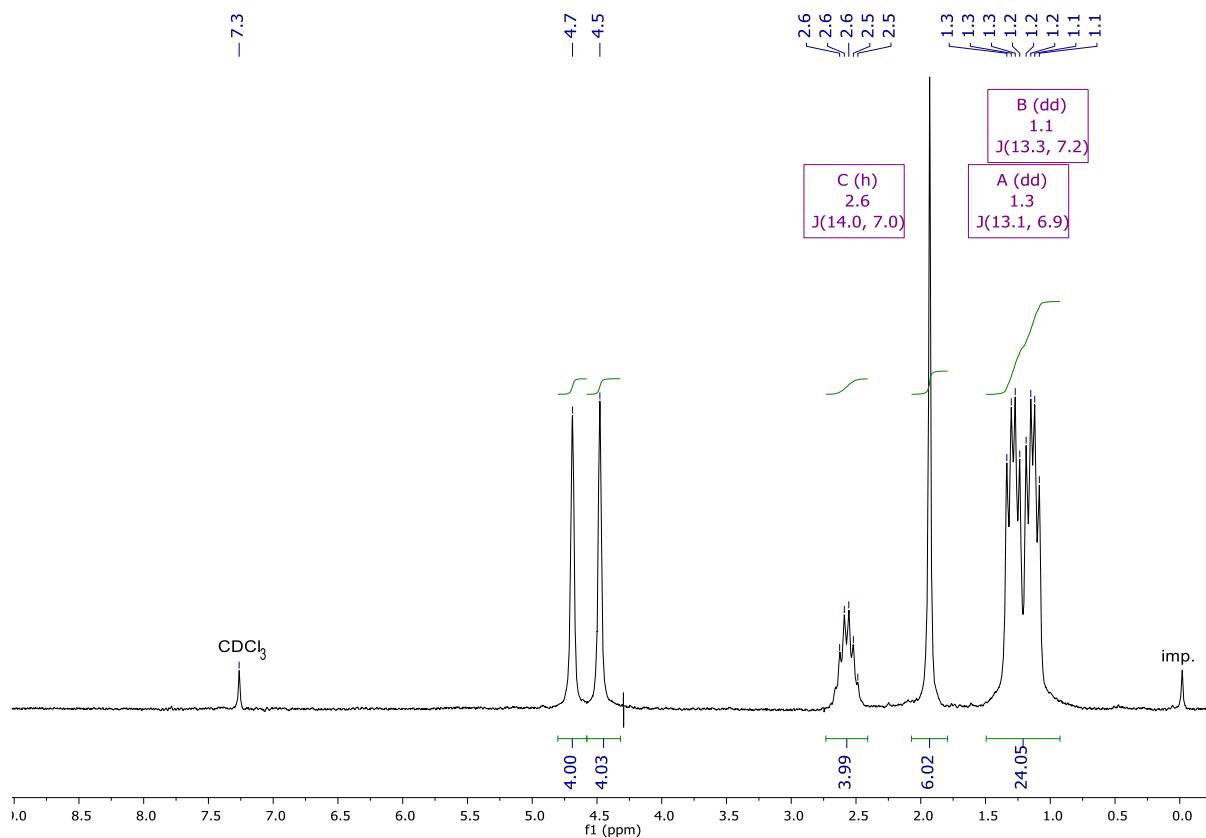


Figure 59 ^1H NMR spectrum of *trans,cis*-Ru(OAc)₂(CO)₂(DiPPF) (**8**) in CDCl₃ at 20 °C

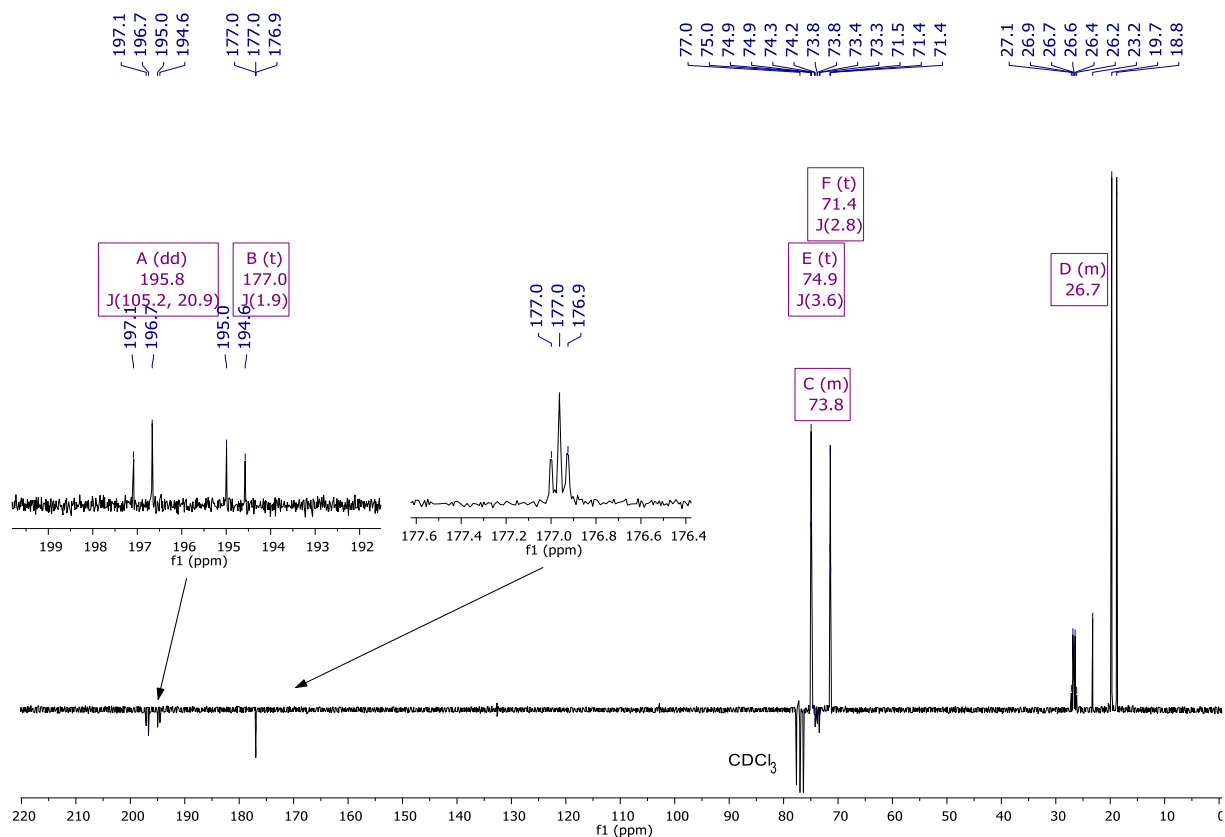


Figure 60 $^{13}\text{C}\{^1\text{H}\}$ NMR of *trans,cis*-Ru(OAc)₂(CO)₂(DiPPF) (**8**) in CDCl₃ at 20 °C

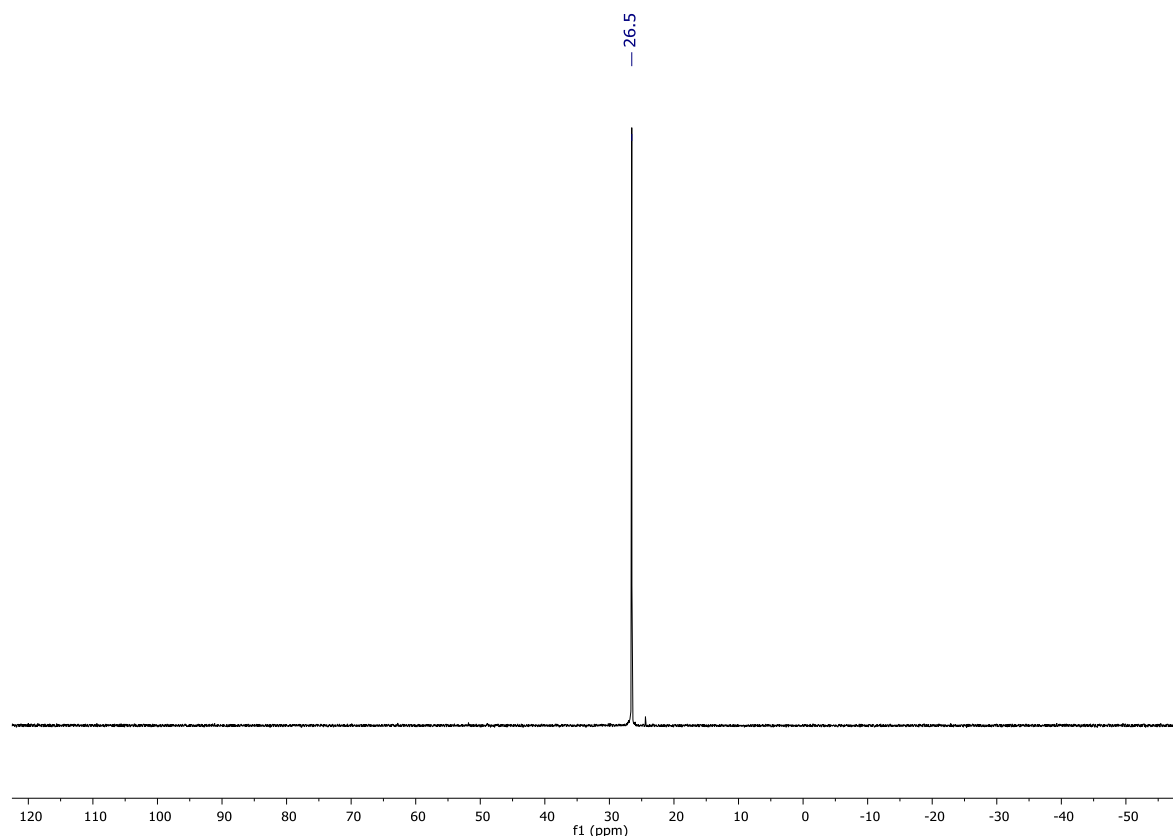
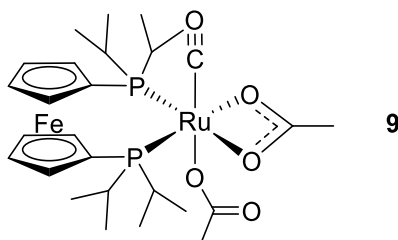


Figure 61 $^{31}\text{P}\{^1\text{H}\}$ NMR spectrum of *trans,cis*- $\text{Ru}(\text{OAc})_2(\text{CO})_2(\text{DiPPF})$ (**8**) in CDCl_3 at $20\text{ }^\circ\text{C}$

Synthesis of $\text{Ru}(\text{OAc})_2(\text{CO})(\text{DiPPF})$ (**9**):



Method a): $\text{Ru}(\text{OAc})_2(\text{DiPPF})$ (**2**) (359 mg, 0.563 mmol) was placed into a three-neck round-bottom flask fitted with a bubbler, subjected to three vacuum-argon cycles and dissolved in 7 mL of degassed toluene. The solution was refluxed for 1 h and then cooled at room temperature. Formaldehyde in water 24% w/w (550 μL , 2.80 mmol, ca. 5 equiv) was added and the biphasic system was stirred at $120\text{ }^\circ\text{C}$ (oil bath temperature) for 2 h. The resulting reddish organic phase was separated from the aqueous fraction and dried with anhydrous MgSO_4 . After filtration, the solvent was evaporated under reduced pressure affording the product as a yellow powder. Yield: 292 mg (78%). ^1H NMR (200.1 MHz, CD_2Cl_2 , $20\text{ }^\circ\text{C}$): $\delta = 4.82$ (br s, 2H; C_5H_4), 4.47

(s, 2H; C₅H₄), 4.40 (s, 2H; C₅H₄), 4.30 (s, 2H; C₅H₄), 2.65 (m, 2H; CH(CH₃)₂), 2.44 (m, 2H; CH(CH₃)₂), 1.92 (s, 6H; CH₃CO₂), 1.62 (dd, ³J(P,H) = 15.9 Hz, ³J(H,H) = 7.0 Hz, 6H; CH(CH₃)₂), 1.30 (dd, ³J(P,H) = 14.2 Hz, ³J(H,H) = 7.1 Hz, 12H; CH(CH₃)₂), 0.95 ppm (dd, ³J(P,H) = 12.0 Hz, ³J(H,H) = 6.9 Hz, 6H; CH(CH₃)₂); ¹³C{¹H} NMR (50.3 MHz, CD₂Cl₂, 20 °C): δ = 74.2 (br s; C₅H₄), 72.6 (d, ²J(C,P) = 8.7 Hz; C₅H₄), 71.9 (br s; C₅H₄), 69.9 (d, ³J(C,P) = 3.0 Hz; C₅H₄), 25.5 (br s; CH(CH₃)₂), 24.5 (t, ³J(C,P) = 1.6 Hz; OCOCH₃), 20.9 (br s; CH(CH₃)₂), 19.8 (s; CH(CH₃)₂), 19.3 (br s; CH(CH₃)₂), 18.6 ppm (br s; CH(CH₃)₂); ³¹P{¹H} NMR (81.0 MHz, CD₂Cl₂, 20 °C): δ = 61.7 ppm (br s); IR: $\tilde{\nu}$ = 1939 (s) cm⁻¹ (C≡O); elemental analysis (%) calcd for C₂₇H₄₂FeO₅P₂Ru: C 48.73, H 6.36; found: C 48.82, H 6.54.

Method b): Ru(OAc)₂(DiPPF) (**2**) (197 mg, 0.309 mmol) and paraformaldehyde (H₂CO)_n (23 mg, 0.77 mmol, 2.5 equiv) were suspended in 5 mL of toluene in a 10 mL Schlenk tube and heated at 120°C for 3 h. The obtained reddish solution was concentrated under reduced pressure to 1 mL, and added of *n*-pentane (2 mL). The resulting yellow precipitate was filtered, washed with diethyl ether (3x10 mL) and finally dried under reduced pressure. Yield: 100 mg (49%).

Method c): Ru(OAc)₂(CO)₂(DiPPF) (**8**) (197 mg, 0.309 mmol) was heated at 120°C under reduced pressure for 16 h affording **9**. Yield: 185 mg (93%).

Method d): [Ru(CO)₂(Cl)₂]_n (131 mg, 0.574 mmol) and DiPPF (264 mg, 0.632) were suspended in 5 mL of degassed toluene and refluxed for 2.5 h. Sodium acetate (236 mg, 2.8 mmol) were added to the yellow suspension than was refluxed for 24 h. The resulting solution was cooled to room temperature and diethyl ether (5 mL) was added, affording a yellow precipitate. The solid was filtered, washed with diethyl ether (2x1 mL) and dried under reduced pressure. Yield 208 mg (53%).

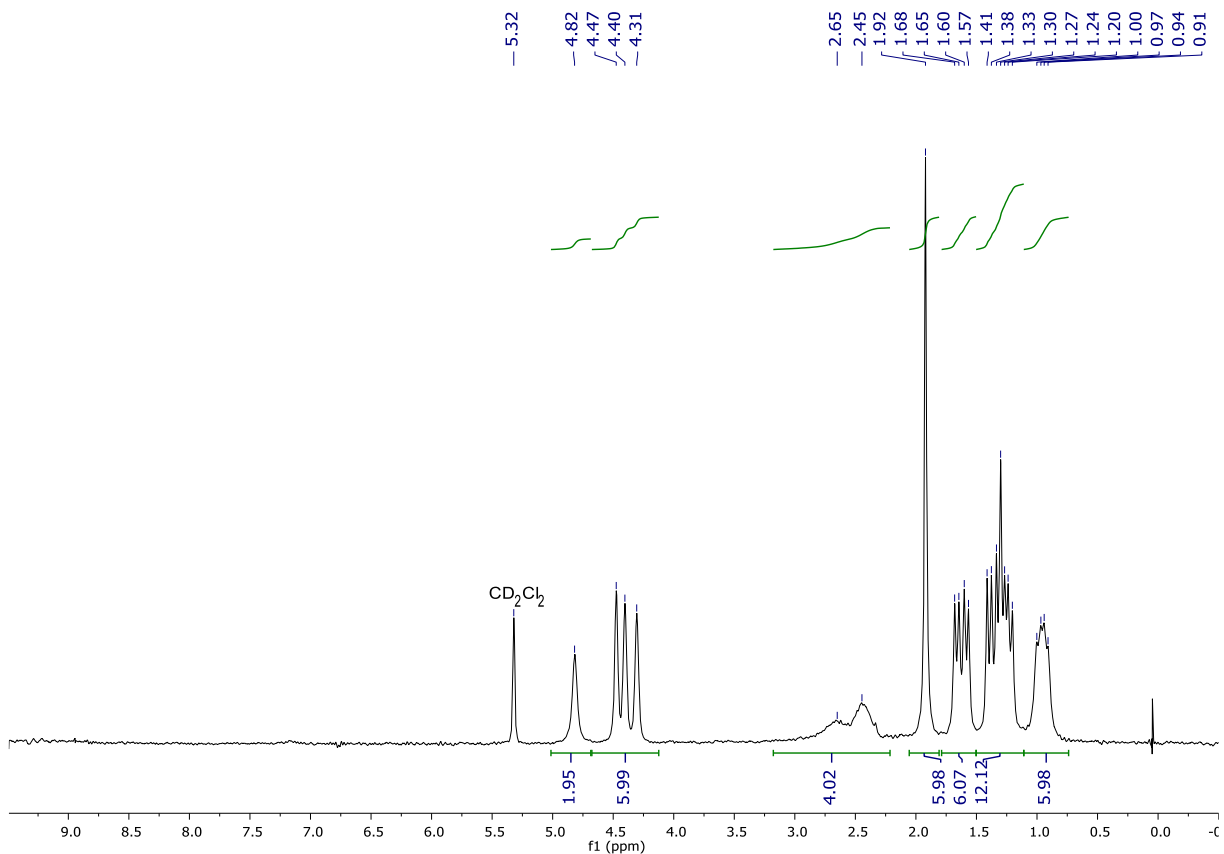


Figure 62 1H NMR spectrum of $Ru(OAc)_2(CO)(DiPPF)$ (**9**) in CD_2Cl_2 at 20 °C

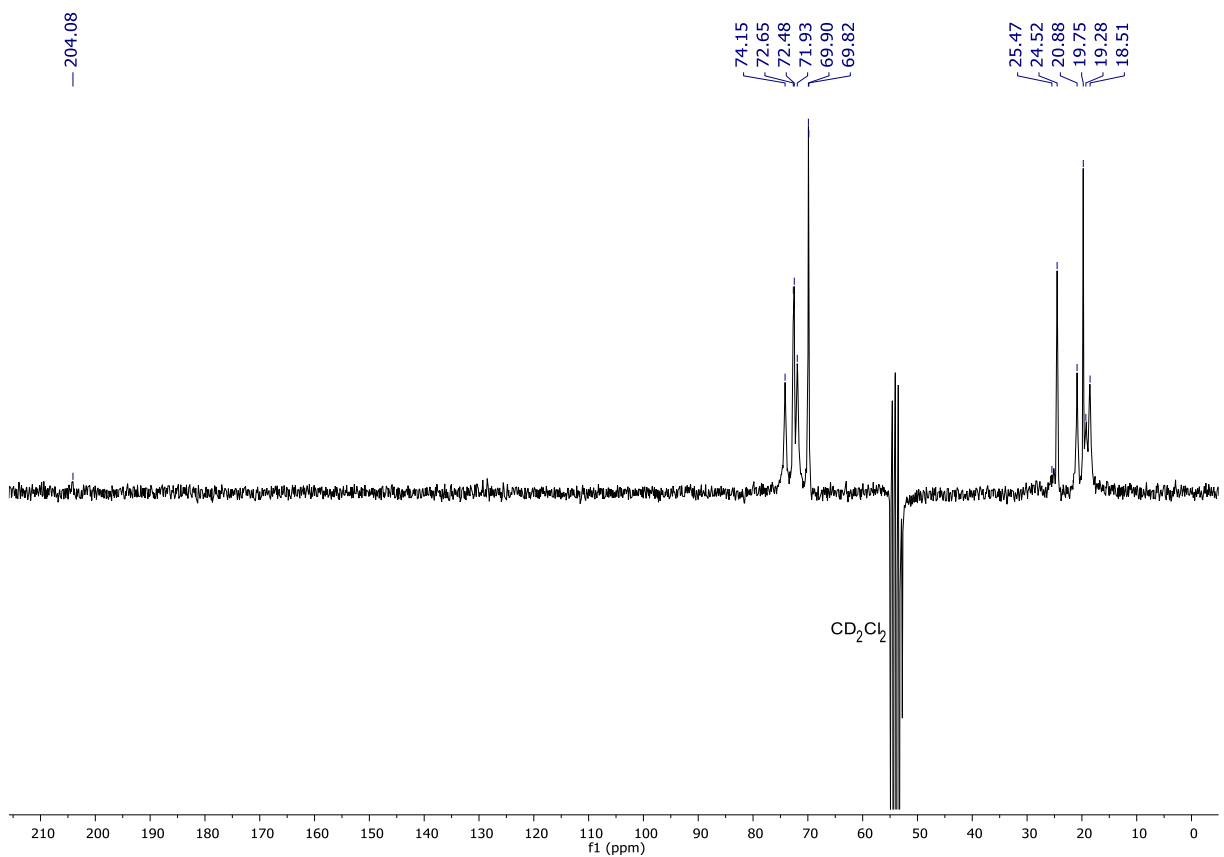


Figure 63 $^{13}C\{^1H\}$ NMR spectrum of $Ru(OAc)_2(CO)(DiPPF)$ (**9**) in CD_2Cl_2 at 20 °C

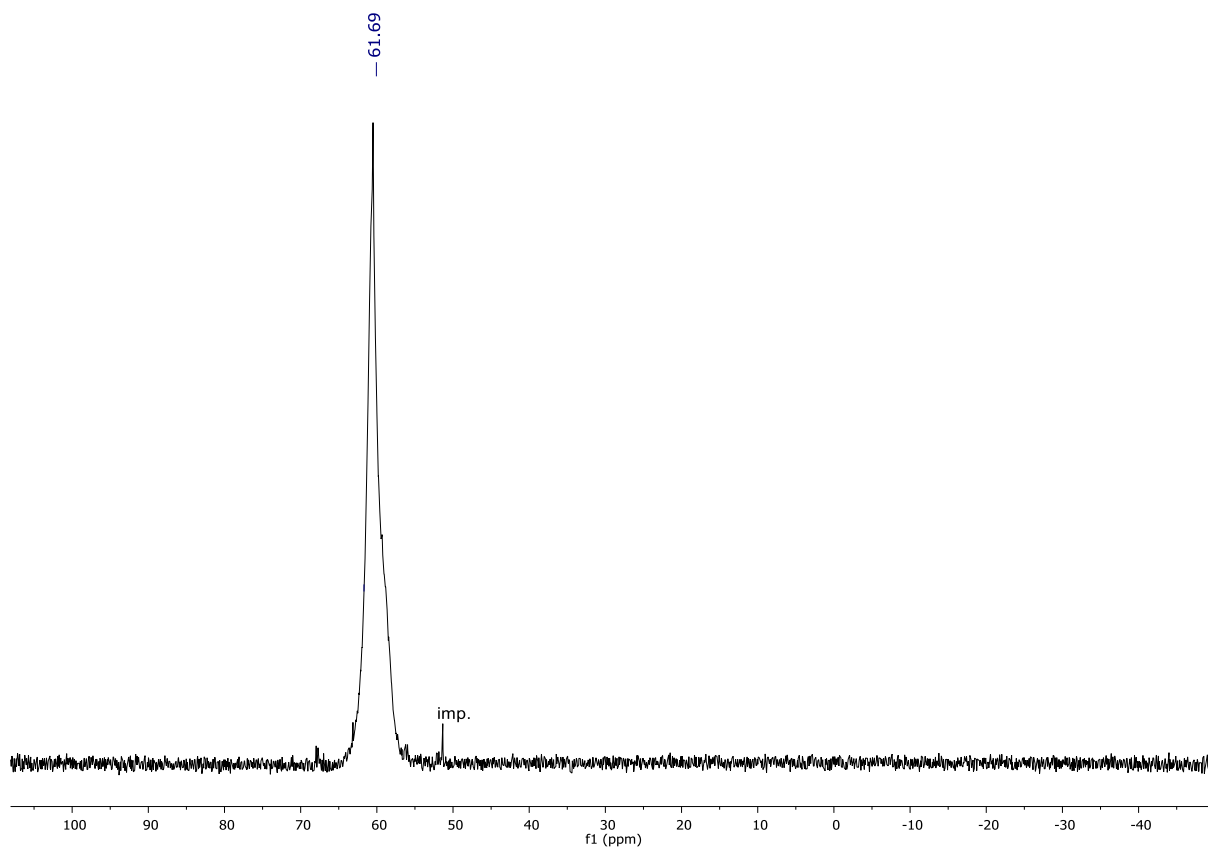


Figure 64 $^{31}\text{P}\{^1\text{H}\}$ NMR spectrum of $\text{Ru}(\text{OAc})_2(\text{CO})(\text{DiPPF})$ (9) in CD_2Cl_2 at 20°C

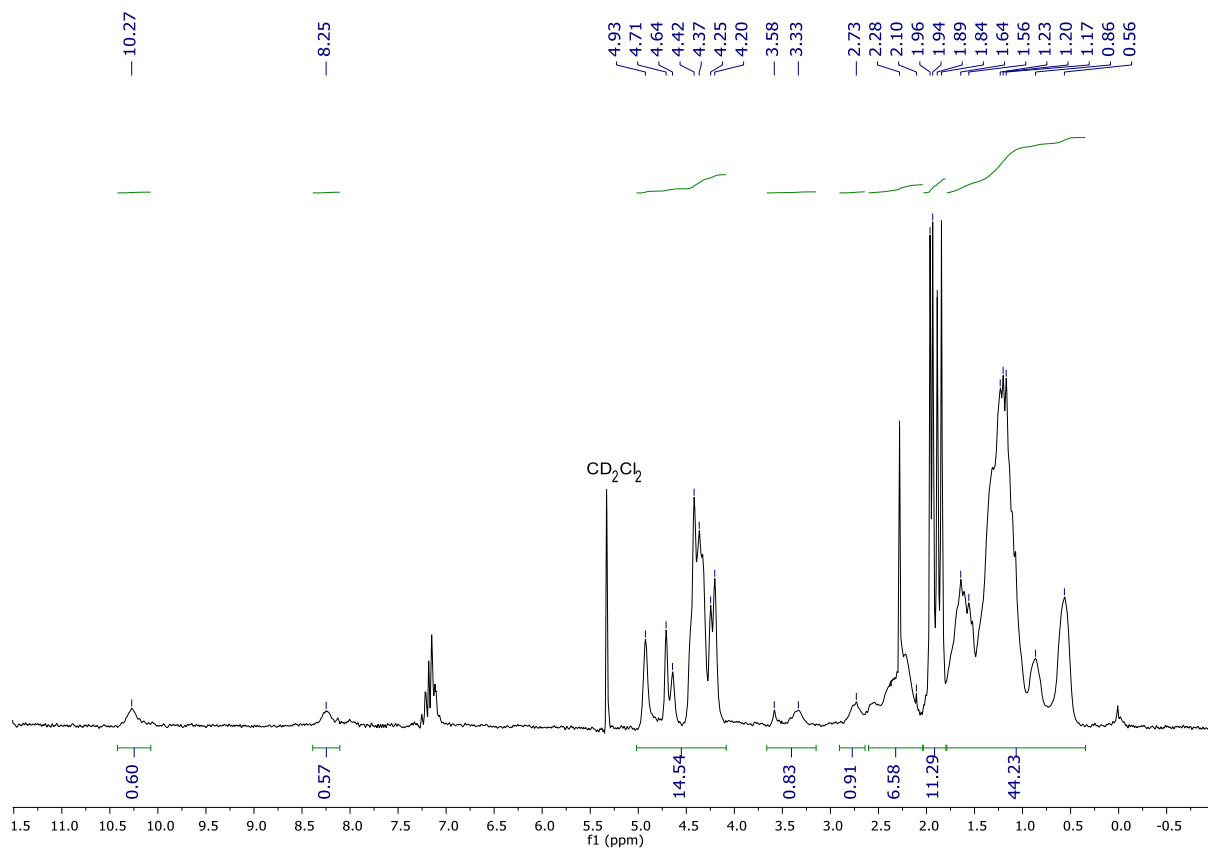


Figure 65 ^1H NMR spectrum of $\text{Ru}(\text{OAc})_2(\text{CO})(\text{DiPPF})$ (9) in CD_2Cl_2 at -75°C

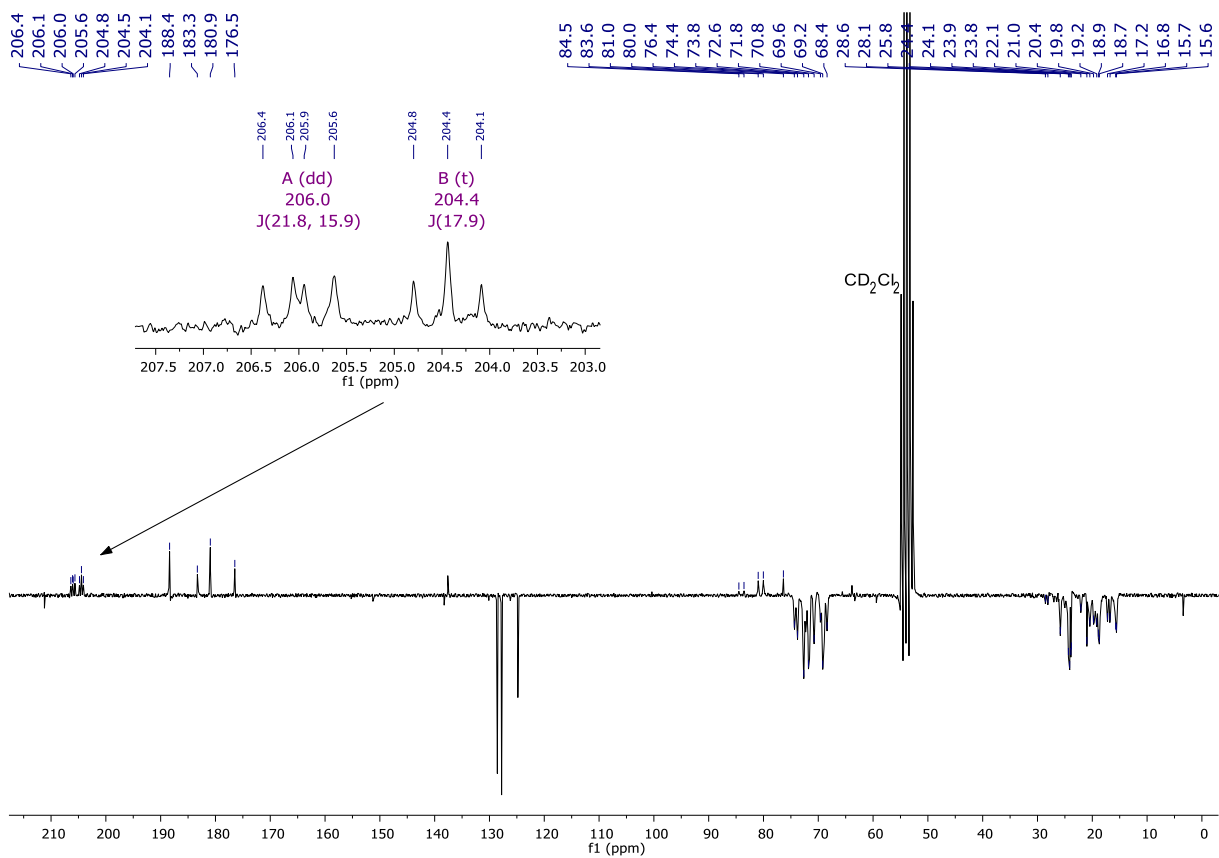


Figure 66 $^{13}\text{C}\{^1\text{H}\}$ NMR spectrum of $\text{Ru}(\text{OAc})_2(\text{CO})(\text{DiPPF})$ (**9**) in CD_2Cl_2 at $-75\text{ }^\circ\text{C}$

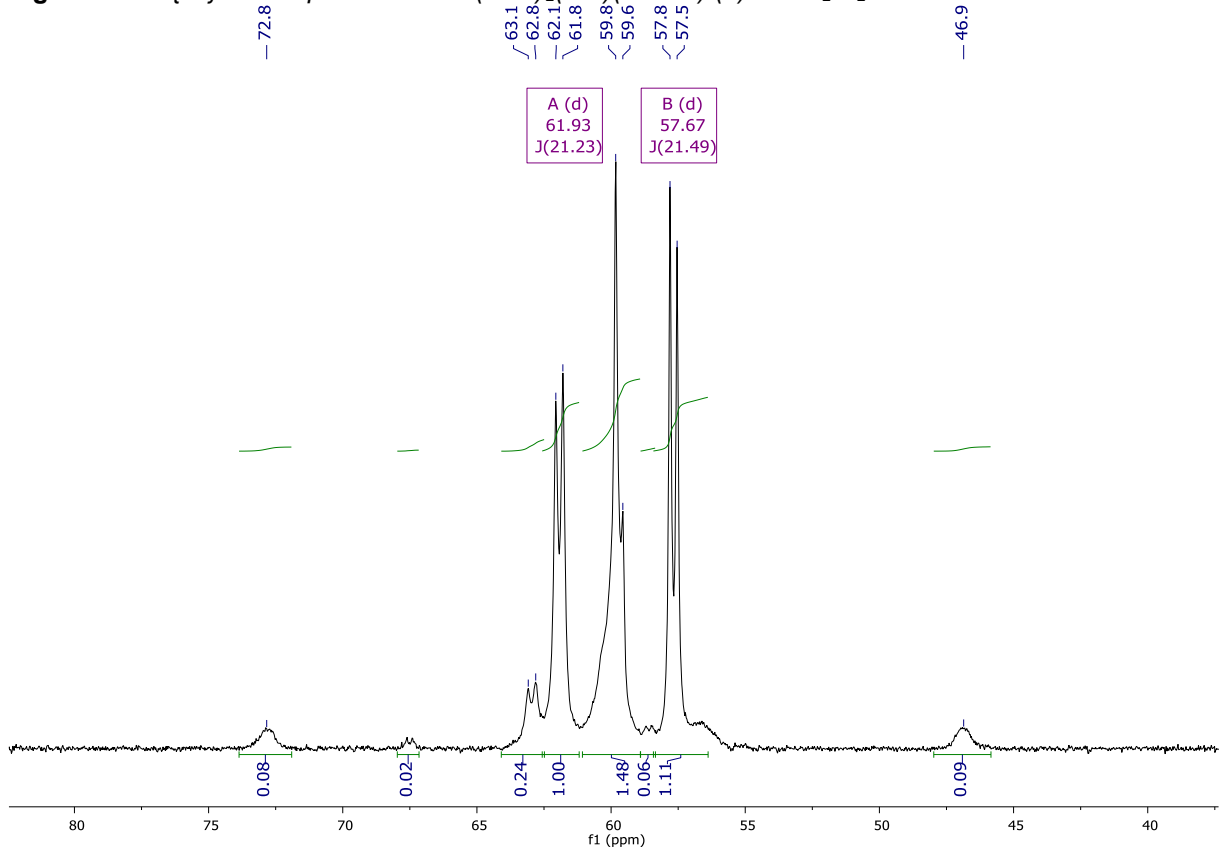
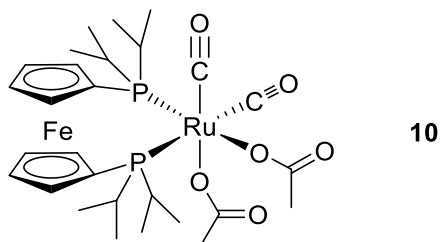


Figure 67 $^{31}\text{P}\{^1\text{H}\}$ NMR spectrum of $\text{Ru}(\text{OAc})_2(\text{CO})(\text{DiPPF})$ (**9**) in CD_2Cl_2 at $-75\text{ }^\circ\text{C}$

Synthesis of *cis,cis*-Ru(OAc)₂(CO)₂(DiPPF) (10):



Ru(OAc)₂(CO)DiPPF (100 mg, 0.150 mmol) was dissolved in degassed CH₂Cl₂ (3 mL), and vigorously stirred under CO atmosphere (1 atm) for 24 h at room temperature. The solvent was evaporated under reduced pressure leading the product as a yellow powder. Yield: 95.7 mg (92%). ¹H NMR (200.1 MHz, CD₂Cl₂, 20 °C): δ = 4.60 (dt, ³J(H,H) = 5.0 Hz, ⁴J(H,H) = 1.5 Hz, 4H; C₅H₄), 4.53-4.46 (m, 4H; C₅H₄), 3.02 (pseudo hept, J(H,H) = 6.8 Hz, 1H; CH(CH₃)₂), 2.86-2.19 (m, 3H; CH(CH₃)₂), 2.00 (s, 3H; CH₃CO₂), 1.93 (s, 3H; CH₃CO₂), 1.75-0.80 ppm (m, 24H; CH(CH₃)₂); ¹³C{¹H} NMR (50.3 MHz, CD₂Cl₂, 20 °C): δ = 201.6 (t, ²J(C,P) = 14.0 Hz; CO), 193.4 (dd, ²J(C,P) = 115.3 Hz, ²J(C,P) = 13.0 Hz; CO), 175.8 (dd, ²J(C,P) = 18.2 Hz, ²J(C,P) = 2.6 Hz; OCOCH₃), 78.1 (d, ¹J(C,P) = 41.6 Hz; ipso-C₅H₄), 78.0 (d, ¹J(C,P) = 41.5 Hz; ipso-C₅H₄), 75.6 (d, J(C,P) = 5.3 Hz; C₅H₄), 75.4 (d, J(C,P) = 5.1 Hz; C₅H₄), 73.6 (d, J(C,P) = 8.5 Hz; C₅H₄), 72.4 (d, J(C,P) = 6.3 Hz; C₅H₄), 71.8 (d, J(C,P) = 5.2 Hz; C₅H₄), 71.4 (d, J(C,P) = 4.8 Hz; C₅H₄), 71.3 (d, J(C,P) = 5.4 Hz; C₅H₄), 69.9 (d, J(C,P) = 3.4 Hz; C₅H₄), 29.5 (d, ¹J(C,P) = 30.0 Hz; CH(CH₃)₂), 27.3 (d, ¹J(C,P) = 25.7 Hz; CH(CH₃)₂), 25.8 (d, ¹J(C,P) = 21.6 Hz; CH(CH₃)₂), 25.3 (d, ¹J(C,P) = 17.6 Hz; CH(CH₃)₂), 24.4 (s; OCOCH₃), 22.8 (d, ²J(C,P) = 4.5 Hz; CH(CH₃)₂), 20.3 (s; OCOCH₃), 20.00 (d, ²J(C,P) = 3.8 Hz; CH(CH₃)₂), 19.8 (br s; CH(CH₃)₂), 19.6 (br s; CH(CH₃)₂), 19.5 (br s; CH(CH₃)₂), 19.4 (d, ²J(C,P) = 4.0 Hz; CH(CH₃)₂), 19.1 (d, ²J(C,P) = 3.5 Hz; CH(CH₃)₂), 18.2 ppm (br s; CH(CH₃)₂); ³¹P{¹H} NMR (81.0 MHz, CD₂Cl₂, 20 °C): δ = 50.8 (d, ²J(P,P) = 20.5 Hz), 32.2 ppm (d, ²J(P,P) = 20.5 Hz); elemental analysis (%) calcd for C₂₈H₄₂FeO₆P₂Ru: C 48.49, H 6.10; found: C 45.30, H 6.30.

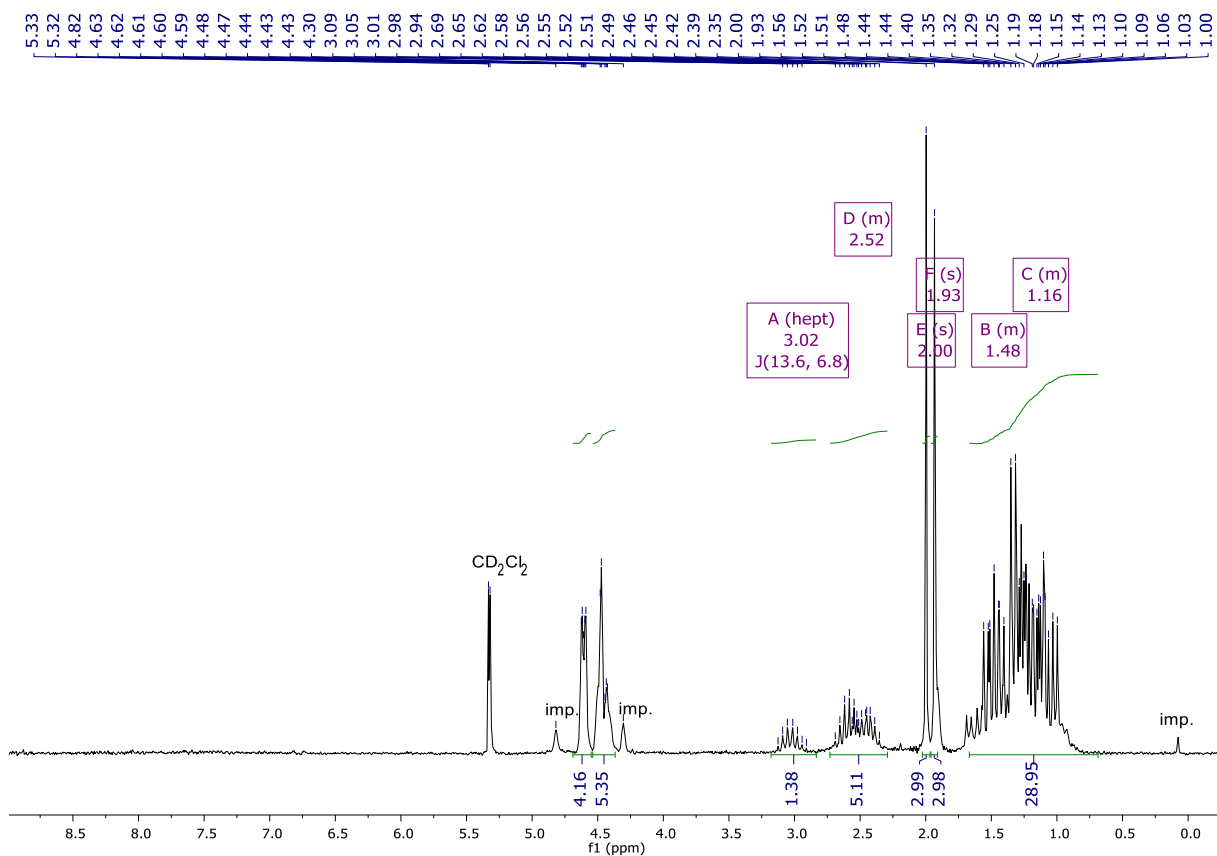


Figure 68 ¹H NMR spectrum of Ru(OAc)₂(CO)₂(DiPPF) (**10**) in CD₂Cl₂ at 20 °C

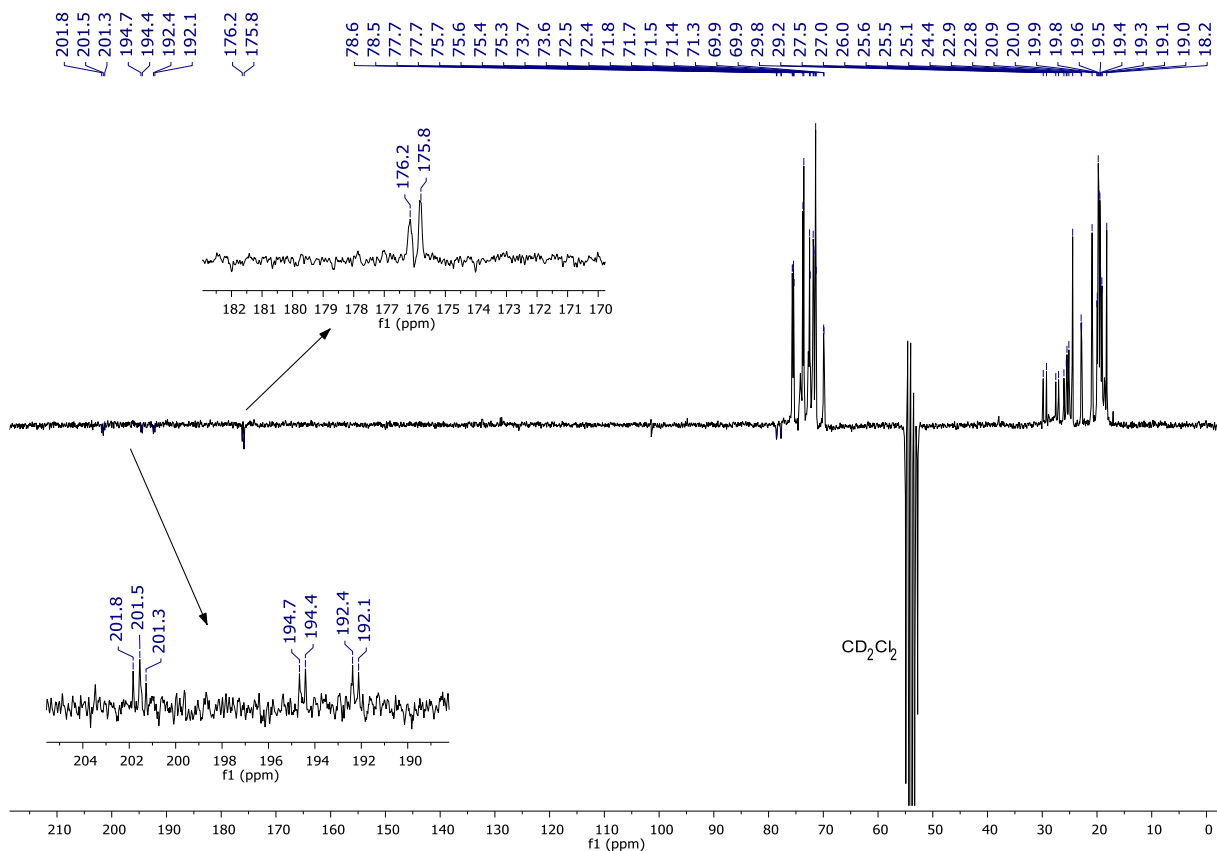


Figure 69 ¹³C{¹H} NMR spectrum of Ru(OAc)₂(CO)₂(DiPPF) (**10**) in CD₂Cl₂ at 20 °C

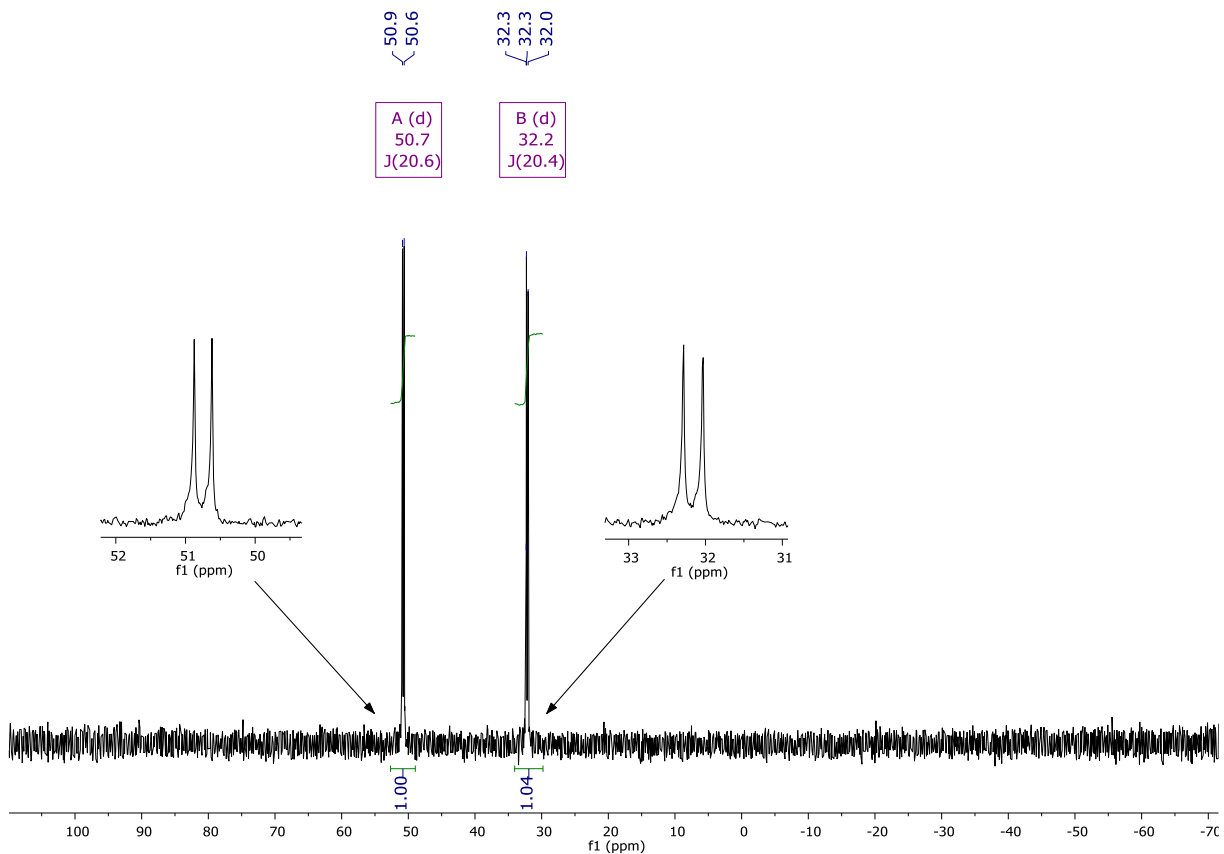


Figure 70 $^{31}\text{P}\{^1\text{H}\}$ NMR spectrum of $\text{Ru}(\text{OAc})_2(\text{CO})_2(\text{DiPPF})$ (**10**) in CD_2Cl_2 at $20\text{ }^\circ\text{C}$

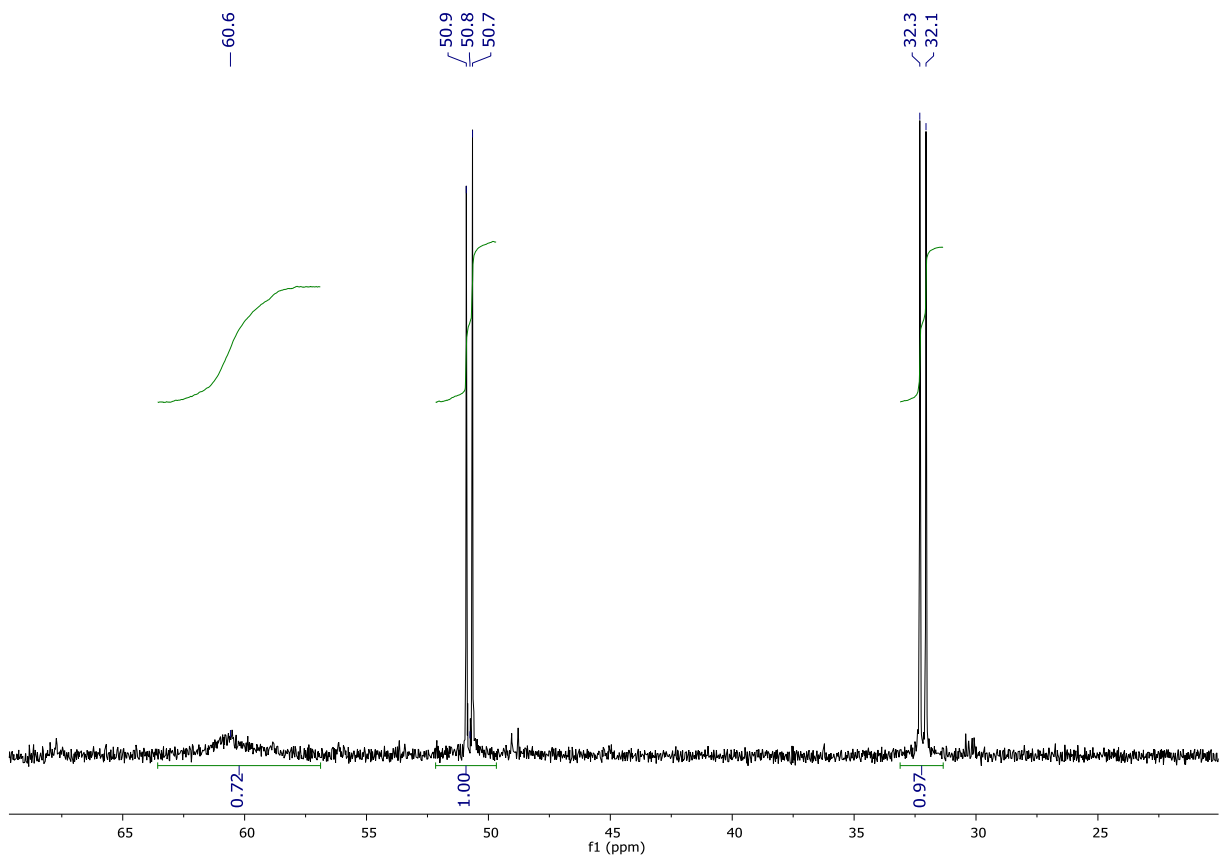
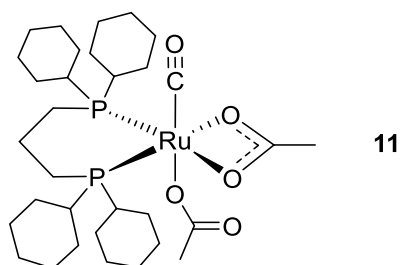


Figure 71 $^{31}\text{P}\{^1\text{H}\}$ NMR spectrum of $\text{Ru}(\text{OAc})_2(\text{CO})_2(\text{DiPPF})$ (**10**) in CD_2Cl_2 after 40 h at $20\text{ }^\circ\text{C}$

Synthesis of Ru(OAc)₂(CO)(DCyPP) (11):



Ru(OAc)₂(CO)(PPh₃)₂ (200 mg, 0.259 mmol) and DCyPP (206.1 mg, 0.50 mmol), 2 equiv) were suspended in degassed cyclohexane (3.5 mL) and heated at 90°C for 6 h. The obtained solution was cooled to room temperature, and leaved at 4 °C overnight affording a precipitate, that was filtered, washed with cold *n*-pentane (3x1 mL) and dried under reduced pressure. Yield: 124 mg (70%). ¹H NMR (200.1 MHz, CD₂Cl₂, 20 °C): δ = 2.69-2.06 (m, 8H; CH of Cy and PCH₂), 1.96 (br s, 6H; CH₃CO₂), 2.06-1.62 (m, 16H; CH₂ of Cy), 1.61-1.04 ppm (m, 28H; CH₂ of Cy and CH₂CH₂P); ³¹P{¹H} NMR (81.0 MHz, CD₂Cl₂, 20°C): δ = 42.7 ppm (br s); IR: $\tilde{\nu}$ = 1932 (s) cm⁻¹ (C≡O); elemental analysis (%) calc. for C₂₇H₄₂FeO₅P₂Ru: C 48.73, H 6.36; found: C 48.82, H 6.54.

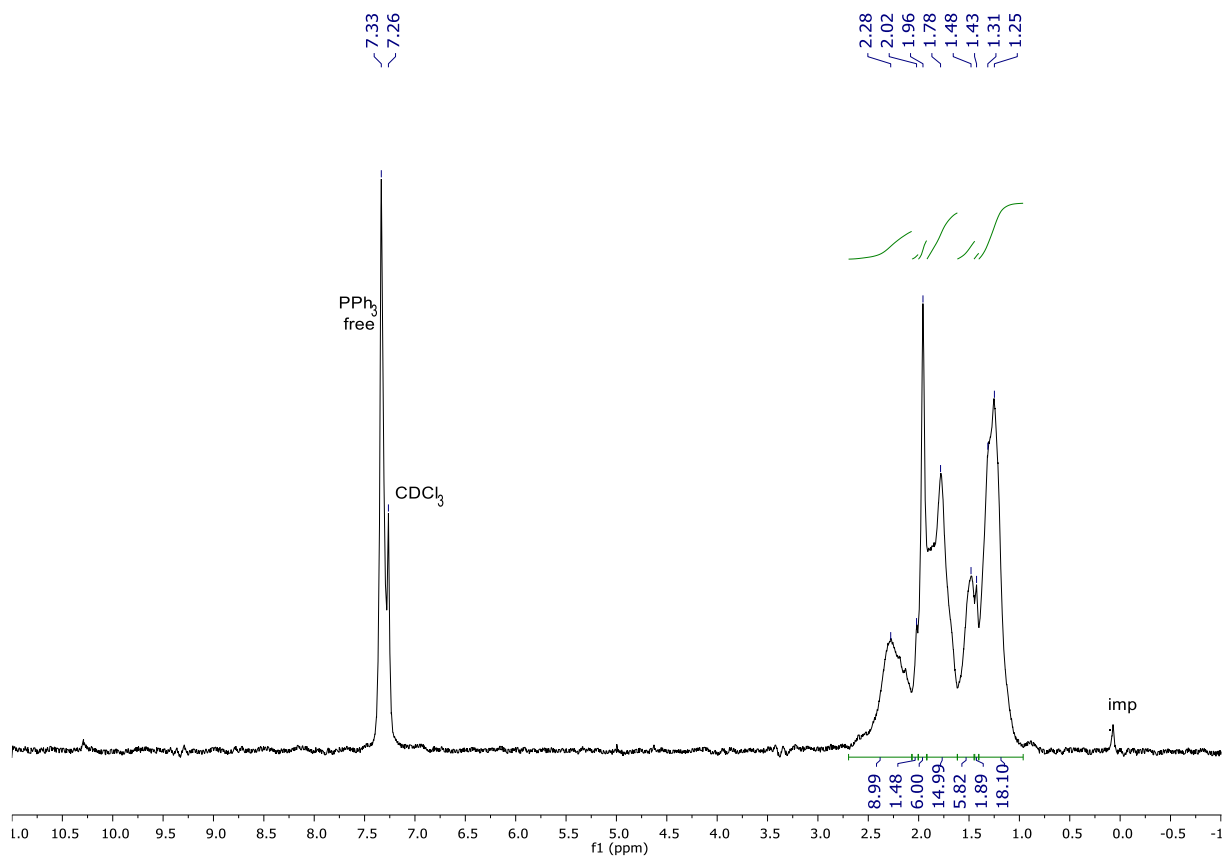


Figure 72 ^1H NMR spectrum of $\text{Ru}(\text{OAc})_2(\text{CO})_2(\text{DCyPP})$ (**11**) in CDCl_3 at $20\text{ }^\circ\text{C}$

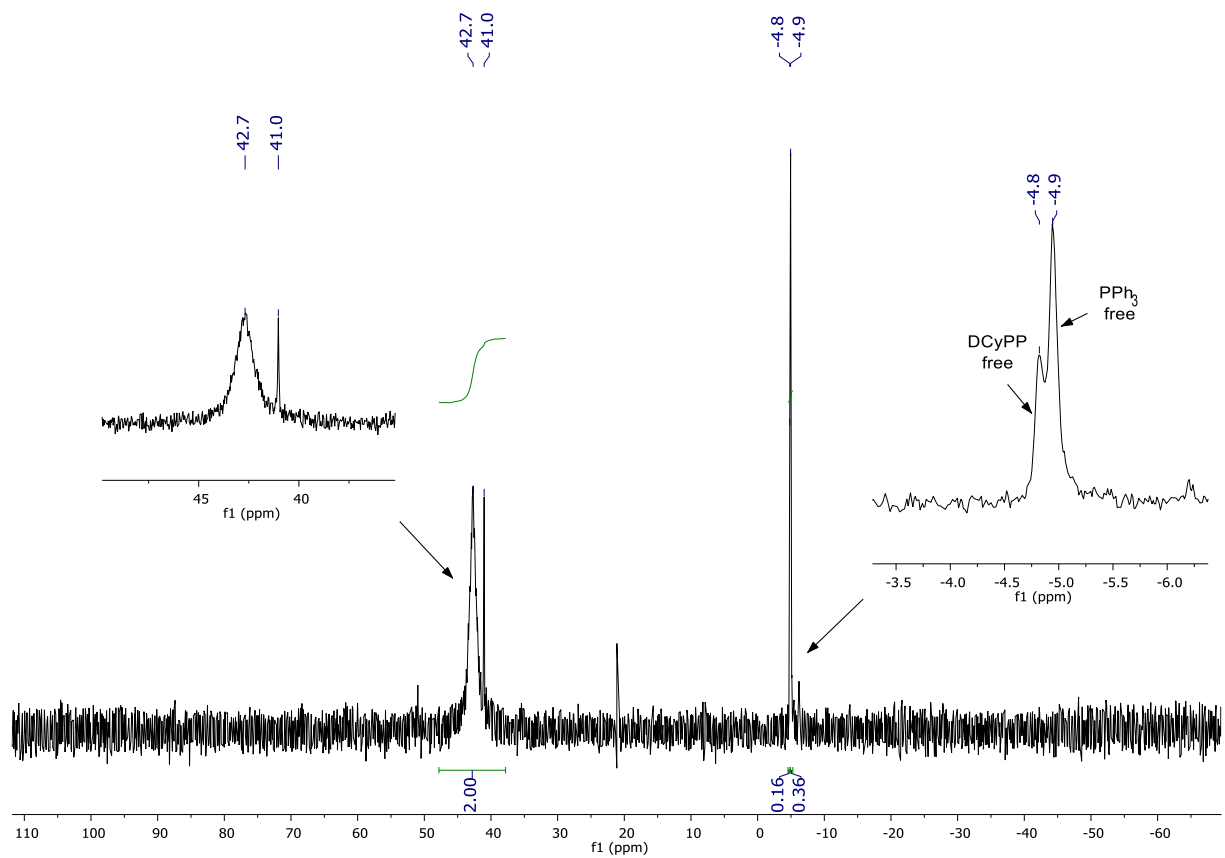
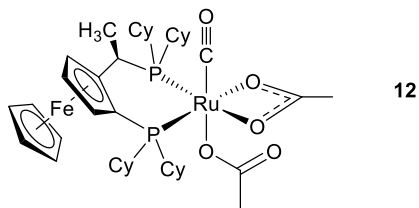


Figure 73 $^{31}\text{P}\{^1\text{H}\}$ NMR spectrum of $\text{Ru}(\text{OAc})_2(\text{CO})_2(\text{DCyPP})$ (**11**) in CDCl_3 at $20\text{ }^\circ\text{C}$

Synthesis of Ru(OAc)₂(CO)(4Cy-Josiphos) (12):



Ru(OAc)₂(CO)(PPh₃)₂ (200 mg, 0.259 mmol) and 4Cy-Josiphos (157 mg, 0.259 mmol) were suspended in 2 mL of degassed toluene and the mixture was heated at 90 °C for 24 h. The resulting solution was cooled to room temperature and concentrated to almost 1 mL, removing the solvent under reduced pressure. Addition of 1 mL of cold *n*-pentane (4 °C) afforded an orange precipitate that was filtered, washed with cold *n*-pentane (2x2 mL) and dried under reduced pressure. Yield: 100 mg (45%). ¹H NMR (200.1 MHz, CD₂Cl₂, 20 °C): δ = 4.46 (br s, 1H; C₅H₃), 4.41 (m, 1H; C₅H₃), 4.35 (m, 1H; C₅H₃), 4.35 (s, 5H; C₅H₅), 3.03 (br s, 1H; CHCH₃), 2.63-2.06 (m, 4H; CH of Cy), 2.04-1.51 (m, 16H; CH₂ of Cy), 1.87 (br s, 6H; CH₃CO₂), 1.68 (dd, ³J(P,H) = 10.7 Hz, ³J(H,H) = 7.3 Hz, 3H; CHCH₃), 1.49-1.22 (m, 16H; CH₂ of Cy), 1.19-1.06 ppm (m, 8H; CH₂ of Cy); ³¹P{¹H} NMR (81.0 MHz, CD₂Cl₂, 20 °C): δ = 77.3 (br s), 46.8 ppm (br m); IR: ν̄ = 1948 (s) cm⁻¹ (C≡O); elemental analysis (%) calc. for C₂₇H₄₂FeO₅P₂Ru: C 48.73, H 6.36; found: C 48.82, H 6.54.

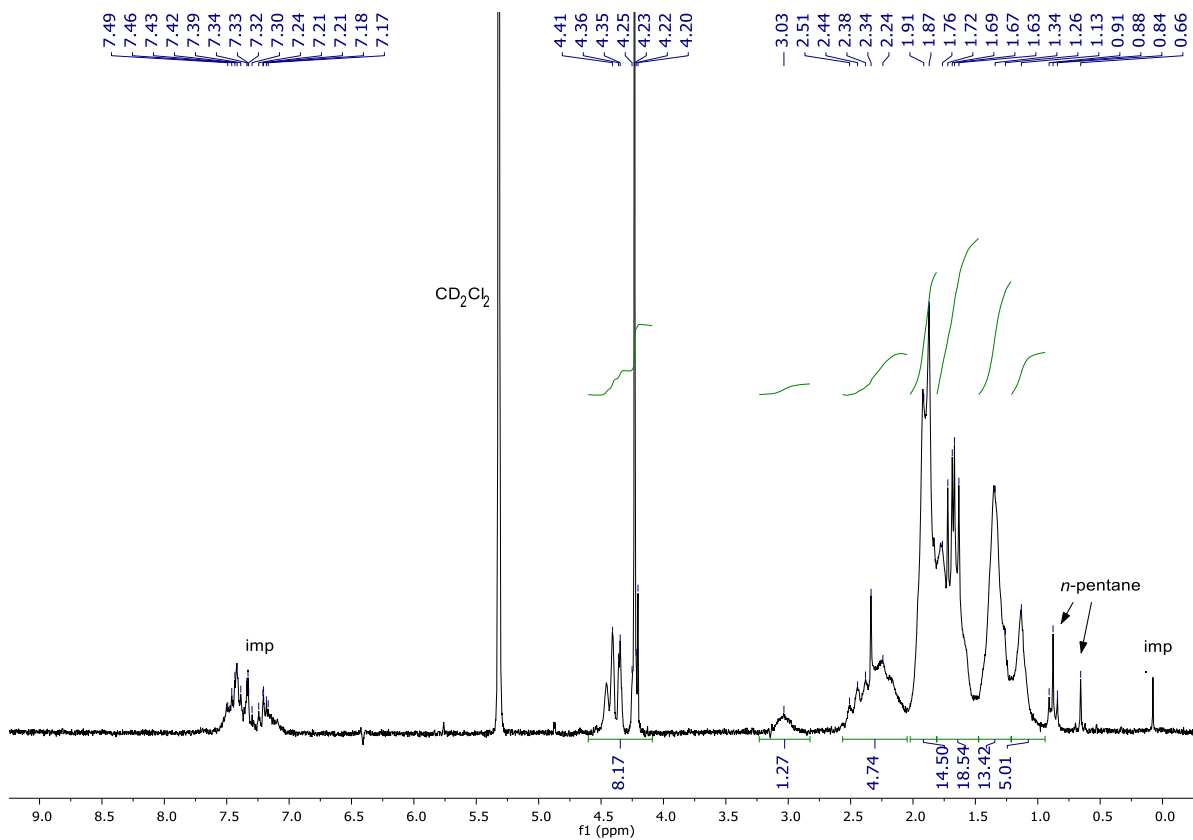


Figure 74 ^1H NMR spectrum of $\text{Ru}(\text{OAc})_2(\text{CO})(4\text{Cy-Josiphos})$ (**12**) in CD_2Cl_2 at 20°C

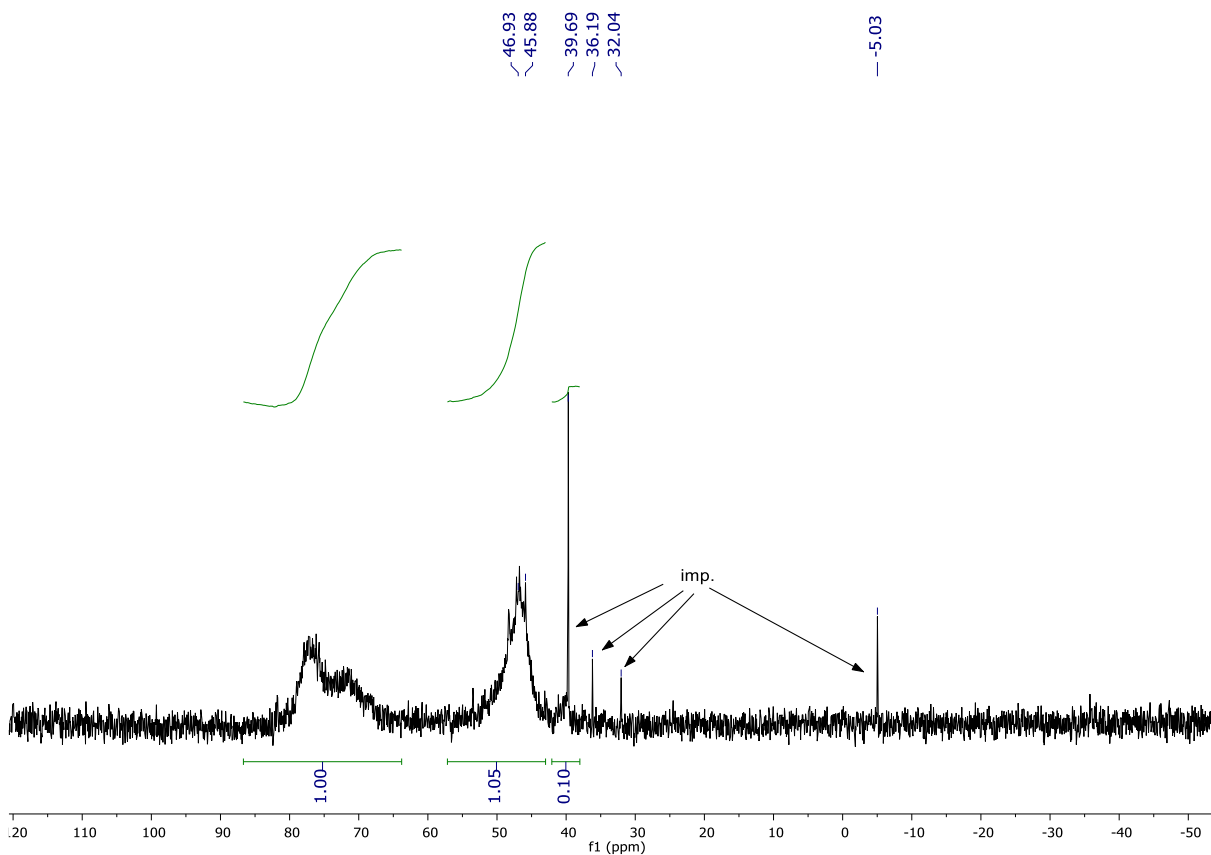
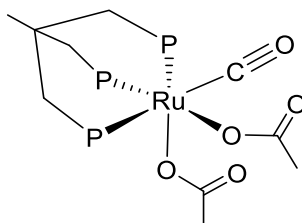


Figure 75 $^{31}\text{P}\{^1\text{H}\}$ NMR spectrum of $\text{Ru}(\text{OAc})_2(\text{CO})(4\text{Cy-Josiphos})$ (**12**) in CD_2Cl_2 at 20°C

Synthesis of Ru(OAc)₂(CO)(Triphos) (13):



13

Ru(OAc)₂(CO)(PPh₃)₂ (180 mg, 0.233 mmol) and triphos (153 mg, 0.2245 mmol) were suspended in 3 mL of degassed toluene and the mixture was heated at 90 °C for 16 h. The resulting suspension was cooled to room temperature and concentrated to ~ 1 mL under reduced pressure. The white solid was filtrate, washed with MTBE (2x3 mL) and dried under reduced pressure. Yield: 125 mg (61%). ¹H NMR (200.1 MHz, CD₂Cl₂, 20 °C): δ = 7.84 (t, ³J(H,H) = 8.8 Hz, 4H; aromatic protons), 7.54 (dd, ³J(H,H) = 10.2 Hz, ³J(H,H) = 7.3 Hz, 3H; aromatic protons), 7.44 (br s, 1H; aromatic proton), 7.30 (dd, ³J(H,H) = 7.3 Hz, ³J(H,H) = 3.0 Hz, 3H; aromatic protons), 7.26-7.10 (m, 15H; aromatic protons), 7.04 (t, ³J(H,H) = 6.3 Hz, 1H; aromatic proton), 6.97 (t, ³J(H,H) = 7.8 Hz, 3H; aromatic protons), 2.51 (d, ²J(P,H) = 8.7 Hz, 2H; PCH₂), 2.44-2.37 (m, 1H; PCH₂), 2.33-2.22 (m, 1H; PCH₂), 2.14 (br s, 2H; PCH₂), 1.97 ppm (q, ⁴J(P,H) = 2.6 Hz, 0.4H; CH₃), 1.86 (br s, 6H; OCOCH₃), 1.63 ppm (q, ⁴J(P,H) = 2.9 Hz, 3H; CH₃). ³¹P{¹H} NMR (81.0 MHz, CD₂Cl₂, 20 °C): δ = 29.4 (AM₂ spin system, d, ²J(P_M,P_A) = 39.0 Hz; P_M), -7.0 ppm (t, ²J(P_M,P_A) = 39.0 Hz, P_A), 34.3 (AM₂ spin system, d, ²J(P_M,P_A) = 35.9 Hz; P_M), 5.7 ppm (t, ²J(P_M,P_A) = 35.9 Hz, P_A); elemental analysis (%) calc. for C₁₀H₁₅O₅P₃Ru: C 29.35, H 3.69; found: C 29.47, H 3.72.

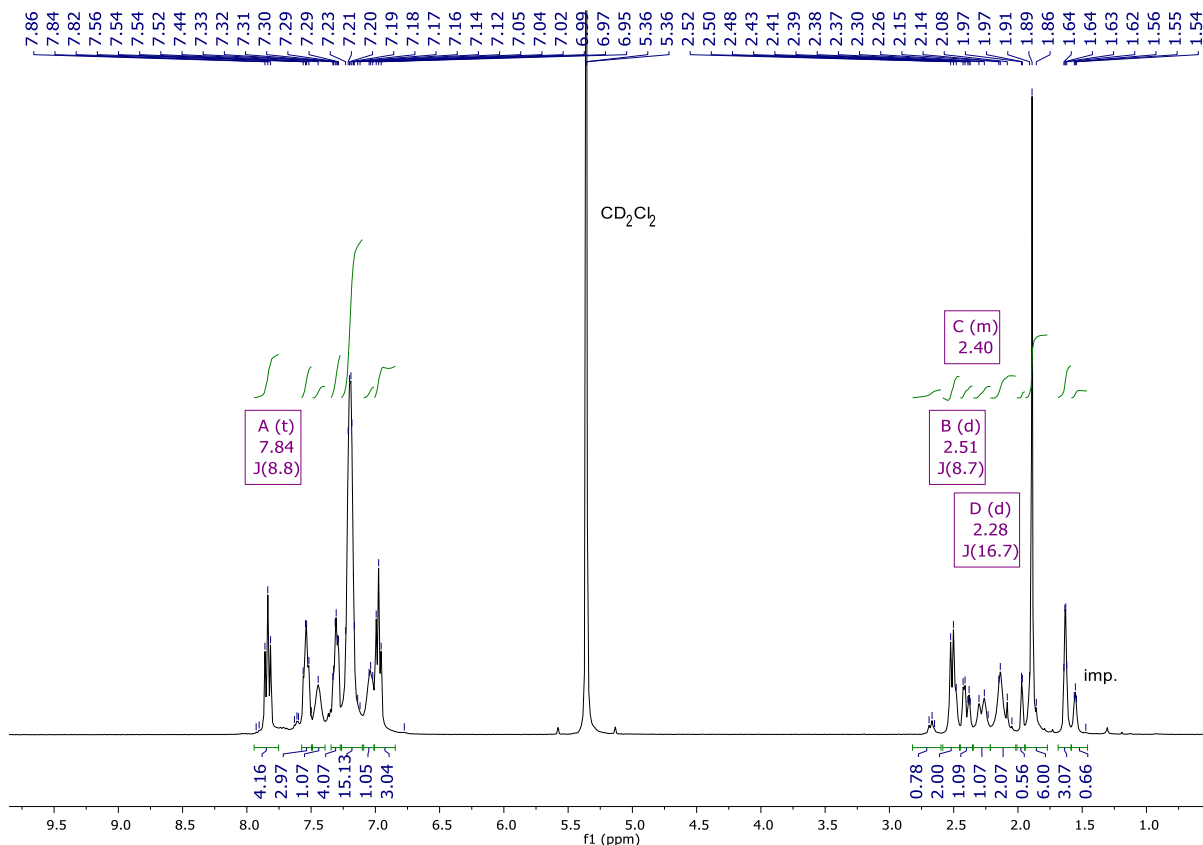


Figure 76 ¹H NMR spectrum of Ru(OAc)₂(CO)₂(triphos) (**13**) in CD₂Cl₂ at 20 °C

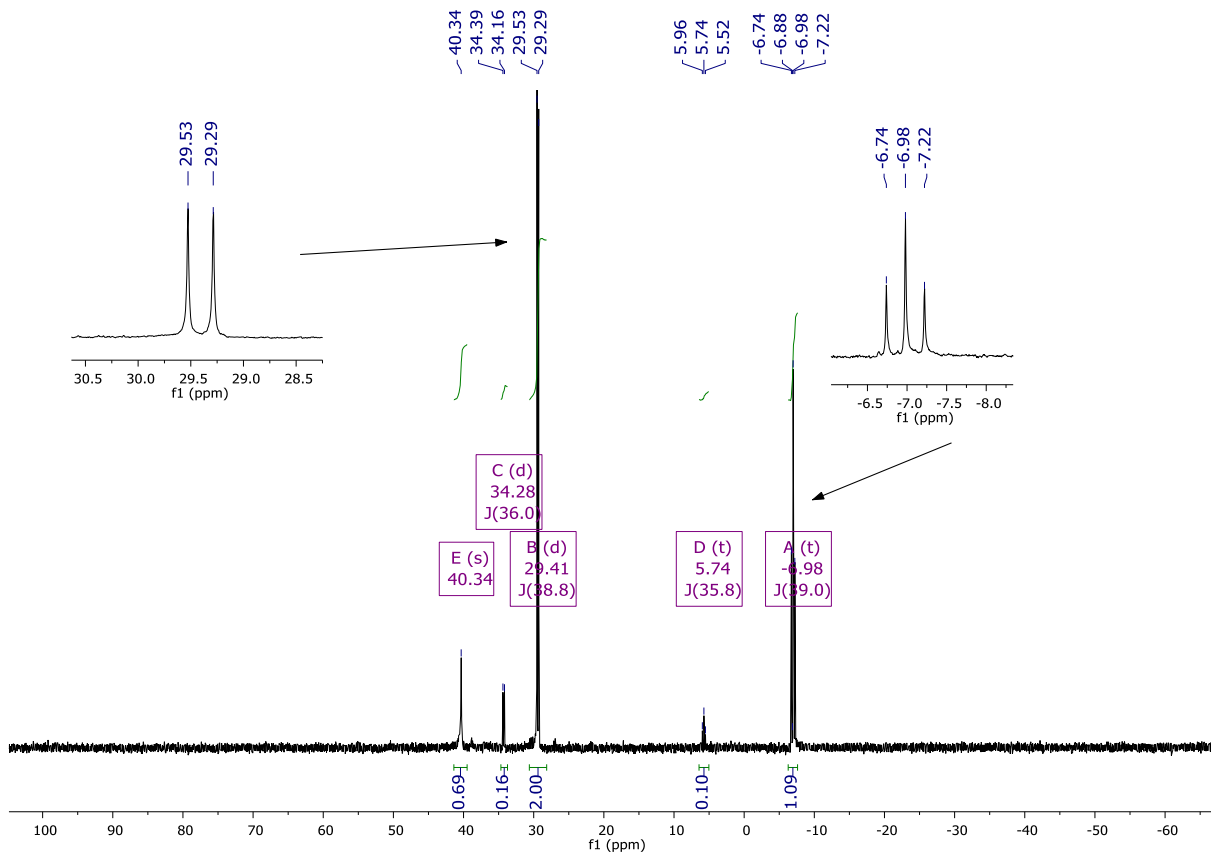
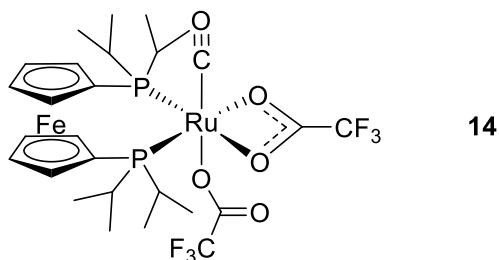


Figure 77 ³¹P{¹H} NMR spectrum of Ru(OAc)₂(CO)(triphos) (**13**) in CD₂Cl₂ at 20 °C showing the A₂X pattern

Synthesis of Ru(k¹-OCOCF₃)(k²-OCOCF₃)₂(CO)(DiPPF) (14):



Ru(OAc)₂(CO)(DiPPF) (**9**) (130 mg, 0.195 mmol) was suspended in distilled and degassed diethyl ether (3 mL). TFA (32 μ L, 0.41 mmol) was added and the mixture was stirred for 30 min at room temperature affording a dark yellow solution. After addition of calcium carbonate (80 mg), the solution was stirred for 2 h at room temperature. The solution was filtered and the solvent was removed under reduced pressure to give the product as a yellow powder. Yield: 90 mg (70%). ¹H NMR (200.1 MHz, [D₈]toluene, 20 °C): δ = 4.73-4.30 (m, 2H; C₅H₄), 4.03 (br s, 2H; C₅H₄), 3.85 (br s, 2H; C₅H₄), 3.80 (s, 2H; C₅H₄), 2.99 (br s, 1H; CH(CH₃)₂), 2.51 (br s, 2H; CH(CH₃)₂), 2.30-2.16 (br m, 1H; CH(CH₃)₂), 1.47 (br s, 6H; CH(CH₃)₂), 1.26 (dd, ³J(P,H) = 16.0 Hz, ³J(H,H) = 7.1 Hz, 6H; CH(CH₃)₂), 1.01 (br s, 6H; CH(CH₃)₂), 0.61 ppm (br s, 6H; CH(CH₃)₂); ¹³C{¹H} NMR (50.3 MHz, CDCl₃, 20 °C): δ = (mancano OCOCF₃, CF₃, ipso-C₅H₄) 203.6 (dd, ²J(C,P) = 24.4 Hz, ²J(C,P) = 12.1 Hz: CO), 74.6 (s; C₅H₄), 72.0 (t, J(C,P) = 3.6 Hz; C₅H₄), 70.2 (t, J(C,P) = 2.7 Hz; C₅H₄), 27.0-25.5 (m; CH(CH₃)₂), 21.0 (br s; CH(CH₃)₂), 19.2 (s; CH(CH₃)₂), 18.9 (br s; CH(CH₃)₂), 18.1 ppm (br s; CH(CH₃)₂); ³¹P{¹H} NMR (81.0 MHz, CDCl₃, 20 °C): δ = 62.0 ppm (s). ¹⁹F{¹H} NMR (188.3 MHz, CDCl₃, 20 °C): δ = - 70.2 (s), - 70.3 ppm (s); elemental analysis (%) calc. for C₂₇H₃₆F₆FeO₅P₂Ru: C 41.93, H 4.69; found: C 42.07, H 4.74.

RF05H038.299

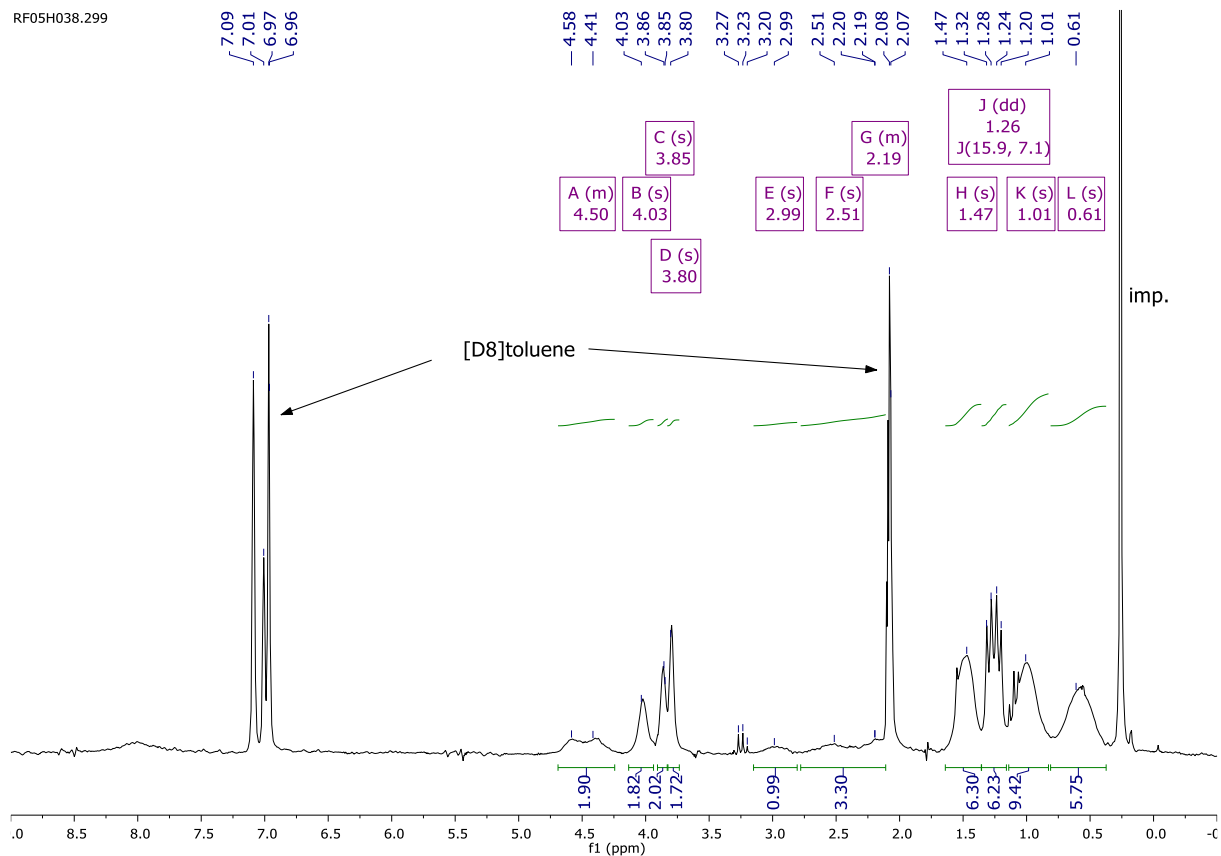


Figure 78 ^1H NMR spectrum of $\text{Ru}(\text{OCOFC}_3)_2(\text{CO})(\text{DiPPF})$ (**14**) in $[\text{D}8]\text{toluene}$ at $20\text{ }^\circ\text{C}$

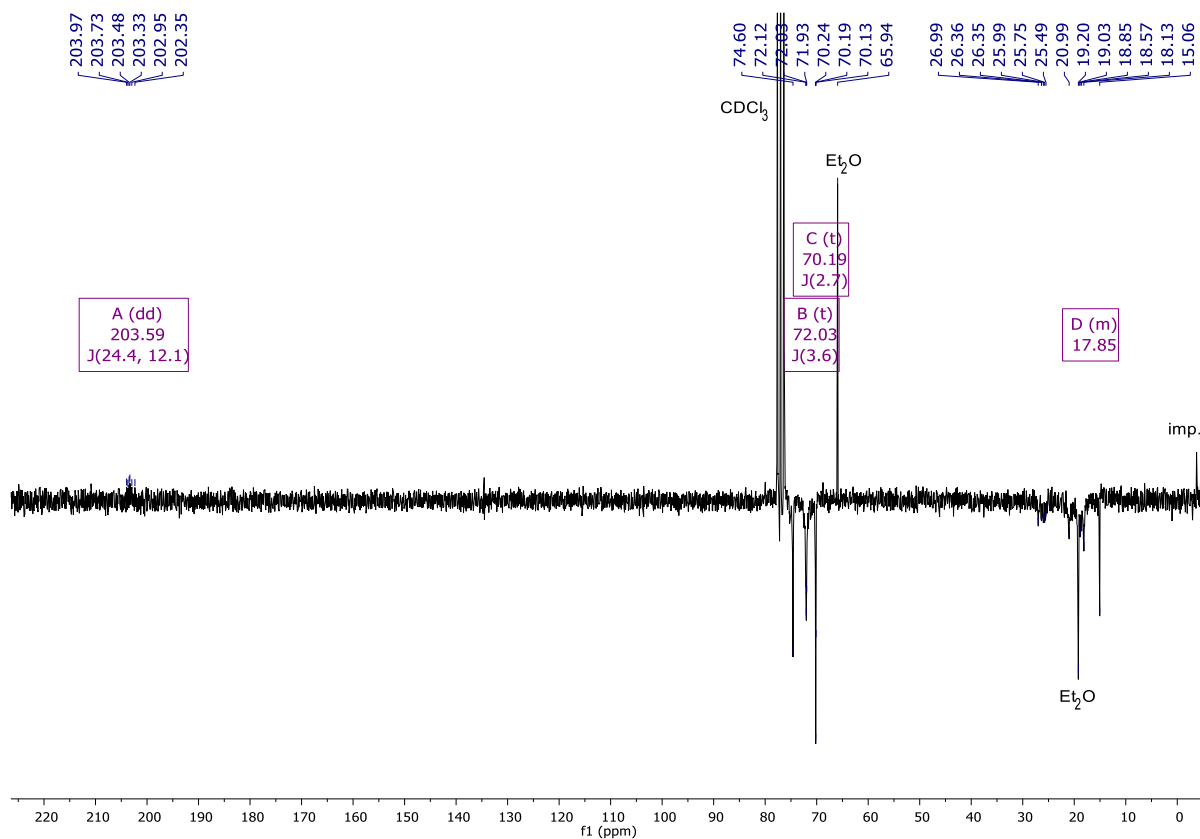


Figure 79 $^{13}\text{C}\{^1\text{H}\}$ NMR spectrum of $\text{Ru}(\text{OCOFC}_3)_2(\text{CO})(\text{DiPPF})$ (**14**) in CDCl_3 at $20\text{ }^\circ\text{C}$

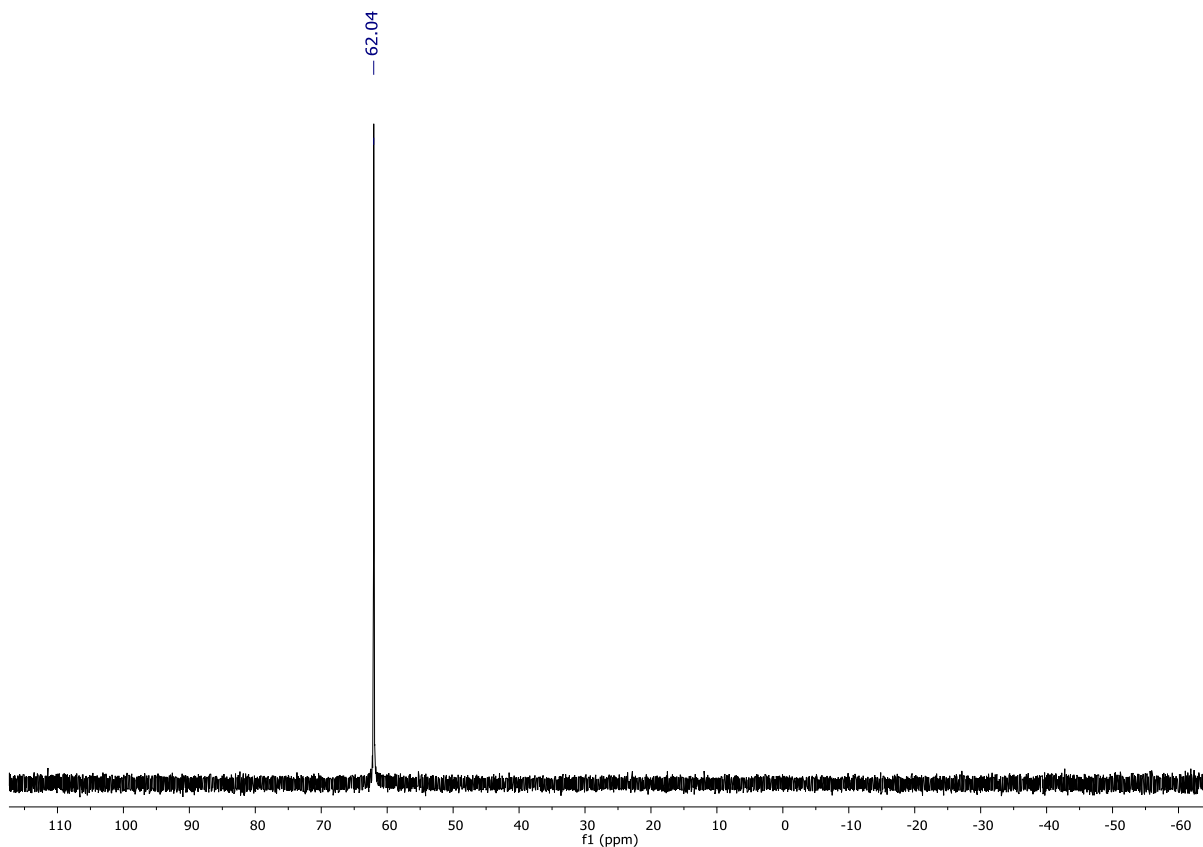


Figure 80 $^{31}\text{P}\{^1\text{H}\}$ NMR spectrum of $\text{Ru}(\text{OCOCF}_3)_2(\text{CO})(\text{DiPPF})$ (**14**) in CDCl_3 at 20 °C

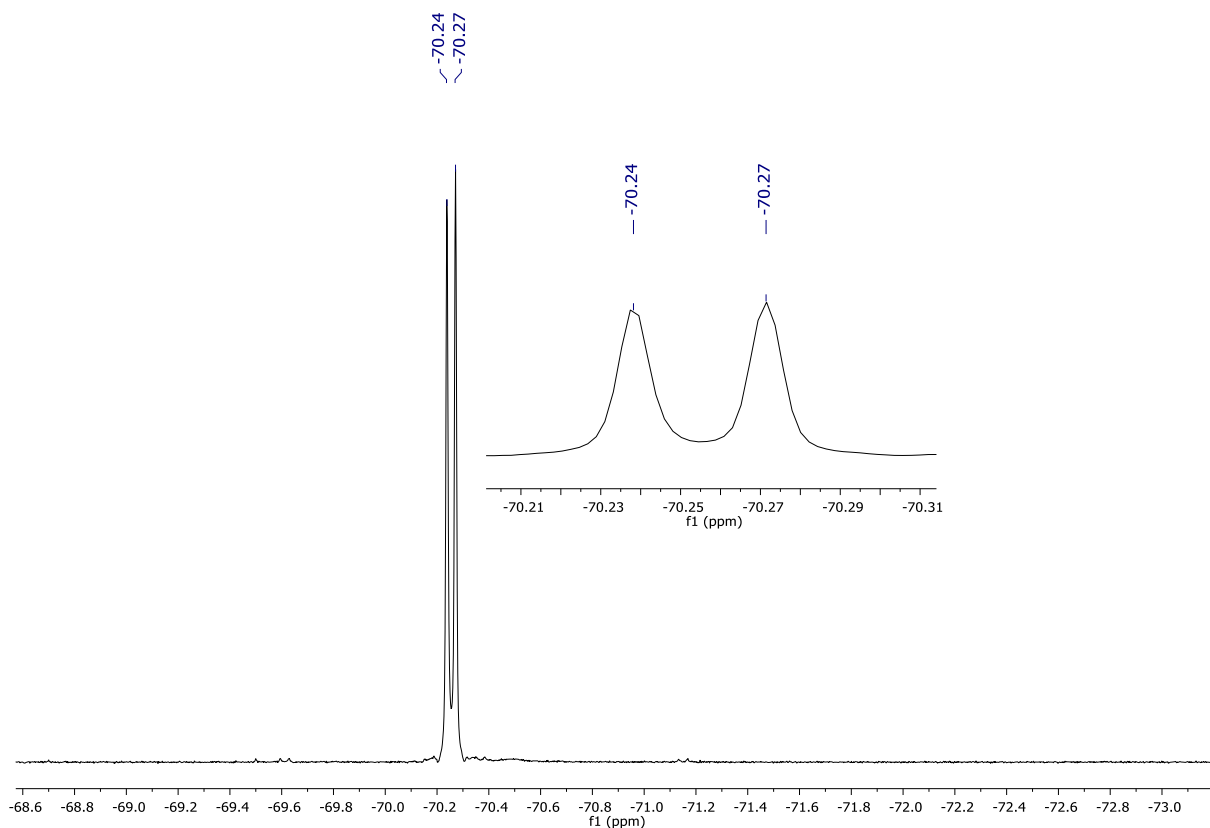


Figure 81 $^{19}\text{F}\{^1\text{H}\}$ NMR spectrum of $\text{Ru}(\text{OCOCF}_3)_2(\text{CO})(\text{DiPPF})$ (**14**) in CDCl_3 at 20 °C

NMR evidences of Ru(OAc)(OCOCF₃)(CO)(DiPPF):

The mixed carboxylate complex was detected after addition of 1 equiv. of TFA to **9** in CD₂Cl₂ in an NMR tube. ¹H NMR (200.1 MHz, CD₂Cl₂, 20 °C): δ = 5.04-4.68 (m, 2H; C₅H₄), 4.52 (m, 2H; C₅H₄), 4.44 (br s, 2H; C₅H₄), 4.34 (s, 2H; C₅H₄), 3.07-2.71 (br m, 1H; CH(CH₃)₂), 2.70-2.25 (br m, 1H; CH(CH₃)₂), 2.42 (h, ³J(H,H) = 7.1 Hz, 1H; CH(CH₃)₂), 1.87 (s; OCOCH₃), 1.81-1.52 (m, 6H; CH(CH₃)₂), 1.50-1.15 (m, 12H; CH(CH₃)₂), 1.12-0.81 ppm (m, 6H; CH(CH₃)₂); ³¹P{¹H} NMR (81.0 MHz, CD₂Cl₂, 20 °C): δ = 67.8 (br s), 59.8 ppm (br s).

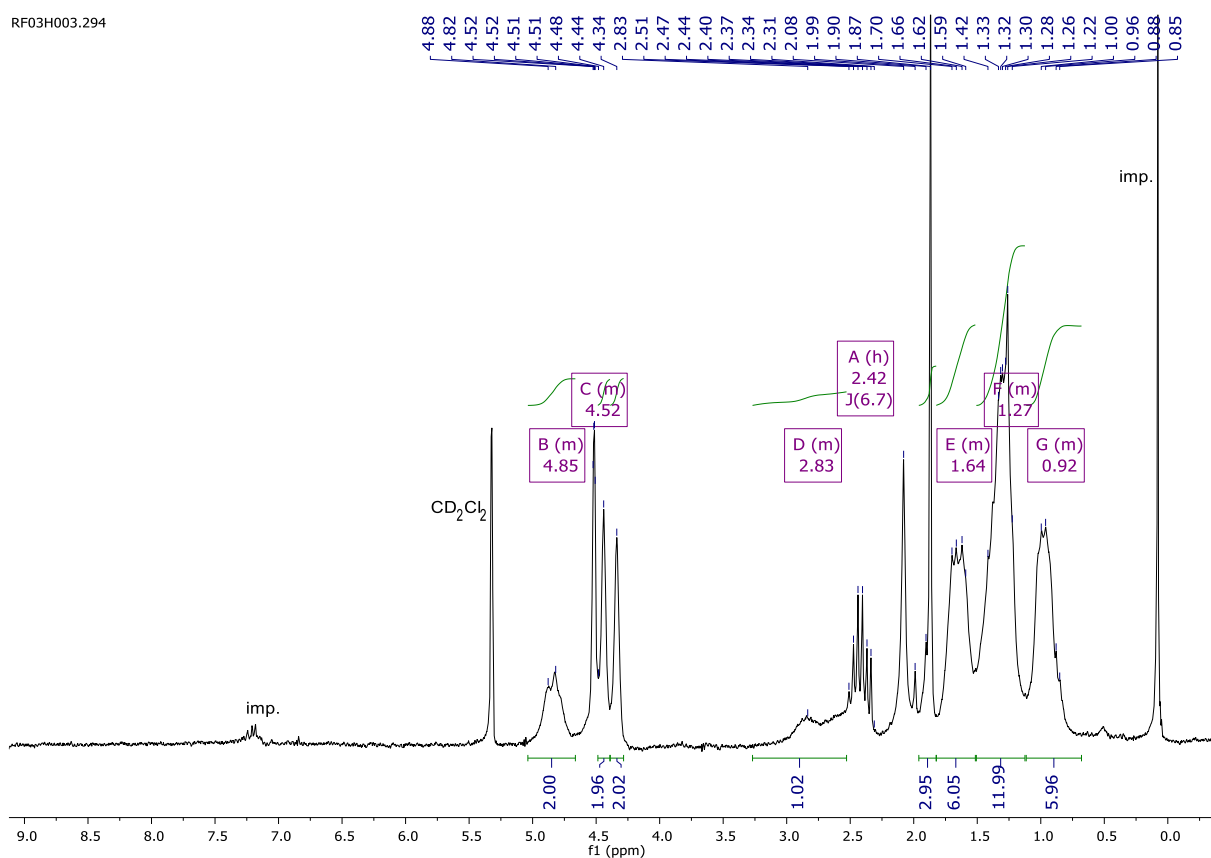


Figure 82 ¹H NMR spectrum of **9** after addition of 1 equiv. of TFA in CD₂Cl₂ at 20 °C

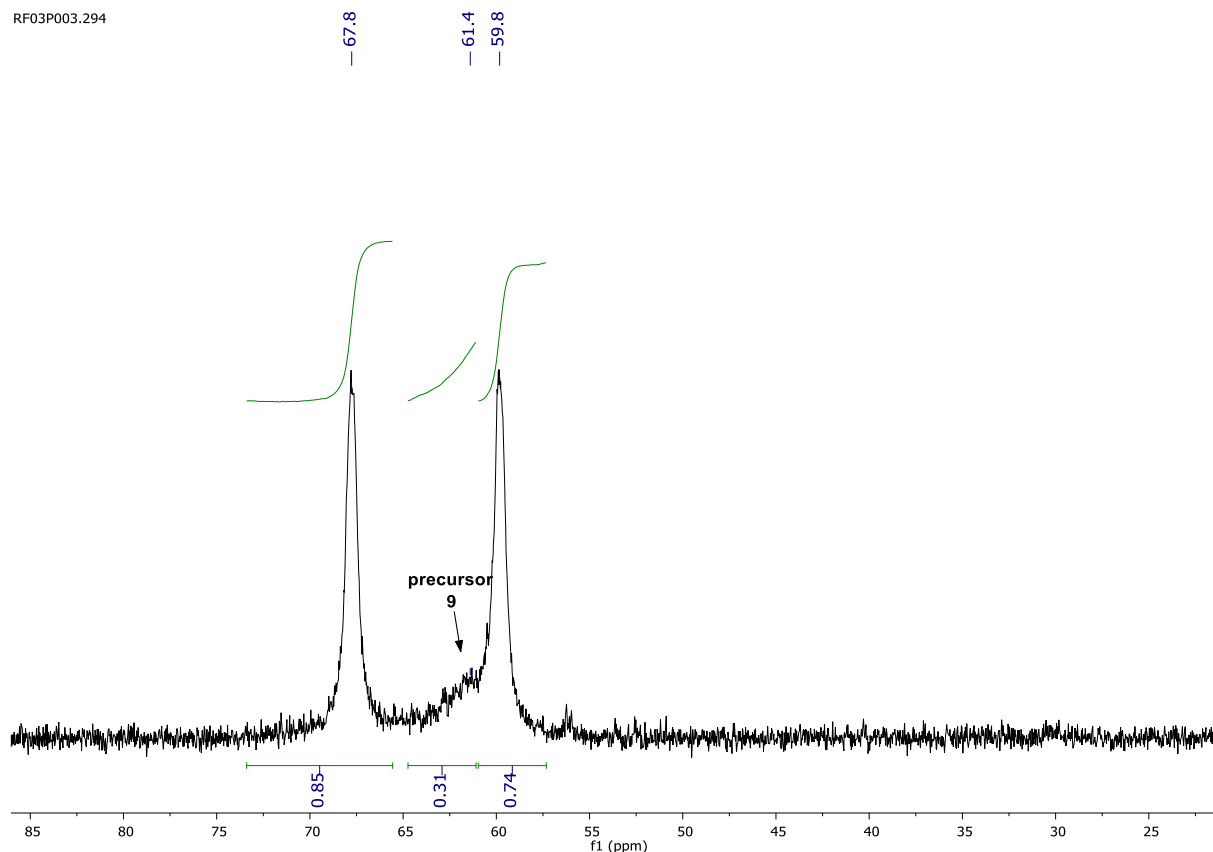
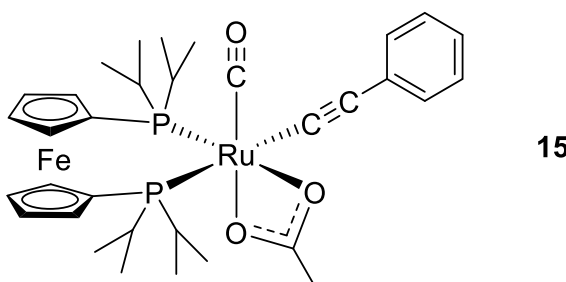


Figure 83 $^{31}\text{P}\{^1\text{H}\}$ NMR spectrum of **9** after addition of 1 equiv. of TFA in CD_2Cl_2 at 20 °C

Synthesis of $\text{Ru}(k^2\text{-OCOCH}_3)_2(\text{CO})(\text{DiPPF})(\text{C}\equiv\text{CPh})$ (**15**):



$\text{Ru}(\text{OAc})_2(\text{CO})(\text{DiPPF})$ (**9**) (100 mg, 0.150 mmol) was suspended in degassed toluene (3 mL) and added of phenylacetylene (18.4 mg, 0.180 mmol, 1.2 equiv) and Py (23.9 μL , 0.30 mmol, 2 equiv). The resulting solution was stirred at 50 °C for 30 minutes, and leaved at 4 °C overnight affording a precipitate, that was filtered, washed with cold *n*-pentane (3x2 mL) and dried under reduced pressure. Yield: 69 mg (65%). ^1H NMR (200.1 MHz, CD_2Cl_2 , 20 °C): δ = 7.37-7.02 (m, 5H; aromatic protons), 4.70 (dd, $^3J(\text{H},\text{H})$ = 2.2 Hz, $^3J(\text{P},\text{H})$ = 1.1 Hz, 1H; C_5H_4), 4.62 (dd, $^3J(\text{H},\text{H})$ = 2.3 Hz, $^3J(\text{P},\text{H})$ = 1.2 Hz, 1H; C_5H_4), 4.47 (m, 2H; C_5H_4), 4.41 (m, 2H; C_5H_4), 4.36 (m, 2H; C_5H_4), 2.94 (hept, $^3J(\text{H},\text{H})$

= 7.1 Hz, 1H; $\text{CH}(\text{CH}_3)_2$), 2.85-2.64 (m, 1H; $\text{CH}(\text{CH}_3)_2$), 2.42 (hept, $^3J(\text{H,H}) = 7.1$ Hz, 2H; $\text{CH}(\text{CH}_3)_2$), 1.92 (s, 6H; OCOCH_3), 1.59 (dd, $^3J(\text{P,H}) = 16.2$ Hz, $^3J(\text{H,H}) = 7.1$ Hz, 3H; $\text{CH}(\text{CH}_3)_2$), 1.48 (dd, $^3J(\text{H,H}) = 7.1$ Hz, $^3J(\text{P,H}) = 3.0$ Hz, 3H; $\text{CH}(\text{CH}_3)_2$), 1.45-1.18 (several m, 15H; $\text{CH}(\text{CH}_3)_2$), 0.92 ppm (dd, $^3J(\text{P,H}) = 13.5$ Hz, $^3J(\text{H,H}) = 7.1$ Hz, 3H; $\text{CH}(\text{CH}_3)_2$); $^{13}\text{C}\{^1\text{H}\}$ NMR (50.3 MHz, CD_2Cl_2 , 20 °C): $\delta = 207.3$ (dd, $^2J(\text{C,P}) = 20.8$ Hz, $^2J(\text{C,P}) = 11.8$ Hz; CO), 186.7 (t, $^2J(\text{C,P}) = 2.3$ Hz; OCOCH_3), 138.7 (s; *ipso*- C_6H_5), 131.3 (d, $^2J(\text{C,P}) = 0.8$ Hz; *o*- C_6H_5), 129.1 (d, $^2J(\text{C,P}) = 2.2$ Hz; $\text{C}\equiv\text{CPh}$), 128.1 (s; *m*- C_6H_5), 124.9 (s; *p*- C_6H_5), 105.0 (dd, $^2J(\text{C,P}) = 23.9$ Hz, $^2J(\text{C,P}) = 2.0$ Hz; $\text{C}\equiv\text{CPh}$), 83.1 (dd, $^1J(\text{C,P}) = 40.5$ Hz, $^3J(\text{C,P}) = 5.5$ Hz; *ipso*- C_5H_4), 78.9 (dd, $^1J(\text{C,P}) = 33.5$ Hz, $^3J(\text{C,P}) = 1.1$ Hz; *ipso*- C_5H_4), 74.4 (d, $J(\text{C,P}) = 3.6$ Hz; C_5H_4), 73.6 (d, $J(\text{C,P}) = 5.0$ Hz; C_5H_4), 73.1 (d, $J(\text{C,P}) = 14.2$ Hz; C_5H_4), 72.9 (d, $J(\text{C,P}) = 11.9$ Hz; C_5H_4), 71.6 (d, $J(\text{C,P}) = 4.9$ Hz; C_5H_4), 71.2 (d, $J(\text{C,P}) = 6.0$ Hz; C_5H_4), 70.4 (d, $J(\text{C,P}) = 4.3$ Hz; C_5H_4), 69.9 (d, $J(\text{C,P}) = 4.9$ Hz; C_5H_4), 28.9 (d, $^1J(\text{C,P}) = 2.9$ Hz; $\text{CH}(\text{CH}_3)_2$), 28.3 (d, $^1J(\text{C,P}) = 11.2$ Hz; $\text{CH}(\text{CH}_3)_2$), 27.5 (d, $^1J(\text{C,P}) = 26.2$ Hz; $\text{CH}(\text{CH}_3)_2$), 26.5 (d, $^1J(\text{C,P}) = 15.3$ Hz; $\text{CH}(\text{CH}_3)_2$), 24.9 (t, $^4J(\text{C,P}) = 1.4$ Hz; OCOCH_3), 20.9 (s; $\text{CH}(\text{CH}_3)_2$), 20.0 (*pseudo*-t, $J(\text{C,P}) = 2.2$ Hz; $\text{CH}(\text{CH}_3)_2$), 19.9 (s; $\text{CH}(\text{CH}_3)_2$), 19.7 (d, $^2J(\text{C,P}) = 1.8$ Hz; $\text{CH}(\text{CH}_3)_2$), 19.3 (d, $^2J(\text{C,P}) = 2.7$ Hz; $\text{CH}(\text{CH}_3)_2$), 19.2 (d, $^2J(\text{C,P}) = 4.7$ Hz; $\text{CH}(\text{CH}_3)_2$), 19.0 ppm (s; $\text{CH}(\text{CH}_3)_2$); $^{31}\text{P}\{^1\text{H}\}$ NMR (81.0 MHz, CD_2Cl_2 , 20 °C): $\delta = 70.0$ (d, $^2J(\text{P,P}) = 15.9$ Hz), 30.3 ppm (d, $^2J(\text{P,P}) = 15.9$ Hz); elemental analysis (%) calc. for $\text{C}_{33}\text{H}_{44}\text{FeO}_3\text{P}_2\text{Ru}$: C 56.02, H 6.27; found: C 55.87, H 6.14.

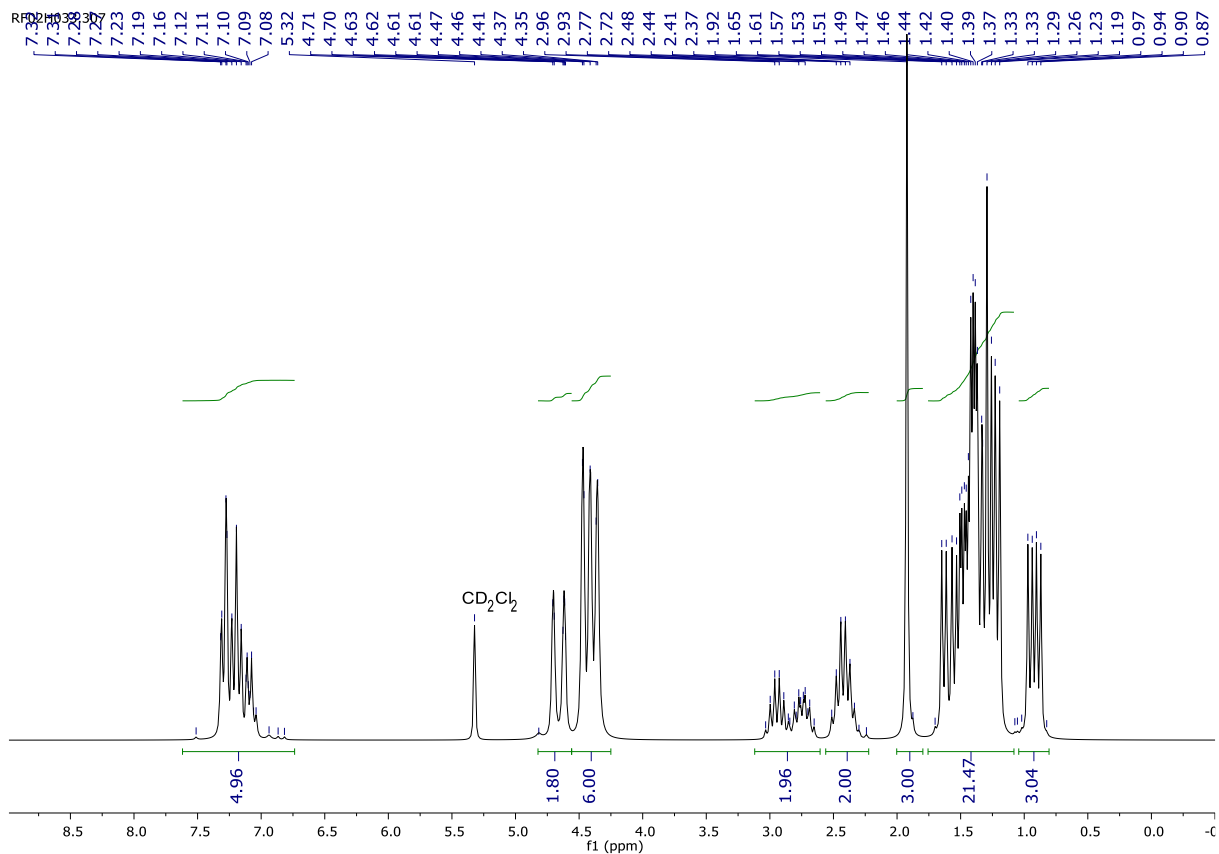


Figure 84 ^1H NMR spectrum of $\text{Ru}(\text{k}^2\text{-OCOCH}_3)_2(\text{CO})(\text{DiPPF})(\text{C}\equiv\text{CPh})$ (**15**) in CD_2Cl_2 at 20°C

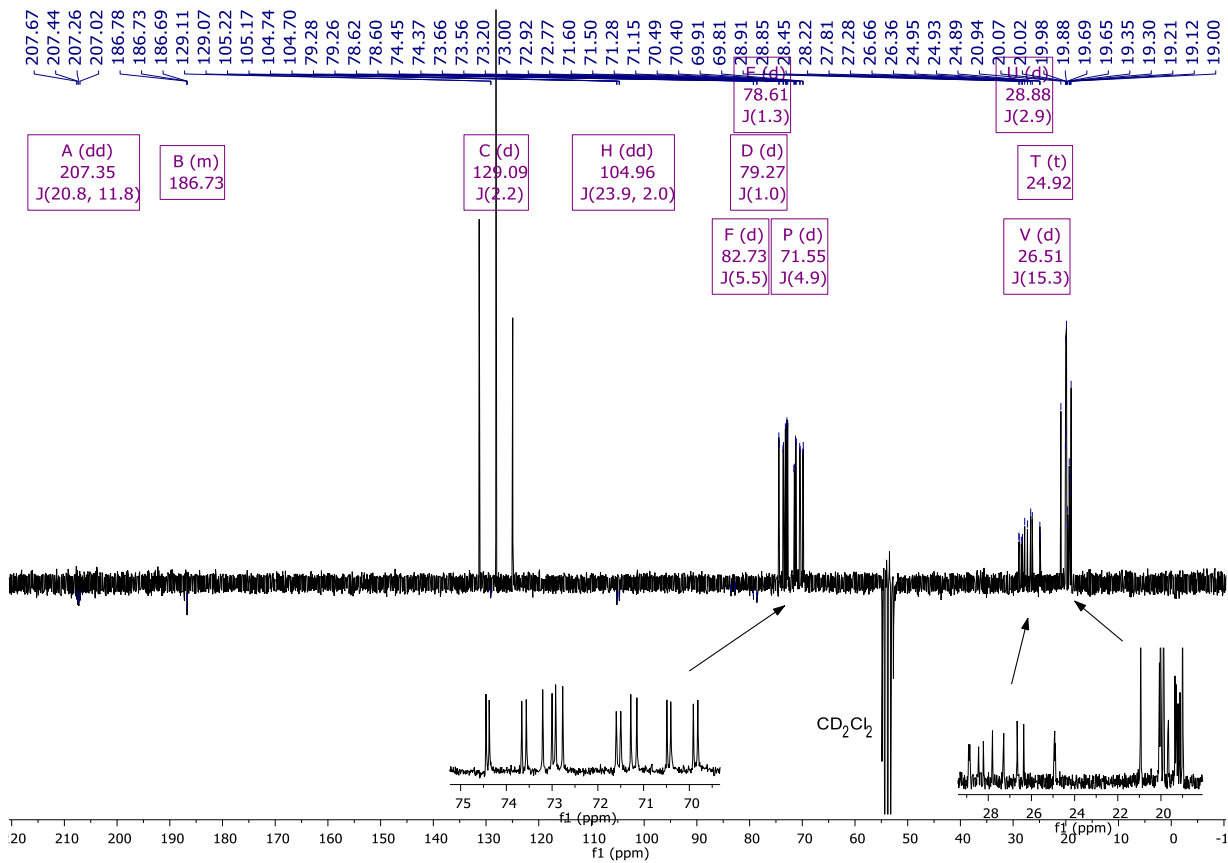


Figure 85 $^{13}\text{C}\{^1\text{H}\}$ NMR spectrum of $\text{Ru}(\text{k}^2\text{-OCOCH}_3)_2(\text{CO})(\text{DiPPF})(\text{C}\equiv\text{CPh})$ (**15**) in CD_2Cl_2 at 20°C

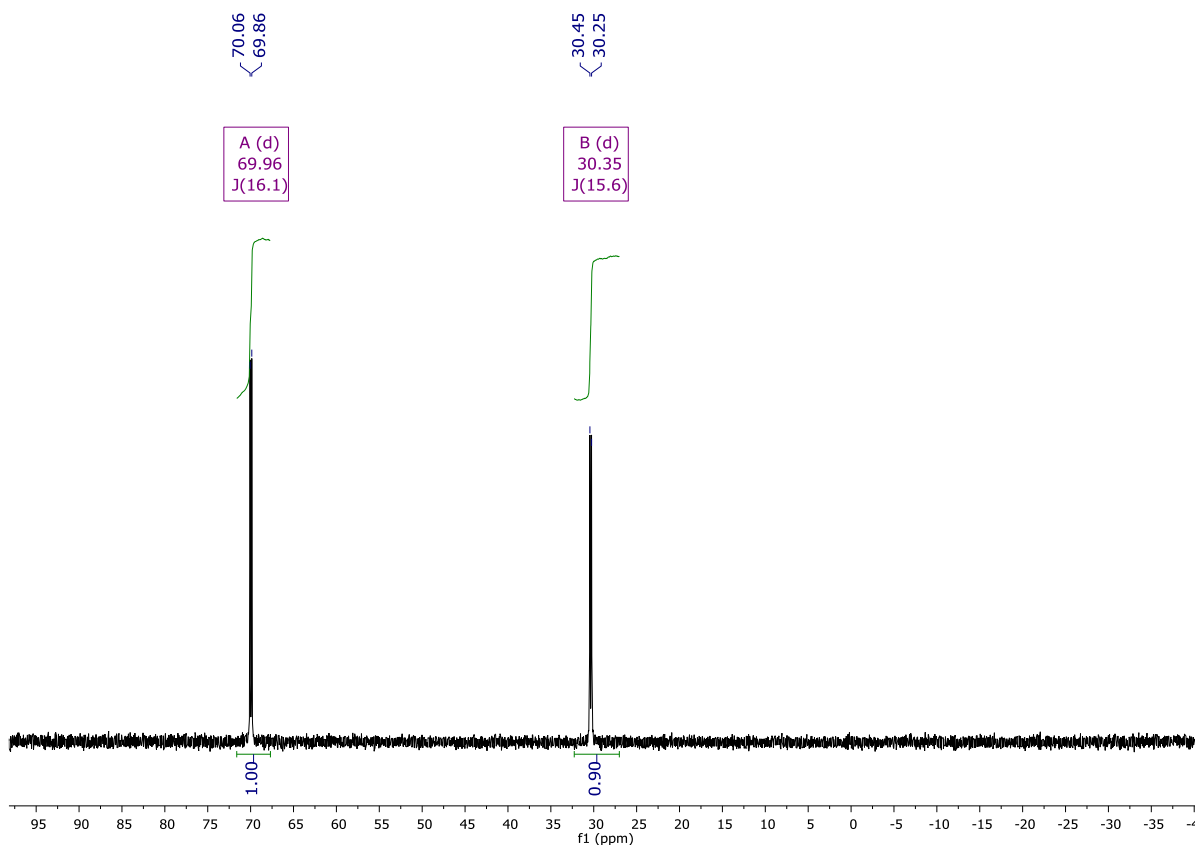


Figure 86 $^{31}\text{P}\{^1\text{H}\}$ NMR spectrum of $\text{Ru}(\kappa^2\text{-OCOCH}_3)_2(\text{CO})(\text{DiPPF})(\text{C}\equiv\text{CPh})$ (**15**) in CD_2Cl_2 at $20\text{ }^\circ\text{C}$

Single Crystal X-Ray Structure Determination of Compound 16.

General Data:

Data were collected on an X-ray single crystal diffractometer equipped with a CCD detector (Bruker APEX II, κ -CCD), a rotating anode (Bruker AXS, FR591) with $\text{MoK}\alpha$ radiation ($\lambda = 0.71073\text{ \AA}$), and a Montel mirror by using the APEX 2 software package.¹ The measurements were performed on a single crystal coated with perfluorinated ether. The crystal was fixed on the top of a glass fiber and transferred to the diffractometer. The crystal was frozen under a stream of cold nitrogen. A matrix scan was used to determine the initial lattice parameters. Reflections were merged and corrected for Lorentz and polarization effects, scan speed, and background using SAINT. Absorption corrections, including odd and even ordered spherical harmonics were performed using SADABS.² Space group assignments were based upon systematic absences, E statistics, and successful refinement of the structures. Structures were solved by direct methods with the aid of successive difference Fourier maps, and were refined against all data using SHELXL-2014 in conjunction with SHELXLE. If not mentioned otherwise, non-hydrogen atoms were refined with

anisotropic displacement parameters. Hydrogen atoms were placed in ideal positions using the SHELXL riding model. Full-matrix least-squares refinements were carried out by minimizing $\Sigma w(F_o^2 - F_c^2)^2$ with SHELXL-2014³ weighting scheme. Neutral atom scattering factors for all atoms and anomalous dispersion corrections for the non-hydrogen atoms were taken from *International Tables for Crystallography*.

Detailed Crystallographic Data:

Compound	Ru(k²-OCOCH₃)₂(CO)(DiPPF)(C≡CPh)
Crystal data	
Chemical formula of the crystal	2(C ₃₃ H ₄₄ O ₃ P ₂ Ru)·2(Fe)·2(C ₇ H ₈)
<i>M_r</i>	1599.35
Crystal system, space group	Monoclinic, <i>P</i> 2 ₁ / <i>c</i>
Temperature (K)	170
<i>a</i> , <i>b</i> , <i>c</i> (Å)	10.1474 (2), 15.3943 (2), 23.8422 (4)
β (°)	96.816 (2)
<i>V</i> (Å ³)	3698.12 (11)
<i>Z</i>	2
Radiation type	Mo <i>K</i> α
μ (mm ⁻¹)	0.92
Crystal size (mm)	0.30 × 0.20 × 0.16
Data collection	
Diffractometer	Xcalibur, Eos
Absorption correction	Analytical <i>CrysAlis Pro</i> 1.171.38.46 (Rigaku Oxford Diffraction, 2015) Analytical numeric absorption correction using a multifaceted crystal model based on expressions derived by R.C. Clark & J.S. Reid. (Clark, R. C. & Reid, J. S. (1995). <i>Acta Cryst.</i> A51, 887-897) Empirical absorption correction using spherical harmonics, implemented in SCALE3 ABSPACK scaling algorithm.
<i>T_{min}</i> , <i>T_{max}</i>	0.906, 0.941
No. of measured, independent and observed [<i>I</i> > 2σ(<i>I</i>)] reflections	83940, 8449, 6809
<i>R_{int}</i>	0.070
(sin θ/λ) _{max} (Å ⁻¹)	0.649
Refinement	
<i>R</i> [<i>F</i> ² > 2σ(<i>F</i> ²)], <i>wR</i> (<i>F</i> ²), <i>S</i>	0.034, 0.076, 1.06

No. of reflections	8449
No. of parameters	434
H-atom treatment	H-atom parameters constrained
$\Delta_{\max}, \Delta_{\min}$ ($e \text{ \AA}^{-3}$)	0.49, -0.33

Table 4 Bond Lengths for Ru(k²-OCOCH₃)₂(CO)(DiPPF)(C≡CPh).

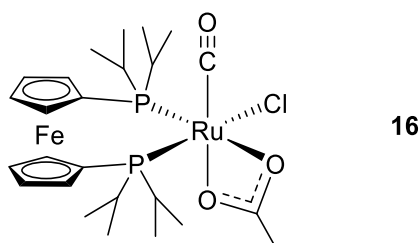
Atom	Atom	Length/Å	Atom	Atom	Length/Å
Ru1	P2	2.3018(6)	C2	C3	1.442(4)
Ru1	P1	2.4658(7)	C26	C27	1.530(4)
Ru1	O3	2.1936(17)	C26	C28	1.541(4)
Ru1	O2	2.2013(17)	C33	C32	1.421(4)
Ru1	C1	2.040(2)	C19	C20	1.427(4)
Ru1	C9	1.816(3)	C22	C21	1.423(4)
P2	C12	1.852(2)	C15	C16	1.528(4)
P2	C18	1.814(2)	C15	C17	1.529(4)
P2	C15	1.860(3)	C3	C4	1.395(4)
P1	C29	1.814(2)	C3	C8	1.396(4)
P1	C23	1.875(3)	C30	C31	1.418(4)
P1	C26	1.876(2)	C21	C20	1.415(4)
O3	C10	1.268(3)	C31	C32	1.412(4)
O2	C10	1.262(3)	C4	C5	1.375(4)
O1	C9	1.159(3)	C8	C7	1.387(4)
C1	C2	1.199(3)	C7	C6	1.375(4)
C12	C13	1.535(3)	C5	C6	1.383(5)
C12	C14	1.528(3)	C40	C35	1.373(5)
C29	C33	1.430(4)	C40	C39	1.393(5)
C29	C30	1.436(4)	C35	C36	1.373(5)
C18	C19	1.436(3)	C35	C34	1.496(5)
C18	C22	1.429(3)	C39	C38	1.353(5)
C10	C11	1.499(4)	C38	C37	1.380(5)
C23	C24	1.525(4)	C36	C37	1.365(5)
C23	C25	1.531(4)			

Table 5 Bond Angles for Ru(k²-OCOCH₃)₂(CO)(DiPPF)(C≡CPh).

Atom	Atom	Atom	Angle/°	Atom	Atom	Atom	Angle/°
P2	Ru1	P1	100.28(2)	O3	C10	C11	120.8(2)
O3	Ru1	P2	104.04(5)	O2	C10	O3	119.0(2)
O3	Ru1	P1	93.70(5)	O2	C10	C11	120.2(2)
O3	Ru1	O2	59.51(6)	C24	C23	P1	112.16(18)
O2	Ru1	P2	162.75(5)	C24	C23	C25	108.1(2)
O2	Ru1	P1	86.76(5)	C25	C23	P1	116.92(19)
C1	Ru1	P2	86.26(7)	C1	C2	C3	175.6(3)
C1	Ru1	P1	172.56(7)	C27	C26	P1	113.79(18)
C1	Ru1	O3	81.18(8)	C27	C26	C28	108.6(2)

C1	Ru1	O2	85.98(8)	C28	C26	P1	115.90(18)
C9	Ru1	P2	88.39(8)	C32	C33	C29	108.4(2)
C9	Ru1	P1	90.10(8)	O1	C9	Ru1	177.2(2)
C9	Ru1	O3	166.10(9)	C20	C19	C18	107.7(2)
C9	Ru1	O2	107.46(9)	C21	C22	C18	108.3(2)
C9	Ru1	C1	93.65(11)	C16	C15	P2	114.35(18)
C12	P2	Ru1	111.44(8)	C16	C15	C17	110.1(2)
C12	P2	C15	102.21(12)	C17	C15	P2	112.42(18)
C18	P2	Ru1	119.28(8)	C4	C3	C2	121.1(3)
C18	P2	C12	104.65(11)	C4	C3	C8	117.8(2)
C18	P2	C15	100.58(12)	C8	C3	C2	121.1(3)
C15	P2	Ru1	116.60(8)	C31	C30	C29	108.5(2)
C29	P1	Ru1	116.07(8)	C20	C21	C22	108.1(2)
C29	P1	C23	101.84(12)	C32	C31	C30	108.1(2)
C29	P1	C26	103.00(11)	C31	C32	C33	108.3(2)
C23	P1	Ru1	119.94(8)	C21	C20	C19	108.4(2)
C23	P1	C26	101.93(12)	C5	C4	C3	121.4(3)
C26	P1	Ru1	111.84(8)	C7	C8	C3	120.5(3)
C10	O3	Ru1	90.71(15)	C6	C7	C8	120.5(3)
C10	O2	Ru1	90.51(15)	C4	C5	C6	120.1(3)
C2	C1	Ru1	172.2(2)	C7	C6	C5	119.6(3)
C13	C12	P2	110.39(17)	C35	C40	C39	120.7(4)
C14	C12	P2	111.65(17)	C40	C35	C34	121.2(4)
C14	C12	C13	110.1(2)	C36	C35	C40	118.2(3)
C33	C29	P1	124.3(2)	C36	C35	C34	120.6(4)
C33	C29	C30	106.7(2)	C38	C39	C40	120.2(4)
C30	C29	P1	128.9(2)	C39	C38	C37	119.2(4)
C19	C18	P2	127.61(19)	C37	C36	C35	121.2(4)
C22	C18	P2	124.8(2)	C36	C37	C38	120.5(4)
C22	C18	C19	107.4(2)				

Synthesis of RuCl(OAc)(CO)(DiPPF) (16):



[Ru(CO)₂(Cl)₂]_n (65 mg, 0.287 mmol) and DiPPF (132 mg, 0.316) were suspended in 2.5 mL of degassed *t*BuOH and the mixture was heated at 100 °C for 1 h. sodium acetate (132 mg, 1.4 mmol) and 450 μL of chloroform were added, and the mixture was refluxed for 24 h then cooled to room temperature. The salt was filtered, and the

solution dried under reduced pressure affording the product as a greenish solid. Yield 91 mg (49%). ^1H NMR (200.1 MHz, CDCl_3 , 20 °C): δ = 4.91 (m, 1H; C_5H_4), 4.75 (m, 1H; C_5H_4), 4.55-4.31 (m, 6H; C_5H_4), 2.94 (hept, $^3J(\text{H,H}) = 7.0$ Hz, 2H; $\text{CH}(\text{CH}_3)_2$), 2.50 (hept, $^3J(\text{H,H}) = 7.1$ Hz, 2H; $\text{CH}(\text{CH}_3)_2$), 1.97 (s, 3H; OCOCH_3), 1.78-1.53 (m, 6H; $\text{CH}(\text{CH}_3)_2$), 1.54-1.17 (m, 12H; $\text{CH}(\text{CH}_3)_2$), 1.08-0.82 ppm (m, 6H; $\text{CH}(\text{CH}_3)_2$); $^{31}\text{P}\{^1\text{H}\}$ NMR (81.0 MHz, CD_2Cl_2 , 20 °C): δ = 67.8 (d, $^2J(\text{P,P}) = 19.1$ Hz), 56.6 ppm (d, $^2J(\text{P,P}) = 19.1$ Hz). elemental analysis (%) calc. for $\text{C}_{25}\text{H}_{39}\text{ClFeO}_3\text{P}_2\text{Ru}$: C 46.78, H 6.12; found: C 46.87, H 6.16.

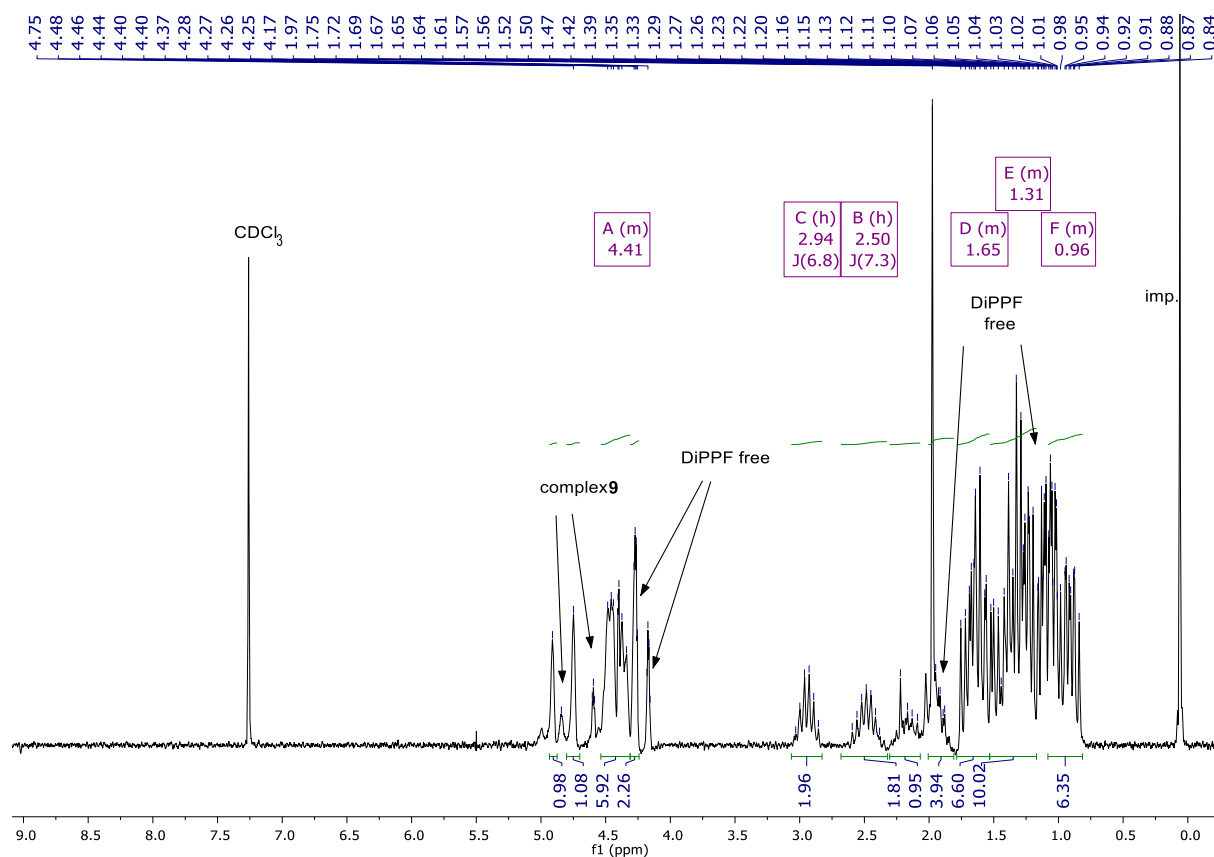


Figure 87 ^1H NMR spectrum of $\text{RuCl}(k^2\text{-OCOCH}_3)(\text{CO})(\text{DiPPF})$ **16** in CDCl_3 at 20 °C

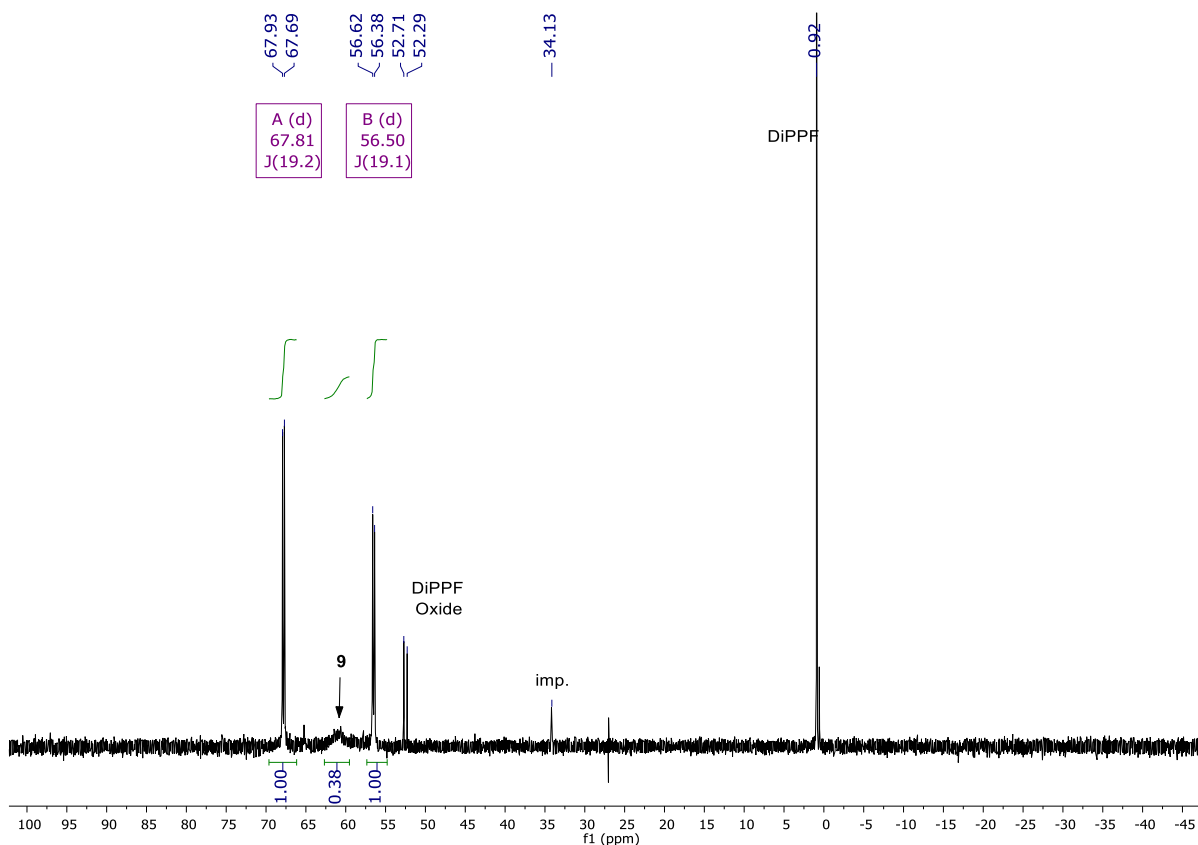


Figure 88 $^{31}\text{P}\{^1\text{H}\}$ NMR spectrum of $\text{RuCl}(k^2\text{-OCOCH}_3)(\text{CO})(\text{DiPPF})$ **16** in CDCl_3 at $20\text{ }^\circ\text{C}$

3.3 Transfer Hydrogenation

General procedure for TH of Acetophenone: The substrate (1.0 mmol) and catalysts were dissolved in 9,7 mL of 2-propanol and heated at $100\text{ }^\circ\text{C}$ under argon, then $200\text{ }\mu\text{L}$ of $\text{NaO}i\text{Pr}$ in 2-propanol (0.1M, 2 mol%, $20\text{ }\mu\text{mol}$) were added. The start of the reaction was considered the addition of the base, the molar ratio of substrate/catalyst (S/C) varied from 1000/1 to 20.000/1, while the molar ratio of substrate/base was fixed to 50/1. The reaction was sampled by removing an aliquot of the reaction mixture, mixture, which was quenched by addition of diethyl ether (1:1 (v/v)), filtered over a short silica pad, and submitted to GC analysis for the determination of the conversion, using a MEGADEX-ETTBDMS- β chiral column.

In the case where the catalyst was generated *in situ*, the acetate pre-catalyst was dissolved in IPA (9,7 mL) followed by addition of 10 equivalent of the chosen NN ligand (ampy, en, Hampt) and refluxed at $100\text{ }^\circ\text{C}$ under argon before addition of the substrate and the base.

3.4 Hydrogenation of aldehydes

General procedure for the hydrogenation of neat aldehydes: The hydrogenation reactions were performed in an 8 vessel Biotage Endeavor apparatus (10 mL each). The desired amount of catalysts (based on the S/C ratio, generally 20'000:1, 0.002 mmol) was weighted in a 10 mL test tube, then the aldehyde (40 mmol), the additive (basic, KOH 1M solution 0.125%, 0.05 mmol, 50 μ L; or acidic TFA, 10 equiv. respect to the catalyst, usually 0.02 mmol, 1.5 μ L) were added at open air. Others additives like ampy (5-10 equiv. respect to the catalyst) or solvents (1-2 mL), may be added. Once 8 test tubes are prepared in this way, they were placed in the vessels, sealed into the apparatus and stirred at 650 rpm. A pressure of 2 bar of N₂ was applied with five venting cycles. The vessels were then charged with H₂ at the desired pressure and slowly vented five times, heated to 90°C, and leaved to react for 16 h. The apparatus monitored the hydrogen uptake, and GC/NMR analyses were performed at the end of the experiment on the crude reaction.

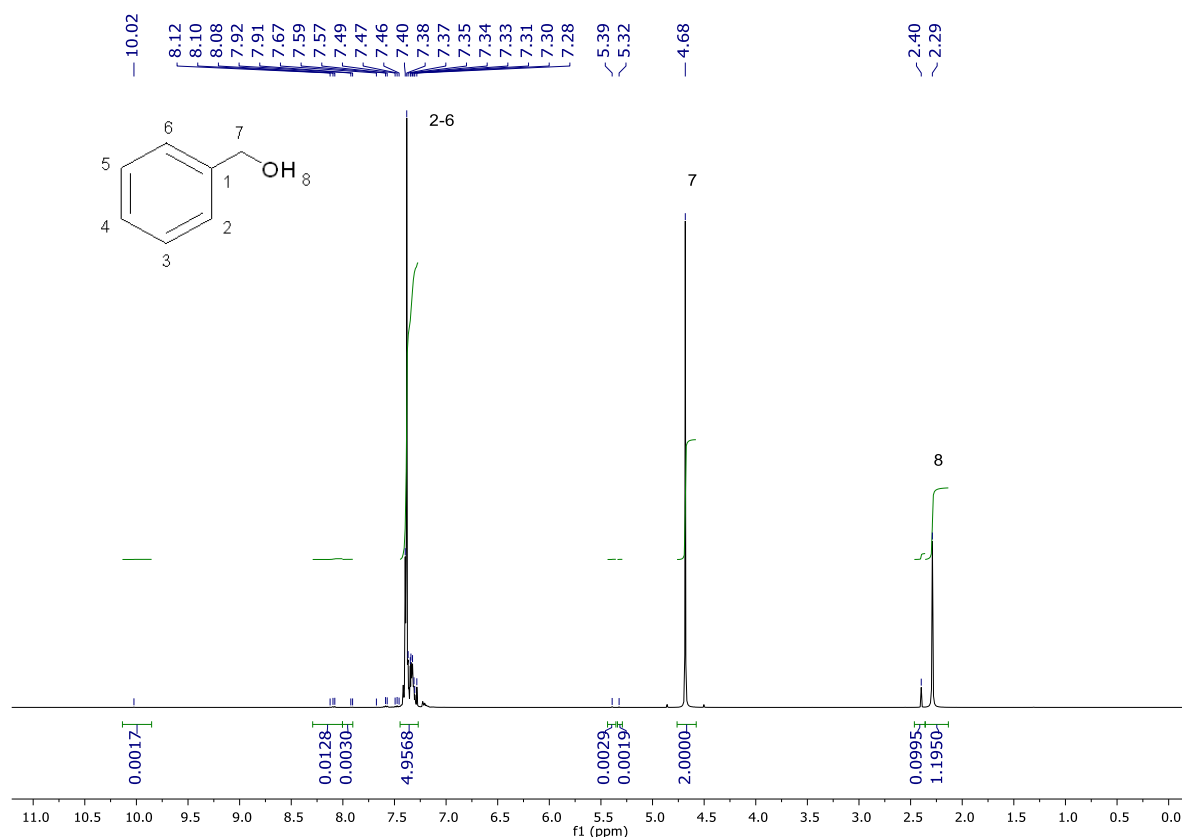


Figure 89 ¹H NMR spectrum of Benzyl Alcohol (crude mixture of entry 2, Table 10) in CDCl₃ at 20 °C.

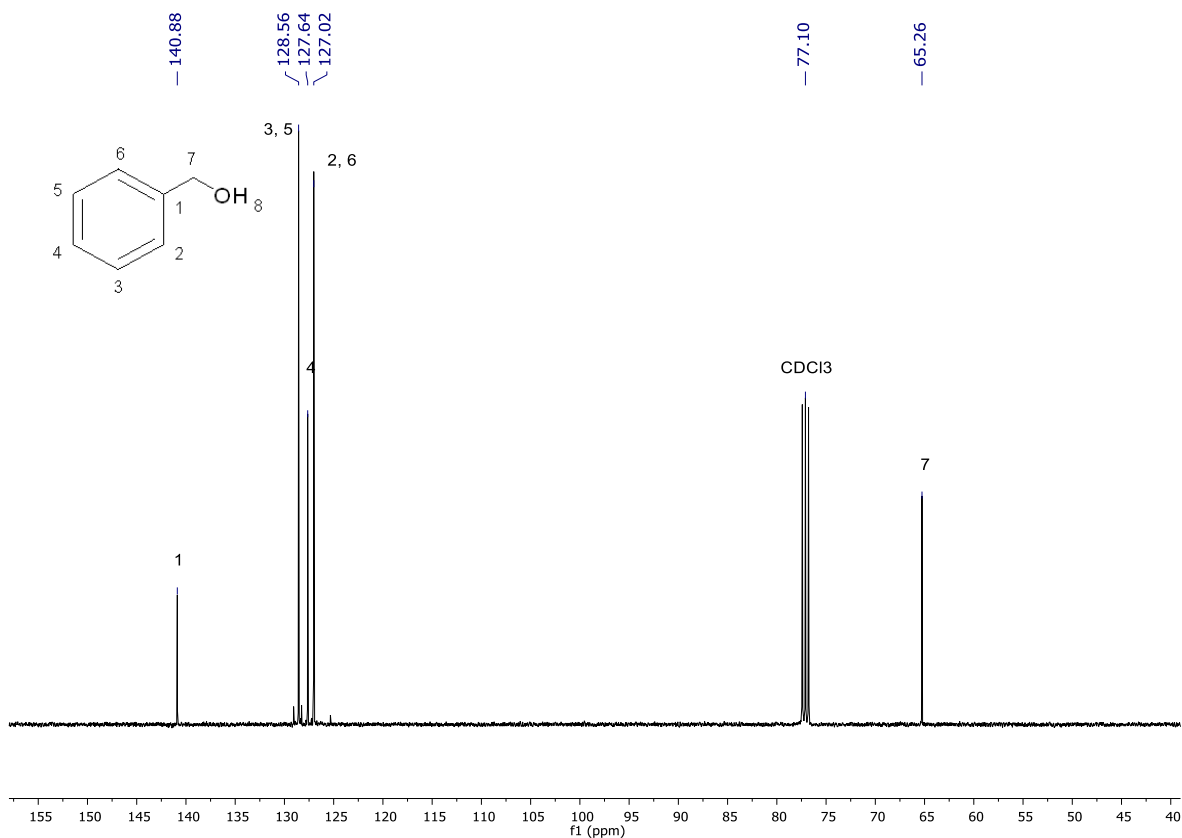


Figure 90 ¹³C{¹H} NMR spectrum of Benzyl Alcohol (crude reaction mixture entry 2, Table 10) in CDCl₃ at 20 °C.

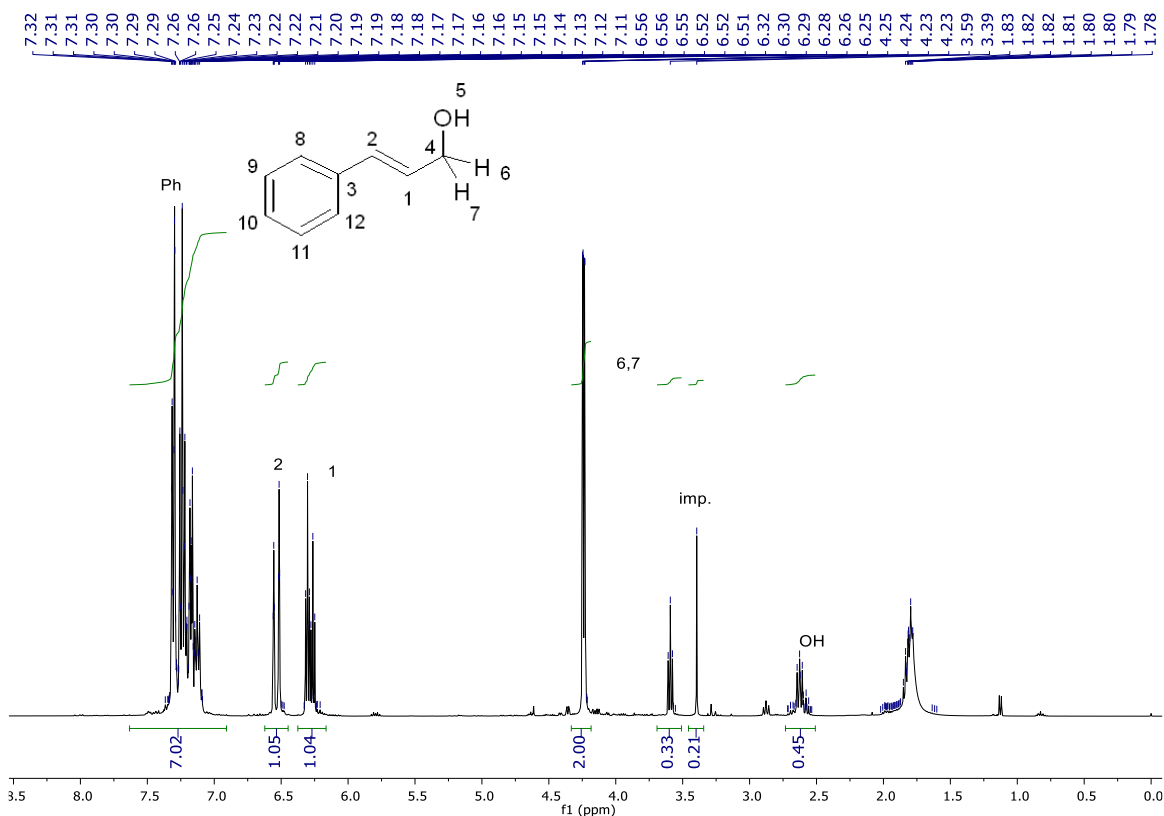


Figure 91 ¹H NMR spectrum of cinnamyl alcohol (crude mixture of entry 18, Table 14) in CDCl₃ at 20 °C.

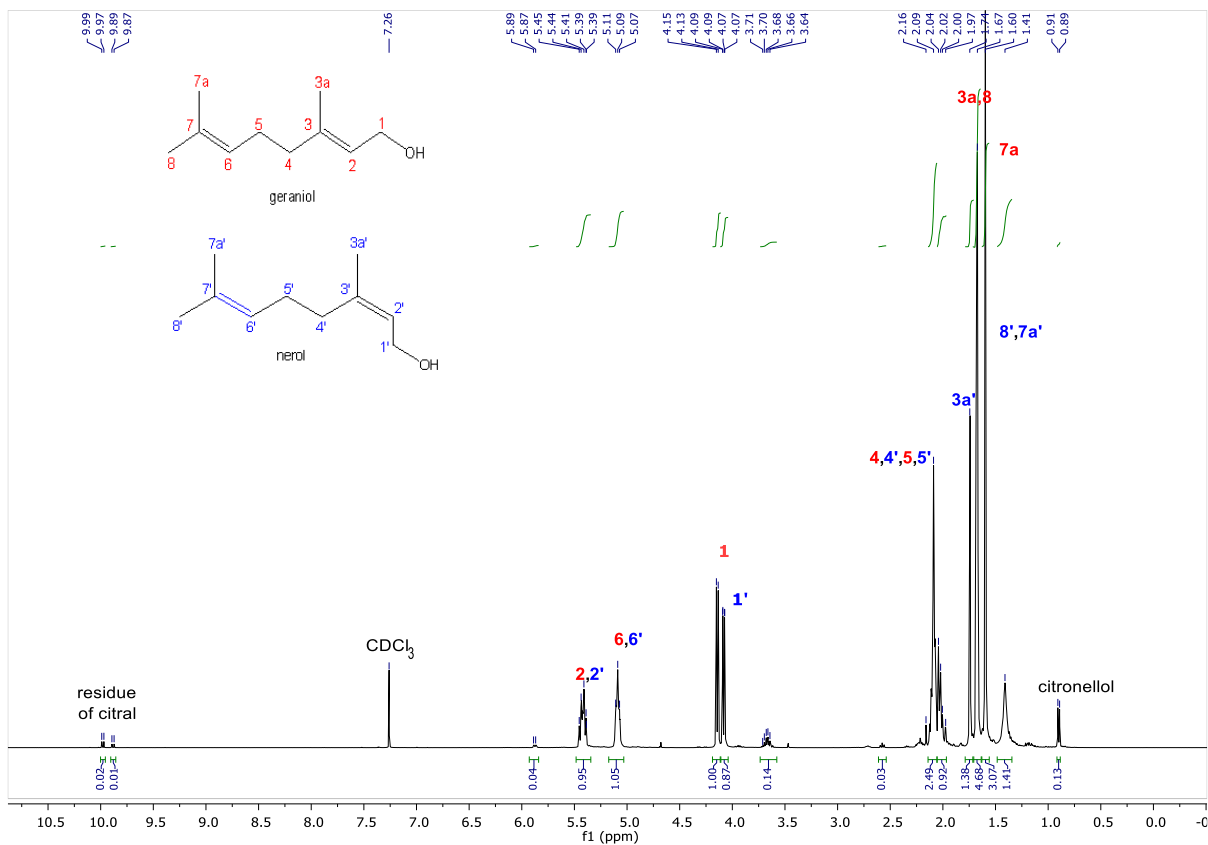


Figure 92 ^1H NMR spectrum of geranio and nerol mixture (crude mixture of entry 5, Table 15) in CDCl_3 at 20°C .

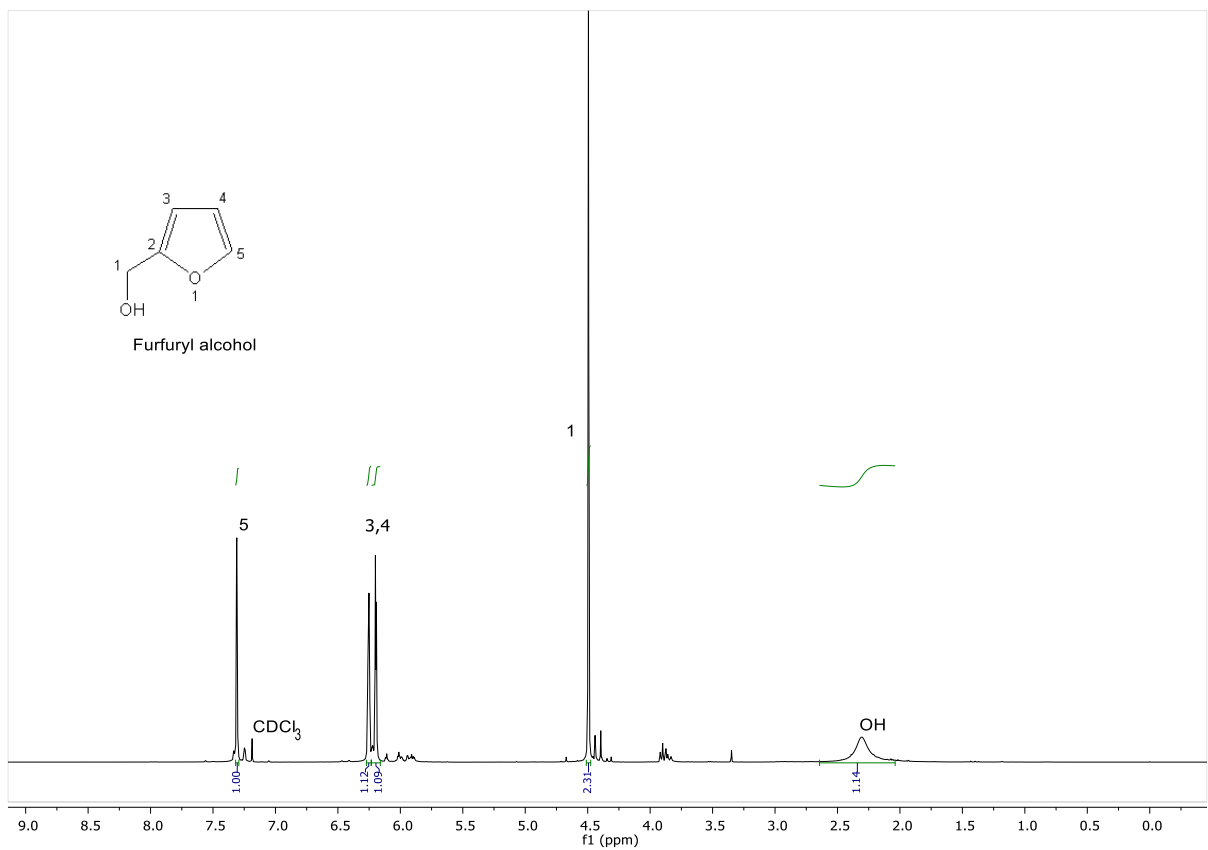


Figure 93 ^1H NMR spectrum of furfuryl alcohol (crude mixture of entry 11, Table 16) in CDCl_3 at 20°C .

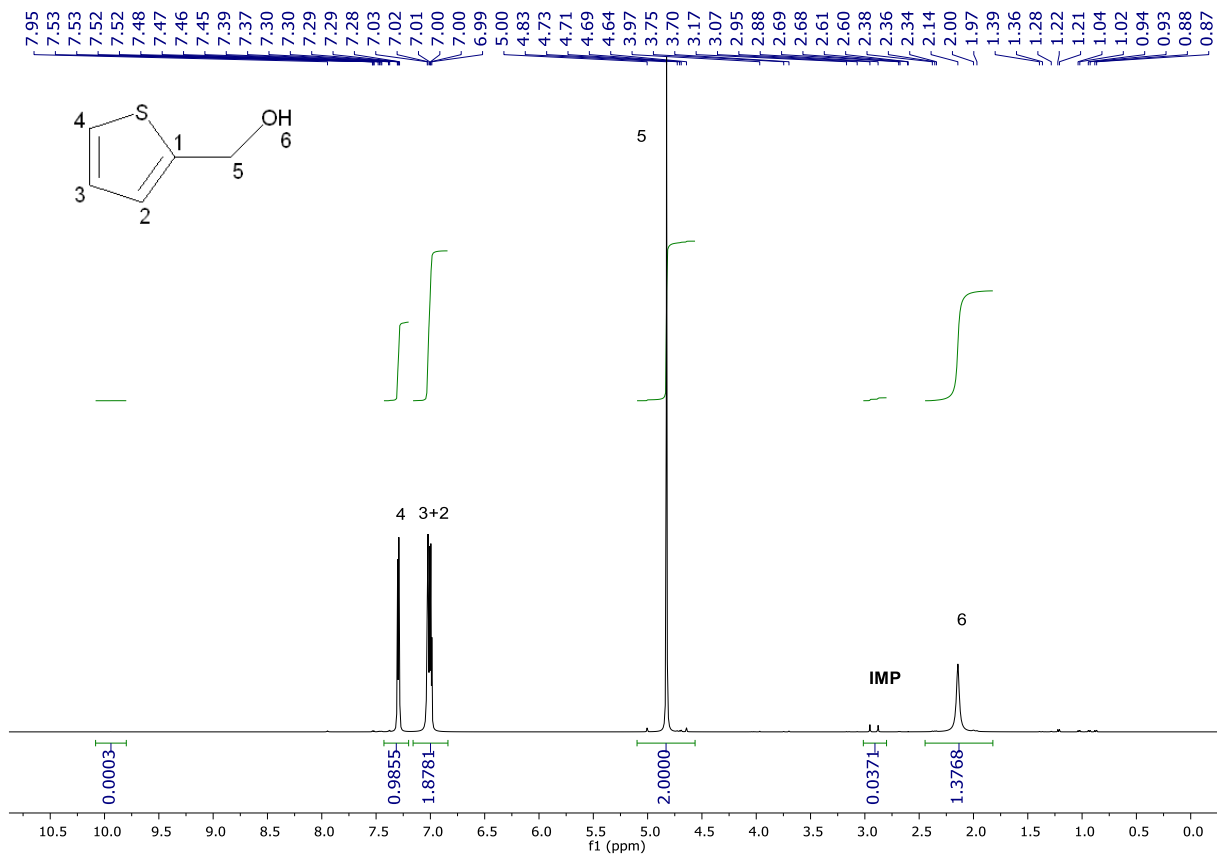


Figure 94 ^1H NMR spectrum of 2-(Hydroxymethyl)thiophene (crude mixture of entry 12, Table 16) in CDCl_3 at 20 °C.

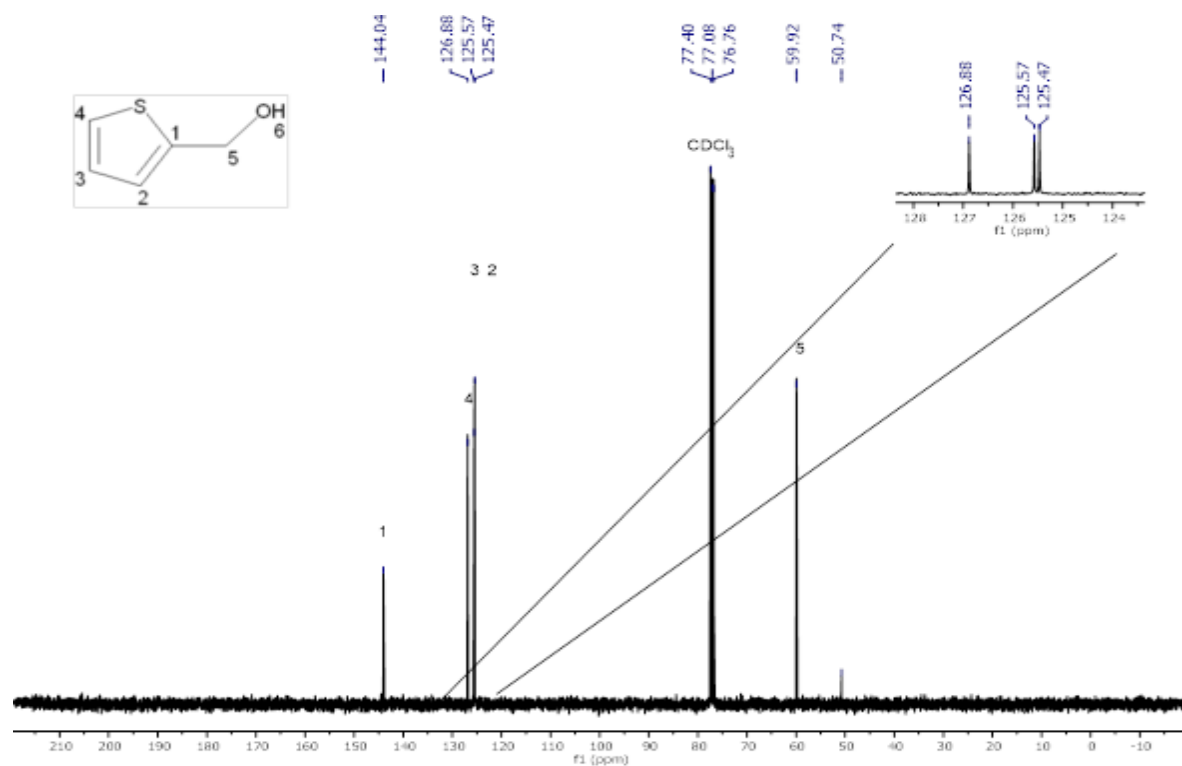


Figure 95 $^{13}\text{C}\{^1\text{H}\}$ NMR spectrum of 2-(Hydroxymethyl)thiophene (crude mixture of entry 12, Table 16) in CDCl_3 at 20 °C.

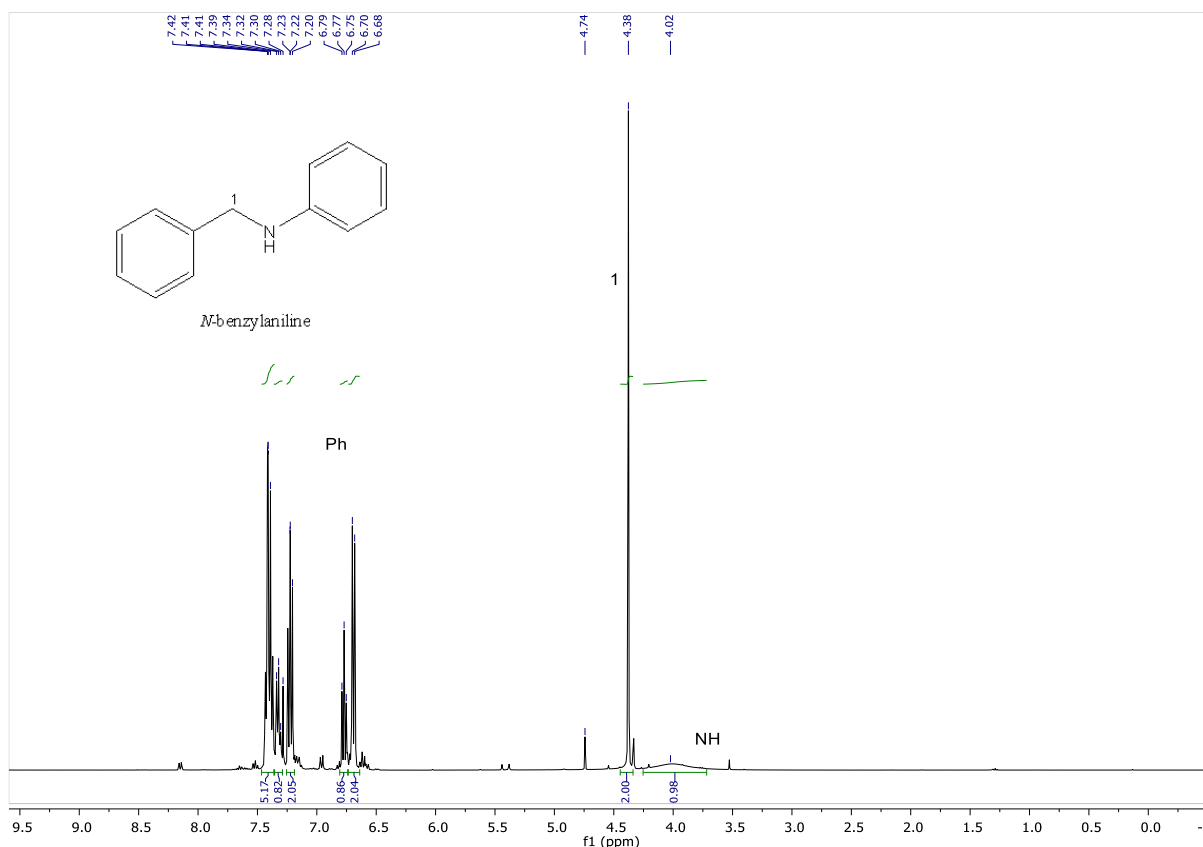


Figure 96 ^1H NMR spectrum of *N*-benzylaniline (crude mixture of entry 1, Table 17) in CDCl_3 at 20°C

3.5 *N*-alkylation

Evidence of the formation of the hydride $\text{RuH}(\text{OAc})(\text{CO})(\text{DiPPF})$ (**17**):

a) with 2-propanol / NEt_3 : Complex **9** (11.8 mg, 0.0178 mmol) was dissolved in 2-propanol (0.4 mL) and NEt_3 (50 μL , 0.359 mmol) was added under argon. The resulting solution was recorded using CDCl_3 as external lock. Signals of **MH** (in the presence of **9**): $^{31}\text{P}\{^1\text{H}\}$ NMR (81.0 MHz, CDCl_3 , 20°C): $\delta = 80.0$ (d, $^2J(\text{P},\text{P}) = 8.2$ Hz), 24.6 ppm (d, $^2J(\text{P},\text{P}) = 7.1$ Hz); ^{31}P NMR (81.0 MHz, CDCl_3 , 20°C): $\delta = 79.8$ (br s), 24.5 ppm (d, $^2J(\text{P},\text{H}) = 135$ Hz).

b) with H_2 : Complex **9** (10 mg, 0.015 mmol) was dissolved in $[\text{D}_8]$ toluene (0.45 mL) and the solution was pressurized with dihydrogen (4 atm) in a quick pressure valve Wildman NMR tube. Signals of **MH** (in the presence of **9**): ^1H NMR (200.1 MHz, $[\text{D}_8]$ -toluene, 20°C): $\delta = -5.98$ ppm (dd, 1H; $^2J(\text{H},\text{P}) = 133$ Hz, $^2J(\text{H},\text{P}) = 31.3$ Hz, 1H; Ru-H); $^{31}\text{P}\{^1\text{H}\}$ NMR (81.0 MHz, $[\text{D}_8]$ toluene, 20°C): $\delta = 79.3$ (d, $^2J(\text{P},\text{P}) = 8.5$ Hz), 25.0 ppm (d, $^2J(\text{P},\text{P}) = 8.5$ Hz).

Catalytic alkylation of amines: The ruthenium complex (0.01 mmol) was dissolved in 580 μL of ethanol (0.01 mol) and, if required, TFA (10 equiv with respect to the catalyst) was added to the catalyst under argon. The solution was kept at the suitable temperature (30, 65, 78 or 100 $^{\circ}\text{C}$) and the amine (1.00 mmol) was added. The reaction was sampled by removing 50 μL of the reaction mixture and diluting it with 2 mL of *n*-pentane. The obtained solution was filtered over a short pad of basic alumina and the conversion was determined by GC analysis ([amine] = 1.7 M; alcohol/amine/Ru = 1000/100/1).

Alkylation of amines with the *in situ* generated catalyst: The precursor $\text{Ru}(\text{OAc})_2(\text{CO})(\text{PPh}_3)_2$ (0.01 mmol, 7.7 mg) and the selected diphosphine (1.5 equiv) were suspended in 2 mL of cyclohexane under argon. The mixture was stirred at reflux temperature for 3 h, the solvent was removed under vacuum and the alkylation of amines was performed following the procedure described above for the isolated catalysts.

Synthesis of 1-benzyl-4-ethylpiperazine: Complex **9** (30 mg, 0.045 mmol) was dissolved in 5.80 mL of ethanol (0.10 mol) and after addition of *N*-benzylpiperazine (**e**) (1.95 mL, 11.2 mmol) at 78 $^{\circ}\text{C}$, the solution was refluxed for 15 h (the ratios ethanol/amine/Ru = 2200/250/1). The solution was allowed to reach room temperature and *n*-pentane (7 mL) was added. The mixture was filtered over basic alumina (7.2 g) resulting in a biphasic system. The upper phase was separated, dried and concentrated under reduced pressure, affording 1.87 g of 1-benzyl-4-ethylpiperazine (81% yield). ^1H NMR (200.1 MHz, CDCl_3 , 20 $^{\circ}\text{C}$): δ = 7.29 (m, 5H; aromatic protons), 3.51 (s, 2H; PhCH_2), 2.49 (s, broad, 8H; NCH_2CH_2), 2.40 (q, $^3J(\text{H},\text{H}) = 7.2$ Hz, 2H; CH_2CH_3), 1.07 ppm (t, $^3J(\text{H},\text{H}) = 7.2$ Hz, 3H; CH_2CH_3); $^{13}\text{C}\{^1\text{H}\}$ NMR (50.3 MHz, CDCl_3 , 20 $^{\circ}\text{C}$): δ = 138.2 (*ipso*- C_6H_5), 129.3 (*o*- C_6H_5), 128.3 (*m*- C_6H_5), 127.0 (*p*- C_6H_5), 63.2 (PhCH_2N), 53.2 ($\text{PhCH}_2\text{NCH}_2$), 52.9 (CH_2NEt), 52.4 (NCH_2CH_3), 12.1 ppm (CH_3).

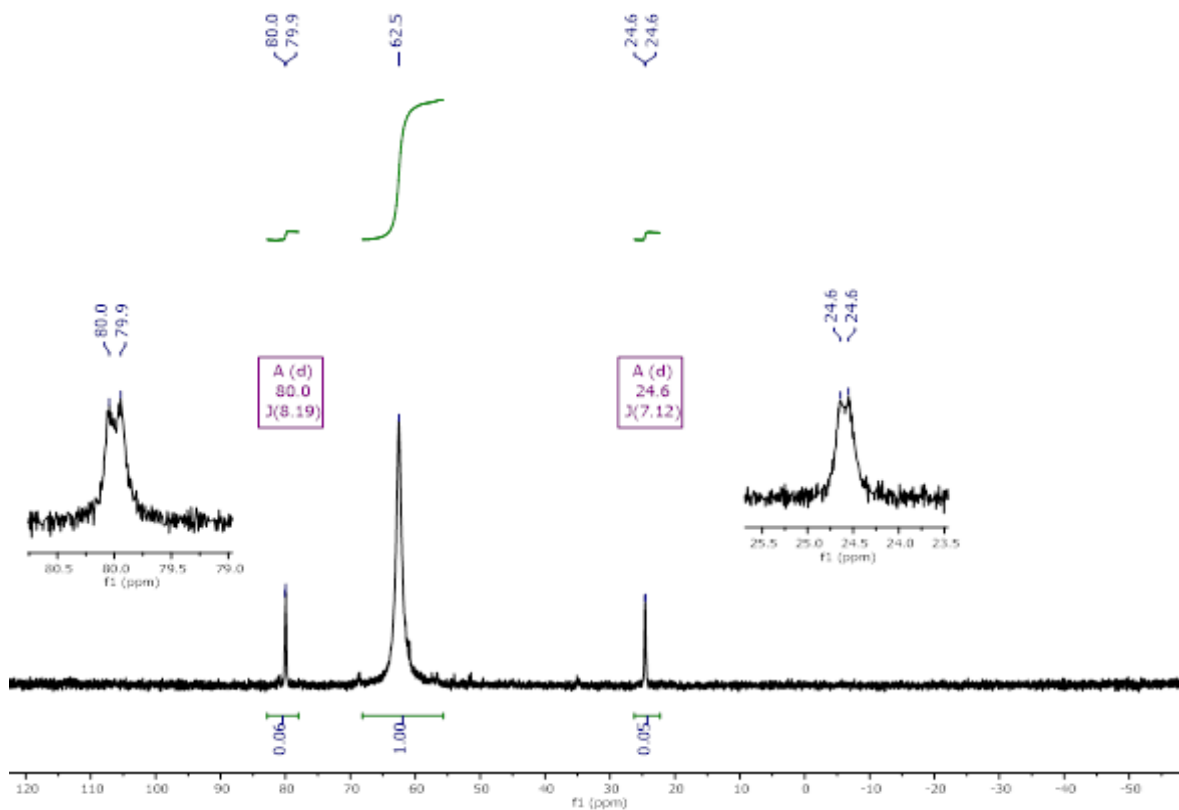


Figure 97. $^{31}\text{P}\{^1\text{H}\}$ NMR spectrum of $\text{Ru}(\text{OAc})_2(\text{CO})(\text{DiPPF})$ (9) and $\text{RuH}(\text{OAc})(\text{CO})(\text{DiPPF})$ (17) mixture, ratio 17/3 = 1/9 in *i*PrOH with 20 equiv NEt_3 (external CDCl_3 lock).

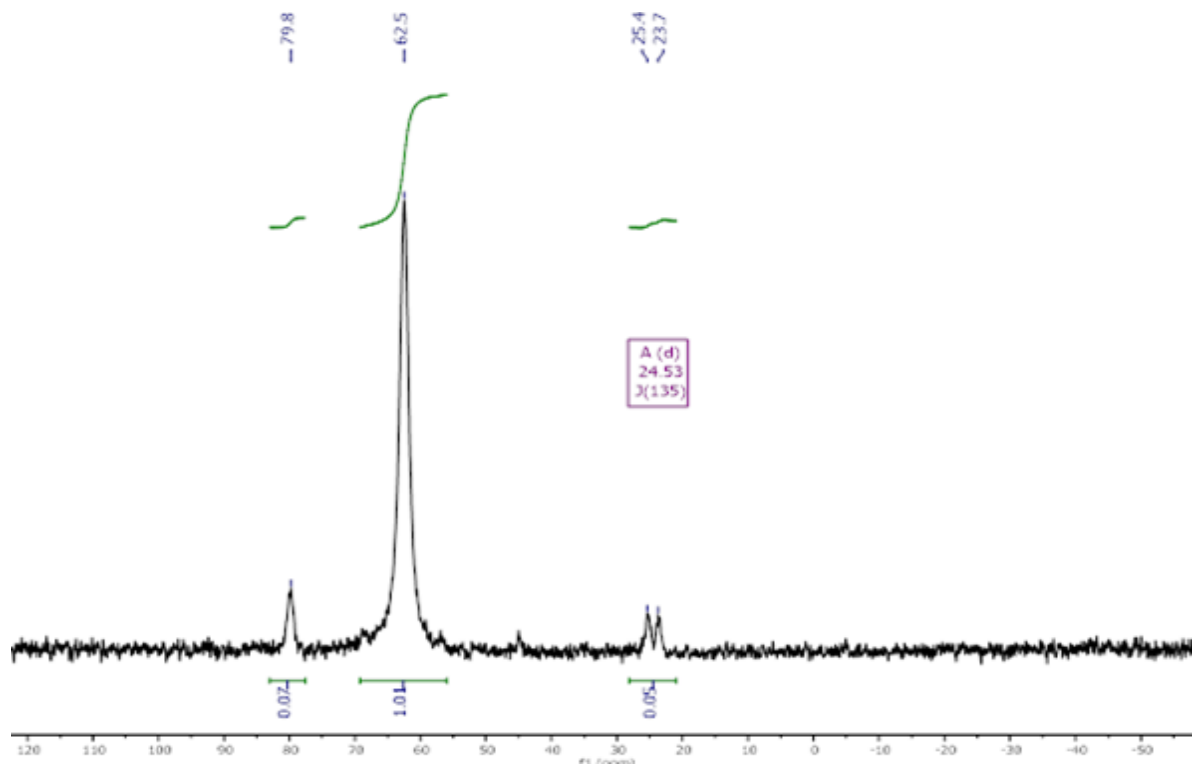


Figure 98. ^{31}P NMR spectrum of $\text{Ru}(\text{OAc})_2(\text{CO})(\text{DiPPF})$ (9) and $\text{RuH}(\text{OAc})(\text{CO})(\text{DiPPF})$ (17) mixture, ratio 17/3 = 1/9, without ^1H decoupling.

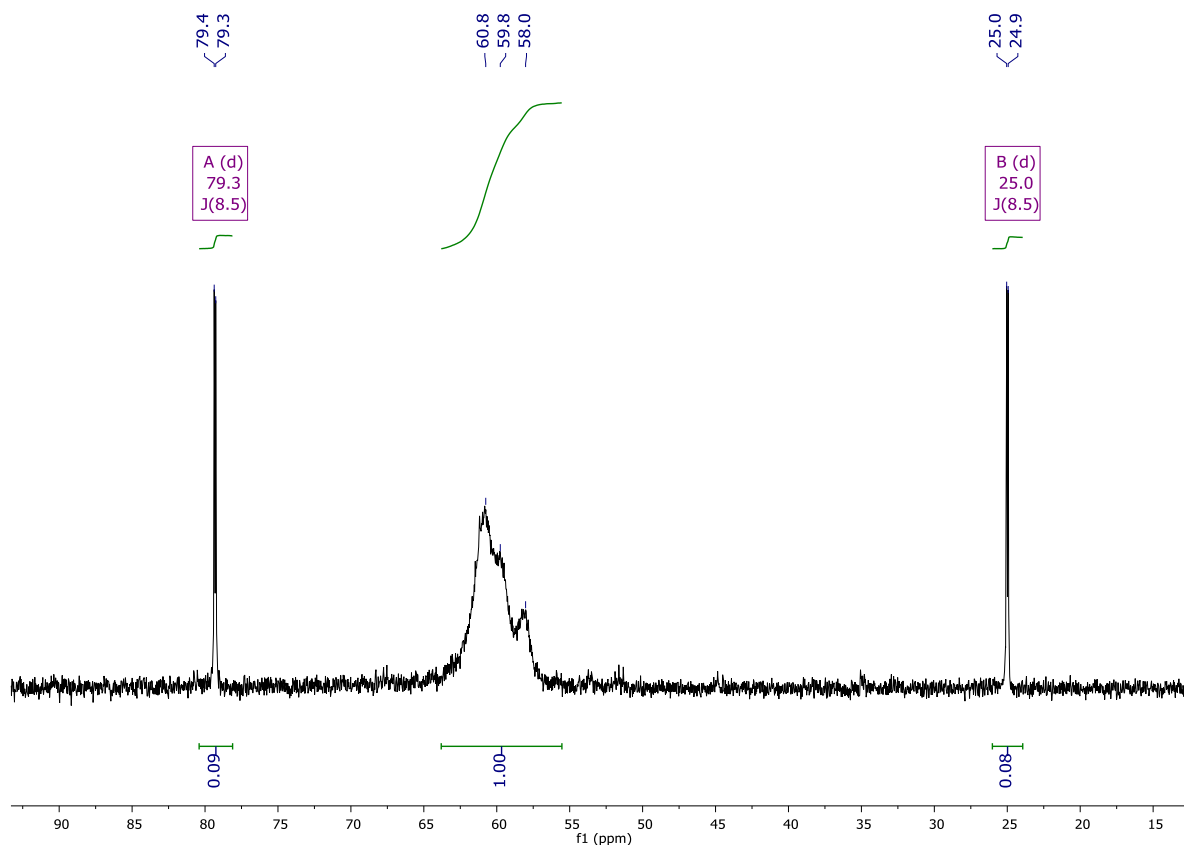


Figure 99 $^{31}\text{P}\{^1\text{H}\}$ NMR spectrum of $\text{Ru}(\text{OAc})_2(\text{CO})(\text{DiPPF})$ (**9**) and $\text{RuH}(\text{OAc})(\text{CO})(\text{DiPPF})$ (**17**) mixture, ratio **17/9** = 1/9, in $[\text{D}_8]\text{toluene}$ with dihydrogen (4 atm).

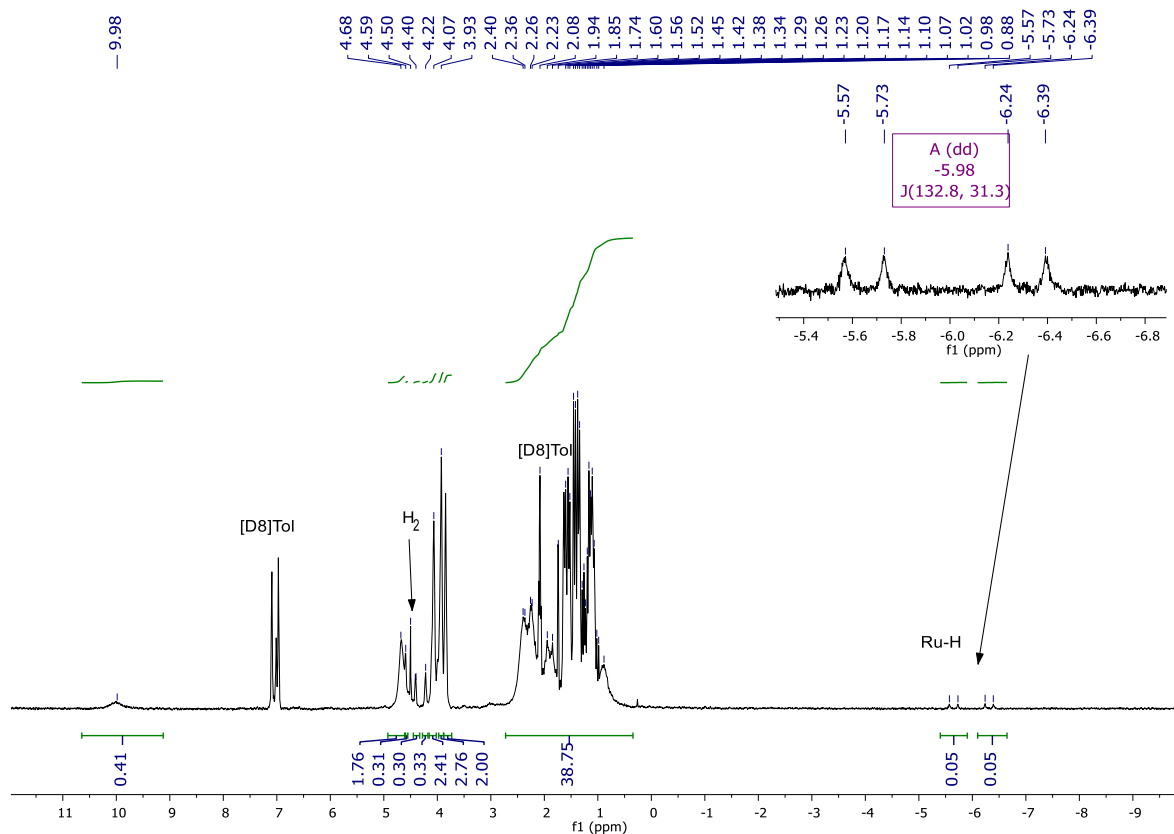


Figure 100 ^1H NMR spectrum of $\text{Ru}(\text{OAc})_2(\text{CO})(\text{DiPPF})$ (**9**) and $\text{RuH}(\text{OAc})(\text{CO})(\text{DiPPF})$ (**17**) mixture, ratio **17/9** = 1/9, in $[\text{D}_8]\text{toluene}$ with dihydrogen (4 atm).

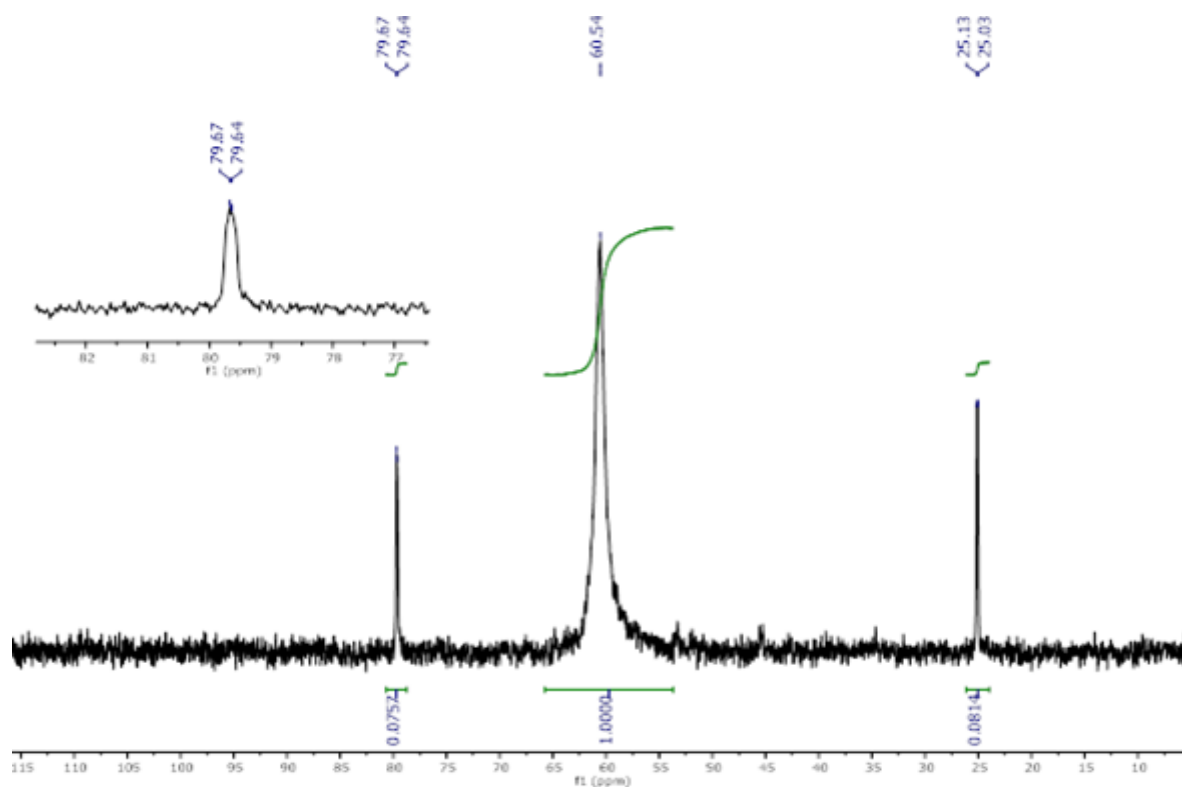


Figure 101 $^{31}\text{P}\{^1\text{H}\}$ NMR spectrum of $\text{Ru}(\text{OAc})_2(\text{CO})(\text{DiPPF})$ (9) and $\text{RuH}(\text{OAc})(\text{CO})(\text{DiPPF})$ (17) mixture, ratio 17/9 = 1/9, heated to 50°C in $[\text{D}_8]\text{toluene}$ with dihydrogen (4 atm).

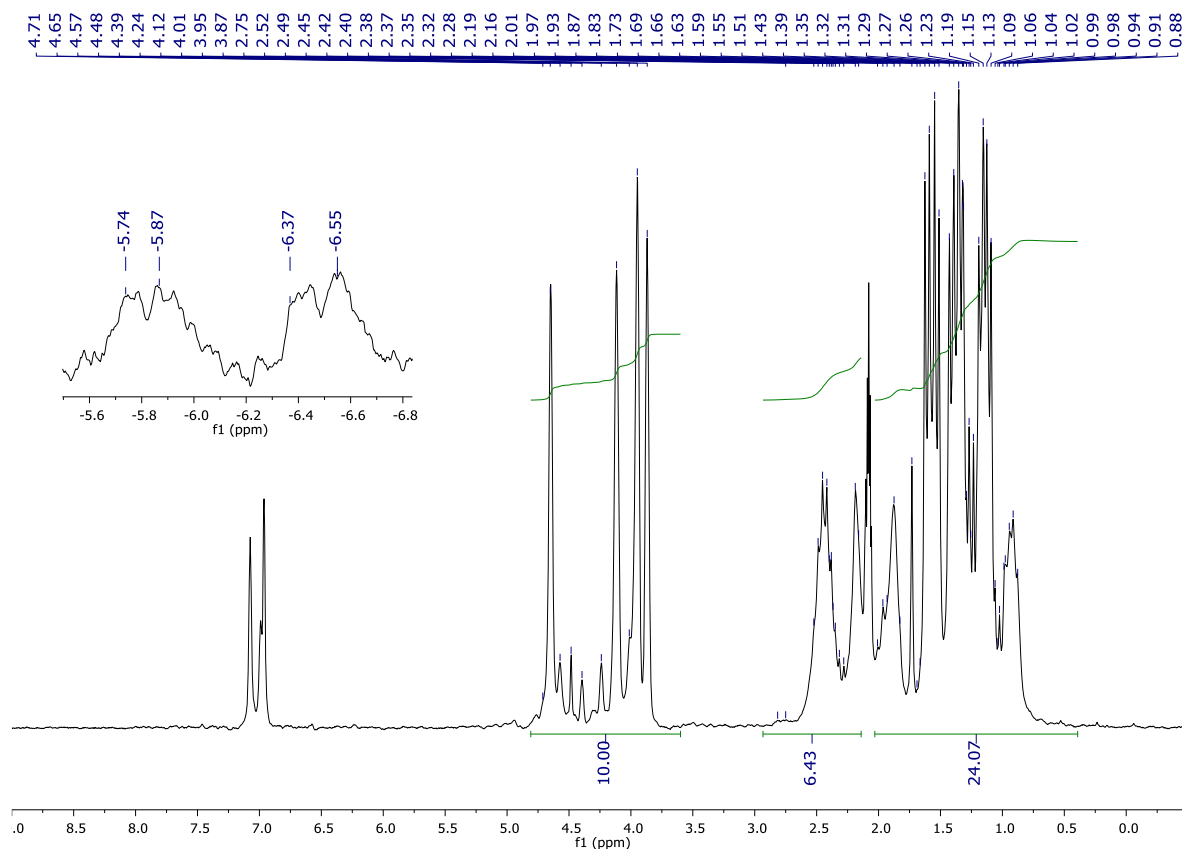
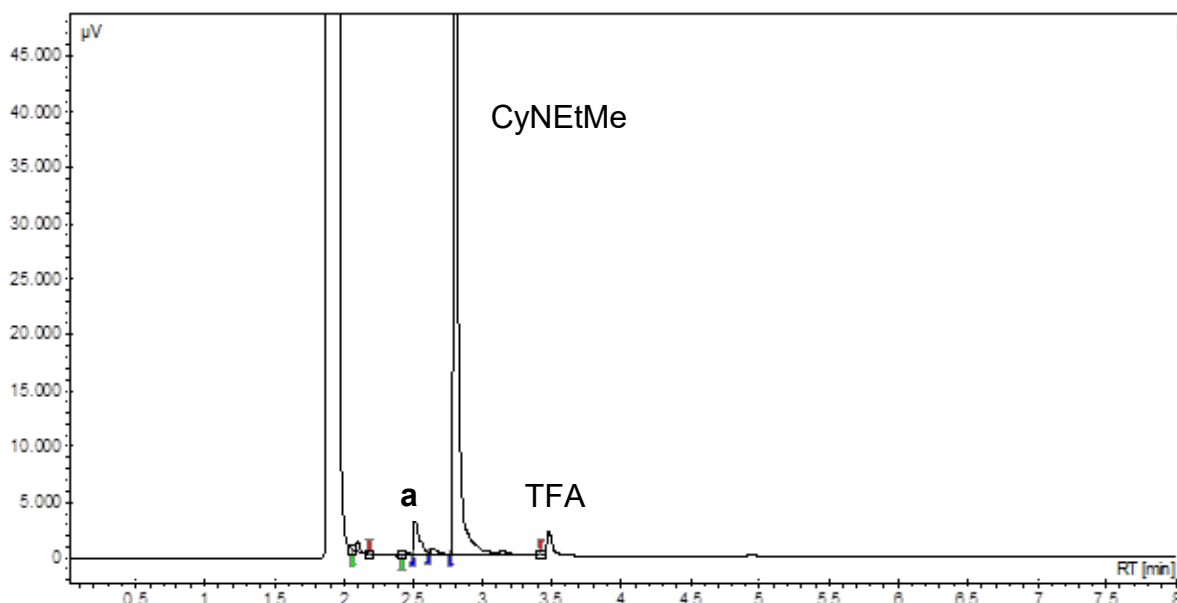
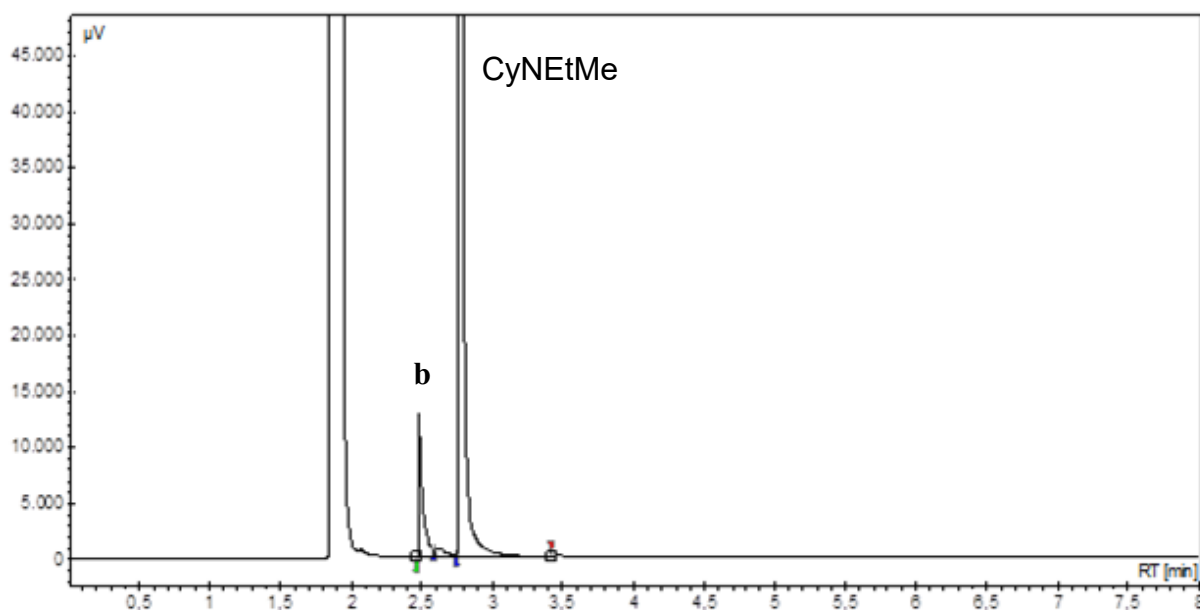


Figure 102 ^1H NMR spectrum of $\text{Ru}(\text{OAc})_2(\text{CO})(\text{DiPPF})$ (9) and $\text{RuH}(\text{OAc})(\text{CO})(\text{DiPPF})$ (17) mixture, ratio 17/9 = 1/9, heated to 50°C in $[\text{D}_8]\text{toluene}$ with dihydrogen (4 atm).



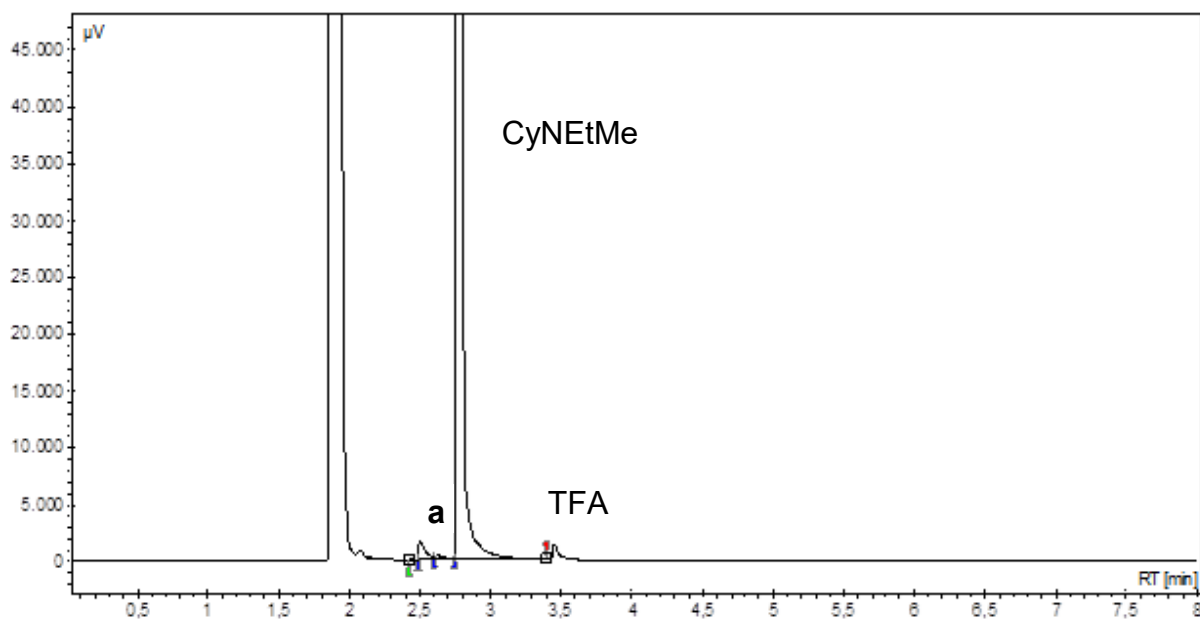
#	Name	Time [Min]	Quantity [% Area]	Height [µV]	Area [µV.Min]	Area [%]
3	CyNHMe (a)	2.52	2.71	3373.5	145.0	2.715
5	CyNEtMe	2.80	95.92	189289.8	5123.4	95.922

Figure 103 GC analysis of N-alkylation of **a** with **2** and TFA at 65°C (Entry 4, Table 18)



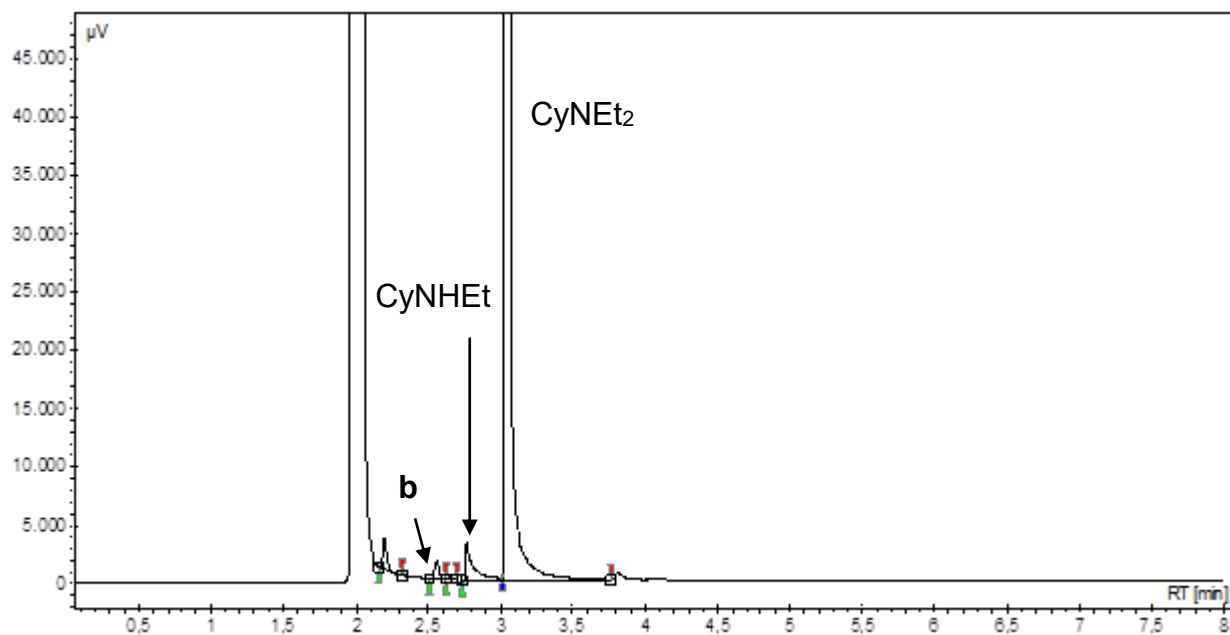
#	Name	Time [Min]	Quantity [% Area]	Height [µV]	Area [µV.Min]	Area [%]
3	CyNHMe (b)	2.48	7.51	12666.4	463.0	7.511
5	CyNEtMe	2.78	91.52	201267.9	56441.1	91.523

Figure 104 GC analysis of N-alkylation of **a** with **9** at 65°C (entry 11, Table 18)



#	Name	Time [Min]	Quantity [% Area]	Height [μV]	Area [μV.Min]	Area [%]
2	CyNHMe (a)	2.50	1.21	1656.8	82.7	1.211
4	CyNEtMe	2.77	98.42	243376.4	6718.7	98.422

Figure 105 GC analysis of N-alkylation of **a** with **9** and TFA at 65°C (entry 12, Table 18)

A)

#	Name	Time [Min]	Quantity [%Area]	Height [μV]	Area [μV.Min]	Area% [%]
2	cyclohexylamine (b)	2.56	0.53	1488.5	44.5	0.525
3	CyNHet	2.77	2.31	3233.7	195.7	2.309
4	CyNEt ₂	3.04	96.01	283953.8	8137.2	96.013

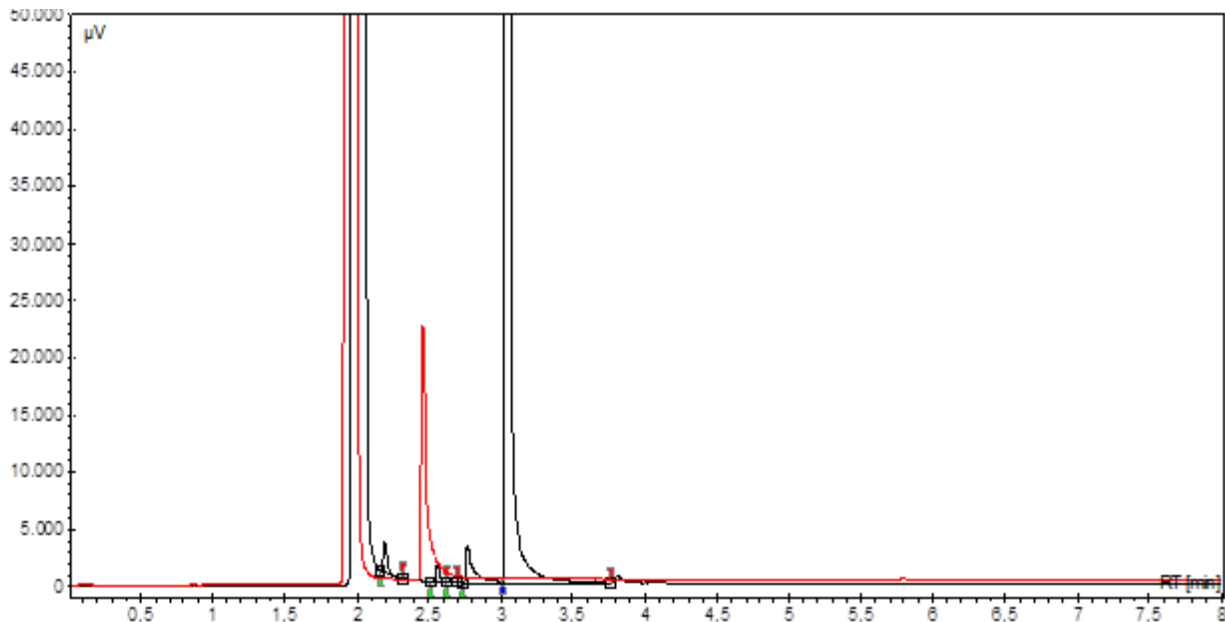
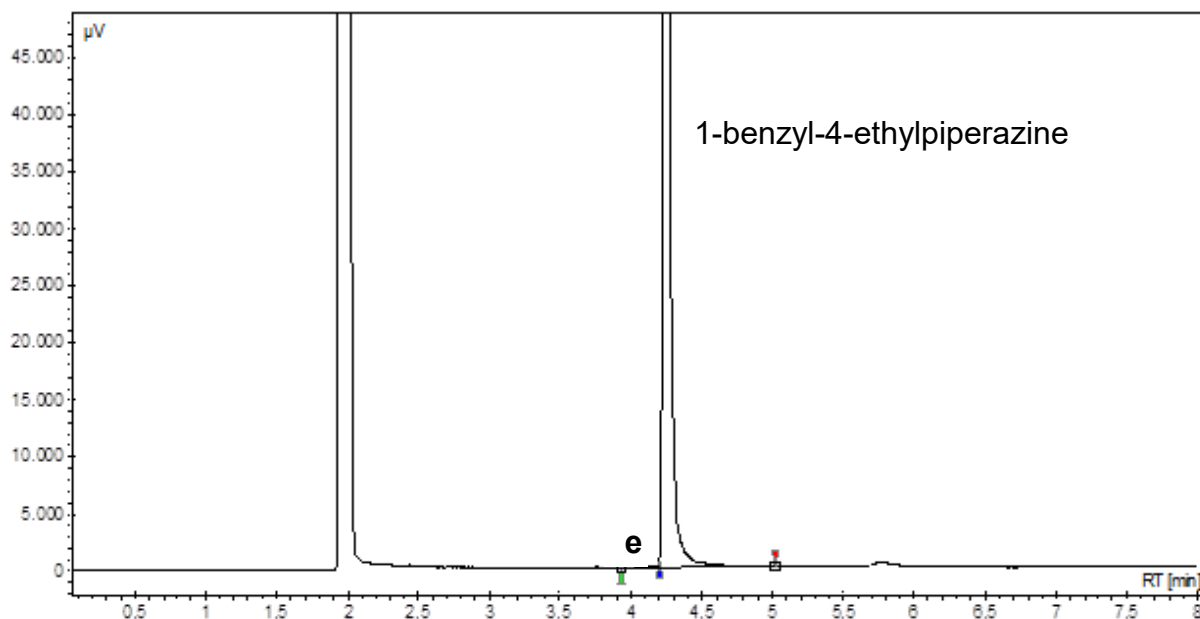
B)

Figure 106 **A)** GC analysis of *N*-alkylation of **b** with **9** at 78 °C (entry 1, Table 19); **B)** superimposition of chromatogram (A) with that of substrate **b** (red line)

A)



#	Name	Time [Min]	Quantity [% Area]	Height [µV]	Area [µV.Min]	Area% [%]
1	1-benzylpiperazine (e)	4.20	0.15	74.4	9.0	0.148
2	1-benzyl-4-ethylpiperazine	4.25	99.85	133660.8	6109.1	99.852

B)

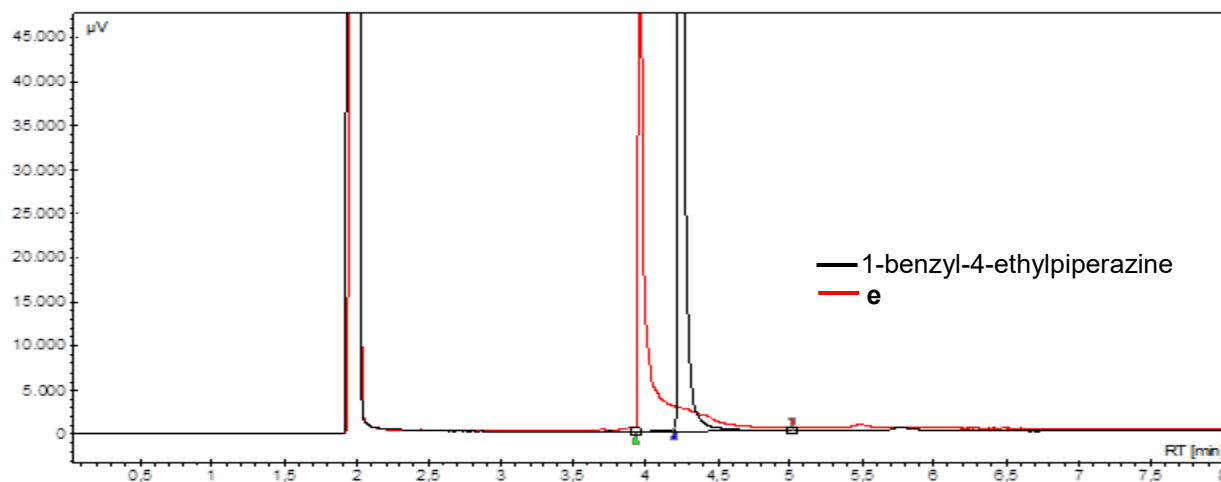


Figure 107 A) GC analysis of N-alkylation of **e** with **9** at 65°C (entry 4, Table 19); B) GC superimposition of chromatogram (A) with that of substrate **e** (red line).

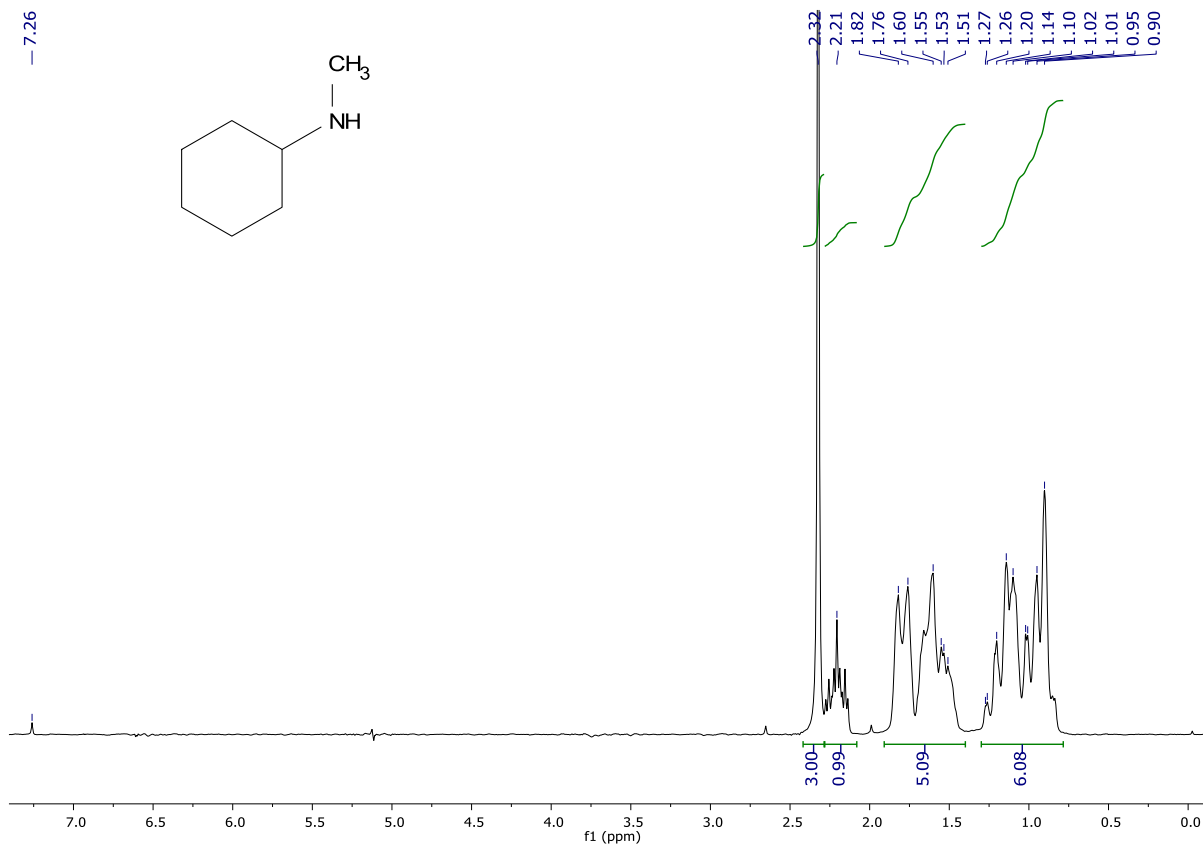


Figure 108. ^1H NMR spectrum of *N*-methylcyclohexylamine (a) in CDCl_3 at 20°C .

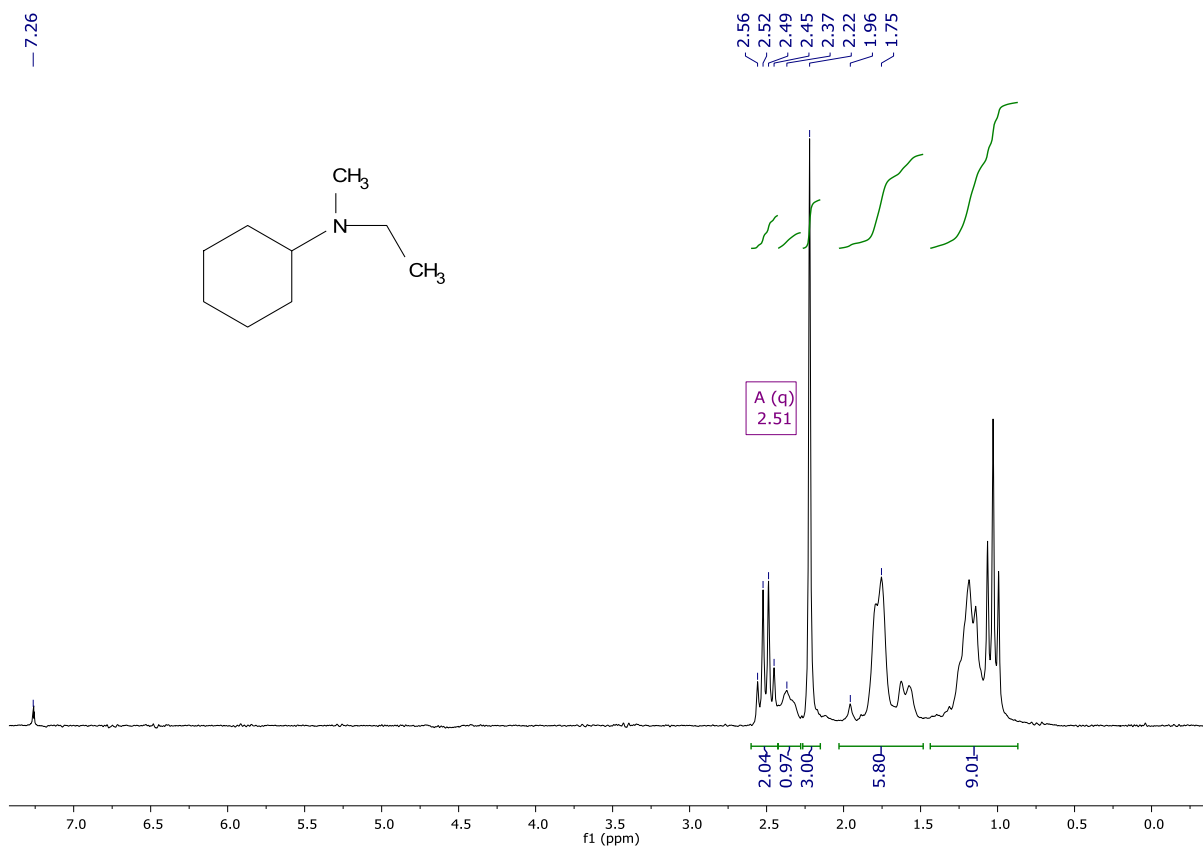


Figure 109 ^1H NMR spectrum of *N*-ethyl-*N*-methylcyclohexylamine in CDCl_3 at 20°C .

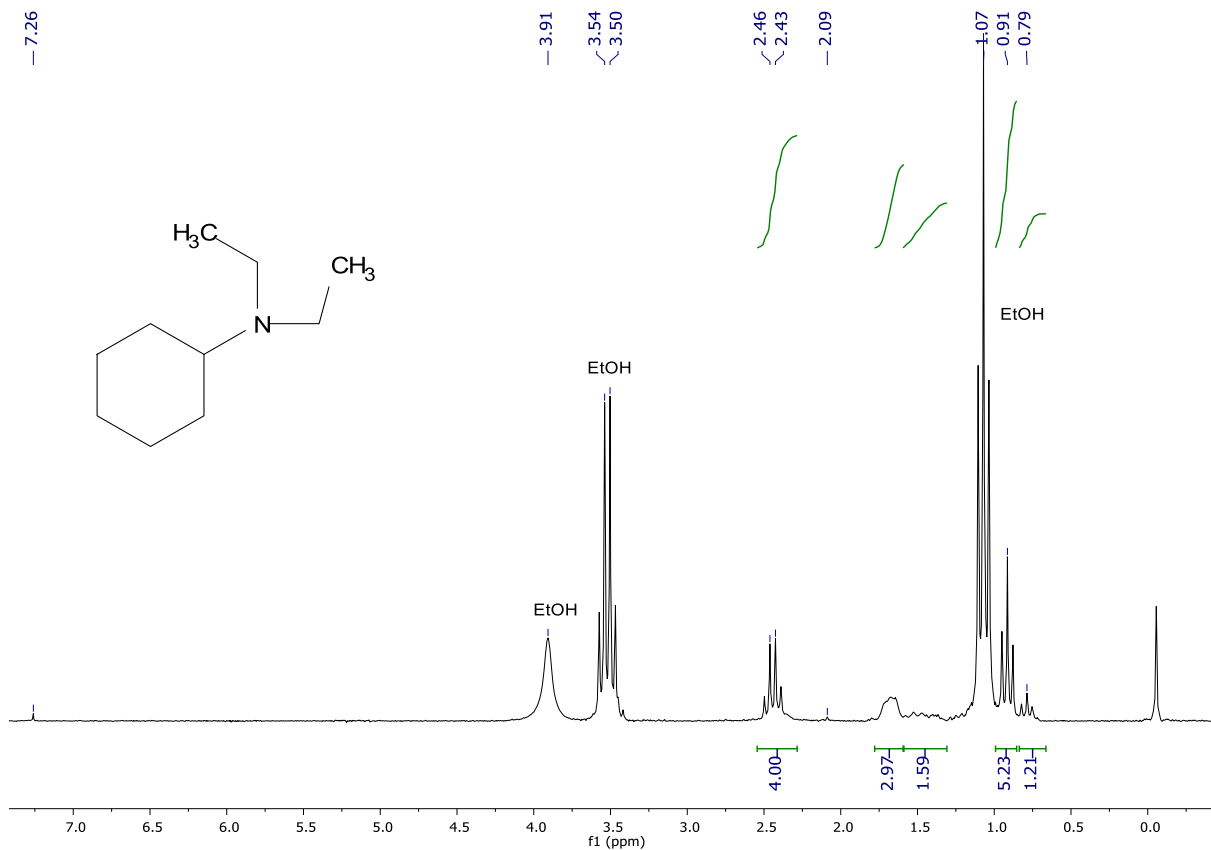


Figure 110 ^1H NMR spectrum of *N,N*-diethylcyclohexylamine in CDCl_3 at 20°C .

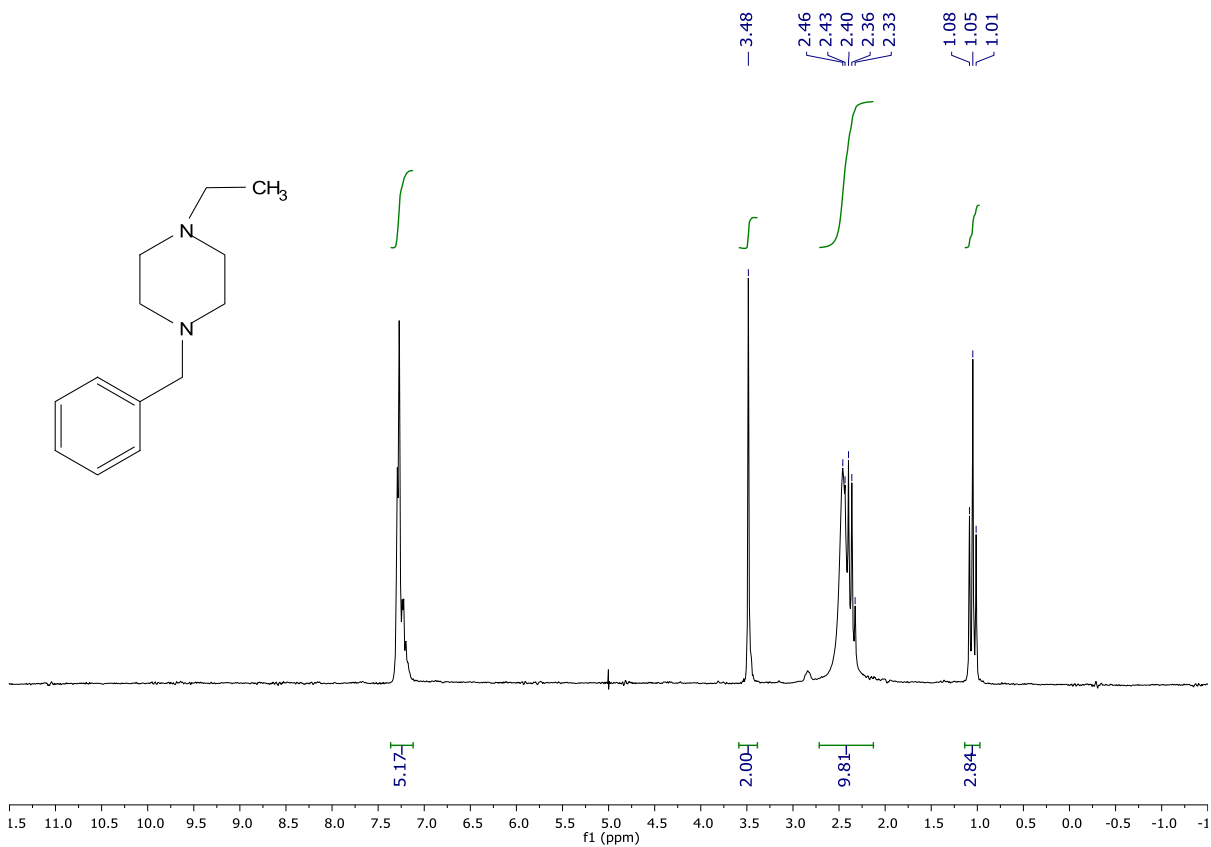


Figure 111 ^1H NMR spectrum of 1-benzyl-4-ethylpiperazine in CDCl_3 at 20°C .

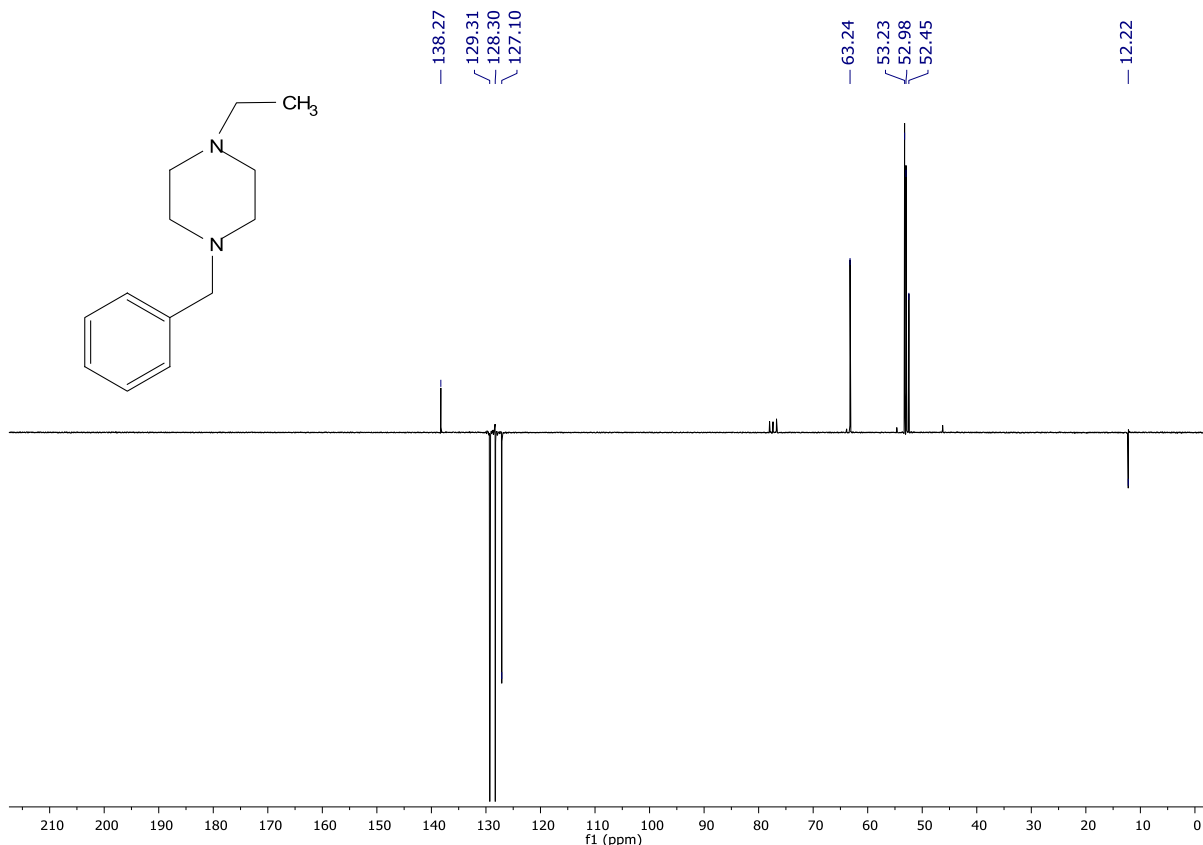


Figure 112 $^{13}\text{C}\{^1\text{H}\}$ NMR spectrum of 1-benzyl-4-ethylpiperazine in CDCl_3 at 20°C .

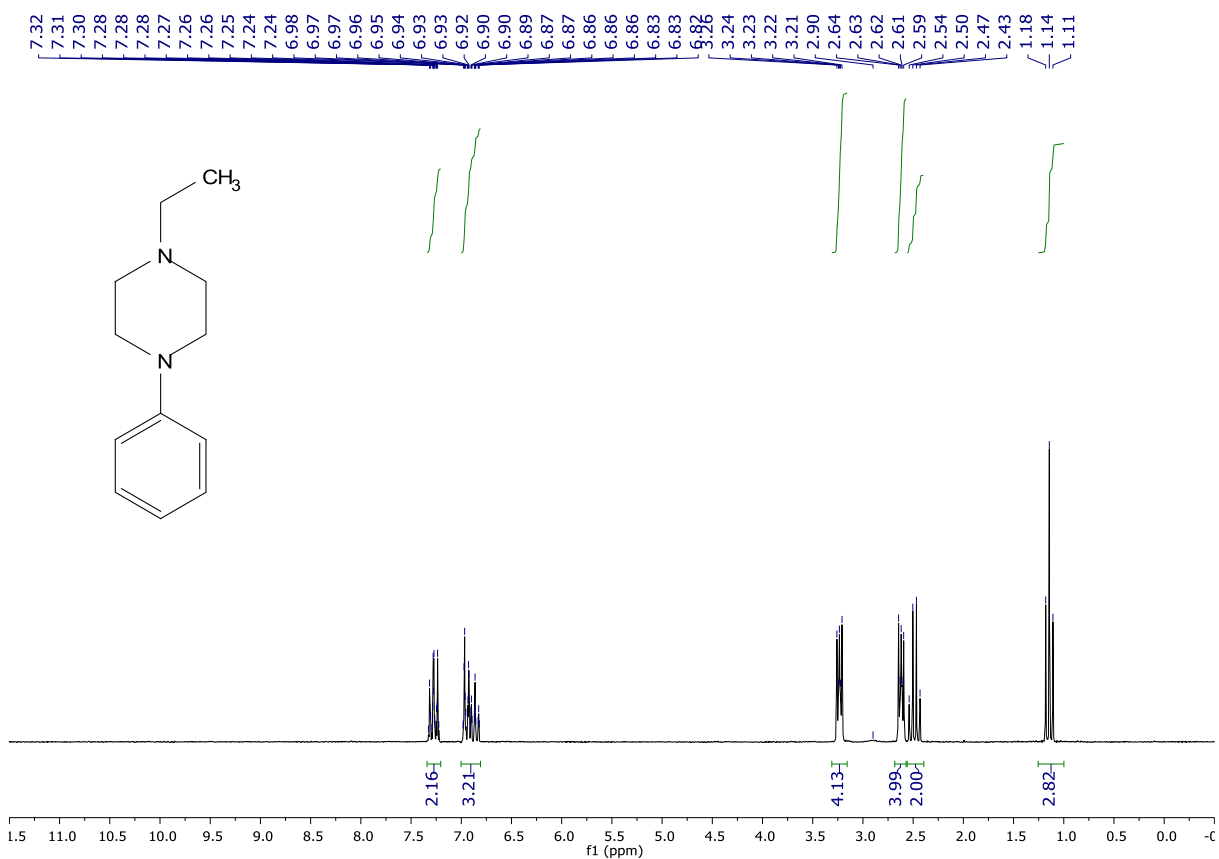


Figure 113 ^1H NMR spectrum of 1-phenyl-4-ethylpiperazine in CDCl_3 at 20°C .

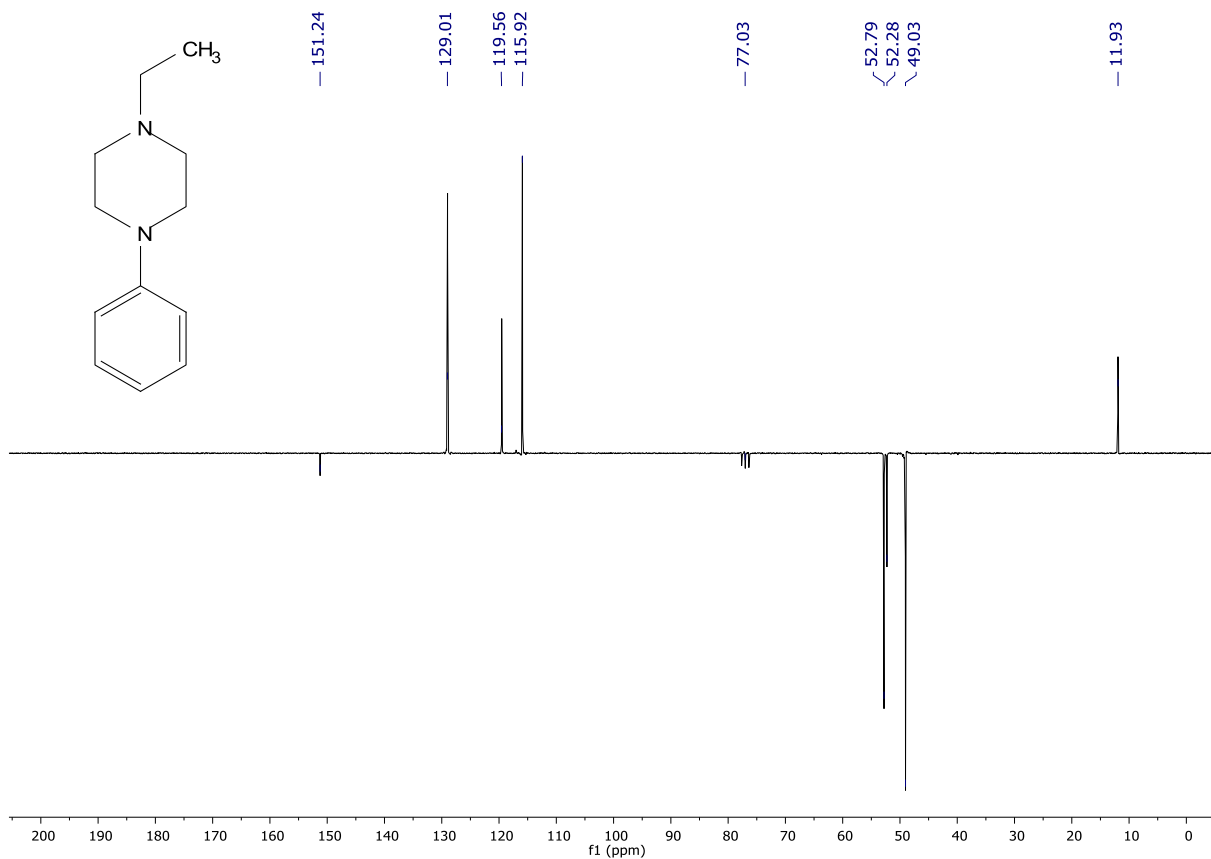


Figure 114 $^{13}\text{C}\{^1\text{H}\}$ NMR spectrum of 1-phenyl-4-ethylpiperazine in CDCl_3 at 20°C .

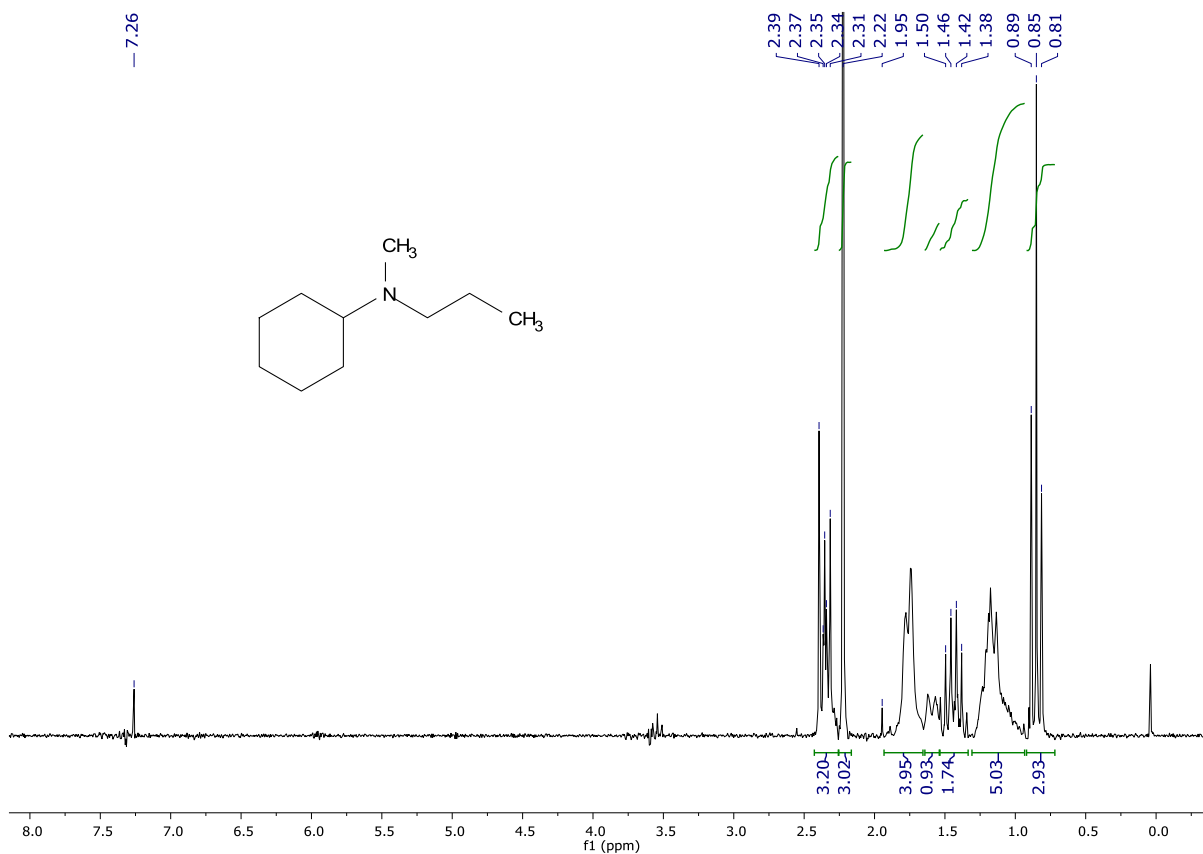


Figure 115 ^1H NMR spectrum of N-methyl-N-propylcyclohexylamine in CDCl_3 at 20°C .

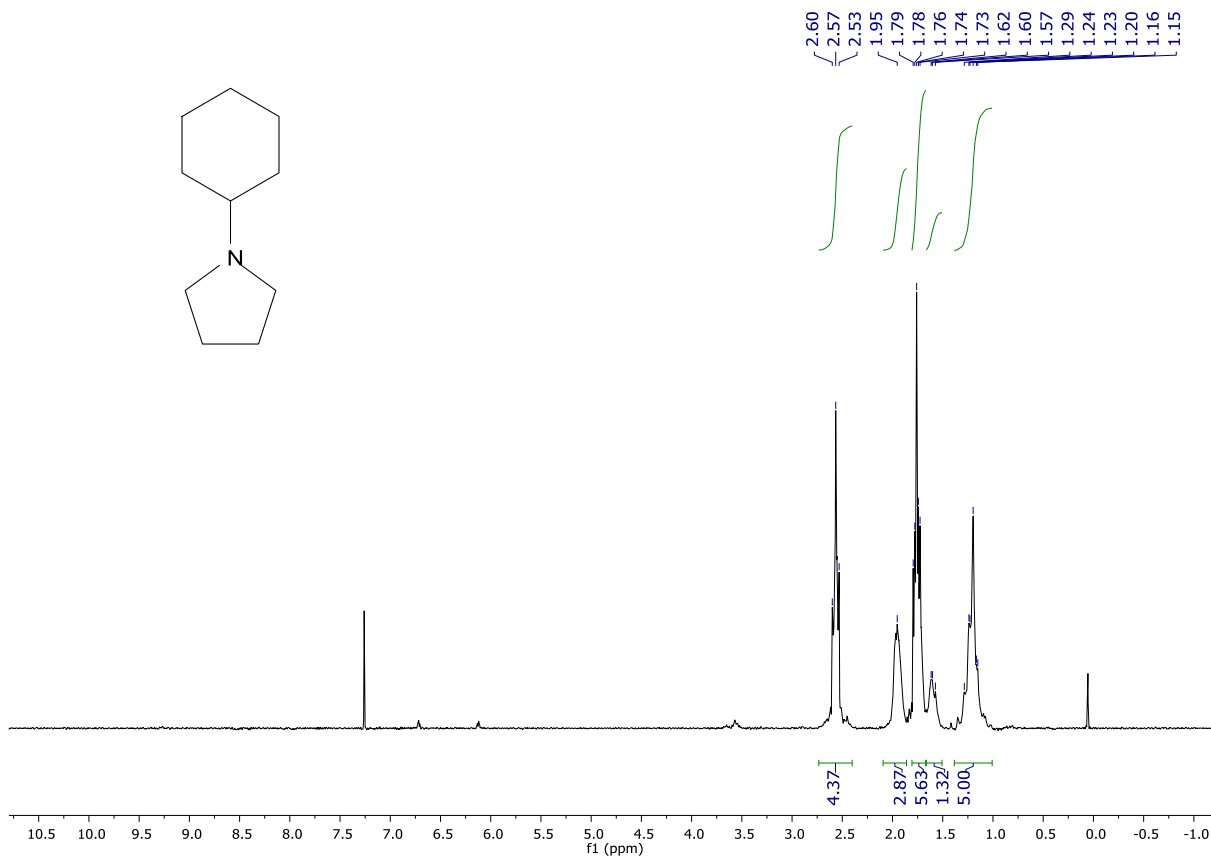


Figure 116 ^1H NMR spectrum of *N*-cyclohexylpyrrolidine in CDCl_3 at 20°C (entry 1, Table 20).

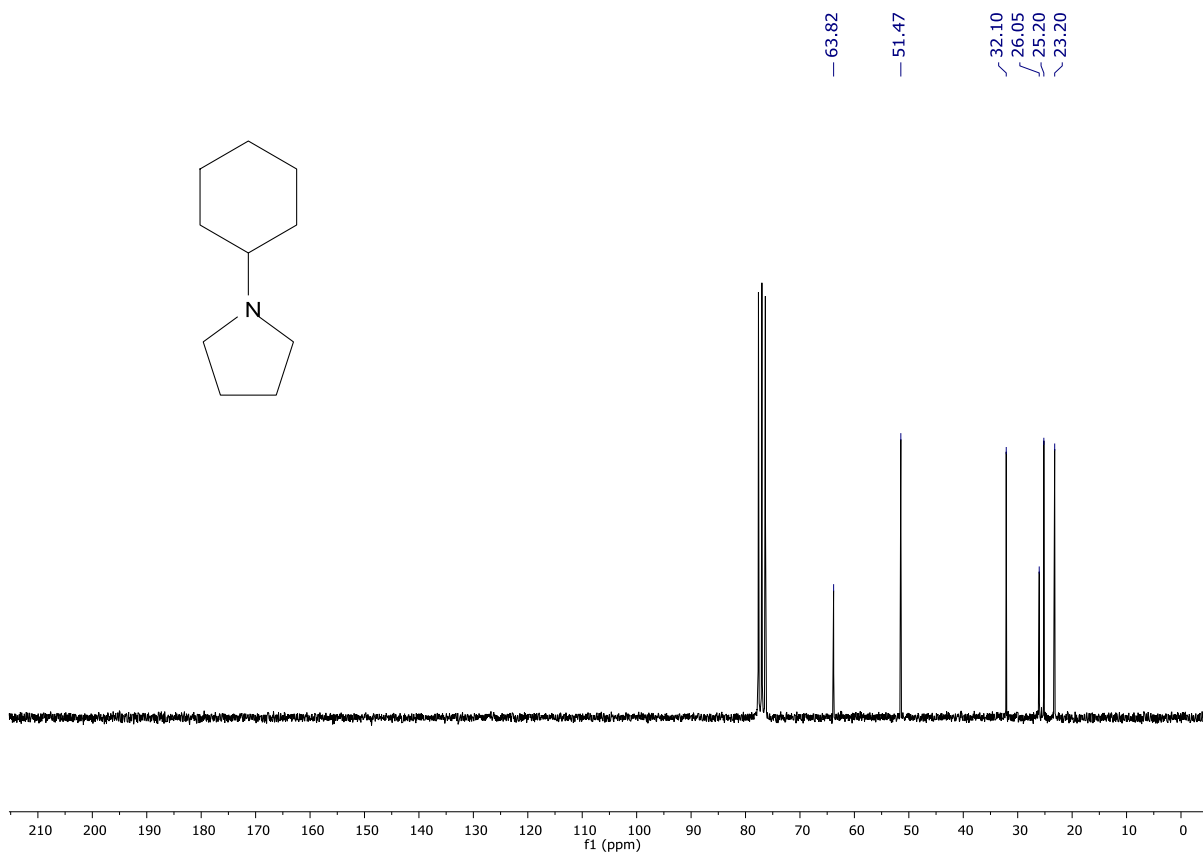


Figure 117 $^{13}\text{C}\{^1\text{H}\}$ NMR spectrum of *N*-cyclohexylpyrrolidine in CDCl_3 at 20°C (entry 1, Table 20)..

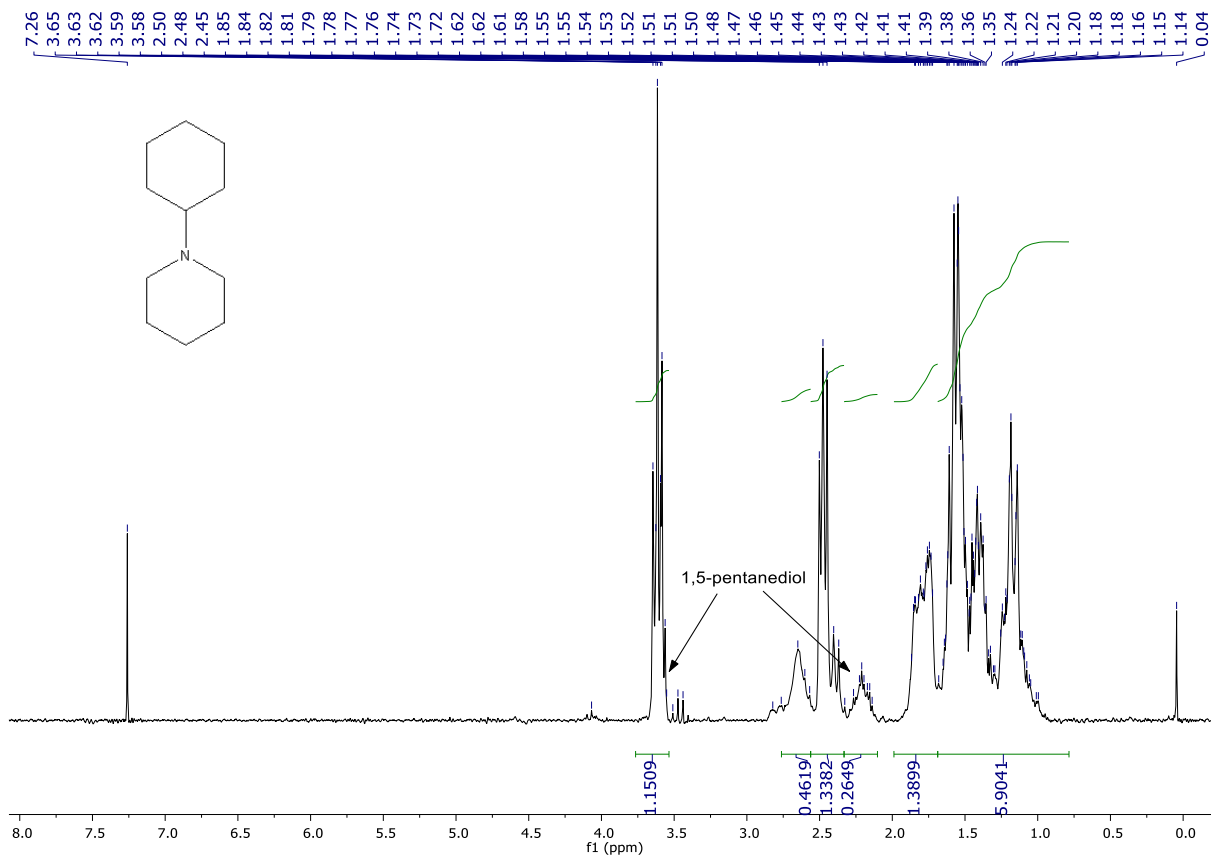


Figure 118 ^1H NMR spectrum of *N*-cyclohexylpiperidine in CDCl_3 at $20\text{ }^\circ\text{C}$ (entry 2, Table 20).

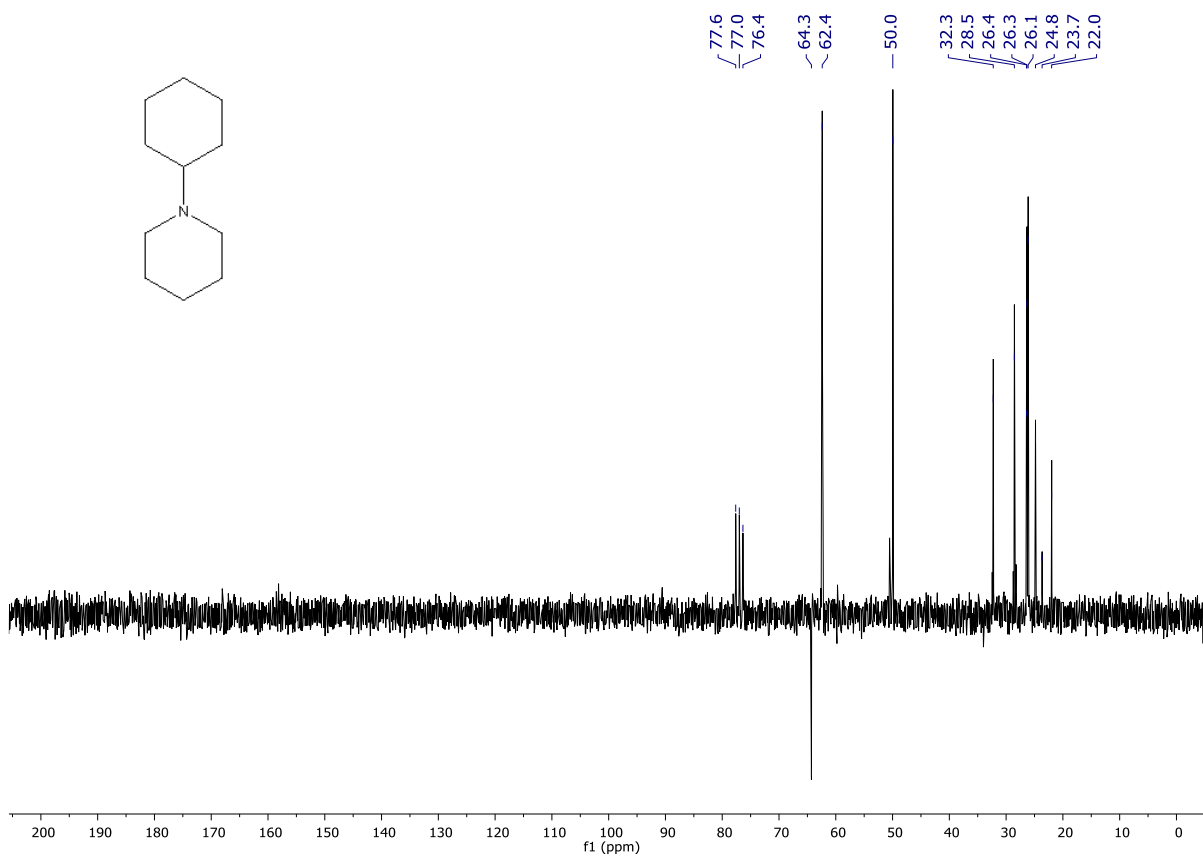


Figure 119 $^{13}\text{C}\{^1\text{H}\}$ NMR spectrum of *N*-cyclohexylpiperidine in CDCl_3 at $20\text{ }^\circ\text{C}$ (entry 2, Table 20).

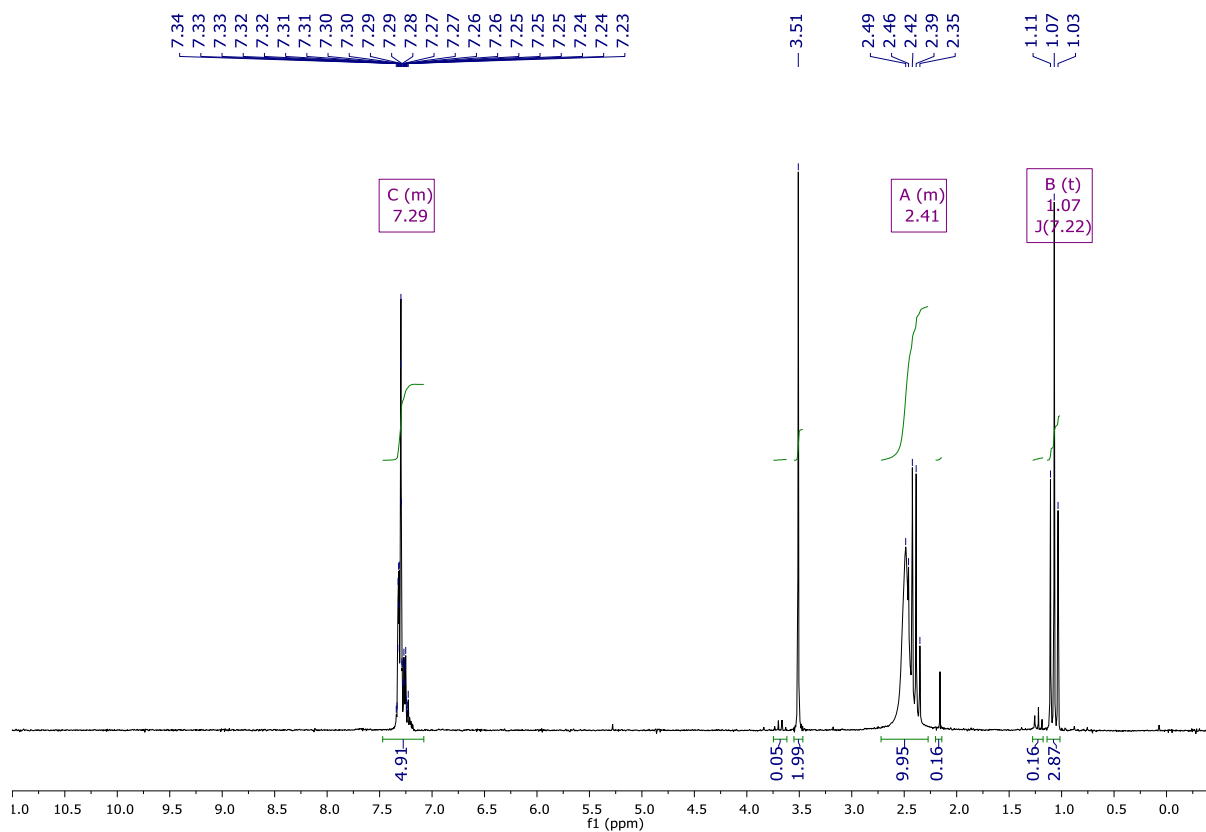


Figure 120 ^1H NMR spectrum of 1-benzyl-4-ethylpiperazine from the gram-scale synthesis.

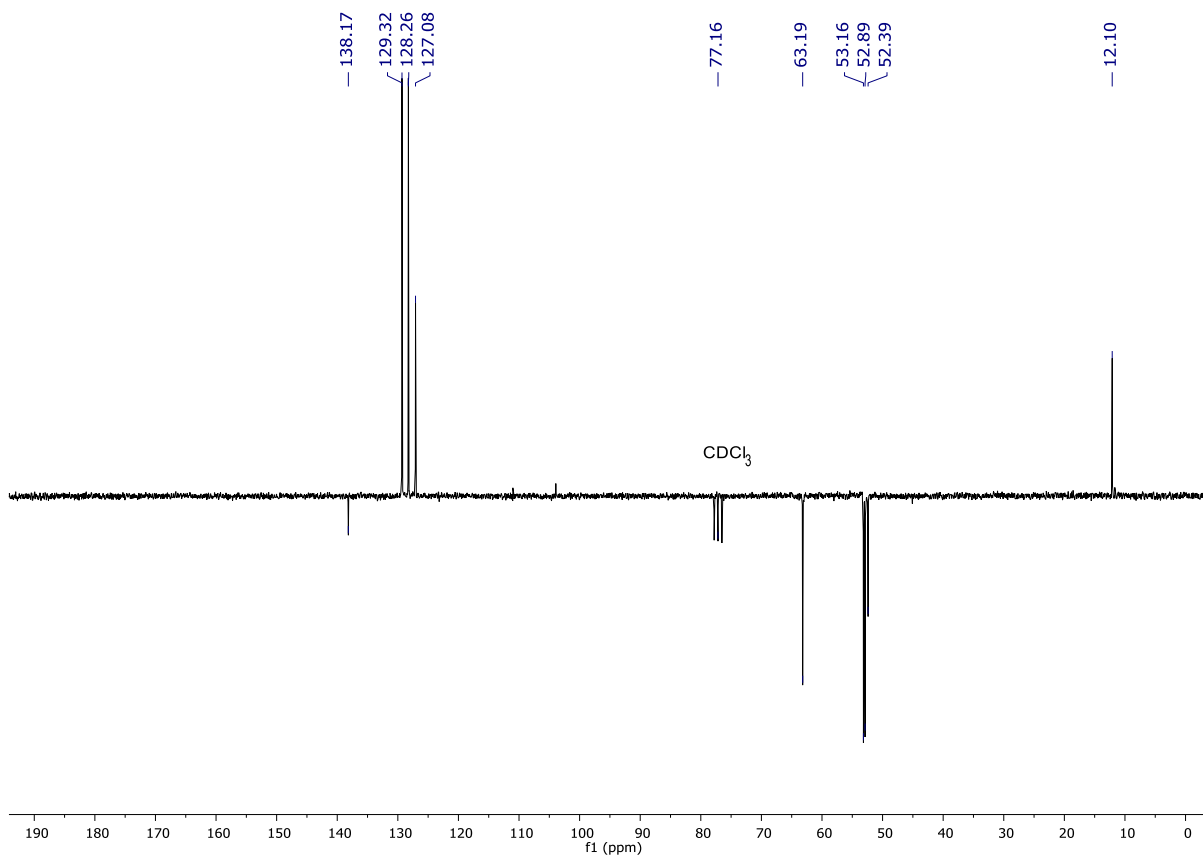


Figure 121 $^{13}\text{C}\{^1\text{H}\}$ NMR spectrum of 1-benzyl-4-ethylpiperazine from the gram-scale synthesis.

4.0 Conclusions and Future Perspectives

During this PhD work several acetate ruthenium complexes bearing bulky and basic bidentate phosphines have been for the first time synthesized and characterized using NMR, IR and, when possible, XRD techniques. The straightforward exchange reaction of triphenylphosphine with metallocene based bulky alkyl-diphosphines DiPPF and DCyPF on the acetate complexes $\text{Ru}(\text{OAc})_2(\text{PPh}_3)_3$ and $\text{Ru}(\text{OAc})_2(\text{CO})(\text{PPh}_3)_3$ afforded novel versatile precursors $\text{Ru}(\text{OAc})_2(\text{PP})$ and $\text{Ru}(\text{OAc})_2(\text{CO})(\text{PP})$. Preliminary studies show that compound $\text{Ru}(\text{OAc})_2(\text{CO})(\text{DiPPF})$ **9** in the presence of TFA easily undergoes protonation of the acetate ligands, affording the corresponding more reactive trifluoroacetate species, whereas interaction of phenylacetylene with **9** in a basic environment, leads to the mono acetylide derivative. Since these systems showed a good versatility reacting with different organic compounds, they were tested in diverse organic transformations.

Firstly, the TH of acetophenone catalysed by the novel acetate complexes $\text{Ru}(\text{OAc})_2(\text{PP})$ (PP= DiPPF, DCyPPF) and $\text{Ru}(\text{OAc})_2(\text{PP})(\text{NN})$ (NN= ampy, en), has been investigated. They showed good activity with TOFs up to 30000 h^{-1} but low TONs up to 2000, but no important differences were observed between the two systems $\text{Ru}(\text{OAc})_2(\text{PP})$ and $\text{Ru}(\text{OAc})_2(\text{PP})(\text{ampy})$. As a matter of fact, the joint steric hindrance and the strong trans-effect of the basic diphosphines weakens the coordination of the ampy ligand, hinting that the $\text{Ru}(\text{OAc})_2(\text{PP})(\text{ampy})$ systems eventually end up in the same catalytic active species of the $\text{Ru}(\text{OAc})_2(\text{PP})$ congeners. This fact likely determines the reduced acceleration effect granted by the bifunctional NH_2 moiety around the metal coordination sphere. On the other hand, the complex $\text{Ru}(\text{OAc})_2(\text{DiPPF})(\text{en})$ with a more coordinating diamine, that appears to release very slowly the nitrogen ligand, shows no significant improvement within the catalytic outcomes. The carbonyl complexes $\text{Ru}(\text{OAc})_2(\text{CO})_n(\text{PP})$ ($n= 1, 2$; PP= DiPPF, Cy-Josiphos) demonstrated good performances with $n=1$, whereas with $n=2$ moderate activities were observed, hinting that the loose of CO is a key step to obtain catalytically active species. The addition of nitrogen ligands to monocarbonyl complexes dramatically increased the reaction rate, suggesting that carbonyl complexes produce more robust and stable species than their $\text{Ru}(\text{OAc})_2(\text{PP})$ congeners.

The carbonyl precursor $\text{Ru}(\text{OAc})_2(\text{CO})(\text{PPh}_3)_2$ in combination with the tridentate ligand Hampt proved to be successful in the reduction of citral to its corresponding alcohol mixture and of bulky (L)-menthone to (-)-menthol with good stereoselectivity and productivity (S/C 1000). Further studies are in progress to better understand the catalytic activity of these complexes and for broadening the scope of the TH reaction to the reduction of other unsaturated moieties, i.e. C=C, C=N.

The $\text{Ru}(\text{OAc})_2(\text{CO})\text{PP}$ type catalyst are proved to be active in the reduction in neat condition, in particular the $\text{Ru}(\text{OAc})_2(\text{CO})(\text{DiPPF})$ complex and the corresponding monochloride $\text{RuCl}(\text{OAc})(\text{CO})(\text{DiPPF})$ are particular active in presence of TFA toward the reduction of all the substrate tested, giving the better performances in terms of activity, loadings and chemoselectivity with respect to the complexes bearing others aliphatic or aryl diphosphines with both basic or acidic additive. Most of the time was dedicated in testing the diacetate thanks to its large availability, while for the chloride-acetate a better synthetic pathway should be developed in order to exploit its reactivity that seems to be comparable or higher in some cases. In view of the set up of a green procedure, also on industrial scale, more tests should be run to take more advantage from the solvent free condition promoted by the TFA, thus avoiding the possible undesired side reactions with the solvent.

The easily achievable carboxylate $\text{Ru}(\text{OAc})_2(\text{CO})(\text{DiPPF})$ **9**, containing the bulky DiPPF diphosphine displayed high activity in the N-alkylation of amines with commercial-grade primary alcohols *via* a borrowing hydrogen reaction. This ruthenium system allowed unprecedented mild N-alkylation of primary and secondary amine at temperature as low as 30°C and without the use of any additional base, resulting one of the most active catalysts reported to date. The carboxylate ligand in combination with basic diphosphines and the carbonyl ligand showed a preference for very concentrated solution of substrate, allowing to perform the reaction in up to “semi-neat” conditions, in which commercial grade alcohols acted as substrates and solvents. The addition of TFA, up to 10 equivalents with respect to the catalyst, has a strong accelerating effect resulted in a rate 4 times higher. Further studies are required to fully rationalize the catalytic cycle in presence of TFA that is involved in the protonation of the amine substrate and in the formation of the labile and active trifluoro carboxylate complexes.

Since catalysis is considered as a crucial enabling green technology for the transformation of organic compounds, the development of novel efficient catalysts for environmentally benign reactions characterized by high atom economy and use of non toxic reagents is of particular importance in this context and follows the vision of the European programs for a sustainable development in which chemistry plays a pivotal role. Given the robustness and the wide reactivity of this new class of Ru catalysts, this PhD work holds promise for a broad application in organic transformations of great interest, including the synthesis of bio-relevant compounds.

5.0 References

- [1] J. J. Berzelius, *Royal Swedish Academy of Sciences* **1835**.
- [2] S. K. Kirchhoff, *Bull. Neusten. Wiss. Naturwiss* **1811**, *10*, 88-92.
- [3] L. J. Thenard, *elementaire theorique et pratique*, Vol. 3, rue de l'Ecole de Medecine, Paris, **1815**.
- [4] J. A. Osborn, F. H. Jardine, J. F. Young, G. Wilkinson, *Journal of the Chemical Society A: Inorganic, Physical, Theoretical* **1966**, 1711-1732.
- [5] a) P. B. Arockiam, C. Bruneau, P. H. Dixneuf, *Chem. Rev.* **2012**, *112*, 5879-5918; b) *Asymmetric Catalysis on Industrial Scale*, 2nd Edition ed., Wiley-VCH Verlag GmbH & Co. KGaA, **2010**; c) S. P. Nolan, H. Clavier, *Chem. Soc. Rev.* **2010**, *39*, 3305-3316; d) M. Beller, K. Kumar, in *Transition Metals for Organic Synthesis*, Vol. 1, 2nd ed. (Eds.: M. Beller, C. Bolm), WILEY-VCH Verlag GmbH & Co. KGaA Weinheim, **2004**, pp. 28-55.
- [6] a) F. a. D. Administration, Q3D Elemental Impurities ed., **2015**; b) E. O. L. 338, (Ed.: E. P. a. t. Council), **13.11.2004**, pp. 4-17.
- [7] R. H. Crabtree, *Chem. Rev.* **2015**, *115*, 127-150.
- [8] D. Wang, D. Astruc, *Chem. Rev.* **2015**, *115*, 6621-6686.
- [9] R. F. Heck, in *Organotransition Metal Chemistry: a Mechanistic Approach*, Vol. 1, 1 ed. (Eds.: P. M. MAITLIS, F. G. A. STONE, R. WEST), Academic Press, New York, **1974**, pp. 55 - 75.
- [10] T. A. Stephenson, G. Wilkinson, *J. Inorg. Nucl. Chem.* **1966**, *28*, 945-956.
- [11] J. Hartwig, *Organotransition Metal Chemistry: From Bonding to Catalysis. J*, Wiley-Blackwell, **2010**.
- [12] R. Noyori, T. Ohkuma, *Angew. Chem. Int. Ed.* **2001**, *40*, 40-73.
- [13] H. Doucet, T. Ohkuma, K. Murata, T. Yokozawa, M. Kozawa, E. Katayama, A. F. England, T. Ikariya, R. Noyori, *Angew. Chem. Int. Ed.* **1998**, *37*, 1703-1707.
- [14] K.-J. Haack, S. Hashiguchi, A. Fujii, T. Ikariya, R. Noyori, *Angew. Chem. Int. Ed. Engl.* **2003**, *36*, 285-288.
- [15] a) G. Chelucci, S. Baldino, W. Baratta, *Coord. Chem. Rev.* **2015**, *300*, 29-85; b) G. Chelucci, S. Baldino, W. Baratta, *Acc. Chem. Res.* **2015**, *48*, 363-379.
- [16] a) W. Baratta, E. Herdtweck, K. Siega, M. Toniutti, P. Rigo, *Organometallics* **2005**, *24*, 1660-1669; b) W. Baratta, K. Siega, M. Toniutti, P. Rigo patent WO2005105819A1, **2005**.
- [17] a) W. Baratta, M. Bosco, G. Chelucci, A. Del Zotto, K. Siega, M. Toniutti, E. Zangrando, P. Rigo, *Organometallics* **2006**, *25*, 4611-4620; b) W. Baratta, K. Siega, P. Rigo, *Adv. Synth. Catal.* **2007**, *349*, 1633-1636; c) W. Baratta, M. Ballico, A. Del Zotto, E. Herdtweck, S. Magnolia, R. Peloso, K. Siega, M. Toniutti, E. Zangrando, P. Rigo, *Organometallics* **2009**, *28*, 4421-4430.
- [18] W. Baratta, M. Ballico, S. Baldino, G. Chelucci, E. Herdtweck, K. Siega, S. Magnolia, P. Rigo, *Chem. Eur. J.* **2008**, *14*, 9148-9160.
- [19] a) W. Baratta, M. Ballico, A. Del Zotto, K. Siega, S. Magnolia, P. Rigo, *Chem. Eur. J.* **2008**, *14*, 2557-2563; b) W. Baratta, C. Barbato, S. Magnolia, K. Siega, P. Rigo, *Chem. Eur. J.* **2010**, *16*, 3201-3206.
- [20] M. Solinas, B. Sechi, S. Baldino, W. Baratta, G. Chelucci, *ChemistrySelect* **2016**, *1*, 2492-2497.
- [21] a) S. Baldino, W. Baratta, A. BLACKABY, R. C. BRYAN, S. FACCHETTI, V. Jurcik, H. G. Nedden (WO2016193761A1), **2016**; b) S. Baldino, S. Facchetti, H. G. Nedden,

- A. Zanotti-Gerosa, W. Baratta, *ChemCatChem* **2016**, *8*, 3195-3198; c) S. Baldino, S. Facchetti, A. Zanotti-Gerosa, H. G. Nedden, W. Baratta, *ChemCatChem* **2016**, *8*, 2279-2288; d) S. Facchetti, V. Jurcik, S. Baldino, S. Giboulot, H. G. Nedden, A. Zanotti-Gerosa, A. Blackaby, R. Bryan, A. Boogaard, D. B. McLaren, E. Moya, S. Reynolds, K. S. Sandham, P. Martinuzzi, W. Baratta, *Organometallics* **2016**, *35*, 277-287.
- [22] a) W. Baratta, G. Bossi, E. Putignano, P. Rigo, *Chem. Eur. J.* **2011**, *17*, 3474-3481; b) G. Bossi, E. Putignano, P. Rigo, W. Baratta, *Dalton Trans.* **2011**, *40*, 8986-8995; c) E. Putignano, G. Bossi, P. Rigo, W. Baratta, *Organometallics* **2012**, *31*, 1133-1142.
- [23] R. C. Mehrotra, *Nature* **1953**, *172*, 74.
- [24] D. C. Bradley, R. C. Mehrotra, I. P. Rothwell, A. Singh, in *Alkoxo and Aryloxo Derivatives of Metals* (Eds.: D. C. Bradley, R. C. Mehrotra, I. P. Rothwell, A. Singh), Academic Press, London, **2001**, pp. 3-181.
- [25] a) A. Spencer, G. Wilkinson, *J. Chem. Soc., Dalton Trans.* **1974**, 786-792; b) A. Dobson, S. D. Robinson, M. F. Uttley, *J. Chem. Soc., Dalton Trans.* **1975**, 370-377.
- [26] a) R. Noyori, M. Ohta, Y. Hsiao, M. Kitamura, T. Ohta, H. Takaya, *J. Am. Chem. Soc.* **1986**, *108*, 7117-7119; b) M. Kitamura, Y. Hsiao, M. Ohta, M. Tsukamoto, T. Ohta, H. Takaya, R. Noyori, *J. Org. Chem.* **1994**, *59*, 297-310.
- [27] a) R. Noyori, T. Ohkuma, M. Kitamura, H. Takaya, N. Sayo, H. Kumobayashi, S. Akutagawa, *J. Am. Chem. Soc.* **1987**, *109*, 5856-5858; b) M. Kitamura, M. Tokunaga, R. Noyori, *J. Org. Chem.* **1992**, *57*, 4053-4054.
- [28] a) F. Micoli, L. Salvi, A. Salvini, P. Frediani, C. Giannelli, *J. Organomet. Chem.* **2005**, *690*, 4867-4877; b) W.-K. Wong, K.-K. Lai, M.-S. Tse, M.-C. Tse, J.-X. Gao, W.-T. Wong, S. Chan, *Polyhedron* **1994**, *13*, 2751-2762; c) A. C. Skapski, F. A. Stephens, *J. Chem. Soc., Dalton Trans.* **1974**, 390-395; d) J. van Buijtenen, J. Meuldijk, J. A. J. M. Vekemans, L. A. Hulshof, H. Kooijman, A. L. Spek, *Organometallics* **2006**, *25*, 873-881; e) V. Cadierno, P. Crochet, J. Díez, S. E. García-Garrido, J. Gimeno, S. García-Granda, *Organometallics* **2003**, *22*, 5226-5234.
- [29] R. W. Mitchell, A. Spencer, G. Wilkinson, *J. Chem. Soc., Dalton Trans.* **1973**, 846-854.
- [30] J. M. Lynam, C. E. Welby, A. C. Whitwood, *Organometallics* **2009**, *28*, 1320-1328.
- [31] M. Ogasawara, S. A. Macgregor, W. E. Streib, K. Folting, O. Eisenstein, K. G. Caulton, *J. Am. Chem. Soc.* **1996**, *118*, 10189-10199.
- [32] F. Požgan, P. H. Dixneuf, *Adv. Synth. Catal.* **2009**, *351*, 1737-1743.
- [33] A. Salvini, P. Frediani, C. Giannelli, L. Rosi, *J. Organomet. Chem.* **2005**, *690*, 371-382.
- [34] C. E. Welby, T. O. Eschemann, C. A. Unsworth, E. J. Smith, R. J. Thatcher, A. C. Whitwood, J. M. Lynam, *Eur. J. Inorg. Chem.* **2011**, *2012*, 1493-1506.
- [35] X. L. Lu, S. Y. Ng, J. J. Vittal, G. K. Tan, L. Y. Goh, T. S. A. Hor, *J. Organomet. Chem.* **2003**, *688*, 100-111.
- [36] C. W. Jung, P. E. Garrou, P. R. Hoffman, K. G. Caulton, *Inorg. Chem.* **1984**, *23*, 726-729.
- [37] a) D. E. Fogg, B. R. James, *Inorg. Chem.* **1997**, *36*, 1961-1966; b) S. D. Drouin, D. Amoroso, G. P. A. Yap, D. E. Fogg, *Organometallics* **2002**, *21*, 1042-1049.
- [38] A. Dobson, S. D. Robinson, *Inorg. Chem.* **1977**, *16*, 137-142.
- [39] C. Chauvier, P. Thuéry, T. Cantat, *Angew. Chem.* **2016**, *128*, 14302-14306.
- [40] N. P. Hiett, J. M. Lynam, C. E. Welby, A. C. Whitwood, *J. Organomet. Chem.* **2011**, *696*, 378-387.

- [41] *The Handbook of Homogeneous Hydrogenation, Vol. 1-3, Vol. 1-3*, WILEY-VCH Verlag GmbH & Co. KGaA Weinheim, **2007**.
- [42] A. Bruneau-Voisine, D. Wang, V. Dorcet, T. Roisnel, C. Darcel, J.-B. Sortais, *Org. Lett.* **2017**, *19*, 3656-3659.
- [43] H. Adkins, R. M. Eloffson, A. G. Rossow, C. C. Robinson, *J. Am. Chem. Soc.* **1949**, *71*, 3622-3629.
- [44] S. E. Clapham, A. Hadzovic, R. H. Morris, *Coord. Chem. Rev.* **2004**, *248*, 2201-2237.
- [45] J. R. Fulton, A. W. Holland, D. J. Fox, R. G. Bergman, *Acc. Chem. Res.* **2002**, *35*, 44-56.
- [46] G. J. Kubas, *Chem. Rev.* **2007**, *107*, 4152-4205.
- [47] H. Itagaki, N. Koga, K. Morokuma, Y. Saito, *Organometallics* **1993**, *12*, 1648-1654.
- [48] O. Blum, D. Milstein, *J. Organomet. Chem.* **2000**, *593-594*, 479-484.
- [49] S. Hashiguchi, A. Fujii, J. Takehara, T. Ikariya, R. Noyori, *J. Am. Chem. Soc.* **1995**, *117*, 7562-7563.
- [50] N. Uematsu, A. Fujii, S. Hashiguchi, T. Ikariya, R. Noyori, *J. Am. Chem. Soc.* **1996**, *118*, 4916-4917.
- [51] a) P. N. Taylor, H. L. Anderson, *J. Am. Chem. Soc.* **1999**, *121*, 11538-11545; b) K. Abdur-Rashid, S. E. Clapham, A. Hadzovic, J. N. Harvey, A. J. Lough, R. H. Morris, *J. Am. Chem. Soc.* **2002**, *124*, 15104-15118; c) C. A. Sandoval, T. Ohkuma, K. Muñiz, R. Noyori, *J. Am. Chem. Soc.* **2003**, *125*, 13490-13503.
- [52] S. Takebayashi, N. Dabral, M. Miskolzie, S. H. Bergens, *J. Am. Chem. Soc.* **2011**, *133*, 9666-9669.
- [53] a) W. Baratta, G. Chelucci, E. Herdtweck, S. Magnolia, K. Siega, P. Rigo, *Angew. Chem. Int. Ed.* **2007**, *46*, 7651-7654; b) S. Zhang, S. Baldino, W. Baratta, *Organometallics* **2013**, *32*, 5299-5304.
- [54] a) A. Nova, D. Balcells, N. D. Schley, G. E. Dobereiner, R. H. Crabtree, O. Eisenstein, *Organometallics* **2010**, *29*, 6548-6558; b) N. D. Schley, G. E. Dobereiner, R. H. Crabtree, *Organometallics* **2011**, *30*, 4174-4179.
- [55] a) W. Baratta, G. Chelucci, S. Gladiali, K. Siega, M. Toniutti, M. Zanette, E. Zangrando, P. Rigo, *Angew. Chem. Int. Ed.* **2005**, *44*, 6214-6219; b) W. Baratta, G. Chelucci, S. Magnolia, K. Siega, P. Rigo, *Chem. Eur. J.* **2009**, *15*, 726-732.
- [56] a) W. Baratta, M. Ballico, G. Chelucci, K. Siega, P. Rigo, *Angew. Chem. Int. Ed.* **2008**, *47*, 4362-4365; b) W. Baratta, F. Benedetti, A. Del Zotto, L. Fanfoni, F. Felluga, S. Magnolia, E. Putignano, P. Rigo, *Organometallics* **2010**, *29*, 3563-3570.
- [57] W. Baratta, G. Chelucci, S. Gladiali, K. Siega, M. Toniutti, M. Zanette, E. Zangrando, P. Rigo, *Angew. Chem. Int. Ed.* **2005**, *44*, 6214-6219.
- [58] a) P. N. Rylander, *Academic Pr.* **1990**; b) H. Rase, *Handbook of Commercial Catalysts.* **2000**; c) C. H. Bartholomew, R. J. Farrauto, **2010**; d) P. Pollak, in *Fine Chemicals, Vol. Fine Chemicals: The Industry and the Business, Second Edition*, Wiley, **2011**.
- [59] R. A. Sheldon, H. v. Bekkum, *Org. Process Res. Dev.* **2002**, *6*, 578-578.
- [60] R. A. Sanchez-Delgado, J. S. Bradley, G. Wilkinson, *J. Chem. Soc., Dalton Trans.* **1976**, 399-404.
- [61] J. Tsuji, H. Suzuki, *Chem. Lett.* **1977**, *6*, 1085-1086.
- [62] R. G. Sanchez-Delgado, A. Andriollo, O. L. De Ochoa, T. Suarez, N. Valencia, *J. Organomet. Chem.* **1981**, *209*, 77-83.
- [63] K. Hotta, *J. Mol. Catal.* **1985**, *29*, 105-107.

- [64] a) T. Ohkuma, H. Ooka, T. Ikariya, R. Noyori, *J. Am. Chem. Soc.* **1995**, *117*, 10417-10418; b) R. Noyori, T. Ohkuma, in *Pure Appl. Chem.*, Vol. 71, **1999**, p. 1493; c) R. Noyori, *Angew. Chem. Int. Ed.* **2002**, *41*, 2008-2022.
- [65] a) *Common Fragrance and Flavor Materials* **2006**; b) L. A. Saudan, *Acc. Chem. Res.* **2007**, *40*, 1309-1319.
- [66] a) A. B. Smith, J. Barbosa, W. Wong, J. L. Wood, *J. Am. Chem. Soc.* **1996**, *118*, 8316-8328; b) Y. Kobayakawa, M. Nakada, *The Journal Of Antibiotics* **2014**, *67*, 483.
- [67] L. Bonomo, L. Kermorvan, P. Dupau, *ChemCatChem* **2015**, *7*, 907-910.
- [68] P. L. Gaus, S. C. Kao, K. Youngdahl, M. Y. Darensbourg, *J. Am. Chem. Soc.* **1985**, *107*, 2428-2434.
- [69] S. M. Geraty, P. Harkin, J. G. Vos, *Inorg. Chim. Acta* **1987**, *131*, 217-220.
- [70] in *The Handbook of Homogeneous Hydrogenation*.
- [71] J. M. DeSimone, *Science* **2002**, *297*, 799.
- [72] P. T. Anastas, M. M. Kirchhoff, *Acc. Chem. Res.* **2002**, *35*, 686-694.
- [73] R. M. Bullock, J.-S. Song, *J. Am. Chem. Soc.* **1994**, *116*, 8602-8612.
- [74] P. Espinet, A. C. Albéniz, in *Current Methods in Inorganic Chemistry*, Vol. 3 (Eds.: H. Kurosawa, A. Yamamoto), Elsevier, Amsterdam, **2003**, pp. 293-371.
- [75] M. B. Smith, *March's Advances Organic Chemistry: Reactions, Mechanisms and Structure*, 7th ed., John Wiley & Sons, Inc, Hoboken, New Jersey, **2013**.
- [76] T. Werner, J. Koch, *Eur. J. Org. Chem.* **2010**, 6904-6907.
- [77] T. A. Geissman, in *Organic Reactions*, Vol. 2 (Ed.: S. E. Denmark), John Wiley & Sons, Inc., Hoboken, New Jersey, **1944**, pp. 94-113.
- [78] F. Christie, A. Zanotti-Gerosa, D. Grainger, **2018**, *10*, 1012-1018.
- [79] P. Dupau, L. Bonomo, L. Kermorvan, **2013**, *52*, 11347-11350.
- [80] a) M. Naruto, S. Saito, *Nature Communications* **2015**, *6*, 8140; b) M. Naruto, S. Agrawal, K. Toda, S. Saito, *Scientific Reports* **2017**, *7*, 3425.
- [81] S. Baldino, W. Baratta, S. Giboulot, H. G. Nedden, A. Zanotti-Gerosa (JM, U. o. Udine), WO2016193762 A1, **2016**.
- [82] D. J. Ager, A. H. M. de Vries, J. G. de Vries, *Chem. Soc. Rev.* **2012**, *41*, 3340-3380.
- [83] P. Mäki-Arvela, J. Hájek, T. Salmi, D. Y. Murzin, *Appl. Catal., A* **2005**, *292*, 1-49.
- [84] R. G. Eilerman, U. b. Staff, in *Kirk-Othmer Encyclopedia of Chemical Technology*, **2014**.
- [85] a) S. Galvagno, A. Donato, G. Neri, R. Pietropaolo, G. Capannelli, *J. Mol. Catal.* **1993**, *78*, 227-236; b) M. Lashdaf, A. Hase, E. Kauppinen, A. O. I. Krause, *Catal. Lett.* **1998**, *52*, 199-204; c) M. Lashdaf, A. O. I. Krause, M. Lindblad, M. Tiitta, T. Venäläinen, *Appl. Catal., A* **2003**, *241*, 65-75; d) Y. Wang, Z. Rong, Y. Wang, P. Zhang, Y. Wang, J. Qu, *J. Catal.* **2015**, *329*, 95-106; e) Y. Wang, T. Yokoi, S. Namba, T. Tatsumi, *Catalysts* **2016**, *6*.
- [86] a) T. Ohkuma, M. Koizumi, K. Muñiz, G. Hilt, C. Kabuto, R. Noyori, *J. Am. Chem. Soc.* **2002**, *124*, 6508-6509; b) L. Diab, T. Šmejkal, J. Geier, B. Breit, *Angew. Chem. Int. Ed.* **2009**, *48*, 8022-8026; c) D. Spasyuk, C. Vicent, D. G. Gusev, *J. Am. Chem. Soc.* **2015**, *137*, 3743-3746; d) X. Tan, G. Wang, Z. Zhu, C. Ren, J. Zhou, H. Lv, X. Zhang, L. W. Chung, L. Zhang, X. Zhang, *Org. Lett.* **2016**, *18*, 1518-1521.
- [87] J. M. Grosselin, C. Mercier, G. Allmang, F. Grass, *Organometallics* **1991**, *10*, 2126-2133.
- [88] G. J. Schroepfer, I. Y. Gore, *J. Lipid Res.* **1963**, *4*, 266-269.
- [89] Z.-J. Yang, D. Zhou, Y.-X. Fang, H.-B. Ji, *Sep. Sci. Technol.* **2016**, *51*, 168-180.
- [90] J.-P. Lange, E. van der Heide, J. van Buijtenen, R. Price, *ChemSusChem* **2011**, *5*, 150-166.

- [91] M. M. Villaverde, N. M. Bertero, T. F. Garetto, A. J. Marchi, *Catal Today* **2013**, *213*, 87-92.
- [92] D. Vargas-Hernández, J. M. Rubio-Caballero, J. Santamaría-González, R. Moreno-Tost, J. M. Mérida-Robles, M. A. Pérez-Cruz, A. Jiménez-López, R. Hernández-Huesca, P. Maireles-Torres, *J. Mol. Catal. A: Chem.* **2014**, *383-384*, 106-113.
- [93] S. Sitthisa, D. E. Resasco, *Catal. Lett.* **2011**, *141*, 784-791.
- [94] a) D. Gramec, L. Peterlin Mašič, M. Sollner Dolenc, *Chem. Res. Toxicol.* **2014**, *27*, 1344-1358; b) K. Martin, V. Jarmila, *Curr. Top. Med. Chem.* **2016**, *16*, 2921-2952.
- [95] G. Guillena, D. J. Ramón, M. Yus, *Chem. Rev.* **2010**, *110*, 1611-1641.
- [96] J. S. Carey, D. Laffan, C. Thomson, M. T. Williams, *Organic & Biomolecular Chemistry* **2006**, *4*, 2337-2347.
- [97] D. G. Hall, *J. Am. Chem. Soc.* **2005**, *127*, 9655-9655.
- [98] a) G. E. Dobereiner, R. H. Crabtree, *Chem. Rev.* **2010**, *110*, 681-703; b) C. Gunanathan, D. Milstein, *Science* **2013**, *341*; c) J. Leonard, A. J. Blacker, S. P. Marsden, M. F. Jones, K. R. Mulholland, R. Newton, *Org. Process Res. Dev.* **2015**, *19*, 1400-1410; d) Q. Yang, Q. Wang, Z. Yu, *Chem. Soc. Rev.* **2015**, *44*, 2305-2329; e) X. Ma, C. Su, Q. Xu, *Top. Curr. Chem.* **2016**, *374*, 27.
- [99] a) R. Martínez, D. J. Ramón, M. Yus, *Tetrahedron* **2006**, *62*, 8982-8987; b) R. Martínez, D. J. Ramón, M. Yus, *Tetrahedron* **2006**, *62*, 8988-9001.
- [100] a) J. U. Nef, *Justus Liebigs Annalen der Chemie* **1901**, *318*, 137-230; b) W. A. Lazier, H. Adkins, *J. Am. Chem. Soc.* **1924**, *46*, 741-746; c) Y. Sprinzak, *J. Am. Chem. Soc.* **1956**, *78*, 3207-3208.
- [101] a) T. Yan, B. L. Feringa, K. Barta, *Nature Communications* **2014**, *5*, 5602; b) S. Elangovan, J. Neumann, J.-B. Sortais, K. Junge, C. Darcel, M. Beller, *Nature Communications* **2016**, *7*, 12641; c) M. Mastalir, M. Glatz, N. Gorgas, B. Stöger, E. Pittenauer, G. Allmaier, L. F. Veiros, K. Kirchner, *Chem. Eur. J.* **2016**, *22*, 12316-12320.
- [102] a) K.-T. Huh, Y. Tsuji, M. Kobayashi, F. Okuda, Y. Watanabe, *Chem. Lett.* **1988**, *17*, 449-452; b) G. Bitsi, E. Schleiffer, F. Antoni, G. Jenner, *J. Organomet. Chem.* **1989**, *373*, 343-352.
- [103] a) A. Tillack, D. Hollmann, D. Michalik, M. Beller, *Tetrahedron Lett.* **2006**, *47*, 8881-8885; b) D. Hollmann, A. Tillack, D. Michalik, R. Jackstell, M. Beller, *Chem. Asian J.* **2007**, *2*, 403-410.
- [104] a) M. H. S. A. Hamid, J. M. J. Williams, *Chem. Commun.* **2007**, 725-727; b) M. H. S. A. Hamid, J. M. J. Williams, *Tetrahedron Lett.* **2007**, *48*, 8263-8265; c) M. H. S. A. Hamid, C. L. Allen, G. W. Lamb, A. C. Maxwell, H. C. Maytum, A. J. A. Watson, J. M. J. Williams, *J. Am. Chem. Soc.* **2009**, *131*, 1766-1774; d) A. B. Enyong, B. Moasser, *J. Org. Chem.* **2014**, *79*, 7553-7563; e) A. Said Stålsmeden, J. L. Belmonte Vázquez, K. van Weerdenburg, R. Rae, P.-O. Norrby, N. Kann, *ACS Sustainable Chemistry & Engineering* **2016**, *4*, 5730-5736.
- [105] V. R. Jumde, L. Gonsalvi, A. Guerriero, M. Peruzzini, M. Taddei, *Eur. J. Org. Chem.* **2015**, *2015*, 1829-1833.
- [106] N. Nakagawa, E. J. Derrah, M. Schelwies, F. Rominger, O. Trapp, T. Schaub, *Dalton Trans.* **2016**, *45*, 6856-6865.
- [107] A. J. Blacker, M. M. Farah, M. I. Hall, S. P. Marsden, O. Saidi, J. M. J. Williams, *Org. Lett.* **2009**, *11*, 2039-2042.
- [108] a) Y. Watanabe, Y. Tsuji, Y. Ohsugi, *Tetrahedron Lett.* **1981**, *22*, 2667-2670; b) A. Arcelli, K. Bui The, G. Porzi, *J. Organomet. Chem.* **1982**, *235*, 93-96; c) Y. Watanabe, Y. Tsuji, H. Ige, Y. Ohsugi, T. Ohta, *J. Org. Chem.* **1984**, *49*, 3359-3363; d) J. A.

- Marsella, *J. Org. Chem.* **1987**, *52*, 467-468; e) S. Ganguly, F. L. Joslin, D. M. Roundhill, *Inorg. Chem.* **1989**, *28*, 4562-4564.
- [109] a) S.-I. Murahashi, K. Kondo, T. Hakata, *Tetrahedron Lett.* **1982**, *23*, 229-232; b) C. S. Cho, J. H. Kim, T.-J. Kim, S. C. Shim, *Tetrahedron* **2001**, *57*, 3321-3329.
- [110] A. Del Zotto, W. Baratta, M. Sandri, G. Verardo, P. Rigo, *Eur. J. Inorg. Chem.* **2003**, *2004*, 524-529.
- [111] a) K. O. Marichev, J. M. Takacs, *ACS Catal.* **2016**, *6*, 2205-2210; b) J. J. A. Celaje, X. Zhang, F. Zhang, L. Kam, J. R. Herron, T. J. Williams, *ACS Catal.* **2017**, *7*, 1136-1142.
- [112] a) C. Gunanathan, D. Milstein, *Angew. Chem.* **2008**, *120*, 8789-8792; b) C. Gunanathan, D. Milstein, *Angew. Chem. Int. Ed.* **2008**, *47*, 8661-8664; c) B. Gnanaprakasam, E. Balaraman, Y. Ben-David, D. Milstein, *Angew. Chem. Int. Ed.* **2011**, *50*, 12240-12244; d) B. Gnanaprakasam, E. Balaraman, Y. Ben-David, D. Milstein, *Angew. Chem.* **2011**, *123*, 12448-12452; e) E. Balaraman, D. Srimani, Y. Diskin-Posner, D. Milstein, *Catal. Lett.* **2015**, *145*, 139-144.
- [113] S. Agrawal, M. Lenormand, B. Martín-Matute, *Org. Lett.* **2012**, *14*, 1456-1459.
- [114] F.-L. Yang, Y.-H. Wang, Y.-F. Ni, X. Gao, B. Song, X. Zhu, X.-Q. Hao, *Eur. J. Org. Chem.* **2017**, *2017*, 3481-3486.
- [115] C. J. Creswell, A. Dobson, D. S. Moore, S. D. Robinson, *Inorg. Chem.* **1979**, *18*, 2055-2059.
- [116] K. D. Nguyen, D. Herkommer, M. J. Krische, *J. Am. Chem. Soc.* **2016**, *138*, 5238-5241.
- [117] P. Espinet, A. C. Albéniz, in *Current Methods in Inorganic Chemistry, Vol. 3* (Eds.: H. Kurosawa, A. Yamamoto), Elsevier, **2003**, pp. 293-371.
- [118] W. Baratta, S. Baldino, M. J. Calhorda, P. J. Costa, G. Esposito, E. Herdtweck, S. Magnolia, C. Mealli, A. Messaoudi, S. A. Mason, L. F. Veiros, *Chem. Eur. J.* **2014**, *20*, 13603-13617.
- [119] S. Oda, J. Franke, M. J. Krische, *Chemical Science* **2016**, *7*, 136-141.
- [120] A. Spencer, G. Wilkinson, *J. Chem. Soc., Dalton Trans.* **1974**, 786-792.